Uniwersytet Mikołaja Kopernika w Toruniu
Wydział Nauk Biologicznych i Weterynaryjnych

Bartosz Szymczak

Rozprawa doktorska

Sygnalizacja purynergiczna w komórkach glejaka – badania *in vitro* nad mechanizmami patologicznymi i możliwościami terapeutycznymi

Promotor:
dr hab. Katarzyna Roszek, prof. UMK

Promotor pomocniczy:
dr Joanna Czarnecka

Katedra Biochemii

Praca doktorska zrealizowana w Szkole Doktorskiej Nauk Ścisłych i Przyrodniczych
„Academia Scientiarum Thoruniensis”

Toruń 2024

Serdeczne podziękowania składam moim mentorkom, promotor ***dr hab. Katarzynie Roszek, prof. UMK*** *i promotor pomocniczej* ***dr Joannie Czarneckiej****. Za wieloletnią współpracę, wsparcie, pomoc, zaufanie, poświęcony czas oraz za ukształtowanie mnie jako badacza, zaangażowanie, przetarcie wielu ścieżek i otwarcie wielu drzwi, które umożliwiły mi zarówno naukowy jak i zawodowy rozwój.*

Szczególne podziękowania kieruję do ***Współautorów*** *publikacji, które są podstawą niniejszej rozprawy doktorskiej. Słowa te kieruję zwłaszcza do zespołu z Università degli Studi di Ferrara, gdzie realizowałem część swoich badań. Za ciepłe przyjęcie, otwartość, pomoc, cenne rady i świeże spojrzenie.*

Słowa uznania kieruję również pod adresem profesora ***Francesco di Virgilio****, niezrównanego autorytetu w świecie sygnalizacji purynergicznej, a którego niedawna śmierć szczególnie mnie dotknęła. Wielkim zaszczytem było dla mnie Go poznać, wielkim żalem jest świadomość, że był to ostatni raz. Za Jego wielką charyzmę, przenikliwość, krytyczne spojrzenie i cenne uwagi.*

Dziękuję również Kolegom i Koleżankom z Katedry Biochemii, za pomoc, ożywione dyskusje i cenne rady, które doprowadziły do powstania tej pracy.

Pracę dedykuję mojej ***Rodzinie****, jako owoc wieloletniego wsparcia, pomocy, pokładanych nadziei i niezmąconej wiary.*

Finansowanie badań:

Badania będące podstawą wyników prezentowanych w niniejszej rozprawie doktorskiej zostały sfinansowane ze środków:

Grantu MINIATURA 3 „Sygnalizacja nukleotydowa jako molekularne wsparcie terapii glejaka - badania wstępne" finansowany przez Narodowe Centrum Nauki (2019/03/X/NZ5/01409), kierownik projektu: dr Joanna Czarnecka

Grantu Grants4NCUStudents „Alterations in mechanisms involved in nucleotide-mediated signaling upon differentiation of glioma cells – a novel therapeutic approach" finansowany przez Uniwersytet Mikołaja Kopernika w Toruniu, w ramach projektu "Inicjatywa Doskonałości – Uczelnia Badawcza" (32/2021/Grants4NCUStudents), kierownik projektu: mgr Bartosz Szymczak

Część badań została zrealizowana przeze mnie w Università degli Studi di Ferrara, podczas dwóch miesięcznych staży naukowych. Pierwszy staż (luty/ marzec 2023) został sfinansowany przez Uniwersytet Mikołaja Kopernika ze środków programu „Mobilności dla doktorantów" w ramach projektu „Inicjatywa doskonałości – Uczelnia Badawcza", natomiast drugi (czerwiec/ lipiec 2023) w ramach programu „Short-term Scientific Mission" ze środków projektu „CA21130 - P2X receptors as a therapeutic opportunity (PRESTO)".

Wykaz publikacji wchodzących w skład rozprawy doktorskiej:

1.	Adinolfi, E., De Marchi, E., Grignolo, M., **Szymczak, B.**, & Pegoraro, A. (2023). The P2X7 receptor in oncogenesis and metastatic dissemination: New insights on vesicular release and adenosinergic crosstalk. International Journal of Molecular Sciences, 24, 18, 13906. https://doi.org/10.3390/ijms241813906	IF (2023) – 4.9 MNiSW – 140pkt
2.	**Szymczak, B.**, Czarnecka, J., Czach, S., Nowak, W., & Roszek, K. (2023). Purinergic approach to effective glioma treatment with temozolomide reveals synergistic anti-cancer effects mediated by P2X7 receptor. Cellular Signalling, 106, 110641. https://doi.org/10.1016/j.cellsig.2023.110641	IF (2023) – 4.4 MNiSW – 100pkt
3.	**Szymczak, B.**, Pegoraro, A., De Marchi, E., Grignolo, M., Maciejewski, B., Czarnecka, J., & Roszek, K. Retinoic acid-induced alterations enhance eATP-mediated anti-cancer effects in glioma cells: implications for P2X7 receptor variants as key players. Praca złożona w BBA - Molecular Basis of Disease – po drugiej odpowiedzi na recenzje	IF (2024) – 4.2 MNiSW – 140pkt
		Sumaryczny IF – 13.5 Suma punktów MNiSW – 380pkt

Spis treści

Streszczenie 7

Abstract 9

I Wstęp 11

II Cel pracy 18

III Materiały i metody 20

1. Materiał biologiczny 20
2. Indukowane różnicowanie i charakterystyka otrzymanych komórek 21
3. Wpływ różnicowania na system sygnalizacji purynergicznej 22
4. Interakcje elementów sygnalizacji purynergicznej z temozolomidem 24
5. Analizy statystyczne 25

IV Omówienie wyników 26

1. Charakterystyka komórek glejaka poddanych różnicowaniu kwasem retinowym (Publikacja 2, 3) 26
2. Zmiany w systemie sygnalizacji purynergicznej pod wpływem różnicowania (Publikacja 2, 3) 27
3. Interakcje receptora P2X7 z temozolomidem (Publikacja 2) 29

V Podsumowanie i wnioski 31

VI Literatura 32

Publikacja 1 37

The P2X7 receptor in oncogenesis and metastatic dissemination: New insights on vesicular release and adenosinergic crosstalk 37

Publikacja 2 53

Purinergic approach to effective glioma treatment with temozolomide reveals synergistic anti-cancer effects mediated by P2X7 receptor 53

Publikacja 3 83

Retinoic acid-induced alterations enhance eATP-mediated anti-cancer effects in glioma cells: implications for P2X7 receptor variants as key players. 83

Oświadczenie o współautorstwie 107

Wykaz skrótów

Ado – adenozyna

ADP – adenozynodifosforan

AMP – adenozynomonofosforan

ATCC – (ang. American Type Cell Culture) – amerykański bank komórek

ATP – adenozynotrifosforan

BGO – kwas 1-hydroksynaftaleno-3,6-disulfonowy

BzATP – 2'(3')-O-(4-benzoilobenzoilo)-adenozyno-5'-fosforan

cDNA – kodujące DNA, cząsteczka DNA powstała po przepisaniu mRNA na DNA w reakcji odwrotnej transkrypcji

CSCs – (ang. Cancer Stem Cells) – komórki macierzyste nowotworu

DMEM-HG – (ang. Dulbecco Minimum Essential Medium High Glucose) – podstawowa pożywka Eagle'a w modyfikacji Dulbecco z podwyższonym stężeniem glukozy

DMSO – dimetylosulfotlenek

DNA – kwas deoksyrybonukleinowy

E-5'NT – ekto-5'-nukleotydaza

E-AK – ekto-kinaza adenylanowa

eATP – ekto-adenozynotrifosforan

EC50 – (ang. effective concentration) – połowa maksymalnego stężenia efektywnego

ELISA – (ang. enzyme-linked immunosorbent assay) – test immunoenzymatyczny

E-NPPaza – ekto-pirofosfataza/ fosfodiesteraza nukleotydów

E-NTPDaza – ekto-fosfohydrolaza di- i trifosfonukleozydów

FBS – (ang. fetal bovine serum) – płodowa surowica cielęca

GBM – (ang. glioblastoma multiforme) – glejak wielopostaciowy

HPLC – (ang. high-performance liquid chromatography) – wysokosprawna chromatografia cieczowa

HRP – (ang. Horseradish peroxidase) – peroksydaza chrzanowa

lncRNA – (ang. long non-coding RNA) – długie niekodujące RNA

MEM – (ang. Minimum Essential Medium) – podstawowa pożywka hodowlana

mRNA – informacyjny RNA

MTIC – 3-metylo- (triazen-1-ylo) imidazolo-4-karboksyamid

MTT – bromek 3-(4,5- dimetylotiazol-2-yl)- 2,5-difenylotetrazoliowy

NEAA – (ang. Non-essential Amino Acids) – aminokwasy nieniezbędne

PDT – (ang. Population Doubling Time) – czas podwajania populacji

RA – kwas retinowy

RNA – kwas rybonukleinowy

RT-qPCR – (ang. Real-Time quantitative Polymerase Chain Reaction) – ilościowa reakcja łańcuchowa polimerazy w czasie rzeczywistym

TMZ – temozolomid

UDP – urydynodifosforan

UTP – urydynotrifosforan

WHO – (ang. World Health Organisation) – Światowa Organizacja Zdrowia

Streszczenie

Glejaki, nowotwory układu nerwowego, wywodzące się z tkanki glejowej, należą do najagresywniejszych i najtrudniejszych w leczeniu rodzajów nowotworów. Rozsiane na obszarze centralnego układu nerwowego i często nie formujące litego guza, stanowią wyzwanie dla chirurgii. Dodatkowo, obecność bariery krew-mózg znacząco ogranicza ilość możliwych do zastosowania chemoterapeutyków, stąd też intensywnie poszukuje się alternatywnych metod terapii. Jedną z takich metod jest indukowane różnicowanie komórek nowotworowych w kierunku komórek neuralnych, które ma na celu obniżenie ich potencjału proliferacyjnego i migracyjnego.

Zewnątrzkomórkowe ATP (eATP) jest dominującym składnikiem mikrośrodowiska nowotworów i jednocześnie naturalnym ligandem dla dwóch rodzin receptorów purynergicznych: metabotropowych P2Y oraz jonotropowych P2X. Spośród nich, najwięcej uwagi poświęca się receptorowi P2X7, a niedawne badania pozwoliły zidentyfikować dwie izoformy tego receptora występujące w organizmie ludzkim - P2X7A oraz P2X7B, biorące udział w regulacji procesów nowotworzenia oraz, zależnie od ich ekspresji w tkance nowotworowej pacjenta, decydujące o powodzeniu terapii przeciwnowotworowych. Aktywacja izoformy P2X7A prowadzi do otwarcia kanału jonowego, natomiast przy przedłużonej stymulacji przekształca się w nieselektywny por, który prowadzi do apoptotycznej śmierci komórek. Izoforma P2X7B jest pozbawiona jednej z wewnątrzkomórkowych domen - zmiana ta sprawia, że taki receptor nie posiada możliwości otwarcia poru, a jego aktywacja ma działanie pro-proliferacyjne.

Przeprowadzone badania miały na celu określenie zmian w mikrośrodowisku purynergicznym w komórkach trzech ludzkich linii komórkowych glejaka: A172, M059K i M059J, poddanych różnicowaniu indukowanemu kwasem retinowym oraz wpływu zmian w systemie sygnalizacji purynergicznej na wrażliwość komórek na chemoterapeutyki.

Analiza zmian poziomu ekspresji markerów neurogenezy potwierdziła różnicowanie badanych komórek w kierunku neuralnym. Zastosowana procedura różnicowania spowodowała obniżenie tempa proliferacji oraz migracji komórek, a także szereg zmian w systemie sygnalizacji purynergicznej. Do najważniejszych z nich należy zaliczyć wzrost poziomu ekspresji receptora P2X7 na poziomie mRNA i białka oraz zmianę stosunku ekspresji izoform P2X7A/B, a także spadek aktywności zewnątrzkomórkowych enzymów degradujących nukleotydy adeninowe. W efekcie

zaobserwowaliśmy zwiększenie wrażliwości komórek na cytotoksyczny efekt eATP oraz BzATP – specyficznego agonisty receptora P2X7, oraz obniżenie tempa migracji komórek – zmiany te były odwracalnie modulowane przez aktywację receptora P2X7. Co więcej, wykazaliśmy, że mimo wzrostu ekspresji pro-proliferacyjnej izoformy P2X7B nie dochodziło do aktywacji wewnątrzkomórkowych szlaków sygnałowych stymulujących proliferację, ponieważ to dominująca, pro-apoptotyczna izoforma P2X7A decydowała o cytotoksycznym działaniu eATP.

Badania mające na celu określenie oddziaływań między elementami sygnalizacji purynergicznej oraz temozolomidem, jednym z najczęściej stosowanych chemoterapeutyków w terapii glejaka wykazały, że jednoczesne stosowanie chemoterapeutyku z ligandami receptora P2X7 znacząco wzmacnia efekt cytotoksyczny, jednocześnie badania *in silico* podparte badaniami *in vitro* wskazują, że temozolomid może działać jako antagonista receptora P2X7.

Uzyskane wyniki wskazują, że różnicowanie kwasem retinowym w połączeniu z kontrolą sygnalizacji purynergicznej w mikrośrodowisku nowotworu mogą mieć potencjał jako terapia wspierająca do obecnie stosowanych kuracji przeciwnowotworowych. Dodatkowo, możliwość wpływania na poziom ekspresji izoform receptora P2X7 i jego warunkowa oraz miejscowo specyficzna aktywacja może w przyszłości stanowić obiecujący cel terapeutyczny.

Słowa kluczowe: glejak, sygnalizacja purynergiczna, eATP, receptor P2X7, różnicowanie, chemioterapia

Abstract

Gliomas, tumors of the nervous system that originate from glial tissue, are considered one of the most aggressive and difficult to treat type of cancer. As they spread throughout the central nervous system and often do not form any solid tumors, they present a challenge to the surgical intervention. In addition, the presence of the blood-brain barrier significantly limits the number of chemotherapeutic agents that can be used, hence the intense search for alternative therapies. One such method is the induction of differentiation towards neural cells, which allows to reduce the proliferative and migratory potential of the cancer cells.

Extracellular ATP (eATP) is the predominant component of the tumor microenvironment, as well as a natural ligand for two families of purinergic receptors: metabotropic P2Y and ionotropic P2X. Among these structures, the P2X7 receptor has received the most attention. Recent studies have identified two distinct isoforms of the P2X7 receptor in the human body: P2X7A and P2X7B. Both of them are involved in the regulation of tumorigenesis. Determination of the success of anti-cancer therapy is dependent on their expression levels in the patient's tumor tissue. Activation of the P2X7A isoform leads to the opening of an ion channel, while with prolonged stimulation it transforms into a non-selective pore, leading to apoptotic cell death. The P2X7B isoform is devoid of one of its intracellular domains - a change that renders such a receptor lacking the pore-opening capacity, whereas its activation has a pro-proliferative effect.

The main research goal was to determine changes in the purinergic microenvironment in cells of three human glioma cell lines, A172, M059K and M059J, subjected to retinoic acid-induced differentiation. Additionally we aimed to access how the alterations in the purinergic signaling system influence cell sensitivity to chemotherapeutics.

Analysis of changes in the expression levels of neurogenesis markers confirmed the differentiation of the cells studied towards the neural lineage. The differentiation procedure resulted in a decrease in cell proliferation and migration rates, as well as a number of modifications in the purinergic signaling system. Among the most important findings were: an increase in the expression level of the P2X7 receptor at the mRNA and protein levels, and a shift in the expression ratio of P2X7A/B isoforms, as well as a decrease in the activity of extracellular adenine nucleotide-degrading enzymes. As a result, we observed an increase in the sensitivity of cells to the cytotoxic effect of eATP

and BzATP, a specific P2X7 receptor agonist, and a decrease in the rate of cell migration - these changes were reversibly modulated by P2X7 receptor activation. Furthermore, we showed that, despite an increase in the expression of the pro-proliferative P2X7B isoform, there was no activation of intracellular signaling pathways that stimulate proliferation, as it was the predominant, pro-apoptotic P2X7A isoform that determined the cytotoxic effect of eATP.

Studies regarding the interactions between elements of purinergic signaling and temozolomide, one of the most commonly used chemotherapeutics in glioma therapy, prove, that concomitant use of a chemotherapeutic agent with P2X7 receptor ligands significantly enhances the cytotoxic effect. At the same time *in silico* studies supported by *in vitro* studies indicate, that temozolomide may act as a P2X7 receptor antagonist.

These results indicate, that retinoic acid differentiation in combination with control of purinergic signaling in the tumor microenvironment, may have potential as a supportive therapy to current anticancer treatments. Additionally, the ability to influence the expression level of P2X7 receptor isoforms and its conditional and site-specific activation may represent a promising therapeutic target in the future.

Keywords: glioma, purinergic signaling, eATP, P2X7 receptor, differentiation, chemotherapy

I Wstęp

1.1 Glejak

Glejak wielopostaciowy (ang. glioblastoma multiforme, GBM) jest najagresywniejszym typem nowotworu występującym w mózgowiu z niekorzystnymi prognozami oscylującymi około 15 miesięcy przeżycia od uzyskania diagnozy [1]. Chociaż czynniki wywołujące glejaka wzbudzają wiele kontrowersji, to obowiązujące teorie zakładają, że powstanie glejaka jest wynikiem nagromadzenia mutacji w neuralnych komórkach macierzystych lub komórkach prekursorowych gleju, które to mutacje prowadzą do niekontrolowanych podziałów i ostatecznie do rozwoju guza [2]. Obecnym standardem w kuracji są interwencje chirurgiczne, a także radioterapia i chemioterapia.

1.2 Możliwości chemioterapii

Liczba środków wykorzystywanych w chemioterapii glejaka jest znacznie ograniczona w porównaniu do innych typów nowotworów, ze względu na barierę krew-mózg – naturalną barierę biologiczną, która jest przepuszczalna jedynie dla niewielkiej liczby cząsteczek o odpowiednio małej masie cząsteczkowej i lipofilowym charakterze. Głównymi chemoterapeutykami stosowanymi w terapii glejaka są temozolomid (TMZ), pochodne nitrozomocznika (np. karmustyna i lomustyna), czy irinotekan [3–5]. Wszystkie wymienione związki mają zbliżony mechanizm działania – są podawane pacjentowi w formie proleku, dostają się do krwiobiegu i penetrują barierę krew-mózg, następnie wnikają do wnętrza komórki, gdzie ulegają konwersji do cząsteczki aktywnej i trwale wiążą się z DNA, uniemożliwiając przeprowadzenie takich procesów jak replikacja czy transkrypcja [6].

Strategia ta nie jest jednak idealna, co można zilustrować na przykładzie TMZ. Związek ten po wniknięciu do komórki powinien przekształcić się do formy pośredniej (MTIC - 3-metylo-(triazen-1-ylo)imidazolo-4-karboksyamid), a następnie w reakcji z wodą, do formy aktywnej (kationu metyloazoniowego), która związałaby się z guaniną w łańcuchu DNA [4]. W praktyce jednak TMZ dość szybko po podaniu pacjentowi ulega konwersji do swojej pośredniej formy (MTIC), która nie posiada zdolności do penetracji błony komórkowej [7]. Szacuje się, że nawet 80% TMZ ulega przekształceniu, zanim dotrze do środowiska guza [8]. To z kolei sprawia, że w terapii konieczne jest podawanie pacjentom dużo wyższych dawek, które w konsekwencji wywołują liczne działania niepożądane, np. nudności, anemia czy małopłytkowość [9].

Ograniczenie możliwości chemioterapii do zaledwie kilku opcji, prowadzi do silnej presji selekcyjnej nowotworu, który po pierwszej fazie remisji powraca jako guz wtórny, niemal zawsze odporny na działanie pierwotnie stosowanego chemoterapeutyku [10].

Wysoka agresywność i niski wskaźnik przeżywalności, w połączeniu z małą liczbą, wciąż niedoskonałych opcji terapeutycznych glejaka są głównymi czynnikami motywacyjnymi do poszukiwania nowych, alternatywnych metod podejścia do terapii tego nowotworu lub zwiększania wydajności tych już istniejących.

1.3 Różnicowanie indukowane kwasem retinowym

Jedną z aktualnie proponowanych metod alternatywnych dla terapii glejaka jest różnicowanie w kierunku neuralnym w oparciu o podawanie czynników różnicujących, a jednym z najczęściej stosowanych jest kwas retinowy (ang. retinoic acid, RA) [11]. RA jest pochodną witaminy A, ma charakter lipofilowy i względnie łatwo penetruje barierę krew-mózg i wnika do wnętrza komórek, gdzie wiąże się ze swoistymi dimerycznymi receptorami jądrowymi, zmieniając ich konformację. Prowadzi to do utraty powinowactwa do białek represorowych, rekrutacji białek aktywatorowych i promowania ekspresji docelowych genów [12]. Chociaż pierwsze doniesienia dotyczące właściwości kwasu retinowego i jego wpływu na komórki glejaka, w tym obniżenia ich potencjału proliferacyjnego, pojawiły się ponad dwadzieścia lat temu, zagadnienie to wciąż wymaga dodatkowych badań.

Główne zarzuty względem stosowania kwasu retinowego w terapii glejaka dotyczą wykształcanych przez nowotwór mechanizmów odporności związanych z utratą ekspresji receptorów kwasu retinowego oraz innych zaburzeń związanych z percepcją i przekazywaniem sygnału od tej cząsteczki [13–15]. Kolejnymi zarzutami są niski odsetek translacji wyników *in vitro* na badania *in vivo*, oraz efekty uboczne stosowanej terapii [16,17].

Z drugiej jednak strony, istnieje szereg badań wskazujących na różnicujący i antyproliferacyjny wpływ kwasu retinowego, zarówno na komórki macierzyste glejaka jak i inne subpopulacje komórek guza [18–20].

1.4 Sygnalizacja purynergiczna

System sygnalizacji purynergicznej jest jednym z najstarszych systemów przekazywania sygnałów w organizmach zwierząt. Na system ten składają się receptory błonowe (podzielone na trzy klasy: P1, P2X oraz P2Y), odpowiedzialne za percepcję

sygnałów ze środowiska zewnątrzkomórkowego oraz zewnątrzkomórkowe enzymy (ekto-enzymy związane z błoną komórkową oraz egzo-enzymy wydzielane do przestrzeni zewnątrzkomórkowej), regulujące stężenie i homeostazę ligandów dla receptorów (Rycina 1.) [21–23].

Do klasy P1 zaliczamy cztery receptory wrażliwe na adenozynę, oznaczone jako P1A1, P1A2a, P1A2b oraz P1A3. Wszystkie one są klasycznymi receptorami metabotropowymi, zbudowanymi z siedmiu domen transbłonowych oraz sprzężonymi z białkami G. W przypadku receptorów P1A1 oraz P1A3 z receptorem najczęściej jest sprzężona podjednostka α_i lub α_q białka G, natomiast w przypadku receptorów P1A2a oraz P1A2b jest to podjednostka α_s [24].

Receptory z klasy P2Y również są receptorami metabotropowymi. Do tej klasy zaliczamy osiem białek oznaczonych numerami: P2Y1, P2Y2, P2Y4, P2Y6, P2Y11, P2Y12, P2Y13, P2Y14. Podobnie jak w przypadku klasy P1, zidentyfikowano różne podjednostki α białka G. W przypadku receptorów P2Y1, P2Y2, P2Y4, P2Y6, P2Y11 są to najczęściej podjednostki α_q, natomiast receptory P2Y12, P2Y13 oraz P2Y14 są najczęściej sprzężone z podjednostką α_i białka G. Receptory klasy P2Y wyróżnia najszersze spektrum ligandów, ponieważ wśród agonistów wykazujących powinowactwo do tych receptorów zidentyfikowano wiele di- i trifosfonukleotydów, m. in. ATP, ADP, UTP, UDP, a nawet UDP-glukozę [25].

Ostatnią klasą są jonotropowe receptory P2X wrażliwe na ATP. Zaliczamy do niej siedem receptorów nazwanych kolejno: P2X1, P2X2, P2X3, P2X4, P2X5, P2X6 oraz P2X7. Funkcjonalny receptor typu P2X jest zbudowany z trzech podjednostek, które tworzą kanał jonowy, przepuszczalny dla kationów. Ze względu na strukturalne podobieństwo, w skład jednego trimeru mogą wchodzić zarówno trzy identyczne podjednostki (homotrimer), jak i różne białka (heterotrimer) [26]. Jedynym wyjątkiem od tej reguły jest receptor P2X7 [27].

W organizmie człowieka zidentyfikowano kilkanaście zewnątrzkomórkowych enzymów metabolizujących nukleotydy, które podzielono z uwagi na rodzaj katalizowanych reakcji (Rycina 1.) [23].

Do klasy hydrolaz należy: sześć E-NTPDaz (ekto-fosfohydrolazy di- i trifosfonukleozydów) katalizujących rozkład trifosfonukleotydów do difosfonukleotydów oraz difosfonukleotydów do monofosfonukleotydów, każdorazowo z uwolnieniem ortofosforanu, trzy E-NPPazy (ekto-pirofosfatazy/ fosfodiesterazy

nukleotydów) katalizujące degradację trifosfonukleotydów do monofosfonukleotydów z wytworzeniem pirofosforanu, ekto-5'-nukleotydaza degradująca monofosfonukleotyd do nukleozydu i ortofosforanu oraz alkaliczna fosfataza – enzym o niskiej specyficzności substratowej, aktywny względem różnych związków zawierających w swojej strukturze resztę fosforanową [28–30].

Oprócz tego występują również enzymy z klasy transferaz i są to: kinaza adenylanowa, katalizująca odwracalną reakcję przenoszenia reszty fosforanowej z ATP na AMP, czego skutkiem jest powstanie dwóch cząsteczek ADP oraz difosfokinaza nukleozydowa, przenosząca grupę fosforanową z dowolnego trifosfonukleotydu na difosfonukleotyd, czego skutkiem może być obniżenie lub podwyższenie stężenia ATP.

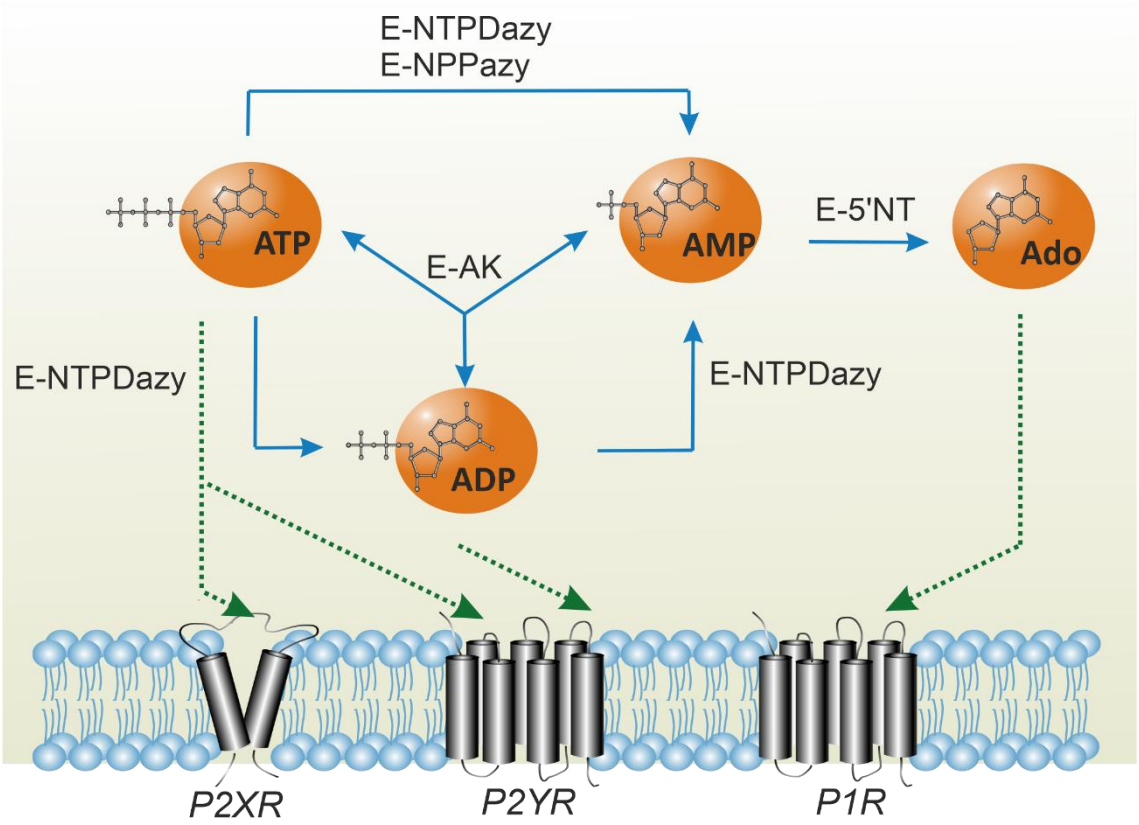

Rycina 1. Schematyczna ilustracja oddziaływania elementów sygnalizacji purynergicznej (Szymczak i wsp. 2023, zmienione).

Receptory purynergiczne, poprzez aktywację wewnątrzkomórkowych szlaków sygnalizacyjnych, regulują takie procesy, jak proliferacja, różnicowanie, neurotransmisja, apoptoza, indukcja stanów zapalnych czy angiogeneza [31]. eATP jest głównym zewnątrzkomórkowym ligandem receptorów purynergicznych obecnych w mikrośrodowisku guza [32]. Wysokie stężenie ATP poza komórką wynika przede

wszystkim z uwalniania go do przestrzeni międzykomórkowej przez komórki nekrotyczne, ale również na skutek jego aktywnego uwalniania w mikropęcherzykach lub poprzez mechanizm dodatniego sprzężenia zwrotnego przy aktywacji receptorów purynergicznych [33]. Rola eATP w procesie nowotworzenia od lat pozostaje przedmiotem sporu, ze względu na sprzeczne doniesienia dotyczące wpływu eATP, wynikające w głównej mierze z wysokiej heterogenności nowotworów. Niemniej, w większości badań uwaga skupia się na receptorze P2X7 i jego udziale w kontroli proliferacji i inwazyjności nowotworów [34–36].

1.5 Receptor P2X7 – charakterystyka, rola w nowotworzeniu, potencjał terapeutyczny (Publikacja 1)

Gen kodujący podjednostkę receptora P2X7 jest w ludzkim genomie zlokalizowany na długim ramieniu 12. chromosomu. Składa się z trzynastu eksonów, a w wyniku jego ekspresji powstaje peptyd o długości 595 aminokwasów. Białko ulega następnie modyfikacjom posttranslacyjnym takim jak glikozylacja, które stanowią swoisty sygnał umożliwiający transport do błony komórkowej [27].

Receptor P2X7, podobnie jak pozostałe receptory purynergiczne z klasy P2X, jest receptorem jonowym zbudowanym z trzech podjednostek, który po otwarciu kanału o średnicy około 0,8 nm umożliwia napływ jonów sodu i wapnia przy jednoczesnym wypływie jonów potasu. Istnieje jednak szereg właściwości, które sprawiają, że jest on wyjątkowy na tle pozostałych receptorów tej klasy [37].

Pierwszą cechą jest fakt, że receptor ten występuje jedynie w formie homotrimeru, podczas gdy pozostałe receptory mogą być zbudowane z różnych podjednostek i funkcjonować jako heterotrimery [38]. Charakterystyczną cechą receptora P2X7 jest również jego próg pobudliwości, wyznaczony na około 100 μM, czyli 10-krotnie wyższy od wartości progowej pozostałych receptorów [39]. Jednak, co wyjątkowe i w kontekście jego potencjału terapeutycznego wydaje się być najważniejsze, przedłużająca się stymulacja receptora prowadzi do trwałej zmiany jego konformacji i typowy dla receptorów P2X kanał jonowy rozszerza się tworząc nieselektywny por o średnicy około 3-5 nm, umożliwiający napływ do komórki większych cząsteczek, takich jak np. barwniki fluorescencyjne [40]. Zgodnie z obecną wiedzą, otwarcie kanału jonowego prowadzi dalej do aktywacji wewnątrzkomórkowych szlaków sygnalizacyjnych związanych z efektem pro-proliferacyjnym komórki, podczas gdy formowanie makroporu jest wiązane z efektem cytotoksycznym [41].

W ludzkim organizmie zidentyfikowano dziesięć form splicingowych receptora (P2X7A-J), z czego cztery są zaangażowane w proces nowotworzenia (P2X7A, P2X7B, P2X7H oraz P2X7J) [42].

Izoforma P2X7A jest podstawową formą białka receptora i powstaje w wyniku pełnej ekspresji wszystkich trzynastu eksonów genu P2X7. Powstałe białko wykazuje zarówno właściwości kanału jonowego, jak i zdolność do otwierania nieselektywnego makroporu [40]. Izoforma P2X7B powstaje w wyniku przerwania procesu transkrypcji po dziesiątym eksonie, a powstały transkrypt podlega procesowi translacji, w wyniku którego powstaje skrócone białko, które wprawdzie posiada zdolność otwierania kanału, jednak nie może formować makroporu [43,44]. Izoforma P2X7J powstaje na skutek przerwania transkrypcji po siódmym eksonie - transkrypt podlega procesowi translacji, jednak nie tworzy funkcjonalnej podjednostki receptora ze względu na brak drugiej, C-końcowej, domeny kotwiczącej w błonie komórkowej. Udowodniono, że ta postać białka receptorowego może zaburzać proces oligomeryzacji izoformy P2X7A [45]. Izoforma P2X7H powstaje w wyniku przerwania procesu transkrypcji po trzecim eksonie, a powstały produkt nie podlega translacji i występuje jako lncRNA, o właściwościach promowania nowotworów [46].

Ze względu na dwoistą naturę receptora P2X7, zależną od obecności izoform splicingowych oraz powszechną ekspresję w różnych typach nowotworów, potwierdzonych dotychczas w takich przypadkach jak: białaczka [47], czerniak [48], glejak [41], neuroblastoma [49], nowotwór prostaty [50], piersi [51], kości [52] czy jelita grubego [53], stał się on obiektem zainteresowania jako potencjalny cel terapeutyczny.

Dotychczas potwierdzono rolę receptora P2X7 w aktywowaniu wielu wewnątrzkomórkowych szlaków związanych z rozprzestrzenianiem guza [54–56], a jego nadekspresja została wykryta w różnych typach nowotworów. Obecnie uważa się, że za pro-nowotworowe działanie receptora P2X7 odpowiada w głównej mierze izoforma P2X7B, która działa jako kanał jonowy, jednak nie posiada zdolności do otwierania makroporu [52]. W wyniku ekspresji tego wariantu splicingowego receptora, komórka mimo wzrastającego stężenia ATP w przestrzeni zewnątrzkomórkowej, nie jest w stanie odbierać tych zmian jako sygnał niebezpieczeństwa („danger signal”), zamiast tego dochodzi do ciągłej stymulacji wewnątrzkomórkowych szlaków sygnalizacyjnych związanych ze wzrostem [57]. Badania potwierdzają, że ekspresja izoformy P2X7B jest

powiązana z procesem metastazy nowotworów kości, prostaty czy skóry, może być też negatywnym czynnikiem prognostycznym [50,58,59].

Kolejnym procesem, w którym istotną rolę odgrywa receptor P2X7, a który jest powiązany z procesem nowotworzenia jest wydzielanie przez komórkę mikropęcherzyków [60]. Struktury te pełnią ważną rolę w komunikacji między komórkami, w tym w mikrośrodowisku guza. Potwierdzono, że stymulacja receptora P2X7 może prowadzić do uwalniania mikropęcherzyków bogatych w ATP, co tworzy swoistą pętlę dodatniego sprzężenia zwrotnego, jeszcze bardziej nasilając aktywację receptora i zwiększając stymulację wewnątrzkomórkowych szlaków sygnalizacyjnych [61]. Oprócz ATP, w pęcherzykach uwalnianych pod wpływem stymulacji receptora P2X7 zidentyfikowano również miRNA, których aktywność wiąże się z procesami proliferacji i migracji komórek [59].

Z drugiej strony, wykazano pozytywny efekt aktywacji receptora P2X7 i działanie antynowotworowe, gdy dominującą izoformą w mikrośrodowisku guza było P2X7A. W takich przypadkach, pod wpływem wzrastającego stężenia zewnątrzkomórkowego ATP dochodzi do trwałej zmiany konformacji receptora z kanału jonowego na nieselektywny por, w wyniku czego efekt pro-proliferacyjny ustępuje na rzecz efektu cytotoksycznego [40]. Wzrost stężenia ATP może być zarówno efektem fizjologicznym, np. na skutek uwalniania ATP przez mikropęcherzyki do środowiska zewnątrzkomórkowego lub w wyniku nekrozy komórek, ale może być również indukowany, np. w wyniku działania chemoterapeutyków [62]. Badania potwierdzają, że efekt cytotoksyczny niektórych chemoterapeutyków, które stymulują wzrost stężenia zewnątrzkomórkowego ATP jest silniejszy w przypadkach, gdy dominującą izoformą receptora jest P2X7A [41,47,49,63,64]. Co więcej, receptor P2X7 ma pozytywne działanie na hamowanie wzrostu guza gdy podlega ekspresji w komórkach odpornościowych, dzięki czemu możliwa jest zarówno produkcja cytokin, jak i hamowanie szlaków immunosupresyjnych zależnych od adenozyny [65–67].

Przytoczone powyżej dane literaturowe dowodzą, że receptor P2X7 może stać się kluczowym celem nowych terapii. Niezbędne jest jednak spersonalizowane podejście oparte na indywidualnym profilu ekspresji izoform receptora w mikrośrodowisku guza danego pacjenta.

II Cel pracy

Zgodnie z danymi WHO, nowotwory stanowią drugą najczęstszą przyczynę zgonów w zachodnim społeczeństwie. Wśród nich szczególną uwagę zwracają glejaki, nowotwory układu nerwowego, które mimo względnie niskiego współczynnika zachorowalności (mniej niż 200 przypadków na milion osób), cechują się jednym z najniższych 5-letnich wskaźników przeżycia na poziomie 5-10% [68,69]. Jest to spowodowane zarówno wysoką złośliwością, jak i naturalnymi barierami ograniczającymi możliwości stosowania konwencjonalnych metod kuracji, takich jak chemioterapia czy zabiegi chirurgiczne, co wymusza poszukiwanie metod alternatywnych lub wspierających dla aktualnie stosowanych terapii.

Jedną z proponowanych metod alternatywnych w terapii glejaka jest różnicowanie komórek w kierunku neuralnym. Glejaki są heterogenną grupą komórek, często na niskim poziomie zróżnicowania. Dotychczasowe badania wskazują, że szczególnie subpopulacja komórek macierzystych guza (ang. Cancer Stem Cells, CSCs), może być wrażliwa na działanie czynników różnicujących. Biorąc pod uwagę, że wraz ze stopniem zróżnicowania może dojść do przeformatowania całego aparatu sygnalizacyjnego komórki, należy dokładnie zbadać jakie konsekwencje może nieść ze sobą proces indukowanego różnicowania.

Dlatego głównym celem niniejszej pracy było określenie, jakie zmiany w systemie sygnalizacji purynergicznej zachodzą w komórkach glejaka poddanych procesowi indukowanego różnicowania w kierunku neuralnym.

Do celów szczegółowych pracy należało:

- Scharakteryzowanie zmian fizjologii komórek glejaka poddanych różnicowaniu, ze szczególnym uwzględnieniem zmian potencjału proliferacyjnego i migracyjnego;
- Określenie różnic w funkcjonowaniu elementów sygnalizacji purynergicznej, w tym aktywności katalitycznej zewnątrzkomórkowych enzymów metabolizujących nukleotydy, poziomie ekspresji receptorów purynergicznych, a w szczególności izoform receptora P2X7 w komórkach glejaka poddanych procesowi różnicowania;
- Zbadanie zmian w odpowiedzi fizjologicznej różnicowanych komórek, na traktowanie ligandami receptora P2X7, w tym określenie efektu cytotoksycznego,

zmian potencjału migracyjnego, a także aktywacji wewnątrzkomórkowych szlaków sygnalizacyjnych;

- Porównanie i wyjaśnienie mechanizmu zmian efektu cytotoksycznego wywoływanego przez chemoterapeutyki oraz chemoterapeutyki podawane wraz z ligandami receptora P2X7, w niezróżnicowanych i zróżnicowanych komórkach glejaka.

III Materiały i metody

1. Materiał biologiczny

1.1 Linie komórkowe i uzasadnienie wyboru

Materiałem badawczym były komórki linii A172 (ludzka linia komórkowa glejaka (ATCC CRL–1620)), M059J (ludzka linia komórkowa glejaka (ATCC CRL-2366)) oraz M059K (ludzka linia komórkowa glejaka (ATCC CRL-2365)).

Linia komórkowa A172 została wyprowadzona w latach 70-tych z próbki guza 53-letniego pacjenta chorującego na glejaka, o niedoprecyzowanej charakterystyce. Komórki linii A172 zostały wybrane do badań, ponieważ są aktualne popularnym i często wybieranym modelem komórkowym wykorzystywanym w badaniach *in vitro*.

Linie komórkowe M059K i M059J zostały wyprowadzone z komórek próbki guza, pochodzącej od 33-letniego pacjenta płci męskiej cierpiącego na glejaka wielopostaciowego. Mimo wspólnego pochodzenia, linie te zasadniczo różnią się od siebie z uwagi na fakt, że linia M059J jest dużo wrażliwsza na działanie promieniowania jonizacyjnego, cytotoksyczny efekt bleomycyny i karmustyny, a także posiada znaczne defekty w mechanizmie naprawy dwuniciowych uszkodzeń DNA. Stąd też równoległe prowadzenie badań na obu liniach komórkowych daje możliwość porównania zróżnicowanych odpowiedzi subpopulacji komórek w obrębie guza.

1.2 Warunki hodowli

Hodowle komórkowe prowadzono w warunkach optymalnych (temperatura 37^{o}C, przy atmosferze 5% CO_2 i o podwyższonej wilgotności), zgodnie z zaleceniem producenta. Medium hodowlane dla linii komórkowej A172 stanowiła mieszanina DMEM-HG, 10% FBS, 100 U/ml penicyliny oraz 0,1 mg/ml streptomycyny, z kolei media hodowlane dla linii komórkowej M059J i M059K stanowiła mieszanina Ham's F12/MEM, 10% FBS, 100 U/ml penicyliny i 0,1 mg/ml streptomycyny oraz 0,5% aminokwasów (ang. non-essential aminoacids, NEAA).

Komórki były pasażowane każdorazowo po osiągnięciu stanu subkonfluencji. Do pasażu wykorzystywano 0,25% roztwór trypsyny w PBS. Ilość wysiewanych komórek była dostosowywana do potrzeb wykonywanego eksperymentu i wykorzystywanych naczyń hodowlanych.

2. Indukowane różnicowanie i charakterystyka otrzymanych komórek

2.1 Protokół różnicowania

W celu indukcji różnicowania wykorzystano zoptymalizowany dwutygodniowy protokół oparty o zastosowanie medium hodowlanego z dodatkiem kwasu retinowego (10 μM w DMSO). Medium było wymieniane dwa razy w tygodniu, a komórki pasażowano raz w tygodniu, po uzyskaniu odpowiedniej gęstości. Ze względu na wrażliwość kwasu retinowego na światło, całość procedury różnicowania wykonywano w ciemności. Po dwóch tygodniach prowadzenia procedury, uzyskane komórki były wykorzystywane do dalszych analiz.

2.2 Ocena zmiany potencjału proliferacyjnego

W celu określenia zmian w tempie proliferacji komórek przeprowadzono analizy tempa podwajania populacji komórek oraz rozkładu faz cyklu komórkowego. Analiza tempa podwajania populacji (ang. population doubling time, PDT) polegała na równoległym prowadzeniu hodowli komórek kontrolnych i indukowanych do różnicowania przez 30 dni i zliczaniu ich liczby dwa razy w tygodniu przy wykorzystaniu komory zliczeniowej Thoma. Komórki były barwione 0,4% błękitem trypanu. Analiza rozkładu faz cyklu komórkowego polegała na utrwaleniu w 70% etanolu i wybarwieniu 20 μg/ml jodkiem propidyny komórek kontrolnych oraz zróżnicowanych, a następnie analizie fluorescencji w cytometrze przepływowym (BriCyte E6 flow cytometer (Mindray, Shenzhen, Chiny)).

2.3 Analiza zmian poziomu ekspresji genów markerowych neurogenezy

Określenie zmian w poziomie ekspresji wybranych genów markerowych neurogenezy wykonano przy pomocy analizy RT-qPCR. Z komórek kontrolnych i różnicowanych wyizolowano RNA przy wykorzystaniu zestawu „RNeasy Mini Kit", firmy Qiagen. Uzyskane RNA zostało poddane reakcji DNazowania przy użyciu zestawu „DNase I, RNase-free" (ThermoFischer Scientific), a następnie przepisane na cDNA w procesie odwrotnej transkrypcji przy zastosowaniu zestawu „RevertAid First Strand cDNA Synthetic Kit" (ThermoFischer Scientific), oba etapy przeprowadzono w termocyklerze T100 Thermal Cycle (BioRad). Uzyskane cDNA zostało wykorzystane jako matryca do reakcji Real-Time qPCR. Analizie poddano trzy geny markerowe neurogenezy: *NES* (kodujący białko nestynę), *NeuroD1* (kodujący czynnik transkrypcyjny o tej samej nazwie), *TUJ1* (kodujący białko β-tubuliny klasy III) oraz

jeden gen markerowy gleju - *GFAP* (gen kodujący kwaśne białko włókienkowe). Reakcję Real-Time qPCR przeprowadzono przy wykorzystaniu zestawu „LightCycler 480 SYBR Green I Master", w termocyklerze LightCycler480 (Roche).

2.4 Pomiar zmian potencjału migracyjnego komórek

Zmiany w potencjale migracyjnym różnicowanych komórek względem komórek kontrolnych określono przy pomocy analiz RT-qPCR oraz testu rysy. Przygotowanie matrycy do reakcji RT-qPCR przeprowadzono w identyczny sposób jak powyżej, natomiast analizie poddano geny *CDH1* (kodujący białko E-kadheryny) i *CDH2* (kodujący białko N-kadheryny). Test rysy polegał na „wydrapaniu" rysy na powierzchni monowarstwy komórek, w którym prowadzono hodowle komórkowe, a następnie wykonaniu zdjęć w czasie 0, 4, 8, 12 i 24 godzin od momentu powstania rysy. Potencjał migracyjny określono jako procent powierzchni rysy na zdjęciu po upływie danego czasu względem powierzchni rysy w momencie jej wykonania.

3. Wpływ różnicowania na system sygnalizacji purynergicznej

3.1 Zmiana aktywności ektoenzymów nukleolitycznych

W celu określenia zmian w aktywności enzymów metabolizujących zewnątrzkomórkowe nukleotydy, przeprowadzono analizę ekspresji wybranych enzymów na poziomie mRNA oraz reakcje enzymatyczne dla wybranych enzymów. Analizie RT-qPCR poddano geny *ENTPD1, ENTPD5*, *ENTPD6, AK1*, *NT5E*, kodujące odpowiednio białka enzymatyczne: NTPDazę 1, NTPDazę 5, NTPDazę 6, kinazę adenylanową oraz ekto-5'-nukleotydazę. Z kolei pomiar aktywności katalitycznej przeprowadzono dla NTPDaz/NPPaz w kierunku degradacji ATP, NTPDaz/NPPaz w kierunku degradacji ADP, kinazy adenylanowej w kierunku metabolizmu ADP oraz ekto-5'-nukleotydazy. Mieszaniny poreakcyjne zebrano i poddano analizie HPLC z użyciem zestawu do chromatografii In- Line Degasser AF, 515 HPLC Pump, Waters Pump Control Module, Waters 2487 Dual Absorbance Detector, Waters 717 Plus Autosampler (Waters Corporation) z detekcją przy długości fali λ=260 nm.

3.2 Analiza zmian w poziomie ekspresji receptora P2X7

Do określenia zmian w poziomie ekspresji izoform receptora P2X7 na poziomie mRNA wykorzystano reakcję RT-qPCR przy wykorzystaniu sond TaqMan i termocyklera AB PRISM 7300 Step One Real-Time PCR system (Applied Biosystems). Przygotowanie matrycy cDNA odbyło się w sposób identyczny do protokołu opisanego powyżej.

W celu określenia zmian w poziomie ekspresji izoform receptora P2X7 na poziomie białka przeprowadzono reakcję Western blot. Lizat komórkowy został rozdzielony w żelu 4-12% NuPAGE Bis-Tris, firmy Thermo Scientific, a następnie transferowany na membranę nitrocelulozową. Membrana była inkubowana przez noc w temperaturze 4^{o}C z króliczymi przeciwciałami anty-P2X7, a następnie z kozimi przeciwciałami wtórnymi anty-króliczymi sprzężonymi z peroksydazą chrzanową (HRP). Analizę chemiluminometryczną wykonano przy użyciu zestawu ECL HRP Chemiluminescent Substrate ETA C ULTRA 2.0, firmy Cyanagen, oraz chemiluminometru C-Digit Model 3600, firmy LI-COR.

Z kolei do wyznaczenia zmian funkcjonalności receptora P2X7 wykorzystano test wychwytu bromku etydyny. Komórki były inkubowane przez 10 minut z bromkiem etydyny w stężeniu 10 μg/ml, a następnie dodano agonistę receptora P2X7 (w zależności od eksperymentu ATP lub BzATP w odpowiednich stężeniach). Pomiar spektrofluorymetryczny prowadzono przez 60 minut przy długościach fali wzbudzenia λ=530 nm i emisji λ=590 nm.

3.3 Ocena zmiany wrażliwości na ligandy receptorów purynergicznych

Analizy zmian żywotności komórek kontrolnych i różnicowanych poddanych działaniu ligandów receptorów sygnalizacji purynergicznej zostały przeprowadzone przy użyciu testu MTT. Komórki były inkubowane przez 24, 48 i 72 godziny z różnymi agonistami receptorów purynergicznych (adenozyna, ADP, ATP) w zakresie stężeń od 0 do 500 μM oraz z BzATP, specyficznym agonistą receptora P2X7 w zakresie stężeń od 0 do 100 μM. Dodatkowo komórki były inkubowane z 1 μM A740003 – specyficznym antagonistą receptora P2X7 oraz 100 μM BGO – inhibitorem zewnątrzkomórkowych enzymów metabolizujących nukleotydy. Po zakończeniu traktowania, komórki były inkubowane przez 30 minut z 0,5 mg/ml MTT, a po tym czasie osad powstałych kryształów formazanu został rozpuszczony w DMSO. Pomiaru spektrofotometrycznego dokonano przy pomocy czytnika płytek Epoch Take 3, przy długości fali λ=570 nm.

3.4 Wpływ zmian profilu ekspresji izoform receptora P2X7 na aktywację wewnątrzkomórkowych szlaków sygnalizacyjnych

W celu określenia zmian w aktywacji wewnątrzkomórkowego szlaku sygnalizacji PI3K/AKT pod wpływem stymulacji receptora P2X7 przeprowadzono test ELISA. Komórki były inkubowane przez 24 godziny razem z ATP lub BzATP oraz w obecności lub bez A740003. Po tym czasie komórki poddano lizie, a uzyskany lizat wykorzystano do przeprowadzenia testu. Do analiz wykorzystano zestaw „Akt (pS473) + total Akt ELISA Kit", firmy Abcam, zgodnie z instrukcjami producenta. Absorbancję barwnych roztworów, będących rezultatami reakcji, poddano pomiarowi spektrofotometrycznemu przy wykorzystaniu czytnika płytek Epoch Take 3.

3.5 Analiza wpływu ligandów receptora P2X7 na potencjał migracyjny komórek

Wpływ ligandów receptora P2X7 na potencjał migracyjny komórek został zmierzony przy pomocy testu rysy, przeprowadzonym zgodnie z protokołem opisanym w części 2.4. Do komórek w stanie konfluencji, którym wykonano sztuczną rysę dodano ATP/BzATP oraz A740003 w odpowiednich stężeniach. Pomiary wykonywano w czasie 0, 4, 8, 12 oraz 24 godzin od momentu wykonania rysy. Potencjał migracyjny określono jako tempo zmniejszenia pola powierzchni rysy w czasie, względem początkowych rozmiarów rysy.

4. Interakcje elementów sygnalizacji purynergicznej z temozolomidem

4.1 Ocena efektu cytotoksycznego ligandów receptora P2X7 podawanych razem z temozolomidem

Zmiany w poziomie żywotności komórek traktowanych temozolomidem zostały określone przy pomocy testu MTT. W pierwszej kolejności komórki były traktowane temozolomidem z zakresie stężeń 0-1000 μM w celu wyznaczenia parametru EC50 dla tego związku. Następnie komórki były inkubowane z temozolomidem o stężeniu odpowiadającemu EC50 oraz ATP (zakres stężeń 80-500 μM) lub BzATP (zakres stężeń 8-100 μM) przez 72 godziny. Po zakończeniu inkubacji przeprowadzono test MTT, zgodnie z protokołem opisanym w części 3.3.

4.2 Analiza potencjału migracyjnego komórek traktowanych ligandami receptora P2X7 i temozolomidem

Wpływ temozolomidu oraz ligandów receptora P2X7 na potencjał migracyjny komórek określono przy pomocy testu rysy, zgodnie z procedurą opisaną wcześniej w części 2.4.

4.3 Wpływ temozolomidu na funkcjonalność receptora P2X7

Interakcje między temozolomidem a receptorem P2X7 określono przy pomocy technik *in silico* oraz *in vitro*. Analizy *in silico* polegały na wygenerowaniu homologicznego modelu ludzkiego receptora P2X7, a następnie na dokowaniu cząsteczki temolozolomidu do kieszeni wiążącej ligand receptora P2X7. Homolog ludzkiego receptora został stworzony na bazie znanej struktury receptora szczurzego przy pomocy oprogramowania SWISS-MODEL, poprawność otrzymanej struktury została zweryfikowana przy pomocy oprogramowania Procheck, z kolei dokowanie cząsteczki temozolomidu do kieszeni wiążącej przeprowadzono przy pomocy oprogramowania SMINA. Analizy *in vitro* opierały się na teście wychwytu bromku etydyny. Badane komórki były inkubowane w obecności zarówno ligandów receptora P2X7 jak i temozolomidu. Test został przeprowadzony zgodnie z protokołem opisanym w części 3.2.

5. Analizy statystyczne

Przeprowadzone eksperymenty były wykonane w czterech, niezależnych powtórzeniach. Wszelkie analizy statystyczne wykonano w programie Past 4.02. Różnice w poziomie ekspresji genów, potencjale migracyjnym, potencjale proliferacyjnym, między komórkami zróżnicowanymi i niezróżnicowanymi określono przy pomocy testu Mann-Whitney'a. Różnice w potencjale migracyjnym, żywotności komórek, aktywacji szlaków wewnątrzkomórkowych, wychwytu bromku etydyny w analizach z wykorzystaniem ligandów receptora P2X7 przeprowadzono z wykorzystaniem dwustronnego testu ANOVA i testu post-hoc Tukey'a. Różnice były uznawane za istotne statystycznie dla wartości $p \leq 0,05$.

IV Omówienie wyników

1. Charakterystyka komórek glejaka poddanych różnicowaniu kwasem retinowym (Publikacja 2, 3)

Różnicowanie komórek glejaka badanych linii komórkowych z wykorzystaniem kwasu retinowego pozwoliło na pogłębioną charakterystykę i porównanie zmian wywołanych poprzez indukcję różnicowania. Badania mające na celu porównanie wybranych markerów neurogenezy pokazują, że w przypadku linii A172 i M059J dochodzi do znaczącego wzrostu wszystkich testowanych genów, natomiast w przypadku komórek M059K ta tendencja jest odwrotna, gdyż zaobserwowano spadek poziomu ekspresji nestyny i TUJ1. Poziom ekspresji GFAP nie zmienił się w żadnej z trzech badanych linii, co potwierdza brak różnicowania i specjalizacji komórek w kierunku gleju.

Wyniki uzyskane dla wszystkich trzech badanych linii komórek glejaka, pokazują, że różnicowanie komórek w kierunku neuralnym obniża ich potencjał proliferacyjny, znacząco spowalniając tempo podziału komórek. Dodatkowe badania przeprowadzone na komórkach M059J i M059K, mające na celu określenie zmian cyklu komórkowego pod wpływem różnicowania wykazały, że o ile w przypadku komórek M059K znacząco wzrósł procentowy udział komórek w fazie G1, przy obniżeniu ilości komórek w fazie S i G2, tak w przypadku komórek M059J nie zaobserwowano znaczących zmian między komórkami kontrolnymi i różnicowanymi, co sugeruje, że za obniżeniem tempa proliferacji stoi inny mechanizm, niż w komórkach M059K.

Analiza zmian w poziomie ekspresji genów kodujących N-kadherynę i E-kadherynę, przeprowadzona dla komórek M059J i M059K pokazuje, że w przypadku linii M059K na skutek różnicowania wzrasta udział N-kadheryny, natomiast w komórkach M059J poziom ekspresji N-kadheryny nie ulega znaczącym zmianom, jednak dochodzi do zahamowania ekspresji E-kadheryny. Co ciekawe, choć wysoki poziom N-kadheryny jest utożsamiany z przejściem epitelialno-mezenchymalnym, wyniki testu rysy pokazują, że komórki A172 i M059K na skutek różnicowania znacząco obniżyły swój potencjał migracyjny, natomiast komórki M059J są komórkami o małym potencjale migracyjnym i proces różnicowania nie zmienił znacząco tych właściwości.

Tym samym, wykazano, że w wyniku różnicowania otrzymano linie komórkowe, które mimo różnych odpowiedzi na neurogenne działanie kwasu retinowego, cechowały się niskim tempem proliferacji i niewielkim potencjałem migracyjnym. Wywołane

kwasem retinowym zmiany fenotypowe w komórkach glejaka stały się punktem wyjścia do drugiej części badań, gdzie sprawdzono jak proces różnicowania wpływa na zmiany systemu sygnalizacji purynergicznej w celu wzmocnienia wstępnie zaindukowanego efektu przeciwnowotworowego.

2. Zmiany w systemie sygnalizacji purynergicznej pod wpływem różnicowania (Publikacja 2, 3)

Hipoteza projektu zakładała, że proces różnicowania może wpłynąć na zmiany w homeostazie systemu sygnalizacji purynergicznej. W pierwszej kolejności określono jakie zmiany zachodzą w środowisku zewnątrzkomórkowym. Oznaczenie aktywności zewnątrzkomórkowych enzymów metabolizujących nukleotydy wykazało, że enzymami, które mają największy udział w utrzymaniu zewnątrzkomórkowej homeostazy nukleotydowej w komórkach niezróżnicowanych są kinaza adenylanowa oraz ekto-5'-nukleotydaza. Po 14-dniowym okresie różnicowania zaobserwowano znaczny spadek aktywności enzymów we wszystkich trzech badanych liniach, przy czym kinaza adenylanowa pozostała dominującym enzymem w przypadku komórek A172. Z drugiej strony jej aktywność całkowicie zanikła w komórkach linii M059J, gdzie dominującym enzymem była ekto-5'-nukleotydaza, natomiast w przypadku linii M059K dominowały NTPDazy/NPPazy metabolizujące ATP. Rezultaty te korelują z wynikami uzyskanymi w analizie RT-qPCR, które wskazały, że poziom ekspresji genów kodujących NTPDazę 5, NTPDazę 6, kinazę adenylanową oraz ekto-5'-nukleotydazę spadał w komórkach zróżnicowanych. Obniżone aktywności enzymów metabolizujących nukleotydy prowadzą do zaburzenia homeostazy nukleotydowej w mikrośrodowisku nowotworu, a tym samym implikują zmiany cytofizjologii komórek glejaka, dlatego następnym etapem było określenie czy dochodzi do zmian również w poziomie ekspresji receptorów purynergicznych.

Analiza zmian poziomu ekspresji receptora P2X7 (na poziomie genu i białka) wykazała, że na skutek różnicowania w komórkach wszystkich trzech linii wzrasta ilość receptora P2X7. Co więcej, badania poświęcone izoformom receptora, przeprowadzone na liniach M059K i M059J wykazały, że na poziomie ekspresji genu dominującym wariantem w komórkach jest izoforma P2X7A, a tendencja ta utrzymuje się również po różnicowaniu. Wyniki metody Western blot dla komórek tych linii pokazały z kolei, że izoforma P2X7A jest dominująca względem P2X7B w obu liniach, jednak pod wpływem

różnicowania przewaga ta zmniejsza się, co mogłoby sugerować, że zmniejszy się liczba funkcjonalnych receptorów formujących por.

Przeprowadzone badania funkcjonalności receptora, polegające na pomiarze wychwytu bromku etydyny przez komórki traktowane ligandami receptora P2X7, wykazały, że we wszystkich badanych liniach komórkowych proces różnicowania prowadzi do zwiększenia efektywności otwarcia poru w błonie komórkowej, co pokrywa się ze zwiększeniem ilości receptorów P2X7A zdolnych do otwarcia poru.

Powyższe wyniki pokazują, że pod wpływem kwasu retinowego wykreowano mikrośrodowisko guza, w którym enzymy degradujące ATP obniżyły swoją aktywność, co pozwala cząsteczkom ATP dłużej utrzymywać się w przestrzeni zewnątrzkomórkowej. Jednocześnie wrażliwy na ATP receptor P2X7 występuje w zwiększonej ilości, a jego dominującą izoformą w tych warunkach jest P2X7A, której aktywacja prowadzi do apoptozy komórek, dlatego w kolejnym etapie zbadano możliwość wzmocnienia tego przeciwnowotworowego potencjału proapoptotycznego wykorzystując ligandy receptora P2X7.

Uzyskane wyniki wykazały, że agoniści receptora P2X7, ATP oraz BzATP, znacząco zwiększyli cytotoksyczne działanie w różnicowanych komórkach wszystkich badanych linii. W przypadku różnicowanych komórek linii A172 już 10 μM ATP i 10 μM BzATP wywołały obniżenie żywotności komórek do około 30%. Niezróżnicowane komórki niezróżnicowane były praktycznie niewrażliwe na ATP i BzATP w badanym zakresie stężeń. Zróżnicowane komórki M059K były wrażliwe na 100 μM ATP i 100 μM BzATP, mimo, że niezróżnicowane komórki tej linii wykazały wrażliwość dopiero na bardzo wysokie (1 mM) stężenia ATP, natomiast dla BzATP nie udało się osiągnąć efektu cytotoksycznego w testowanym zakresie stężeń. Komórki M059J wykazały najmniejsze zmiany wrażliwości na ligandy receptora P2X7 po różnicowaniu, ponieważ spadek żywotności do 50% w obu wariantach zaobserwowano w obecności ATP o stężeniu 1000 μM i około 100 μM BzATP. Co jednak istotne, dla każdej z testowanych linii, efekt cytotoksyczny był częściowo znoszony w obecności A740003, specyficznego antagonisty receptora P2X7, co potwierdziło przypuszczenia, że efekt cytotoksyczny jest w znacznej mierze modulowany przez aktywację receptora P2X7.

Sprawdzono również, jak obecność ligandów receptorów purynergicznych w środowisku zewnątrzkomórkowym wpłynie na potencjał migracyjny komórek. Uzyskane wyniki pokazują, że w większości testowanych wariantów ligandy receptora

P2X7 nie wpływają na tempo migracji komórek, jednak w przypadku niezróżnicowanych komórek A172 i M059K, czyli komórek o najwyższym potencjale migracyjnym, zaobserwowano, że dodanie 100 μM ATP lub 10 μM BzATP do środowiska zewnątrzkomórkowego obniża tempo migracji o ok. 20% w przypadku komórek A172 i o ok. 33% w przypadku komórek M059K.

Ponieważ wykazano, że pod wpływem różnicowania zmienia się stosunek izoform P2X7A/B, założono, że ta zmiana może mieć wpływ na aktywację wewnątrzkomórkowego szlaku sygnalizacyjnego PI3K/AKT. Uzyskane wyniki wskazują jednak, że niezależnie od zmian w stosunku izoform P2X7A do P2X7B, białka zaangażowane we wtórne przekazywanie sygnału w szlaku PI3K/AKT ściśle związanym z proliferacją komórek nie są w sposób istotny bardziej fosforylowane w porównaniu do komórek niestymulowanych ligandami, niezależnie od poziomu zróżnicowania. Oznacza to, że to dominująca izoforma receptora P2X7, a nie ich bezwzględny stosunek jest czynnikiem decydującym o aktywacji wewnątrzkomórkowych szlaków sygnałowych.

3. Interakcje receptora P2X7 z temozolomidem (Publikacja 2)

Ostatnim etapem badań było określenie jak proces różnicowania i indukowane zmiany w systemie sygnalizacji purynergicznej wpłyną na wrażliwość komórek na chemoterapeutyki. W tym celu porównano efekt cytotoksyczny temozolomidu między komórkami kontrolnymi i zróżnicowanymi. Wykazano, że na skutek procesu różnicowania obniża się wartość EC50 (z 500 μM do 125 μM), co świadczy o zwiększeniu wrażliwości komórek glejaka na ten chemoterapeutyk. Dodatkowo, badania podczas których jednocześnie podawano do komórek temozolomid, w stężeniu odpowiadającym parametrowi EC50, oraz ATP i BzATP w zakresie stężeń odpowiednio od 80 do 500 μM i od 8 do 100 μM wykazały, że obecność agonistów znacząco zwiększa efekt cytotoksyczny, jednocześnie efekt ten został zniesiony w obecności A740003, co ponownie potwierdziło, że efekt ten jest modulowany przez receptor P2X7.

Eksperymenty *in silico* pozwoliły na uzyskanie wysokiej jakości homologicznego receptora P2X7, o odwzorowanej strukturze kieszeni wiążącej ligand. Testy polegające na molekularnym dokowaniu BzATP, ATP a także temozolomidu i jego metabolitu – MTIC wykazały, że struktura TMZ wykazuje powinowactwo do kieszeni wiążącej ligand i może nawiązywać z nią interakcje. Chociaż wartość energii swobodnej takiego wiązania jest wyższa od naturalnego liganda jakim jest ATP, co świadczy o niższym

powinowactwie, to w przypadku, gdy w mikrośrodowisku guza stężenie TMZ przewyższa ATP, może dochodzić do konkurencji o miejsce wiązania.

Testy *in vitro* potwierdziły to założenie, ponieważ doświadczenie z wychwytem bromku etydyny w warunkach jednoczesnej obecności ligandów receptora P2X7 (ATP lub BzATP) oraz TMZ powodowały zmniejszenie napływu EtBr w porównaniu do wariantu, w którym komórki były stymulowane samym agonistą receptora. Uzyskane wyniki świadczą o negatywnym oddziaływaniu TMZ na receptor P2X7 sugerując jego antagonistyczną naturę względem receptora. Wyniki te sugerują również, że możliwe jest zwiększenie dostępności TMZ dla komórek i efektywności jego przeciwnowotworowego działania przy jednoczesnym zastosowaniu ATP (lub BzATP) w stężeniu pozwalającym na otwarcie poru receptora P2X7.

V Podsumowanie i wnioski

Przeprowadzone w niniejszej pracy badania rozszerzają wiedzę na temat zmian zachodzących w komórkach glejaka pod wpływem indukowanego różnicowania w kierunku neuralnym i po raz pierwszy zwracają uwagę na zmiany zachodzące w systemie sygnalizacji purynergicznej.

Podsumowując, uzyskane wyniki dowodzą, że:

- Proces indukowanego różnicowania obniża potencjał proliferacyjny i migracyjny komórek glejaka;
- Pod wpływem różnicowania dochodzi do obniżenia aktywności zewnątrzkomórkowych enzymów metabolizujących zewnątrzkomórkowe nukleotydy oraz podwyższenia ekspresji receptora P2X7;
- W efekcie różnicowania dochodzi do zwiększenia cytotoksycznego działania zewnątrzkomórkowego ATP, które jest modulowane przez receptor P2X7;
- Mimo wzrostu poziomu ekspresji izoformy P2X7B, ilościowa przewaga izoformy P2X7A decyduje o aktywacji wewnątrzkomórkowych szlaków PI3K/AKT;
- Pod wpływem różnicowania dochodzi także do zwiększenia dostępności i działania anty-nowotworowego temozolomidu, a efekt cytotoksyczny jest dodatkowo wzmacniany przez obecność ligandów receptorów purynergicznych;
- Strukturalne podobieństwo temozolomidu do naturalnych agonistów receptora P2X7 umożliwia interakcję tego związku z kieszenią wiążącą ligand receptora i działania TMZ jako antagonisty receptora.

Wyniki wskazują, że różnicowanie kwasem retinowym w połączeniu z kontrolą sygnalizacji purynergicznej w mikrośrodowisku nowotworu posiadają potencjał jako terapia wspierająca do obecnie stosowanych kuracji przeciwnowotworowych. Dodatkowo, możliwość wpływania na poziom ekspresji izoform receptora P2X7 i jego warunkowa oraz miejscowo specyficzna aktywacja jest obiecującym celem terapeutycznym.

VI Literatura

1 Stupp R, Brada M, van den Bent MJ, Tonn JC, Pentheroudakis G. High-grade glioma: ESMO Clinical Practice Guidelines for diagnosis, treatment and follow-up. *Ann. Oncol. Off. J. Eur. Soc. Med. Oncol.* 25 Suppl 3, 93–101 (2014).

2 Kim HJ, Park JW, Lee JH. Genetic Architectures and Cell-of-Origin in Glioblastoma. *Front. Oncol.* 10, 615400 (2021).

3 Brada M, Stenning S, Gabe R *et al.* Temozolomide versus procarbazine, lomustine, and vincristine in recurrent high-grade glioma. *J. Clin. Oncol.* 28(30), 4601–4608 (2010).

4 Zhang J, F.G. Stevens M, D. Bradshaw T. Temozolomide: Mechanisms of Action, Repair and Resistance.

5 Vredenburgh JJ, Desjardins A, Reardon DA, Friedman HS. Experience with irinotecan for the treatment of malignant glioma. *Neuro. Oncol.* 11(1), 80–91 (2009).

6 Taal W, Bromberg JEC, Bent MJ Van Den. CNS Oncology Chemotherapy in glioma. *CNS Oncol.* 4(3), 179–192 (2015).

7 Ramalho MJ, Andrade S, Coelho MÁN, Loureiro JA, Pereira MC. Biophysical interaction of temozolomide and its active metabolite with biomembrane models: The relevance of drug-membrane interaction for Glioblastoma Multiforme therapy. *Eur. J. Pharm. Biopharm.* 136(August 2018), 156–163 (2019).

8 Ostermann S, Csajkag C, Buclin T *et al.* Plasma and Cerebrospinal Fluid Population Pharmacokinetics of Temozolomide in Malignant Glioma Patients. *Clin. Cancer Res.* 10(11), 3728–3736 (2004).

9 Bae SH, Park MJ, Lee MM *et al.* Toxicity profile of temozolomide in the treatment of 300 malignant glioma patients in Korea. *J. Korean Med. Sci.* 29(7), 980–984 (2014).

10 Lee SY. Temozolomide resistance in glioblastoma multiforme. *Genes Dis.* 3(3), 198–210 (2016).

11 Dreyfus M, El-Atifi M, Court M *et al.* Reprogramming glioma cell cultures with retinoic acid: Additional arguments for reappraising the potential of retinoic acid in the context of personalized glioma therapy. *Glioma* 1(2), 66 (2018).

12 Mahony S, Mazzoni EO, McCuine S, Young RA, Wichterle H, Gifford DK. Ligand-dependent dynamics of retinoic acid receptor binding during early neurogenesis. *Genome Biol.* 12(1), 1–15 (2011).

13 Rodriguez VW, Bailey R, Gilbert M. Abstract 2900: Sumoylation of the retinoic acid receptor alpha protein represses transcriptional activity and contributes to retinoic acid resistance in glioma stem cells. *Cancer Res.* 76(14_Supplement), 2900–2900 (2016).

14 Campos B, Weisang S, Osswald F *et al.* Retinoid resistance and multifaceted impairment of retinoic acid synthesis in glioblastoma. *Glia* 63(10), 1850–1859 (2015).

15 Liu RZ, Li S, Garcia E *et al.* Association between cytoplasmic CRABP2, altered retinoic acid signaling, and poor prognosis in glioblastoma. *Glia* 64(6), 963–976 (2016).

16 See SJ, Levin VA, Yung WKA, Hess KR, Groves MD. 13-cis-Retinoic acid in the treatment of recurrent glioblastomamultiforme. *Neuro. Oncol.* 6(3), 253–258 (2004).

17 Wismeth C, Hau P, Fabel K *et al.* Maintenance therapy with 13-cis retinoid acid in high-grade glioma at complete response after first-line multimodal therapy - A phase-II study. *J. Neurooncol.* 68(1), 79–86 (2004).

18 Shi Z, Lou M, Zhao Y, Zhang Q, Cui D, Wang K. Effect of all-trans retinoic acid on the differentiation of u87 glioma stem/progenitor cells. *Cell. Mol. Neurobiol.* 33(7), 943–951 (2013).

19 Wang R, Liu C. All-trans retinoic acid therapy induces asymmetric division of glioma stem cells from the U87MG cell line. *Oncol. Lett.* 18(4), 3646–3654 (2019).

20 Liang C, Yang L, Guo S. All-trans retinoic acid inhibits migration, invasion and proliferation, and promotes apoptosis in glioma cells in vitro. *Oncol. Lett.* 9(6), 2833–2838 (2015).

21 Burnstock G. Purinergic Nerves. *Pharmacol. Rev.* 24(3) (1972).

22 Abbracchio MP, Burnstock G. Purinoceptors: Are there families of P2X and P2Y purinoceptors? *Pharmacol. Ther.* 64(3), 445–475 (1994).

23 Porowinska D, Czarnecka J, Komoszynski M. Rola enzymów metabolizujących ektonukleotydy w sygnalizacji z udziałem puryn. *Postepy Biochem.* 57(3) (2011).

24 Peleli M, Fredholm BB, Sobrevia L, Carlström M. Pharmacological targeting of adenosine receptor signaling. *Mol. Aspects Med.* 55, 4–8 (2017).

25 Von Kügelgen I, Hoffmann K. Pharmacology and structure of P2Y receptors. *Neuropharmacology* 104, 50–61 (2016).

26 North RA. P2X receptors. *Philos. Trans. R. Soc. B Biol. Sci.* 371(1700) (2016).

27 Sluyter R. The P2X7 Receptor. *Adv. Exp. Med. Biol.* 1051, 17–53 (2017).

28 Robson SC, Sévigny J, Zimmermann H. The E-NTPDase family of ectonucleotidases: Structure function relationships and pathophysiological significance. *Purinergic Signal.* 2(2), 409–430 (2006).

29 Stefan C, Jansen S, Bollen M. NPP-type ectophosphodiesterases: Unity in diversity. *Trends Biochem. Sci.* 30(10), 542–550 (2005).

30 Sträter N. Ecto-5′-nucleotidase: Structure function relationships. *Purinergic Signal.* 2(2), 343–350 (2006).

31 Burnstock G. Pathophysiology and Therapeutic Potential of Purinergic Signaling. *Pharmacol. Rev.* 58(1), 58–86 (2006).

32 Burnstock G, Di Virgilio F. Purinergic signalling and cancer. *Purinergic Signal.* 9(4), 491–540 (2013).

33 Adinolfi E, De Marchi E, Grignolo M, Szymczak B, Pegoraro A. The P2X7 Receptor in Oncogenesis and Metastatic Dissemination: New Insights on Vesicular Release and Adenosinergic Crosstalk. *Int. J. Mol. Sci.* 24(18) (2023).

34 Lara R, Adinolfi E, Harwood CA *et al.* P2X7 in Cancer: From Molecular Mechanisms to Therapeutics. *Front. Pharmacol.* 11(June) (2020).

35 Di Virgilio F. P2X7 is a cytotoxic receptor….maybe not: implications for cancer.

Purinergic Signal. 17(1), 55–61 (2021).

36 Sarti AC, Vultaggio-Poma V, Di Virgilio F. P2X7: a receptor with a split personality that raises new hopes for anti-cancer therapy. *Purinergic Signal.* 17(2), 175–178 (2021).

37 Virginio C, Mackenzie A, North RA, Surprenant A. Kinetics of cell lysis, dye uptake and permeability changes in cells expressing the rat P2X7 receptor. *J. Physiol.* 519(Pt 2), 335 (1999).

38 North RA. Molecular physiology of P2X receptors. *Physiol. Rev.* 82(4), 1013–1067 (2002).

39 Koles L, Furst S, Illes P. Purine Ionotropic (P2X) Receptors. *Curr. Pharm. Des.* 13(23), 2368–2384 (2007).

40 Di Virgilio F, Schmalzing G, Markwardt F. The Elusive P2X7 Macropore. *Trends Cell Biol.* 28(5), 392–404 (2018).

41 Zanoni M, Sarti AC, Zamagni A *et al.* Irradiation causes senescence, ATP release, and P2X7 receptor isoform switch in glioblastoma. *Cell Death Dis. 2022 131* 13(1), 1–14 (2022).

42 Pegoraro A, De Marchi E, Adinolfi E. P2X7 Variants in Oncogenesis. *Cells 2021, Vol. 10, Page 189* 10(1), 189 (2021).

43 Adinolfi E, Cirillo M, Woltersdorf R *et al.* Trophic activity of a naturally occurring truncated isoform of the P2X7 receptor. *FASEB J.* 24(9), 3393–3404 (2010).

44 Giuliani AL, Colognesi D, Ricco T *et al.* Trophic Activity of Human P2X7 Receptor Isoforms A and B in Osteosarcoma. *PLoS One* 9(9), e107224 (2014).

45 Feng YH, Li X, Zeng R, Gorodeski GI. Endogenously Expressed Truncated P2X7 Receptor Lacking the C-Terminus is Preferentially Upregulated in Epithelial Cancer Cells and Fails to Mediate Ligand-Induced Pore Formation and Apoptosis. *Nucleosides, Nucleotides and Nucleic Acids* 25(9–11), 1271–1276 (2006).

46 Pan H, Ni H, Zhang LL *et al.* P2RX7-V3 is a novel oncogene that promotes tumorigenesis in uveal melanoma. *Tumor Biol.* 37(10), 13533–13543 (2016).

47 Pegoraro A, Orioli E, De Marchi E *et al.* Differential sensitivity of acute myeloid leukemia cells to daunorubicin depends on P2X7A versus P2X7B receptor expression. *Cell Death Dis. 2020 1110* 11(10), 1–12 (2020).

48 Pegoraro A, De Marchi E, Ferracin M *et al.* P2X7 promotes metastatic spreading and triggers release of miRNA-containing exosomes and microvesicles from melanoma cells. *Cell Death Dis. 2021 1212* 12(12), 1–12 (2021).

49 Arnaud-Sampaio VF, Bento CA, Glaser T, Adinolfi E, Ulrich H, Lameu C. P2X7 receptor isoform B is a key drug resistance mediator for neuroblastoma. *Front. Oncol.* 12 (2022).

50 Song H, Arredondo Carrera HM, Sprules A *et al.* C-terminal variants of the P2X7 receptor are associated with prostate cancer progression and bone metastasis – evidence from clinical and pre-clinical data. *Cancer Commun.* 43(3), 400 (2023).

51 Zhu X, Li Q, Song W, Peng X, Zhao R. P2X7 receptor: a critical regulator and potential target for breast cancer. *J. Mol. Med.* 99(3), 349–358 (2021).

52 Giuliani AL, Colognesi D, Ricco T *et al.* Trophic Activity of Human P2X7 Receptor Isoforms A and B in Osteosarcoma. *PLoS One* 9(9), e107224 (2014).

53 Roliano GG, Azambuja JH, Brunetto VT, Butterfield HE, Kalil AN, Braganhol E. Colorectal Cancer and Purinergic Signalling: An Overview. *Cancers 2022, Vol. 14, Page 4887* 14(19), 4887 (2022).

54 Hill LM, Gavala ML, Lenertz LY, Bertics PJ. Extracellular ATP May Contribute to Tissue Repair by Rapidly Stimulating Purinergic Receptor X7-Dependent Vascular Endothelial Growth Factor Release from Primary Human Monocytes. *J. Immunol.* 185(5), 3028–3034 (2010).

55 Sheng G, Gao Y, Ding Q *et al.* P2RX7 promotes osteosarcoma progression and glucose metabolism by enhancing c-Myc stabilization. *J. Transl. Med.* 21(1), 1–23 (2023).

56 Gu LQ, Li FY, Zhao L *et al.* Association of XIAP and P2X7 receptor expression with lymph node metastasis in papillary thyroid carcinoma. *Endocrine* 38(2), 276–282 (2010).

57 Rodrigues RJ, Tomé AR, Cunha RA. ATP as a multi-target danger signal in the brain. *Front. Neurosci.* 9(APR), 138219 (2015).

58 Tattersall L, Shah KM, Lath DL *et al.* The P2RX7B splice variant modulates osteosarcoma cell behaviour and metastatic properties. *J. bone Oncol.* 31 (2021).

59 Pegoraro A, De Marchi E, Ferracin M *et al.* P2X7 promotes metastatic spreading and triggers release of miRNA-containing exosomes and microvesicles from melanoma cells. *Cell Death Dis.* 12(12) (2021).

60 Lombardi M, Gabrielli M, Adinolfi E, Verderio C. Role of ATP in Extracellular Vesicle Biogenesis and Dynamics. *Front. Pharmacol.* 12, 654023 (2021).

61 Vultaggio-Poma V, Falzoni S, Chiozzi P *et al.* Extracellular ATP is increased by release of ATP-loaded microparticles triggered by nutrient deprivation. *Theranostics* 12(2), 859 (2022).

62 Adinolfi E, De Marchi E, Grignolo M, Szymczak B, Pegoraro A. The P2X7 Receptor in Oncogenesis and Metastatic Dissemination: New Insights on Vesicular Release and Adenosinergic Crosstalk. *Int. J. Mol. Sci. 2023, Vol. 24, Page 13906* 24(18), 13906 (2023).

63 Randic T, Magni S, Philippidou D *et al.* Single-cell transcriptomics of NRAS-mutated melanoma transitioning to drug resistance reveals P2RX7 as an indicator of early drug response. *Cell Rep.* 42(7), 112696 (2023).

64 Ma Y, Adjemian S, Yang H *et al.* ATP-dependent recruitment, survival and differentiation of dendritic cell precursors in the tumor bed after anticancer chemotherapy. *Oncoimmunology* 2(6) (2013).

65 Benzaquen J, Dit Hreich SJ, Heeke S *et al.* P2RX7B is a new theranostic marker for lung adenocarcinoma patients. *Theranostics* 10(24), 10849–10860 (2020).

66 Adinolfi E, Capece M, Franceschini A *et al.* Accelerated tumor progression in mice lacking the ATP receptor P2X7. *Cancer Res.* 75(4), 635–644 (2015).

67 De Marchi E, Pegoraro A, Turiello R, Di Virgilio F, Morello S, Adinolfi E. A2A Receptor Contributes to Tumor Progression in P2X7 Null Mice. *Front. Cell Dev. Biol.* 10, 876510 (2022).

68 Tran B, Rosenthal MA. Survival comparison between glioblastoma multiforme and other incurable cancers. *J. Clin. Neurosci.* 17(4), 417–421 (2010).

69 Batash R, Asna N, Schaffer P, Francis N, Schaffer M. Glioblastoma Multiforme, Diagnosis and Treatment; Recent Literature Review. *Curr. Med. Chem.* 24(27) (2017).

Publikacja 1

The P2X7 receptor in oncogenesis and metastatic dissemination: New insights on vesicular release and adenosinergic crosstalk

Autorzy: Adinolfi, E., De Marchi, E., Grignolo, M., **Szymczak, B.,** & Pegoraro, A.

Rok publikacji: 2023

DOI: https://doi.org/10.3390/ijms241813906

Artykuł wydany w czasopiśmie: International Journal of Molecular Sciences

Wydawnictwo: MDPI

Punktacja według wykazu Ministerstwa Nauki i Szkolnictwa Wyższego (2023): 140 pkt

Journal Impact Factor (2023): 4,9 pkt

Liczba cytowań: 4 (Web of Science, stan na 09.2024);

5 (Google Scholar, stan na 09.2024)

International Journal of
Molecular Sciences

MDPI

Review

The P2X7 Receptor in Oncogenesis and Metastatic Dissemination: New Insights on Vesicular Release and Adenosinergic Crosstalk

Elena Adinolfi [1,*], Elena De Marchi [1], Marianna Grignolo [1], Bartosz Szymczak [2] and Anna Pegoraro [1]

[1] Section of Experimental Medicine, Department of Medical Sciences, University of Ferrara, 44121 Ferrara, Italy; elena.demarchi@unife.it (E.D.M.); marianna.grignolo@unife.it (M.G.); anna.pegoraro@unife.it (A.P.)
[2] Department of Biochemistry, Faculty of Biological and Veterinary Sciences, Nicolaus Copernicus University in Torun, 87-100 Torun, Poland; b_szymczak@doktorant.umk.pl
* Correspondence: elena.adinolfi@unife.it; Tel.: +39-(0)-532-455445

Abstract: The tumor niche is an environment rich in extracellular ATP (eATP) where purinergic receptors have essential roles in different cell subtypes, including cancer, immune, and stromal cells. Here, we give an overview of recent discoveries regarding the role of probably the best-characterized purinergic receptor in the tumor microenvironment: P2X7. We cover the activities of the P2X7 receptor and its human splice variants in solid and liquid cancer proliferation, dissemination, and crosstalk with immune and endothelial cells. Particular attention is paid to the P2X7-dependent release of microvesicles and exosomes, their content, including ATP and miRNAs, and, in general, P2X7-activated mechanisms favoring metastatic spread and niche conditioning. Moreover, the emerging role of P2X7 in influencing the adenosinergic axis, formed by the ectonucleotidases CD39 and CD73 and the adenosine receptor A2A in cancer, is analyzed. Finally, we cover how antitumor therapy responses can be influenced by or can change P2X7 expression and function. This converging evidence suggests that P2X7 is an attractive therapeutic target for oncological conditions.

Keywords: P2X7; ATP; cancer; metastasis; exosomes; microvesicles

Citation: Adinolfi, E.; De Marchi, E.; Grignolo, M.; Szymczak, B.; Pegoraro, A. The P2X7 Receptor in Oncogenesis and Metastatic Dissemination: New Insights on Vesicular Release and Adenosinergic Crosstalk. *Int. J. Mol. Sci.* **2023**, *24*, 13906. https://doi.org/10.3390/ijms241813906

Academic Editor: Eric Huet

Received: 3 August 2023
Revised: 1 September 2023
Accepted: 5 September 2023
Published: 9 September 2023

1. Extracellular ATP and Its Receptors in the Tumor Microenvironment

Extracellular ATP (eATP) is an established tumor microenvironment (TME) component that can be released following tumor and adjacent tissue necrosis via active release, mediated by proteins such as those of the ABC cassette family, or inside vesicles released from the tumor, immune, and stroma cells [1,2] (Figure 1). The live measurement of eATP in murine models was made possible by the development of the luciferase-based probe pmeLUC that, thanks to its specific placement at the extracellular facet of the plasma membrane, allows for distinguishing it from intracellular ATP [3–5]. Several studies, taking advantage of either pmeLUC or similar probes, have demonstrated eATP abundance in the TME, and that different treatments, including chemotherapy and caloric restriction, can affect its levels [6–9]. These data led Kamata-Sakurai and colleagues to develop a CD137 targeting antibody endowed with an ATP binding domain allowing for its specific release only at tumor sites, thus preventing systemic drug toxicity [10]. eATP is the natural ligand of two families of purinergic receptors: ionotropic P2Xs and metabotropic P2Ys [11]. Both classes of proteins are expressed at different levels by the cells of the TME and activate signaling pathways favoring growth, invasion, angiogenesis, and chemotherapy resistance, but also regulate, in a tumor-promoting or tumor-eradicating fashion, the immune system [1,2,12,13]. This overview focuses on the role of probably the most studied ATP receptor in cancer: P2X7. Converging evidence supports the view that P2X7 is the receptor for eATP most heavily involved in tumor–host interactions [14]. In the TME, ligands and receptors are involved in a positive feedback loop as eATP ligates P2X7 and triggers P2X7-mediated responses, among which is release of ATP; therefore, P2X7 can upregulate the concentration of its agonist [15]. Here, we cover the involvement of P2X7 in cancer growth,

neovascularization, interactions with the immune system, and metastasis, concentrating on recent discoveries related to the release of miRNA-containing vesicles and the crosstalk among P2X7/CD39/CD73 and A2A receptors.

2. The P2X7 Receptor and Its Splice Variants

The P2X7 receptor is a low-affinity ATP-gated channel mediating, upon ligand engagement, the cellular influx of sodium and calcium and the efflux of potassium ions. P2X7-dependent potassium flux is associated with probably the best-known function of the receptor: activation of the NLRP3 inflammasome followed by maturation and secretion of the pro-inflammatory cytokines IL-1β and IL-18 [16–18]. Prolonged stimulation of the P2X7 receptor with high concentrations (mM range) of ATP also mediates the opening of large non-selective macropores permeable to solutes, such as ethidium, propidium, and lucifer yellow [19,20]. Macropore opening is associated with cell death by necrosis, apoptosis, or pyroptosis, depending upon the involved cell type [17,21]. However, basal stimulation of the receptor with subthreshold concentrations of the agonist, such as those in the TME, was also associated with trophic properties [1,22]. The functional P2X7 receptor is a homotrimer [23] formed by subunits of 595 amino acids whose tridimensional structure was recently identified and exploited for identifying and designing new receptor ligands [24–30]. The P2X7 subunit is formed by a short N terminal domain, two transmembrane regions, a large extracellular domain with ligand binding sites, and a long intracellular C terminal tail. The C terminal domain is responsible for macropore formation [31] and interactions with several proteins [32,33]. In humans, the gene for P2X7 is located on chromosome 12 [34]; it is highly polymorphic and, upon alternative splicing, can give rise to several variants [35,36]. The fully functional receptor is termed P2X7A. Among the other splice variants, P2X7B, P2X7H, and P2X7J have also been associated with oncogenic conditions [37–44]. The P2X7B isoform gives rise to a functional ion channel that lacks the pore-forming and apoptotic activity associated with P2X7A [37,45]. The alternative splicing is due to the retention of an intron between exons 10 and 11 of the full-length receptor that determines the addition of 18 extra amino acids after residue 346, followed by a stop codon leading to truncation of the entire C tail [37]. Moreover, when associated with P2X7A in a heterotrimer, P2X7B is a potentiating subunit upregulating both the channel and macropore activity [39,45].

On the contrary, P2X7J does not give rise to a functional protein but behaves as an antagonizing subunit toward P2X7A [38]. P2X7H, also called P2RX7-V3, generates a long non-coding RNA endowed with tumor-promoting activities [40]. Clinical studies with a blocking antibody specifically recognizing the so-called non-functional P2X7 (nfP2X7) [46] have been carried out by the Biosceptre company, showing promising results both in human and feline patients [14,47]. Although, probably for propriety reasons, we do not know the exact nature of the nfP2X7 variant, we do know that it does not entirely lose the channel activity. At the same time, it is not functional as an ion macropore [46]. Recent studies and overviews have addressed the role of alternatively spliced P2X7 isoforms in health and disease—we refer the reader to the literature for further detail on their activity [35,36,48,49].

3. The P2X7 Receptor in Cancer Growth and Immune Responses

The notion that the P2X7 receptor, under particular circumstances (i.e., low ATP concentrations or certain cell types not able to form cytolytic pores), could also exert trophic activity dates back to approximately twenty years ago [22,50,51] when we demonstrated that the receptor upregulates mitochondrial and reticular calcium levels, leading to increased metabolic activity [22,52]. However, many scientists were sceptical about the ability of a cytotoxic receptor to facilitate cancer growth until in vivo proof clearly emerged [53]. Since then, many papers have confirmed P2X7-dependent cancer-promoting activity and associated the expression of the receptor with increased cell metabolism, neovascularization, and, in general, poor patient prognoses [1,14,54–59]. Several solid and liquid cancer types overexpress P2X7, for which P2X7-targeting drugs are potential therapeutic tools; these include acute myeloid and chronic lymphocytic leukemia [9,42,60–63],

melanoma [43,64,65], glioma [66–68], neuroblastoma [41,44,55,69,70] prostate, breast, bone, and colorectal cancer [71–77]. As the above-cited literature demonstrate, P2X7 growth-promoting roles have been covered elsewhere; therefore, its extensive characterization is beyond the scope of the present overview. The wealth of observations on P2X7 in such a plethora of cancers suggest that the receptor acts as a positive regulator of tumor formation and evolution and, therefore, that its pharmacological blockade could be advantageous for oncological patients [14,78]. However, in the TME, P2X7 is expressed not only by cancer cells but also by many components of the innate and cell-mediated immunity, and it plays a role in both pro-inflammatory and tolerogenic responses [12,13]. Indeed, P2X7 activation increases inflammatory responses favoring cancer immune eradication but can even promote tolerance by causing TGF-β release from myeloid-derived suppressor cells (MDSCs) [79]. Hence, the impact of P2X7 on cancer growth versus tumor immune control is complicated. Indeed, we and others demonstrated that a lack of host P2X7, for example in null mice, could favor tumor growth by significantly reducing immune infiltrates and pro-inflammatory cytokines and increasing intratumoral Tregs and adenosinergic pathways related to immune suppression [15,80–84]. However, even in P2X7 null-hosts, when an implanted tumor expresses P2X7, the administration of P2X7 antagonists causes a significant reduction in neoplastic growth accompanied by a substantial increase in $CD4^+$ infiltrates, and also a decrease in the expression of the fitness marker CD73 in Tregs [15]. On the contrary, in tumor models where the expression of P2X7 is mainly restricted to immune cells, a P2X7 positive allosteric modulator, if administered with anti-PD-1 molecules, could prove beneficial [85,86]. Moreover, specific cytokine profiles affected by P2X7 activation could be either antitumoral or tumor-promoting, depending on the TME context [8,87].

This picture is further complicated by the effects that, via P2X7, eATP exerts on different T cell populations, including effector and regulatory T cells, their ability to survive as memory cells, and exhaustion or senescence processes [12,13,88]. For example, two research groups proposed exploiting P2X7 activity in tumor-infiltrating cytotoxic T cells to improve adoptive cell therapy potential, but achieved opposing results [14,89]. Romagani and colleagues suggested that a lack of P2X7 could be beneficial to overcome tumor-infiltrating lymphocyte (TIL) senescence [14]. At the same time, Wanhaimer and collaborators proposed that in the same cellular and tumoral model, P2X7 plays a central role in maintaining the mitochondrial fitness of TILs and controlled activation of the receptor before injection can even increase the antitumoral activity of these lymphocytes [89]. Although these contrasting results could be partially reconciled by the different cytokine cocktails administered to TILs before reinjection [89], they suggest caution when considering the administration of P2X7-targeting compounds in therapeutic settings. In general, a personalized medicine approach with negative or positive allosteric modulators of P2X7, derived from preventive evaluation of the receptor in tumor samples, including cancer and immune cells, would be advisable from our point of view.

4. P2X7 and Metastasis

Metastatic cancer forms still represent one of the leading causes of tumor-related death. Metastasis formation is a multistep process that requires gaining a series of mutations or other acquired abilities from tumor cells that lead to dissemination, local invasion, systemic resistance to immune cells, pre-conditioning, and colonization of secondary sites, also known as the metastatic niche. The advancement of metastasis is strongly influenced by the ability of transformed cancer cells to co-opt the host immune system and transition to distinct states, a fact attributable to their stemness capabilities [90]. Among the first reports relating P2X7 to cancer pathogenesis are those that demonstrated the receptor favoring cancer cell migration and dissemination [91–94] and reported its influence on epithelial–mesenchymal transition (EMT) [95–98]. EMT is a process of cell transdifferentiation originally adopted during embryogenesis and co-opted during metastasis, causing an increase in cancer cell migration linked to loss of cell polarity and down-regulation of adhesion molecules [99]. This mechanism was confirmed as the basis of P2X7-mediated

invasiveness in recent publications covering the negative prognostic role of the receptor in oncological conditions as different as neuroblastoma [44], triple-negative breast cancer [100] and muscle-invasive bladder carcinoma [101]. In addition to EMT, metastasis is favored by signaling pathways and mechanisms implicated in tissue regeneration, wound healing, and adaptation to stress [90] that have been associated with P2X7 activity both in cancer and other physio-pathological conditions [17,53,55,84,96,102–108]. Among those pathways activated by the P2X7 receptor, the HIF1α/VEGF axis is one of the best studied [53,84,109,110]. Moreover, P2X7 is associated with increased Myc expression in cancer [42,111], a condition promoting metastasis by increasing the invasion and survival of cancer cells in the bloodstream [112]. Finally, P2X7 promotes autophagy [17,44,106–108] and unfolded protein responses [113], which help confer metabolic and immune evasive plasticity in solid cancers [90]. Given the involvement of the P2X7 receptor in the aforementioned metastasis-promoting signaling pathways and mechanisms, it is not surprising that overexpression of the receptor was associated with metastatic stages of multiple cancers [43,55,101,114–118]. Accordingly, P2X7 antagonism proved efficacious in reducing the in vivo dissemination of cancer cells in animal models of metastasis [41,43,78,91,92,96,119].

Interestingly, an increasing amount of evidence tends to associate the metastatic properties of P2X7 with its isoform B. As previously mentioned, P2X7B is a splice variant, present only in humans, which retains the calcium channel properties of P2X7 but lacks the activity of the macropore [37]. We first associated the expression of this isoform with increased metabolic activities in HEK293 cells [45] and a stem-like proliferation-associated phenotype in osteosarcoma cells and patients [39]. Subsequently, Lameu and colleagues demonstrated that the metastatic properties conferred by bradykinin treatment to neuroblastoma cells could be reverted by blocking P2X7B [41]. The same authors later confirmed that in the absence of bradykinin, P2X7 isoform B was central in conferring a series of pro-metastatic features to neuroblastoma cells, including the acquisition of a stem-like phenotype, the suppression of autophagy and induction of EMT [44]. These data are in line with those obtained by Tattersall and colleagues who examined osteosarcoma murine models, where they demonstrated that P2X7B expression could reduce cell adhesion, promote invasion, and upregulate a genetic axis, including FN1/LOX/PDGFB/IGFBP3/BMP4 [75]. The same study also proved that P2X7B could increase osteosarcoma's propensity to spread in mouse lungs, and that administration of its antagonist A740003 could abrogate cancer-associated ectopic bone formation [75]. More recently, P2X7B overexpression was also reported in cohorts of metastatic melanoma [43] and prostate cancer patients with bone metastases [76]. In this latest study, Wang and colleagues also suggested that P2X7 truncated variants can double bone skeletal tumors, thus strongly reducing survival in metastatic mice models via a bone tropism-related mechanism, including the production of IL-6 [76].

5. Role of the P2X7 Receptor in Cancer-Associated Vesicle Release

The release of vesicles from cells is an essential process in cell–cell communication during physiological and pathological processes. Extracellular vesicles (EVs) comprise double membranous particles of different sizes and composition. They can derive from the direct budding of cell membrane cell or the fusion of the intraluminal vesicles with the membrane. EVs can carry proteins, lipids, and nucleic acids, thereby affecting microenvironment composition and cell behavior [120]. Moreover, EVs released from cancer cells can promote pre-metastatic niche formation in organs distant from primary tumors [121–123]. Different stimuli can induce the release of vesicles and ATP through its receptors—P2X7 is one such receptor [124] (Figure 1). Activation of the receptor by ATP induces Ca^{2+} influx, eliciting the exocytosis of EVs in the extracellular space [125]. P2X7-dependent release of vesicles was initially demonstrated in immune cells such as macrophages [126,127], dendritic cells [128,129], and microglia [130] (Figure 1).

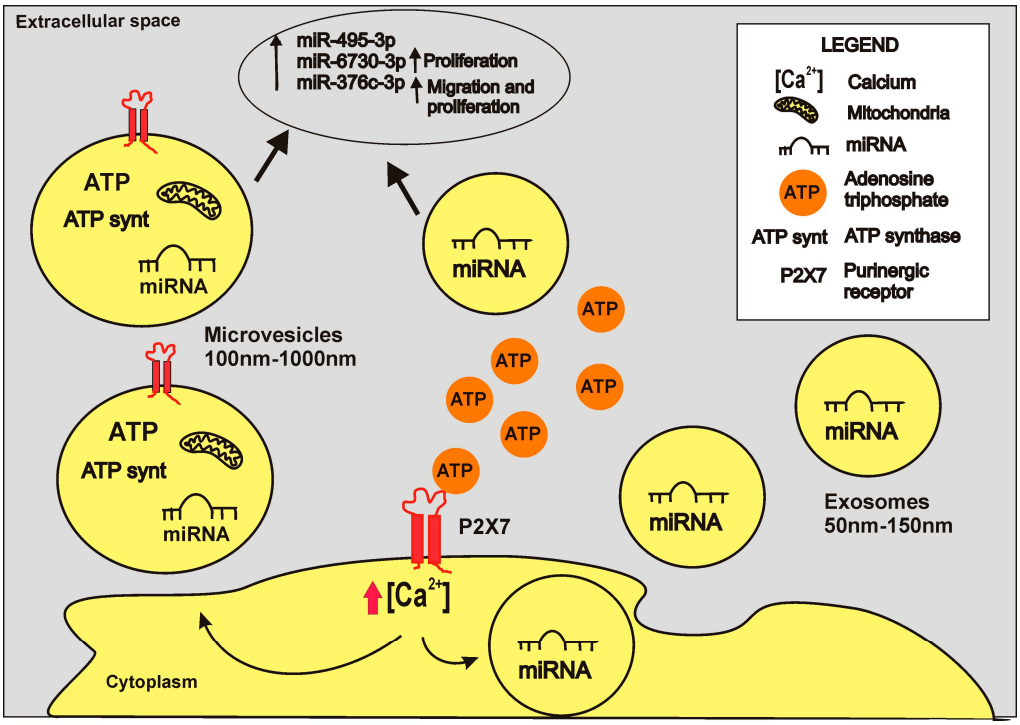

Figure 1. P2X7-dependent vesicle release. Upon ligation with extracellular ATP, P2X7 triggers the release of vesicles of different dimensions and natures from immune, cancer, neuronal, and glial cells. The figure represents vesicles released from tumor cells, including microvesicles/particles ranging in size from 100 to 1000 nm and containing ATP, miRNAs, mitochondria, and ATP synthase [43,58,131], and also exosomes ranging in size from 50 to 150 nm and containing miRNAs [43]. P2X7 activation increases the content of miRNAs, including miR-495-3p, miR-6730-3p, and miR-376c-3p in both vesicular fractions, while antagonism can block their release [43]. Some of these miRNAs have been shown to increase melanoma cells' proliferation and migratory ability [43]. By carrying mitochondria and ectopic ATP synthase, microparticles can produce internal ATP [58,131]. Finally, vesicles also retain P2X7 on their surface, thus possibly facilitating the release of their content in areas rich in eATP.

These vesicles contain inflammatory cytokines and are central players in phlogistic reactions [129,132,133]. In recent years, several studies have focused on this cellular process, demonstrating the release of EVs following P2X7 stimulation from different cancer types, such as neuroblastoma [131,134], lung [131], prostate [135], breast cancers [131,136], and also melanoma [43,58]. EVs contribute to tumor progression, cell migration [43,136], and pre-metastatic niche conditioning [136]. P2X7 activation can induce the release of heterogeneous small and large vesicles [43,131], which different authors have identified as microvesicles, microparticles, exosomes, and oncosomes; therefore, exploring their contents can help to elucidate their biological effects. P2X7 stimulation can induce the release of vesicles containing ATP, thereby increasing its concentration in the TME [58]. ATP is loaded into vesicles thanks to the vesicular nucleotide transporter (VNUT) [137]. However, ATP can also be generated inside EVs in the extracellular environment thanks to glycolytic enzymes located inside the vesicles released from cancer cells [138]. In line with these data, analysis of the content of EVs released upon P2X7 activation demonstrated that they contain other essential players in ATP production: mitochondria [58] and the ectopic ATP synthase [131]. Vesicular ATP can also activate P2X7 in neighboring or distant cells, favoring a positive P2X7-dependent EV release loop [131,134,139]. Additionally, it can support several cellular processes involved in cancer progression, among which cell migration is fundamental for metastatic spread [124,140]. P2X7 can be delivered in vesicles [43,130,137] and, together with ATP, reach distant sites to potentially induce a pro-tumoral microenvironment and metastatic niche formation. The role of P2X7 expressed on the surface of EVs is not clear

yet; however, it is possible to hypothesize that the receptor, via macropore formation, could trigger the release of EV content in eATP-rich areas, such as those associated with inflammation or the TME itself [58]. Together with ATP, other molecules, such as microRNAs (miRNA), are carried by EVs and can potentially modify cell behavior [141]. miRNAs are small non-coding RNA molecules that negatively regulate gene expression. Vesicle miRNA expression changes with cancer types and can promote diverse effects [141]. P2X7, through the interaction with the RNA-binding protein FMR1 can select the miRNA content of small EVs [142]. In line with these data, we demonstrated that microvesicles and exosomes released upon P2X7 stimulation contained a miRNA expression profile profoundly different from vesicles collected from unstimulated cells. Among the miRNAs upregulated in EVs released following P2X7 activation, miR-495-3p, miR-376c-3p, and miR-6730-3p showed proliferation and migration-promoting effects. Treatment of cells with the P2X7 antagonist A740003, before stimulation of EV release, reduced the expression of all three miRNAs [43], thus suggesting P2X7 antagonism as a possible pharmacological strategy to prevent pro-tumoral effects associated with vesicular release.

6. P2X7R and Its Crosstalk with the Adenosinergic Axis in Cancer

Recent data by us and other groups revealed an interplay between P2X7 and the adenosinergic axis formed by ectonucleotidases and adenosine receptors in the TME. This is unsurprising as eATP and its hydrolytic derivative adenosine are constituents of the TME [1]. As mentioned above, in the TME, eATP promotes tumor growth and immune-mediated tumor eradication, mainly via the P2X7 receptor [1]. Adenosine, generated from eATP via CD39 and CD73 ectonucleotidases, is an immune suppressant facilitating tumor escape, acting as an immune cell "don't eat me" signal mainly via its activity at the A2A receptor (A2AR) [84,143–145]. However, the effects of both eATP and adenosine are not limited to immune cells, as often through the same receptors expressed by cancer cells, they can also promote cancer growth, vascularization, and metastasis [56] (Figure 2). To further complicate the picture, the effect of purines on immune cells is not always clearly pro- or antitumoral; for example, both ATP and adenosine are possibly required to produce the primary tumor-eradicating cytokine: IFN-γ [146]. Indeed, ATP and adenosine cooperatively stimulate the upregulation of the major histocompatibility complexes in dendritic cells, thus favoring the activation of T cells designated to IFN-γ secretion [125]. As mentioned above in the TME, the activity of the ectonucleotidases CD39 and CD73 closely controls eATP concentration. P2X7 can interfere with this process by modulating the expression of CD73 and CD39 in cancer-infiltrating immune cells and influencing the level of PD-1 in Tregs [15]. The overexpression of ectonucleotidases is one of the mechanisms causing a reduction in eATP in the TME in tumor-bearing P2X7 null mice [15]. The importance of the crosstalk between P2X7 and CD39 in the TME is further confirmed by the finding that CD39-targeting antibodies require a functional P2X7 receptor in immune cells to work appropriately as antitumoral agents in primary and metastatic murine tumor models [82,83]. These data are further corroborated by a recent study from Casey et al. demonstrating that P2X7 signaling was essential for the favorable effects of CD39 blockade in diffuse large B-cell lymphoma. Indeed, antagonism of CD39 caused an accumulation of eATP that acted on macrophage P2X7, favoring lymphoma cell phagocytosis. eATP-activated P2X7-dependent phagocytosis reinforced the activity of the lymphoma-targeting antibodies rituximab and daratumumab and facilitated therapy resistance [147].

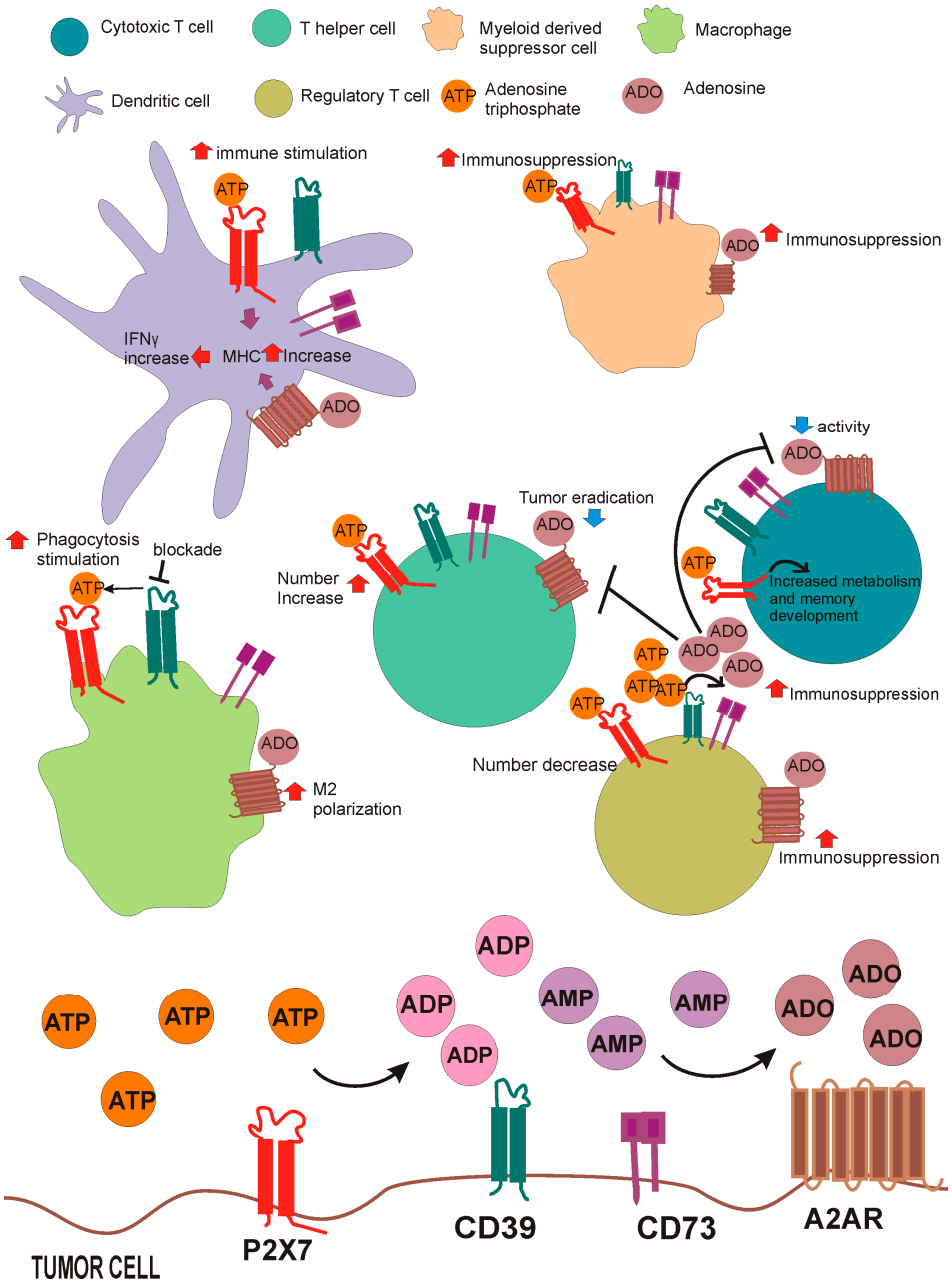

Figure 2. Molecules of the purinergic/adenosinergic axis are expressed by cancer and immune cells in the TME. The TME is rich in eATP due to necrosis and active release of the nucleotide. eATP acts on P2X7 and is then degraded by CD39 and CD73 to adenosine (ADO) acting as the primary source of this purine in the extracellular milieu [1,2]. The P2X7 receptor, the ectonucleotidases CD39 and CD73, and the A2A receptor are expressed by different immune cells involved in both tumor immune-eradication and suppression. In dendritic cells, eATP through P2X7 favors immune stimulation and MHC increase, which are also positively affected by ADO. In macrophages, adenosine sustains M2 polarization, while CD39 blockade, which causes eATP accumulation, stimulates phagocytosis via P2X7. Both eATP and ADO favor myeloid-derived suppressor cell (MDSC) activity [79,144]. ADO, produced in Tregs thanks to CD39/CD73, blocks the proliferation of effector $CD4^+$ and $CD8^+$ T cells via A2AR, contemporarily upregulating immune suppressive activity in Tregs. On the contrary, ATP via P2X7 reduces Treg numbers in tumor infiltrates [15]. P2X7 positively affects tumor infiltration via $CD4^+$ T helper effector cells [15]. ADO via A2AR reduces cytotoxic cell activity [148,149], while P2X7 increases their metabolic activity, thus sustaining responses mediated by memory cells [88].

Recent data from our laboratory and others also point to an interaction between P2X7 and the A2AR in the TME. Indeed, tumors growing in P2X7 null mice overexpressed A2AR [84], possibly due to altered adenosine levels deriving from reduced eATP levels and increased ectonucleotidase activity in the TME [15]. Overexpression of A2AR is not limited to tumors but also affects spleen cells, leading to a systemic immune suppressive phenotype with a significant reduction in circulating IL-1β, TNF-α, IL-6, IL-12, IL-17, and IFN-γ levels, and an increase in TGF-β [84]. Interestingly, inside tumors, A2AR was incremented in necrotic areas, thereby increasing neovascularization, and its blockade caused a substantial reduction in VEGF production in tumor-bearing P2X7 null mice [84]. In a similar vein, a recent study reported upregulation of the P2X7 receptor in melanoma-bearing mice treated with the A2AR antagonist istradefylline [150].

Interestingly, this A2AR blocker increased P2X7 inside the tumors and in lymphoid organs and showed an effect on P2X7 expression even in the absence of cancer [133]. All the described evidence suggests that when developing anti-cancer treatments targeting single components of the P2X7/CD39/CD73/A2AR axis, scientists should consider their effects on the other members of the pathway that might reinforce or impair the efficacy of single protein-targeting drugs. New therapeutic approaches involving multiple targeting strategies could help overcome this issue.

7. P2X7 Receptor in Antitumoral Therapy Resistance

An increasing number of studies have associated P2X7 and its splice variants with either reinforcement or resistance to standard antitumoral therapeutic regimes [2]. eATP levels in the TME may be substantially increased by cytotoxic interventions, such as radio or chemotherapy, while certain antitumoral drugs, such as doxorubicin, daunorubicin, and oxaliplatin were even shown to induce extra release of ATP, which correlated with the onset of immunogenic cell-death-related tumor-eradicating immune responses [8,151]. In this context, opening P2X7A macropores in cancer cells can increase the efficacy of cytotoxic therapies, leading to better prognoses following treatments [42,44,67,152,153]. On the contrary, P2X7B, due to its different gating properties, may be positively selected by eATP and increased in the TME by these treatments, to sustain therapy resistance and relapse [42,44,152]. P2X7-dependent amplification of therapy efficiency was linked to the facilitation of daunorubicin intracellular load in AML blasts [42], increased cytotoxic activity of temozolomide in glioma cells [153], and enhanced differentiating efficacy of retinoic acid in neuroblastoma cells [44]. P2X7A overexpression is also a positive predictor of therapy responses in RAS-mutated melanoma patients, where it is associated with prolonged overall and progression-free survival and in general, early drug responses [65]. In this context, it is envisaged that the administration of positive allosteric modulators of P2X7A, in combination with standard therapy to reinforce their efficacy, can be followed by anti-P2X7B drugs to prevent resistance and relapse after classic therapy cycles [2,42,44,152].

8. Conclusions

Since the first publications proving the direct involvement of the P2X7 receptor in liquid and solid cancer growth [53,60,69], the number of studies analyzing its role in oncogenesis has increased tremendously, reaching more than 700 publications in PubMed (as of August 2023). Both the previous and recent literature strongly suggest that the P2X7 receptor is a suitable therapeutic target for oncological conditions, depending on the type of tumor, the splice variants of the receptor expressed, and the adenosinergic context. Old and recent literature strongly suggest the P2X7 receptor as a suitable therapeutic target in oncologic conditions. Depending on the type of tumor, the splice variants expressed and the adenosinergic context, P2X7 could be exploited to develop new therapeutic strategies based on its antagonism or agonism. Additionally, P2X7 targeting drugs could be or co-administered with traditional or innovative anti-cancer treatments to improve their efficacy. Finally, P2X7-blocking drugs could facilitate the development of novel therapeutic

strategies to block the release of EVs from cancer or immune cells or alter their content to combat their metastasis-promoting activities.

Author Contributions: E.A. and A.P. conceptualized the manuscript. E.A., E.D.M., B.S. and A.P. wrote the original draft. M.G. and E.D.M. prepared the figures. E.A. acquired the funding for publication. All authors have read and agreed to the published version of the manuscript.

Funding: This article is based upon work from PRESTO COST Action CA21130, supported by COST (European Cooperation in Science and Technology) www.cost.eu; www.p2xcost.eu. B.S. took part in a Short Term Mission funded by the Action to visit the laboratory of E.A., during which time he helped prepare this manuscript. E.A. was supported by an Italian Association for Cancer Research (AIRC) grant (IG22837), PUR-THER TRANSCAN-3 JTC2021 Project, and institutional funds from the University of Ferrara.

Conflicts of Interest: The authors declare no conflict of interest. The funders had no role in the interpretation of the data or in the writing of the manuscript.

References

1. Di Virgilio, F.; Sarti, A.C.; Falzoni, S.; De Marchi, E.; Adinolfi, E. Extracellular ATP and P2 purinergic signalling in the tumour microenvironment. *Nat. Rev. Cancer* **2018**, *18*, 601–618. [CrossRef]
2. Zanoni, M.; Pegoraro, A.; Adinolfi, E.; De Marchi, E. Emerging roles of purinergic signaling in anti-cancer therapy resistance. *Front. Cell Dev. Biol.* **2022**, *10*, 1006384. [CrossRef]
3. Pellegatti, P.; Falzoni, S.; Pinton, P.; Rizzuto, R.; Di Virgilio, F. A novel recombinant plasma membrane-targeted luciferase reveals a new pathway for ATP secretion. *Mol. Biol. Cell* **2005**, *16*, 3659–3665. [CrossRef]
4. Pellegatti, P.; Raffaghello, L.; Bianchi, G.; Piccardi, F.; Pistoia, V.; Di Virgilio, F. Increased level of extracellular ATP at tumor sites: In vivo imaging with plasma membrane luciferase. *PLoS ONE* **2008**, *3*, e2599. [CrossRef]
5. De Marchi, E.; Orioli, E.; Pegoraro, A.; Adinolfi, E.; Di Virgilio, F. Detection of Extracellular ATP in the Tumor Microenvironment, Using the pmeLUC Biosensor. *Methods Mol. Biol.* **2020**, *2041*, 183–195. [CrossRef] [PubMed]
6. Michaud, M.; Martins, I.; Sukkurwala, A.Q.; Adjemian, S.; Ma, Y.; Pellegatti, P.; Shen, S.; Kepp, O.; Scoazec, M.; Mignot, G.; et al. Autophagy-dependent anticancer immune responses induced by chemotherapeutic agents in mice. *Science* **2011**, *334*, 1573–1577. [CrossRef]
7. Pietrocola, F.; Pol, J.; Vacchelli, E.; Rao, S.; Enot, D.P.; Baracco, E.E.; Levesque, S.; Castoldi, F.; Jacquelot, N.; Yamazaki, T.; et al. Caloric Restriction Mimetics Enhance Anticancer Immunosurveillance. *Cancer Cell* **2016**, *30*, 147–160. [CrossRef] [PubMed]
8. Lecciso, M.; Ocadlikova, D.; Sangaletti, S.; Trabanelli, S.; De Marchi, E.; Orioli, E.; Pegoraro, A.; Portararo, P.; Jandus, C.; Bontadini, A.; et al. ATP Release from Chemotherapy-Treated Dying Leukemia Cells Elicits an Immune Suppressive Effect by Increasing Regulatory T Cells and Tolerogenic Dendritic Cells. *Front. Immunol.* **2017**, *8*, 1918. [CrossRef] [PubMed]
9. He, X.; Wan, J.; Yang, X.; Zhang, X.; Huang, D.; Li, X.; Zou, Y.; Chen, C.; Yu, Z.; Xie, L.; et al. Bone marrow niche ATP levels determine leukemia-initiating cell activity via P2X7 in leukemic models. *J. Clin. Investig.* **2021**, *131*, e140242. [CrossRef]
10. Kamata-Sakurai, M.; Narita, Y.; Hori, Y.; Nemoto, T.; Uchikawa, R.; Honda, M.; Hironiwa, N.; Taniguchi, K.; Shida-Kawazoe, M.; Metsugi, S.; et al. Antibody to CD137 Activated by Extracellular Adenosine Triphosphate Is Tumor Selective and Broadly Effective In Vivo without Systemic Immune Activation. *Cancer Discov.* **2021**, *11*, 158–175. [CrossRef]
11. Muller, C.E.; Namasivayam, V. Recommended tool compounds and drugs for blocking P2X and P2Y receptors. *Purinergic Signal* **2021**, *17*, 633–648. [CrossRef] [PubMed]
12. Adinolfi, E.; De Marchi, E.; Orioli, E.; Pegoraro, A.; Di Virgilio, F. Role of the P2X7 receptor in tumor-associated inflammation. *Curr. Opin. Pharmacol.* **2019**, *47*, 59–64. [CrossRef]
13. Grassi, F.; De Ponte Conti, B. The P2X7 Receptor in Tumor Immunity. *Front. Cell Dev. Biol.* **2021**, *9*, 694831. [CrossRef]
14. Lara, R.; Adinolfi, E.; Harwood, C.A.; Philpott, M.; Barden, J.A.; Di Virgilio, F.; McNulty, S. P2X7 in Cancer: From Molecular Mechanisms to Therapeutics. *Front. Pharmacol.* **2020**, *11*, 793. [CrossRef] [PubMed]
15. De Marchi, E.; Orioli, E.; Pegoraro, A.; Sangaletti, S.; Portararo, P.; Curti, A.; Colombo, M.P.; Di Virgilio, F.; Adinolfi, E. The P2X7 receptor modulates immune cells infiltration, ectonucleotidases expression and extracellular ATP levels in the tumor microenvironment. *Oncogene* **2019**, *38*, 3636–3650. [CrossRef] [PubMed]
16. Adinolfi, E.; Giuliani, A.L.; De Marchi, E.; Pegoraro, A.; Orioli, E.; Di Virgilio, F. The P2X7 receptor: A main player in inflammation. *Biochem. Pharmacol.* **2018**, *151*, 234–244. [CrossRef] [PubMed]
17. Orioli, E.; De Marchi, E.; Giuliani, A.L.; Adinolfi, E. P2X7 Receptor Orchestrates Multiple Signalling Pathways Triggering Inflammation, Autophagy and Metabolic/Trophic Responses. *Curr. Med. Chem.* **2017**, *24*, 2261–2275. [CrossRef] [PubMed]
18. Di Virgilio, F.; Dal Ben, D.; Sarti, A.C.; Giuliani, A.L.; Falzoni, S. The P2X7 Receptor in Infection and Inflammation. *Immunity* **2017**, *47*, 15–31. [CrossRef]
19. Karasawa, A.; Michalski, K.; Mikhelzon, P.; Kawate, T. The P2X7 receptor forms a dye-permeable pore independent of its intracellular domain but dependent on membrane lipid composition. *elife* **2017**, *6*, e31186. [CrossRef] [PubMed]
20. Di Virgilio, F.; Schmalzing, G.; Markwardt, F. The Elusive P2X7 Macropore. *Trends Cell Biol.* **2018**, *28*, 392–404. [CrossRef]

21. You, R.; He, X.; Zeng, Z.; Zhan, Y.; Xiao, Y.; Xiao, R. Pyroptosis and Its Role in Autoimmune Disease: A Potential Therapeutic Target. *Front. Immunol.* **2022**, *13*, 841732. [CrossRef]
22. Adinolfi, E.; Callegari, M.G.; Ferrari, D.; Bolognesi, C.; Minelli, M.; Wieckowski, M.R.; Pinton, P.; Rizzuto, R.; Di Virgilio, F. Basal activation of the P2X7 ATP receptor elevates mitochondrial calcium and potential, increases cellular ATP levels, and promotes serum-independent growth. *Mol. Biol. Cell* **2005**, *16*, 3260–3272. [CrossRef]
23. Nicke, A. Homotrimeric complexes are the dominant assembly state of native P2X7 subunits. *Biochem. Biophys. Res. Commun.* **2008**, *377*, 803–808. [CrossRef] [PubMed]
24. Karasawa, A.; Kawate, T. Structural basis for subtype-specific inhibition of the P2X7 receptor. *elife* **2016**, *5*, e22153. [CrossRef] [PubMed]
25. Ahmadi, M.; Nowroozi, A.; Shahlaei, M. Constructing an atomic-resolution model of human P2X7 receptor followed by pharmacophore modeling to identify potential inhibitors. *J. Mol. Graph. Model.* **2015**, *61*, 243–261. [CrossRef] [PubMed]
26. Di Virgilio, F.; Jiang, L.H.; Roger, S.; Falzoni, S.; Sarti, A.C.; Vultaggio-Poma, V.; Chiozzi, P.; Adinolfi, E. Structure, function and techniques of investigation of the P2X7 receptor (P2X7R) in mammalian cells. *Methods Enzymol.* **2019**, *629*, 115–150. [CrossRef]
27. Jiang, L.H.; Caseley, E.A.; Muench, S.P.; Roger, S. Structural basis for the functional properties of the P2X7 receptor for extracellular ATP. *Purinergic Signal* **2021**, *17*, 331–344. [CrossRef]
28. Muller, C.E.; Namasivayam, V. Agonists, Antagonists, and Modulators of P2X7 Receptors. *Methods Mol. Biol.* **2022**, *2510*, 31–52. [CrossRef]
29. Pasqualetto, G.; Zuanon, M.; Brancale, A.; Young, M.T. Identification of a novel P2X7 antagonist using structure-based virtual screening. *Front. Pharmacol.* **2022**, *13*, 1094607. [CrossRef]
30. Ghafir El Idrissi, I.; Podlewska, S.; Abate, C.; Bojarski, A.J.; Lacivita, E.; Leopoldo, M. Structure-Activity Relationships and Therapeutic Potential of Purinergic P2X7 Receptor Antagonists. *Curr. Med. Chem.* 2023, *ahead of Print*. [CrossRef]
31. Surprenant, A.; Rassendren, F.; Kawashima, E.; North, R.A.; Buell, G. The cytolytic P2Z receptor for extracellular ATP identified as a P2X receptor (P2X7). *Science* **1996**, *272*, 735–738. [CrossRef]
32. Kim, M.; Jiang, L.H.; Wilson, H.L.; North, R.A.; Surprenant, A. Proteomic and functional evidence for a P2X7 receptor signalling complex. *EMBO J.* **2001**, *20*, 6347–6358. [CrossRef] [PubMed]
33. Kopp, R.; Krautloher, A.; Ramirez-Fernandez, A.; Nicke, A. P2X7 Interactions and Signaling—Making Head or Tail of It. *Front. Mol. Neurosci.* **2019**, *12*, 183. [CrossRef] [PubMed]
34. Rassendren, F.; Buell, G.N.; Virginio, C.; Collo, G.; North, R.A.; Surprenant, A. The permeabilizing ATP receptor, P2X7. Cloning and expression of a human cDNA. *J. Biol. Chem.* **1997**, *272*, 5482–5486. [CrossRef] [PubMed]
35. Pegoraro, A.; De Marchi, E.; Adinolfi, E. P2X7 Variants in Oncogenesis. *Cells* **2021**, *10*, 189. [CrossRef]
36. De Salis, S.K.F.; Li, L.; Chen, Z.; Lam, K.W.; Skarratt, K.K.; Balle, T.; Fuller, S.J. Alternatively Spliced Isoforms of the P2X7 Receptor: Structure, Function and Disease Associations. *Int. J. Mol. Sci.* **2022**, *23*, 8174. [CrossRef] [PubMed]
37. Cheewatrakoolpong, B.; Gilchrest, H.; Anthes, J.C.; Greenfeder, S. Identification and characterization of splice variants of the human P2X7 ATP channel. *Biochem. Biophys. Res. Commun.* **2005**, *332*, 17–27. [CrossRef]
38. Feng, Y.H.; Li, X.; Wang, L.; Zhou, L.; Gorodeski, G.I. A truncated P2X7 receptor variant (P2X7-j) endogenously expressed in cervical cancer cells antagonizes the full-length P2X7 receptor through hetero-oligomerization. *J. Biol. Chem.* **2006**, *281*, 17228–17237. [CrossRef]
39. Giuliani, A.L.; Colognesi, D.; Ricco, T.; Roncato, C.; Capece, M.; Amoroso, F.; Wang, Q.G.; De Marchi, E.; Gartland, A.; Di Virgilio, F.; et al. Trophic activity of human P2X7 receptor isoforms A and B in osteosarcoma. *PLoS ONE* **2014**, *9*, e107224. [CrossRef]
40. Pan, H.; Ni, H.; Zhang, L.; Xing, Y.; Fan, J.; Li, P.; Li, T.; Jia, R.; Ge, S.; Zhang, H.; et al. P2RX7-V3 is a novel oncogene that promotes tumorigenesis in uveal melanoma. *Tumour Biol.* **2016**, *37*, 13533–13543. [CrossRef]
41. Ulrich, H.; Ratajczak, M.Z.; Schneider, G.; Adinolfi, E.; Orioli, E.; Ferrazoli, E.G.; Glaser, T.; Correa-Velloso, J.; Martins, P.C.M.; Coutinho, F.; et al. Kinin and Purine Signaling Contributes to Neuroblastoma Metastasis. *Front. Pharmacol.* **2018**, *9*, 500. [CrossRef]
42. Pegoraro, A.; Orioli, E.; De Marchi, E.; Salvestrini, V.; Milani, A.; Di Virgilio, F.; Curti, A.; Adinolfi, E. Differential sensitivity of acute myeloid leukemia cells to daunorubicin depends on P2X7A versus P2X7B receptor expression. *Cell Death Dis.* **2020**, *11*, 876. [CrossRef] [PubMed]
43. Pegoraro, A.; De Marchi, E.; Ferracin, M.; Orioli, E.; Zanoni, M.; Bassi, C.; Tesei, A.; Capece, M.; Dika, E.; Negrini, M.; et al. P2X7 promotes metastatic spreading and triggers release of miRNA-containing exosomes and microvesicles from melanoma cells. *Cell Death Dis.* **2021**, *12*, 1088. [CrossRef]
44. Arnaud-Sampaio, V.F.; Bento, C.A.; Glaser, T.; Adinolfi, E.; Ulrich, H.; Lameu, C. P2X7 receptor isoform B is a key drug resistance mediator for neuroblastoma. *Front. Oncol.* **2022**, *12*, 966404. [CrossRef]
45. Adinolfi, E.; Cirillo, M.; Woltersdorf, R.; Falzoni, S.; Chiozzi, P.; Pellegatti, P.; Callegari, M.G.; Sandona, D.; Markwardt, F.; Schmalzing, G.; et al. Trophic activity of a naturally occurring truncated isoform of the P2X7 receptor. *FASEB J.* **2010**, *24*, 3393–3404. [CrossRef]
46. Gilbert, S.M.; Oliphant, C.J.; Hassan, S.; Peille, A.L.; Bronsert, P.; Falzoni, S.; Di Virgilio, F.; McNulty, S.; Lara, R. ATP in the tumour microenvironment drives expression of nfP2X(7), a key mediator of cancer cell survival. *Oncogene* **2019**, *38*, 194–208. [CrossRef] [PubMed]

47. Gilbert, S.M.; Gidley Baird, A.; Glazer, S.; Barden, J.A.; Glazer, A.; Teh, L.C.; King, J. A phase I clinical trial demonstrates that nfP2X(7) -targeted antibodies provide a novel, safe and tolerable topical therapy for basal cell carcinoma. *Br. J. Dermatol.* **2017**, *177*, 117–124. [CrossRef] [PubMed]
48. Benzaquen, J.; Heeke, S.; Janho Dit Hreich, S.; Douguet, L.; Marquette, C.H.; Hofman, P.; Vouret-Craviari, V. Alternative splicing of P2RX7 pre-messenger RNA in health and diseases: Myth or reality? *Biomed. J.* **2019**, *42*, 141–154. [CrossRef] [PubMed]
49. Olla, I.; Santos-Galindo, M.; Elorza, A.; Lucas, J.J. P2X7 Receptor Upregulation in Huntington's Disease Brains. *Front. Mol. Neurosci.* **2020**, *13*, 567430. [CrossRef] [PubMed]
50. Baricordi, O.R.; Melchiorri, L.; Adinolfi, E.; Falzoni, S.; Chiozzi, P.; Buell, G.; Di Virgilio, F. Increased proliferation rate of lymphoid cells transfected with the P2X(7) ATP receptor. *J. Biol. Chem.* **1999**, *274*, 33206–33208. [CrossRef] [PubMed]
51. Adinolfi, E.; Pizzirani, C.; Idzko, M.; Panther, E.; Norgauer, J.; Di Virgilio, F.; Ferrari, D. P2X(7) receptor: Death or life? *Purinergic Signal* **2005**, *1*, 219–227. [CrossRef]
52. Adinolfi, E.; Callegari, M.G.; Cirillo, M.; Pinton, P.; Giorgi, C.; Cavagna, D.; Rizzuto, R.; Di Virgilio, F. Expression of the P2X7 receptor increases the Ca^{2+} content of the endoplasmic reticulum, activates NFATc1, and protects from apoptosis. *J. Biol. Chem.* **2009**, *284*, 10120–10128. [CrossRef] [PubMed]
53. Adinolfi, E.; Raffaghello, L.; Giuliani, A.L.; Cavazzini, L.; Capece, M.; Chiozzi, P.; Bianchi, G.; Kroemer, G.; Pistoia, V.; Di Virgilio, F. Expression of P2X7 receptor increases in vivo tumor growth. *Cancer Res.* **2012**, *72*, 2957–2969. [CrossRef]
54. Amoroso, F.; Falzoni, S.; Adinolfi, E.; Ferrari, D.; Di Virgilio, F. The P2X7 receptor is a key modulator of aerobic glycolysis. *Cell Death Dis.* **2012**, *3*, e370. [CrossRef]
55. Amoroso, F.; Capece, M.; Rotondo, A.; Cangelosi, D.; Ferracin, M.; Franceschini, A.; Raffaghello, L.; Pistoia, V.; Varesio, L.; Adinolfi, E. The P2X7 receptor is a key modulator of the PI3K/GSK3beta/VEGF signaling network: Evidence in experimental neuroblastoma. *Oncogene* **2015**, *34*, 5240–5251. [CrossRef]
56. Di Virgilio, F.; Adinolfi, E. Extracellular purines, purinergic receptors and tumor growth. *Oncogene* **2017**, *36*, 293–303. [CrossRef]
57. Rabelo, I.L.A.; Arnaud-Sampaio, V.F.; Adinolfi, E.; Ulrich, H.; Lameu, C. Cancer Metabostemness and Metabolic Reprogramming via P2X7 Receptor. *Cells* **2021**, *10*, 1782. [CrossRef] [PubMed]
58. Vultaggio-Poma, V.; Falzoni, S.; Chiozzi, P.; Sarti, A.C.; Adinolfi, E.; Giuliani, A.L.; Sanchez-Melgar, A.; Boldrini, P.; Zanoni, M.; Tesei, A.; et al. Extracellular ATP is increased by release of ATP-loaded microparticles triggered by nutrient deprivation. *Theranostics* **2022**, *12*, 859–874. [CrossRef]
59. Sarti, A.C.; Vultaggio-Poma, V.; Falzoni, S.; Missiroli, S.; Giuliani, A.L.; Boldrini, P.; Bonora, M.; Faita, F.; Di Lascio, N.; Kusmic, C.; et al. Mitochondrial P2X7 Receptor Localization Modulates Energy Metabolism Enhancing Physical Performance. *Function* **2021**, *2*, zqab005. [CrossRef] [PubMed]
60. Adinolfi, E.; Melchiorri, L.; Falzoni, S.; Chiozzi, P.; Morelli, A.; Tieghi, A.; Cuneo, A.; Castoldi, G.; Di Virgilio, F.; Baricordi, O.R. P2X7 receptor expression in evolutive and indolent forms of chronic B lymphocytic leukemia. *Blood* **2002**, *99*, 706–708. [CrossRef]
61. De Marchi, E.; Pegoraro, A.; Adinolfi, E. P2X7 Receptor in Hematological Malignancies. *Front. Cell Dev. Biol.* **2021**, *9*, 645605. [CrossRef] [PubMed]
62. He, X.; Zhang, Y.; Xu, Y.; Xie, L.; Yu, Z.; Zheng, J. Function of the P2X7 receptor in hematopoiesis and leukemogenesis. *Exp. Hematol.* **2021**, *104*, 40–47. [CrossRef] [PubMed]
63. Pegoraro, A.; Adinolfi, E. The ATP/P2X7 axis is a crucial regulator of leukemic initiating cells proliferation and homing and an emerging therapeutic target in acute myeloid leukemia. *Purinergic Signal* **2021**, *17*, 319–321. [CrossRef]
64. da Silva, G.B.; Yamauchi, M.A.; Zanini, D.; Bagatini, M.D. Novel possibility for cutaneous melanoma treatment by means of rosmarinic acid action on purinergic signaling. *Purinergic Signal* **2022**, *18*, 61–81. [CrossRef]
65. Randic, T.; Magni, S.; Philippidou, D.; Margue, C.; Grzyb, K.; Preis, J.R.; Wroblewska, J.P.; Nazarov, P.V.; Mittelbronn, M.; Frauenknecht, K.B.M.; et al. Single-cell transcriptomics of NRAS-mutated melanoma transitioning to drug resistance reveals P2RX7 as an indicator of early drug response. *Cell Rep.* **2023**, *42*, 112696. [CrossRef]
66. McLarnon, J.G. Roles of purinergic P2X(7) receptor in glioma and microglia in brain tumors. *Cancer Lett.* **2017**, *402*, 93–99. [CrossRef] [PubMed]
67. Gehring, M.P.; Kipper, F.; Nicoletti, N.F.; Sperotto, N.D.; Zanin, R.; Tamajusuku, A.S.; Flores, D.G.; Meurer, L.; Roesler, R.; Filho, A.B.; et al. P2X7 receptor as predictor gene for glioma radiosensitivity and median survival. *Int. J. Biochem. Cell Biol.* **2015**, *68*, 92–100. [CrossRef]
68. Kan, L.K.; Williams, D.; Drummond, K.; O'Brien, T.; Monif, M. The role of microglia and P2X7 receptors in gliomas. *J. Neuroimmunol.* **2019**, *332*, 138–146. [CrossRef]
69. Raffaghello, L.; Chiozzi, P.; Falzoni, S.; Di Virgilio, F.; Pistoia, V. The P2X7 receptor sustains the growth of human neuroblastoma cells through a substance P-dependent mechanism. *Cancer Res.* **2006**, *66*, 907–914. [CrossRef]
70. Benito-Leon, M.; Gil-Redondo, J.C.; Perez-Sen, R.; Delicado, E.G.; Ortega, F.; Gomez-Villafuertes, R. BCI, an inhibitor of the DUSP1 and DUSP6 dual specificity phosphatases, enhances P2X7 receptor expression in neuroblastoma cells. *Front. Cell Dev. Biol.* **2022**, *10*, 1049566. [CrossRef]
71. Wang, Z.; Zhu, S.; Tan, S.; Zeng, Y.; Zeng, H. The P2 purinoceptors in prostate cancer. *Purinergic Signal* **2023**, *19*, 255–263. [CrossRef]
72. Zhu, X.; Li, Q.; Song, W.; Peng, X.; Zhao, R. P2X7 receptor: A critical regulator and potential target for breast cancer. *J. Mol. Med.* **2021**, *99*, 349–358. [CrossRef]

73. Adinolfi, E.; Amoroso, F.; Giuliani, A.L. P2X7 Receptor Function in Bone-Related Cancer. *J. Osteoporos.* **2012**, *2012*, 637863. [CrossRef]
74. Agrawal, A.; Gartland, A. P2X7 receptors: Role in bone cell formation and function. *J. Mol. Endocrinol.* **2015**, *54*, R75–R88. [CrossRef]
75. Tattersall, L.; Shah, K.M.; Lath, D.L.; Singh, A.; Down, J.M.; De Marchi, E.; Williamson, A.; Di Virgilio, F.; Heymann, D.; Adinolfi, E.; et al. The P2RX7B splice variant modulates osteosarcoma cell behaviour and metastatic properties. *J. Bone Oncol.* **2021**, *31*, 100398. [CrossRef]
76. Song, H.; Arredondo Carrera, H.M.; Sprules, A.; Ji, Y.; Zhang, T.; He, J.; Lawrence, E.; Gartland, A.; Luo, J.; Wang, N. C-terminal variants of the P2X7 receptor are associated with prostate cancer progression and bone metastasis—Evidence from clinical and pre-clinical data. *Cancer Commun.* **2023**, *43*, 400–404. [CrossRef] [PubMed]
77. Roliano, G.G.; Azambuja, J.H.; Brunetto, V.T.; Butterfield, H.E.; Kalil, A.N.; Braganhol, E. Colorectal Cancer and Purinergic Signalling: An Overview. *Cancers* **2022**, *14*, 4887. [CrossRef]
78. De Marchi, E.; Pegoraro, A.; Adinolfi, E. Administration of P2X7 Receptor Blockers in Oncological Experimental Models. *Methods Mol. Biol.* **2022**, *2510*, 303–314. [CrossRef] [PubMed]
79. Bianchi, G.; Vuerich, M.; Pellegatti, P.; Marimpietri, D.; Emionite, L.; Marigo, I.; Bronte, V.; Di Virgilio, F.; Pistoia, V.; Raffaghello, L. ATP/P2X7 axis modulates myeloid-derived suppressor cell functions in neuroblastoma microenvironment. *Cell Death Dis.* **2014**, *5*, e1135. [CrossRef]
80. Adinolfi, E.; Capece, M.; Franceschini, A.; Falzoni, S.; Giuliani, A.L.; Rotondo, A.; Sarti, A.C.; Bonora, M.; Syberg, S.; Corigliano, D.; et al. Accelerated tumor progression in mice lacking the ATP receptor P2X7. *Cancer Res.* **2015**, *75*, 635–644. [CrossRef] [PubMed]
81. Hofman, P.; Cherfils-Vicini, J.; Bazin, M.; Ilie, M.; Juhel, T.; Hebuterne, X.; Gilson, E.; Schmid-Alliana, A.; Boyer, O.; Adriouch, S.; et al. Genetic and pharmacological inactivation of the purinergic P2RX7 receptor dampens inflammation but increases tumor incidence in a mouse model of colitis-associated cancer. *Cancer Res.* **2015**, *75*, 835–845. [CrossRef]
82. Li, X.Y.; Moesta, A.K.; Xiao, C.; Nakamura, K.; Casey, M.; Zhang, H.; Madore, J.; Lepletier, A.; Aguilera, A.R.; Sundarrajan, A.; et al. Targeting CD39 in Cancer Reveals an Extracellular ATP- and Inflammasome-Driven Tumor Immunity. *Cancer Discov.* **2019**, *9*, 1754–1773. [CrossRef]
83. Yan, J.; Li, X.Y.; Roman Aguilera, A.; Xiao, C.; Jacoberger-Foissac, C.; Nowlan, B.; Robson, S.C.; Beers, C.; Moesta, A.K.; Geetha, N.; et al. Control of Metastases via Myeloid CD39 and NK Cell Effector Function. *Cancer Immunol. Res.* **2020**, *8*, 356–367. [CrossRef] [PubMed]
84. De Marchi, E.; Pegoraro, A.; Turiello, R.; Di Virgilio, F.; Morello, S.; Adinolfi, E. A2A Receptor Contributes to Tumor Progression in P2X7 Null Mice. *Front. Cell Dev. Biol.* **2022**, *10*, 876510. [CrossRef] [PubMed]
85. Benzaquen, J.; Dit Hreich, S.J.; Heeke, S.; Juhel, T.; Lalvee, S.; Bauwens, S.; Saccani, S.; Lenormand, P.; Hofman, V.; Butori, M.; et al. P2RX7B is a new theranostic marker for lung adenocarcinoma patients. *Theranostics* **2020**, *10*, 10849–10860. [CrossRef] [PubMed]
86. Douguet, L.; Janho Dit Hreich, S.; Benzaquen, J.; Seguin, L.; Juhel, T.; Dezitter, X.; Duranton, C.; Ryffel, B.; Kanellopoulos, J.; Delarasse, C.; et al. A small-molecule P2RX7 activator promotes anti-tumor immune responses and sensitizes lung tumor to immunotherapy. *Nat. Commun.* **2021**, *12*, 653. [CrossRef]
87. Missiroli, S.; Perrone, M.; Gafa, R.; Nicoli, F.; Bonora, M.; Morciano, G.; Boncompagni, C.; Marchi, S.; Lebiedzinska-Arciszewska, M.; Vezzani, B.; et al. PML at mitochondria-associated membranes governs a trimeric complex with NLRP3 and P2X7R that modulates the tumor immune microenvironment. *Cell Death Differ.* **2023**, *30*, 429–441. [CrossRef]
88. Santiago-Carvalho, I.; Banuelos, A.; Borges da Silva, H. Tissue- and temporal-specific roles of extracellular ATP on T cell metabolism and function. *Immunometabolism* **2023**, *5*, e00025. [CrossRef]
89. Wanhainen, K.M.; Peng, C.; Zhou, M.H.; Macedo, B.G.; O'Flanagan, S.; Yang, T.; Kelekar, A.; Burbach, B.J.; Borges da Silva, H.; Jameson, S.C. P2RX7 Enhances Tumor Control by CD8+ T Cells in Adoptive Cell Therapy. *Cancer Immunol. Res.* **2022**, *10*, 871–884. [CrossRef]
90. Gerstberger, S.; Jiang, Q.; Ganesh, K. Metastasis. *Cell* **2023**, *186*, 1564–1579. [CrossRef]
91. Jelassi, B.; Chantome, A.; Alcaraz-Perez, F.; Baroja-Mazo, A.; Cayuela, M.L.; Pelegrin, P.; Surprenant, A.; Roger, S. P2X(7) receptor activation enhances SK3 channels- and cystein cathepsin-dependent cancer cells invasiveness. *Oncogene* **2011**, *30*, 2108–2122. [CrossRef]
92. Jelassi, B.; Anchelin, M.; Chamouton, J.; Cayuela, M.L.; Clarysse, L.; Li, J.; Gore, J.; Jiang, L.H.; Roger, S. Anthraquinone emodin inhibits human cancer cell invasiveness by antagonizing P2X7 receptors. *Carcinogenesis* **2013**, *34*, 1487–1496. [CrossRef] [PubMed]
93. Qiu, Y.; Li, W.H.; Zhang, H.Q.; Liu, Y.; Tian, X.X.; Fang, W.G. P2X7 mediates ATP-driven invasiveness in prostate cancer cells. *PLoS ONE* **2014**, *9*, e114371. [CrossRef] [PubMed]
94. Bai, X.; Li, Q.; Peng, X.; Li, X.; Qiao, C.; Tang, Y.; Zhao, R. P2X7 receptor promotes migration and invasion of non-small cell lung cancer A549 cells through the PI3K/Akt pathways. *Purinergic Signal* 2023, 1–13, *ahead of Print*. [CrossRef] [PubMed]
95. Yang, R.; Yu, T.; Kou, X.; Gao, X.; Chen, C.; Liu, D.; Zhou, Y.; Shi, S. Tet1 and Tet2 maintain mesenchymal stem cell homeostasis via demethylation of the P2rX7 promoter. *Nat. Commun.* **2018**, *9*, 2143. [CrossRef]
96. Zhang, Y.; Cheng, H.; Li, W.; Wu, H.; Yang, Y. Highly-expressed P2X7 receptor promotes growth and metastasis of human HOS/MNNG osteosarcoma cells via PI3K/Akt/GSK3beta/beta-catenin and mTOR/HIF1alpha/VEGF signaling. *Int. J. Cancer* **2019**, *145*, 1068–1082. [CrossRef]

97. Ziberi, S.; Zuccarini, M.; Carluccio, M.; Giuliani, P.; Ricci-Vitiani, L.; Pallini, R.; Caciagli, F.; Di Iorio, P.; Ciccarelli, R. Upregulation of Epithelial-To-Mesenchymal Transition Markers and P2X7 Receptors Is Associated to Increased Invasiveness Caused by P2X7 Receptor Stimulation in Human Glioblastoma Stem Cells. *Cells* **2019**, *9*, 85. [CrossRef]
98. Brisson, L.; Chadet, S.; Lopez-Charcas, O.; Jelassi, B.; Ternant, D.; Chamouton, J.; Lerondel, S.; Le Pape, A.; Couillin, I.; Gombault, A.; et al. P2X7 Receptor Promotes Mouse Mammary Cancer Cell Invasiveness and Tumour Progression, and Is a Target for Anticancer Treatment. *Cancers* **2020**, *12*, 2342. [CrossRef]
99. Yang, J.; Antin, P.; Berx, G.; Blanpain, C.; Brabletz, T.; Bronner, M.; Campbell, K.; Cano, A.; Casanova, J.; Christofori, G.; et al. Guidelines and definitions for research on epithelial-mesenchymal transition. *Nat. Rev. Mol. Cell Biol.* **2020**, *21*, 341–352. [CrossRef]
100. Huang, X.; Jia, Z.; Li, X.; Hu, Z.; Yu, X.; Xia, J. Asiaticoside hampers epithelial-mesenchymal transition by promoting PPARG expression and suppressing P2RX7-mediated TGF-beta/Smad signaling in triple-negative breast cancer. *Phytother. Res.* **2023**, *37*, 1771–1786. [CrossRef]
101. Ledderose, S.; Rodler, S.; Eismann, L.; Ledderose, G.; Rudelius, M.; Junger, W.G.; Ledderose, C. P2X1 and P2X7 Receptor Overexpression Is a Negative Predictor of Survival in Muscle-Invasive Bladder Cancer. *Cancers* **2023**, *15*, 2321. [CrossRef] [PubMed]
102. Pfalzgraff, A.; Barcena-Varela, S.; Heinbockel, L.; Gutsmann, T.; Brandenburg, K.; Martinez-de-Tejada, G.; Weindl, G. Antimicrobial endotoxin-neutralizing peptides promote keratinocyte migration via P2X7 receptor activation and accelerate wound healing in vivo. *Br. J. Pharmacol.* **2018**, *175*, 3581–3593. [CrossRef] [PubMed]
103. Minns, M.S.; Teicher, G.; Rich, C.B.; Trinkaus-Randall, V. Purinoreceptor P2X7 Regulation of Ca^{2+} Mobilization and Cytoskeletal Rearrangement Is Required for Corneal Reepithelialization after Injury. *Am. J. Pathol.* **2016**, *186*, 285–296. [CrossRef]
104. Fabbrizio, P.; Apolloni, S.; Bianchi, A.; Salvatori, I.; Valle, C.; Lanzuolo, C.; Bendotti, C.; Nardo, G.; Volonte, C. P2X7 activation enhances skeletal muscle metabolism and regeneration in SOD1G93A mouse model of amyotrophic lateral sclerosis. *Brain Pathol.* **2020**, *30*, 272–282. [CrossRef] [PubMed]
105. Jorgensen, N.R. The purinergic P2X7 ion channel receptor-a 'repair' receptor in bone. *Curr. Opin. Immunol.* **2018**, *52*, 32–38. [CrossRef]
106. Kimura, T.; Katayama, J. Regularity of approaching visual stimuli influences spatial expectations for subsequent somatosensory stimuli. *Exp. Brain Res.* **2017**, *235*, 1657–1663. [CrossRef]
107. Li, Z.; Huang, Z.; Zhang, H.; Lu, J.; Wei, Y.; Yang, Y.; Bai, L. IRE1-mTOR-PERK Axis Coordinates Autophagy and ER Stress-Apoptosis Induced by P2X7-Mediated Ca^{2+} Influx in Osteoarthritis. *Front. Cell Dev. Biol.* **2021**, *9*, 695041. [CrossRef]
108. Ikutama, R.; Peng, G.; Tsukamoto, S.; Umehara, Y.; Trujillo-Paez, J.V.; Yue, H.; Nguyen, H.L.T.; Takahashi, M.; Kageyama, S.; Komatsu, M.; et al. Cathelicidin LL-37 Activates Human Keratinocyte Autophagy through the P2X(7), Mechanistic Target of Rapamycin, and MAPK Pathways. *J. Investig. Dermatol.* **2023**, *143*, 751–761.e7. [CrossRef]
109. Hill, L.M.; Gavala, M.L.; Lenertz, L.Y.; Bertics, P.J. Extracellular ATP may contribute to tissue repair by rapidly stimulating purinergic receptor X7-dependent vascular endothelial growth factor release from primary human monocytes. *J. Immunol.* **2010**, *185*, 3028–3034. [CrossRef]
110. Yang, C.; Shi, S.; Su, Y.; Tong, J.S.; Li, L. P2X7R promotes angiogenesis and tumour-associated macrophage recruitment by regulating the NF-kappaB signalling pathway in colorectal cancer cells. *J. Cell Mol. Med.* **2020**, *24*, 10830–10841. [CrossRef] [PubMed]
111. Sheng, G.; Gao, Y.; Ding, Q.; Zhang, R.; Wang, T.; Jing, S.; Zhao, H.; Ma, T.; Wu, H.; Yang, Y. P2RX7 promotes osteosarcoma progression and glucose metabolism by enhancing c-Myc stabilization. *J. Transl. Med.* **2023**, *21*, 132. [CrossRef] [PubMed]
112. Maddipati, R.; Norgard, R.J.; Baslan, T.; Rathi, K.S.; Zhang, A.; Saeid, A.; Higashihara, T.; Wu, F.; Kumar, A.; Annamalai, V.; et al. MYC Levels Regulate Metastatic Heterogeneity in Pancreatic Adenocarcinoma. *Cancer Discov.* **2022**, *12*, 542–561. [CrossRef]
113. Akhtari, M.; Jalal Zargar, S.; Javinani, A.; Ashraf-Ganjouei, A.; Vojdanian, M.; Jamshidi, A.; Mahmoudi, M. Prototypic P2X7 Receptor Agonist, BzATP, Induced the Expression of Unfolded Protein Response Genes in Human M1 Macrophages. *Iran. J. Allergy Asthma Immunol.* **2022**, *21*, 73–80. [CrossRef]
114. Gu, L.Q.; Li, F.Y.; Zhao, L.; Liu, Y.; Chu, Q.; Zang, X.X.; Liu, J.M.; Ning, G.; Zhao, Y.J. Association of XIAP and P2X7 receptor expression with lymph node metastasis in papillary thyroid carcinoma. *Endocrine* **2010**, *38*, 276–282. [CrossRef]
115. Zhang, Y.; Ding, J.; Wang, L. The role of P2X7 receptor in prognosis and metastasis of colorectal cancer. *Adv. Med. Sci.* **2019**, *64*, 388–394. [CrossRef]
116. Calik, I.; Calik, M.; Sarikaya, B.; Ozercan, I.H.; Arslan, R.; Artas, G.; Dagli, A.F. P2X7 receptor as an independent prognostic indicator in gastric cancer. *Bosn. J. Basic. Med. Sci.* **2020**, *20*, 188–196. [CrossRef] [PubMed]
117. Calik, I.; Calik, M.; Turken, G.; Ozercan, I.H. A promising independent prognostic biomarker in colorectal cancer: P2X7 receptor. *Int. J. Clin. Exp. Pathol.* **2020**, *13*, 107–121.
118. Wang, X.; Chang, X.; He, C.; Fan, Z.; Yu, Z.; Yu, B.; Wu, X.; Hou, J.; Li, J.; Su, L.; et al. ATP5B promotes the metastasis and growth of gastric cancer by activating the FAK/AKT/MMP2 pathway. *FASEB J.* **2021**, *35*, e20649. [CrossRef]
119. Ren, S.; Zhang, Y.; Wang, Y.; Lui, Y.; Wei, W.; Huang, X.; Mao, W.; Zuo, Y. Targeting P2X(7) receptor inhibits the metastasis of murine P388D1 lymphoid neoplasm cells to lymph nodes. *Cell Biol. Int.* **2010**, *34*, 1205–1211. [CrossRef] [PubMed]
120. van Niel, G.; D'Angelo, G.; Raposo, G. Shedding light on the cell biology of extracellular vesicles. *Nat. Rev. Mol. Cell Biol.* **2018**, *19*, 213–228. [CrossRef]

121. Feng, W.; Dean, D.C.; Hornicek, F.J.; Shi, H.; Duan, Z. Exosomes promote pre-metastatic niche formation in ovarian cancer. *Mol. Cancer* **2019**, *18*, 124. [CrossRef]
122. Hood, J.L.; San, R.S.; Wickline, S.A. Exosomes released by melanoma cells prepare sentinel lymph nodes for tumor metastasis. *Cancer Res.* **2011**, *71*, 3792–3801. [CrossRef]
123. Zhao, H.; Achreja, A.; Iessi, E.; Logozzi, M.; Mizzoni, D.; Di Raimo, R.; Nagrath, D.; Fais, S. The key role of extracellular vesicles in the metastatic process. *Biochim. Biophys. Acta Rev. Cancer* **2018**, *1869*, 64–77. [CrossRef] [PubMed]
124. Lombardi, M.; Gabrielli, M.; Adinolfi, E.; Verderio, C. Role of ATP in Extracellular Vesicle Biogenesis and Dynamics. *Front. Pharmacol.* **2021**, *12*, 654023. [CrossRef] [PubMed]
125. Becherer, U.; Pasche, M.; Nofal, S.; Hof, D.; Matti, U.; Rettig, J. Quantifying exocytosis by combination of membrane capacitance measurements and total internal reflection fluorescence microscopy in chromaffin cells. *PLoS ONE* **2007**, *2*, e505. [CrossRef]
126. Gulinelli, S.; Salaro, E.; Vuerich, M.; Bozzato, D.; Pizzirani, C.; Bolognesi, G.; Idzko, M.; Di Virgilio, F.; Ferrari, D. IL-18 associates to microvesicles shed from human macrophages by a LPS/TLR-4 independent mechanism in response to P2X receptor stimulation. *Eur. J. Immunol.* **2012**, *42*, 3334–3345. [CrossRef] [PubMed]
127. Thomas, L.M.; Salter, R.D. Activation of macrophages by P2X7-induced microvesicles from myeloid cells is mediated by phospholipids and is partially dependent on TLR4. *J. Immunol.* **2010**, *185*, 3740–3749. [CrossRef]
128. Baroni, M.; Pizzirani, C.; Pinotti, M.; Ferrari, D.; Adinolfi, E.; Calzavarini, S.; Caruso, P.; Bernardi, F.; Di Virgilio, F. Stimulation of P2 (P2X7) receptors in human dendritic cells induces the release of tissue factor-bearing microparticles. *FASEB J.* **2007**, *21*, 1926–1933. [CrossRef]
129. Pizzirani, C.; Ferrari, D.; Chiozzi, P.; Adinolfi, E.; Sandona, D.; Savaglio, E.; Di Virgilio, F. Stimulation of P2 receptors causes release of IL-1beta-loaded microvesicles from human dendritic cells. *Blood* **2007**, *109*, 3856–3864. [CrossRef] [PubMed]
130. Bianco, F.; Pravettoni, E.; Colombo, A.; Schenk, U.; Moller, T.; Matteoli, M.; Verderio, C. Astrocyte-derived ATP induces vesicle shedding and IL-1 beta release from microglia. *J. Immunol.* **2005**, *174*, 7268–7277. [CrossRef]
131. Kao, Y.C.; Chang, Y.W.; Lai, C.P.; Chang, N.W.; Huang, C.H.; Chen, C.S.; Huang, H.C.; Juan, H.F. Ectopic ATP synthase stimulates the secretion of extracellular vesicles in cancer cells. *Commun. Biol.* **2023**, *6*, 642. [CrossRef] [PubMed]
132. MacKenzie, A.; Wilson, H.L.; Kiss-Toth, E.; Dower, S.K.; North, R.A.; Surprenant, A. Rapid secretion of interleukin-1beta by microvesicle shedding. *Immunity* **2001**, *15*, 825–835. [CrossRef]
133. Soni, S.; O'Dea, K.P.; Tan, Y.Y.; Cho, K.; Abe, E.; Romano, R.; Cui, J.; Ma, D.; Sarathchandra, P.; Wilson, M.R.; et al. ATP redirects cytokine trafficking and promotes novel membrane TNF signaling via microvesicles. *FASEB J.* **2019**, *33*, 6442–6455. [CrossRef]
134. Gutierrez-Martin, Y.; Bustillo, D.; Gomez-Villafuertes, R.; Sanchez-Nogueiro, J.; Torregrosa-Hetland, C.; Binz, T.; Gutierrez, L.M.; Miras-Portugal, M.T.; Artalejo, A.R. P2X7 receptors trigger ATP exocytosis and modify secretory vesicle dynamics in neuroblastoma cells. *J. Biol. Chem.* **2011**, *286*, 11370–11381. [CrossRef] [PubMed]
135. Kholia, S.; Jorfi, S.; Thompson, P.R.; Causey, C.P.; Nicholas, A.P.; Inal, J.M.; Lange, S. A novel role for peptidylarginine deiminases in microvesicle release reveals therapeutic potential of PAD inhibition in sensitizing prostate cancer cells to chemotherapy. *J. Extracell. Vesicles* **2015**, *4*, 26192. [CrossRef]
136. Park, M.; Kim, J.; Phuong, N.T.T.; Park, J.G.; Park, J.H.; Kim, Y.C.; Baek, M.C.; Lim, S.C.; Kang, K.W. Involvement of the P2X7 receptor in the migration and metastasis of tamoxifen-resistant breast cancer: Effects on small extracellular vesicles production. *Sci. Rep.* **2019**, *9*, 11587. [CrossRef]
137. Giuliani, A.L.; Berchan, M.; Sanz, J.M.; Passaro, A.; Pizzicotti, S.; Vultaggio-Poma, V.; Sarti, A.C.; Di Virgilio, F. The P2X7 Receptor Is Shed Into Circulation: Correlation With C-Reactive Protein Levels. *Front. Immunol.* **2019**, *10*, 793. [CrossRef]
138. Ronquist, K.G.; Ek, B.; Stavreus-Evers, A.; Larsson, A.; Ronquist, G. Human prostasomes express glycolytic enzymes with capacity for ATP production. *Am. J. Physiol. Endocrinol. Metab.* **2013**, *304*, E576–E582. [CrossRef]
139. Ronquist, K.G.; Ek, B.; Morrell, J.; Stavreus-Evers, A.; Strom Holst, B.; Humblot, P.; Ronquist, G.; Larsson, A. Prostasomes from four different species are able to produce extracellular adenosine triphosphate (ATP). *Biochim. Biophys. Acta* **2013**, *1830*, 4604–4610. [CrossRef]
140. Svitkina, T. The Actin Cytoskeleton and Actin-Based Motility. *Cold Spring Harb. Perspect. Biol.* **2018**, *10*, a018267. [CrossRef] [PubMed]
141. Yang, Q.; Diamond, M.P.; Al-Hendy, A. The emerging role of extracellular vesicle-derived miRNAs: Implication in cancer progression and stem cell related diseases. *J. Clin. Epigenet.* **2016**, *2*, 13. [PubMed]
142. Wozniak, A.L.; Adams, A.; King, K.E.; Dunn, W.; Christenson, L.K.; Hung, W.T.; Weinman, S.A. The RNA binding protein FMR1 controls selective exosomal miRNA cargo loading during inflammation. *J. Cell Biol.* **2020**, *219*, e201912074. [CrossRef] [PubMed]
143. Antonioli, L.; Blandizzi, C.; Pacher, P.; Hasko, G. Immunity, inflammation and cancer: A leading role for adenosine. *Nat. Rev. Cancer* **2013**, *13*, 842–857. [CrossRef] [PubMed]
144. Morello, S.; Pinto, A.; Blandizzi, C.; Antonioli, L. Myeloid cells in the tumor microenvironment: Role of adenosine. *Oncoimmunology* **2016**, *5*, e1108515. [CrossRef]
145. Vijayan, D.; Young, A.; Teng, M.W.L.; Smyth, M.J. Targeting immunosuppressive adenosine in cancer. *Nat. Rev. Cancer* **2017**, *17*, 765. [CrossRef]
146. Furuta, K.; Onishi, H.; Ikada, Y.; Masaki, K.; Tanaka, S.; Kaito, C. ATP and its metabolite adenosine cooperatively upregulate the antigen-presenting molecules on dendritic cells leading to IFN-gamma production by T cells. *J. Biol. Chem.* **2023**, *299*, 104587. [CrossRef]

147. Casey, M.; Segawa, K.; Law, S.C.; Sabdia, M.B.; Nowlan, B.; Salik, B.; Lee, C.; Winterford, C.; Pearson, S.; Madore, J.; et al. Inhibition of CD39 unleashes macrophage antibody-dependent cellular phagocytosis against B-cell lymphoma. *Leukemia* **2023**, *37*, 379–387. [CrossRef]
148. Cekic, C.; Linden, J. Adenosine A2A receptors intrinsically regulate CD8+ T cells in the tumor microenvironment. *Cancer Res.* **2014**, *74*, 7239–7249. [CrossRef] [PubMed]
149. Antonioli, L.; Fornai, M.; Pellegrini, C.; D'Antongiovanni, V.; Turiello, R.; Morello, S.; Hasko, G.; Blandizzi, C. Adenosine Signaling in the Tumor Microenvironment. *Adv. Exp. Med. Biol.* **2021**, *1270*, 145–167. [CrossRef]
150. Gutknecht da Silva, J.L.; Passos, D.F.; Cabral, F.L.; Miron, V.V.; Schetinger, M.R.C.; Cardoso, A.A.; Dal Piva, C.H.; Gomes, C.O.; Ebone, R.S.; Leal, D.B.R. Istradefylline induces A2A/P2X7 crosstalk expression inducing pro-inflammatory signal, and reduces AKT/mTOR signaling in melanoma-bearing mice. *Med. Oncol.* **2023**, *40*, 178. [CrossRef]
151. Ma, Y.; Adjemian, S.; Yang, H.; Catani, J.P.; Hannani, D.; Martins, I.; Michaud, M.; Kepp, O.; Sukkurwala, A.Q.; Vacchelli, E.; et al. ATP-dependent recruitment, survival and differentiation of dendritic cell precursors in the tumor bed after anticancer chemotherapy. *Oncoimmunology* **2013**, *2*, e24568. [CrossRef] [PubMed]
152. Zanoni, M.; Sarti, A.C.; Zamagni, A.; Cortesi, M.; Pignatta, S.; Arienti, C.; Tebaldi, M.; Sarnelli, A.; Romeo, A.; Bartolini, D.; et al. Irradiation causes senescence, ATP release, and P2X7 receptor isoform switch in glioblastoma. *Cell Death Dis.* **2022**, *13*, 80. [CrossRef] [PubMed]
153. Szymczak, B.; Czarnecka, J.; Czach, S.; Nowak, W.; Roszek, K. Purinergic approach to effective glioma treatment with temozolomide reveals enhanced anti-cancer effects mediated by P2X7 receptor. *Cell Signal* **2023**, *106*, 110641. [CrossRef] [PubMed]

Publikacja 2

Purinergic approach to effective glioma treatment with temozolomide reveals synergistic anti-cancer effects mediated by P2X7 receptor

Autorzy: **Szymczak, B.**, Czarnecka, J., Czach, S., Nowak, W., & Roszek, K.

Rok publikacji: 2023

DOI: https://doi.org/10.1016/j.cellsig.2023.110641

Artykuł wydany w czasopiśmie: Cellular Signalling

Wydawnictwo: Elsevier

Punktacja według wykazu Ministerstwa Nauki i Szkolnictwa Wyższego (2023): 100 pkt

Journal Impact Factor (2023): 4,4 pkt

Liczba cytowań: 2 (Web of Science, stan na 09.2024);

2 (Google Scholar, stan na 09.2024)

Cellular Signalling 106 (2023) 110641

Contents lists available at ScienceDirect

Cellular Signalling

journal homepage: www.elsevier.com/locate/cellsig

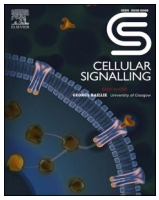

Purinergic approach to effective glioma treatment with temozolomide reveals enhanced anti-cancer effects mediated by P2X7 receptor

Bartosz Szymczak [a], Joanna Czarnecka [a], Sylwia Czach [b], Wiesław Nowak [b], Katarzyna Roszek [a,*]

[a] Department of Biochemistry, Faculty of Biological and Veterinary Sciences, Nicolaus Copernicus University in Torun, Lwowska 1, 87-100 Torun, Poland
[b] Institute of Physics, Faculty of Physics, Astronomy and Informatics, Nicolaus Copernicus University in Torun, Grudziądzka 5, 87-100 Torun, Poland

ARTICLE INFO

Keywords:
Glioma
Purinergic signaling
Temozolomide
P2X7 receptor
Molecular docking

ABSTRACT

The purinergic signaling pathway is the oldest evolutionary transmitter system that regulates a wide array of physiological and pathophysiological processes in central nervous system. However, the question of how the purinergic compounds interact with administrated drugs is rarely addressed. We aimed to clarify the interplay between purinergic signaling and chemotherapeutic drug temozolomide (TMZ) in human glioma cell line.

We applied an initial retinoic acid-induced differentiation of A172 glioma cells and tested the P2X7 receptor expression in undifferentiated and differentiated gliomas. We compared the P2X7 receptor agonists/antagonists influence and their co-action with TMZ in both cell types through assessment of cell proliferation, viability and migrative properties. Molecular docking allowed to indicate the potential binding site for TMZ in the structure of hP2X7 receptor. Differentiated cells turned out to be more susceptible to ATP and TMZ alone but also to the concerted action of TMZ and ATP. Enhanced effects triggered by ATP and TMZ treatment include the decreased by 70% viability, and reduced migration ability of differentiated A172 glioma cells. Noteworthy, these results can be achieved already at low non-toxic ATP concentration and at reduced to 125 μM effective concentration of TMZ.

Therefore, ATP molecules must be present and maintained at appropriate concentration in glioma cells microenvironment to achieve their co-action with TMZ and enhanced anti-cancer activity. All that, in turn, could shorten the therapy, increase its efficacy and limit the side effects for the patient. Our purinergic approach creates a promising perspective for developing novel combined oncological therapies.

1. Introduction

Glioblastoma multiforme (GBM) is the most aggressive type of malignant tumor in the brain. Current hypothesis assumes that GBM arises from an accumulation of somatic mutations in neural stem cells (NSCs) and glial precursor cells that confer selective growth promotion, resulting in uncontrolled proliferation [1,2]. Another model has suggested that GBM arises from committed precursor cells, such as glial precursor cells (GPCs), oligodendrocyte precursors, and astrocytes. Regardless the cell origin and several existing therapeutic modalities, GBM still has a poor prognosis and high mortality rates. The outcome results from a low differentiation of cells, genetic instability, and increased incidence of cancer cells invasion into surrounding tissue, however gliomas almost never metastasize out of the brain [3–5].

The most commonly used chemotherapeutic agents include temozolomide, a cytostatic drug that binds to the DNA structure, and nitrosourea derivatives with an alkylating effect [6,7]. Temozolomide (TMZ, chemical name: 4-oxo-3-(trideuteriomethyl)imidazo[5,1-d][1,2,3,5]tetrazine-8-carboxamide) is a small (194 Da) lipophilic molecule administrated *via* oral route. TMZ is rapidly absorbed in intact form due to its stability at acidic pH. At pH values over 7.4, TMZ undergoes spontaneous breakdown to form monomethyl triazene 5-(3-methyltriazen-1-yl)-imidazole-4-carboxamide (MTIC). MTIC further reacts with water to liberate 5-aminoimidazole-4-carboxamide (AIC) and the highly reactive methyldiazonium cation [8]. Inside the cells, active TMZ derivatives methylate irreversibly DNA bases leading to G2/M cell cycle arrest and apoptosis [6,8].

TMZ molecules exhibit relatively high affinity to biological membranes; however, the prodrug concentration decreases after administration. Its cationic form, MTIC, has a low affinity to biological membranes and permeability through barriers, so it is challenging to reach the target cells in effective concentrations [9]. Consequently, high

* Corresponding author.
E-mail address: kroszek@umk.pl (K. Roszek).

https://doi.org/10.1016/j.cellsig.2023.110641
Received 4 December 2022; Received in revised form 22 February 2023; Accepted 23 February 2023
Available online 28 February 2023

doses of the drug should be administered, which augments the side effects (gastrointestinal troubles such as nausea and vomiting, fatigue, anemia, thrombocytopenia) of the therapy [10]. Moreover, in the long run, monotherapy with chemotherapeutic agents causes the phenomenon of selection pressure, leading to the formation of secondary chemoresistant neoplasms [11].

The limitations of the current treatment modalities call for the development of novel therapeutic approaches targeting cancer cell-specific biological features and pathways. Recently, induction of cellular differentiation has become an attractive therapeutic strategy against glioma cell proliferation and tumorigenicity. Several differentiation-inducing agents, including neomycin and retinoic acid (RA), have been tested with promising outcomes [12,13].

Extracellular purine nucleosides (adenosine, guanosine) and nucleotides (mainly ATP and GTP) have been widely accepted as signaling molecules acting in different cells and tissues throughout the human body, including cancer cells. The purinergic signaling system is the oldest evolutionary transmitter system that regulates a wide array of physiological and pathophysiological processes [14,15]. The finding that ecto-ATP is an abundant constituent of the tumor microenvironment is perhaps one of the most important recent discoveries in cancer biology [16]. Consistently, different cancer cells express high P2X7 receptor (P2X7R) levels. P2X7R has attracted much scientific attention as a potential new target of anti-cancer therapies for various and sometimes opposite reasons [17,18]. On one side, it has been proposed that its growth-promoting activity could be targeted. Thus, we could take advantage of the multiple and well-known highly selective P2X7R inhibitors developed by the pharma industry [19]. On the other, it was suggested that P2X7R-initiated cytotoxic activity could be exploited to kill tumor cells, presumably sparing healthy cells, thanks to their lower level of P2X7R expression [20].

Concerted action of various ecto-nucleotidases leads to sequential hydrolysis of extracellular nucleotides, thus, the precise control of enzymatic activity allows for maintaining the ecto-nucleotides/nucleosides balance in the tumor microenvironment. ATP can be metabolised by ecto-NTPDases (ecto-nucleoside triphosphate diphosphohydrolases), NPPs (nucleotide pyrophosphatase/phosphodiesterases) or adenylate kinase to ADP and AMP [21]. Ecto-adenosine is then produced from AMP by ecto-5′-nucleotidase (CD73), an enzyme highly expressed in many solid tumors [22,23]. Adenosine has been considered as a critical factor enhancing the progression of tumors, and CD73 emerges recently as a target for glioblastoma treatment [24]. In conclusion, ectonucleotidases create an indispensable enzyme system and an emerging target of innovative therapies [21].

The high heterogeneity of glioblastoma multiforme has been reflected in their response to purinergic signals. Several human glioblastoma cell lines such as U-138MG, U-87MG, and U-251MG were reported to increase their proliferation rate in the presence of both ATP and adenosine [25,26]. The mechanism of this phenomenon stays unclear. On one hand, the increase in proliferation and migration of glioblastoma cells has been attributed to activation of the P2X7 receptor [27]; on the other - P2X7 receptor expression is decreased in gliomas [28,29]. However, some human glioblastoma cell lines have retained the "physiological" expression and function of the P2X7 receptor, and ATP in concentrations above 1 mM is cytotoxic to them [25]. Thus, the M059J cells with a high level of P2X7 receptor expression are sensitive to ionizing radiation and ATP-mediated cell death [30].

Adenosine stimulates the progression of glioma cells through the activation of the A2a receptor [31] and A3 receptor, which promotes migration [32]. On the other hand, adenosine was reported to have antiproliferative activity in different glioblastoma cell lines [33], and to reduce the pool of glioblastoma stem cells.

Considering these existing inconclusive results, we aimed to reinvestigate the anti-cancer effects of purine signaling molecules in model A172 glioma cells, and shed more light on their interactions within the cell microenvironment. We proposed a completely novel approach: a prior differentiation of glioma cells and subjecting them to purinergic signals. Additionally, we considered the interplay between purinergic signaling and established therapeutic – temozolomide, and its effects on human glioma cells. We have elucidated, for the first time, the possible hP2X7R interaction with TMZ. Within therapeutic context, we provide relevant data on the effects triggered by RA-mediated differentiation and combined ATP/TMZ treatment in human glioma cells.

2. Experimental part

2.1. Materials and methods

2.1.1. Cell line

Cells of human glioma cell line A172 were purchased from American Type Culture Collection (ATCC) were grown according to manufacturer protocol in high-glucose DMEM medium with 4.5 g/L glucose (Biowest, France) supplemented with 10% fetal bovine serum (FBS) (Biowest, France), 100 IU/mL penicillin and 100 μg/mL streptomycin (Biowest, France), and cultured in a humidified incubator supplied with 5% CO_2 at 37 °C.

2.1.2. Differentiation of A172 cells

The neuronal differentiation protocol was based on the literature data [13,34]. Cells were seeded at a density of 10,000 cells/cm^2 in the culture medium described above. After adhesion, the culture medium was replaced with high-glucose DMEM, 10% FBS, 100 IU/mL penicillin, and 100 μg/mL streptomycin supplemented with 10 μM retinoic acid (Sigma-Aldrich, Germany). The culture was carried out for 14 days, and the medium was changed every 72 h. The passages were performed on the 5th and 11th day from the start of differentiation, in the 1: 3 ratio.

2.1.3. The growth kinetics of undifferentiated and differentiated A172 cells

Cell growth was assessed by determination of the total cell number and their proliferation rate. Initially, cells were seeded at a density of 2.5×10^5 per plate of 6 cm diameter, and cultured under standard conditions, with or without 10 μM retinoic acid (for differentiated and undifferentiated cells, respectively). The cells were passaged every 3 days, and the cell number was counted using Thoma chamber, after 0.4% trypan blue staining.

2.1.4. The gene expression analysis in undifferentiated and differentiated A172 cells

Gene expression was analyzed at the mRNA level. Undifferentiated and differentiated A172 cells at a subconfluent state were detached with 0.25% trypsin and re-suspended in lysis buffer. mRNA was isolated using the RNeasy Mini Kit (Qiagen, Germany). The concentration of the RNA preparation was determined spectrophotometrically using an Epoch Take 3 reader (Agilent BioTek, USA). The obtained material was DNAsed with the DNase I, RNase-free kit (ThermoFischer Scientific, USA) using T100 Thermal Cycler (BioRad, USA).

The mRNA was used as a substrate in the reverse transcription (RT) reaction (RevertAid First Strand cDNA Synthesis Kit, ThermoFischer Scientific, USA). The reaction was carried out for 60 min at 42 °C and stopped for 5 min at 70 °C in a T100 Thermal Cycler (BioRad, USA). The obtained cDNA served as a template for the quantitative analysis of the genes expression level in the Real-Time qPCR reaction.

The Real-Time PCR reaction was performed using the LightCycler 480 SYBR Green I Master kit (Roche, Switzerland), 50 ng cDNA, and synthesized primers (IBB PAN, Poland) listed below with a final concentration of 0.4 μM using LightCycler480 (Roche, Switzerland). Subsequent stages of reaction were as follows: initial denaturation 95 °C, 5 min. (1 cycle); denaturation 95 °C, 10 s.; annealing 60 °C, 20 s.; extending 72 °C, 20 s. (45 cycles). The results were analyzed with the LightCycler 480 SW 1.5.1 software (Roche, Switzerland) with reference

to the expression level of actin and GAPDH genes.

Primers' sequences for the analyzed genes. Primers were designed with the Primer3Plus software (http://www.bioinformatics.nl/cgi-bin/primer3plus/primer3plus.cgi) based on cDNA sequences from the NCBI database (https://www.ncbi.nlm.nih.gov/). Primers parameters were analyzed in OligoAnalyzer Tool (https://eu.idtdna.com/calc/analyzer), specificity was confirmed using the Primer BLAST software (https://www.ncbi.nlm.nih.gov/tools/primer-blast/).

Gene name	Access number	Primer sequence: Forward (5′ → 3′) Reverse (5′ → 3′)	Product (bp)
NES	>NM_006617.1	F: GGAAGAGAACCTGGGAAAGG R: GATTCAGCTCTGCCTCATCC	188
GFAP	>S40719.1	F: GTGGTGAAGACCGTGGAGAT R: CGGAGCAACTATCCTGCTTC	145
TUJ1	>U47634.1	F: GAAGAGGGCGAGATGTACGA R: TTTAGACACTGCTGGCTTCG	122
P2X7	>Y09561.1	F: GACGCTCTGTTCCTCTGACC R: TCACAGGTCTTCTGGTTCCC	111
NTPDase1	>NM_001776.6	F: GGGAAAGACGAGGAAAGAG R: TCTGGCAATGCTTTGTTCTG	176
NTPDase5	>NM_001249.4	F: GCATTTGCCAACACCTTTTT R: ACAGGGCTCTCTGTGATGCT	179
NTPDase6	>NM_001247.5	F: GCACTGAAGCCAGGTCTTTC R: GGGCCTTTTCTCCAGGTAAC	172
AK	>NM_000476.3	F: GGCTTCCTGATTGATGGCTA R: CTGGTCTCTCCACGTTTCAAG	143
5' NT	>NC_000006.12	F: CGCAACAATGGCACAATTAC R: CAGGTTTTCGGGAAAGATCA	196
GAPDH	>NC_000012.12	F: GAGTCAACGGATTTGGTCGT R: GACAAGCTTCCCGTTCTCAG	185
Actin	>NC_000007.14	F: ATCCACGAAACTACCTTCAA R: TCTTGATCTTCATTGTGCTG	166

2.1.5. Western blotting analysis

Undifferentiated and differentiated A172 cells at a subconfluent state were detached with 0.25% trypsin and re-suspended in lysis buffer. Twenty micrograms of total protein was loaded on Bolt™ 4 to 12%, Bis-Tris, 1.0 mm precast gels (Invitrogen) and transferred to NC membranes (Invitrogen) by dry transfer. Membranes were blocked with 5% skim milk solution in TBS-Tween (0.1%) buffer for 1 h at room temperature and incubated overnight at 4 °C with primary antibody against P2X7R (1:200, rabbit polyclonal, Sigma-Aldrich). The blots were incubated with appropriate secondary antibodies conjugated to alkaline phosphatase (1:1000, Sigma-Aldrich) and visualized using NBT/BCIP Tablets (Roche). The density of bands was measured with ScienceLab software.

2.2. Cell viability assays

Cell viability screening was assessed using MTT test based on the activity of mitochondrial enzymes and their ability to reduce MTT salts to formazan. Undifferentiated and differentiated A172 cells were seeded at density 15,000 cells/cm^2 in 48-well plates. After 24 h, the culture media were replaced with 80–500 μM ATP, ADP, adenosine (Sigma-Aldrich, Germany), 8–100 μM BzATP (2′(3′)-O-(4-Benzoylbenzoyl) adenosine 5′-triphosphate; Sigma-Aldrich, Germany), 1 μM A740003 (Sigma-Aldrich, Germany), 100–1000 μM temozolomide (TMZ) (Sigma-Aldrich, Germany), respectively, or combination of various compounds. After 72 h of incubation, the medium was replaced with 0.5 mg/mL MTT (Sigma-Aldrich, Germany) in the culture medium. After 30 min of incubation at 37 °C, the MTT solution was removed, and the formed formazan crystals were dissolved in 300 μL of DMSO (Chempur, Poland). The absorbance of the solution was measured at 570 nm, using an Epoch Take 3 plate reader. The experiment was performed in 4 replications. Cell viability was calculated as a percentage of the untreated samples reflecting positive control (100%).

Analogously, for treatment with temozolomide and ATP, undifferentiated and differentiated A172 cells were seeded at density 15,000 cells/cm^2 in 48-well plates. After adhesion, the culture medium was removed, fresh medium was supplemented with 500 μM TMZ for undifferentiated cells and 125 μM TMZ (approx. EC50 values) for differentiated cells, whereas control cells media did not contain TMZ. Concentrations between 80 and 500 μM ATP with NTPDase inhibitor, 100 μM BGO (1-naphthol-3,6-disulfonic acid; BG0136, Sigma-Aldrich, Germany) [35] or P2 receptor agonist, 8–100 μM BzATP were added to the fresh culture medium. Cell viability was tested after 72 h by the trypan blue staining and MTT test according to the procedure described above, as well as by the neutral red uptake (NRU) assay.

NRU assay is based on the cell capability to uptake the dye by functional lysosomes. Aliquots of 0.33% neutral red (Sigma-Aldrich, Germany) were added to the medium of growing cells and incubated for 50 min, then the solution was aspirated and cells washed with pre-warmed PBS. To dissolve the accumulated dye, 1% acetic acid in 50% ethanol was added. All samples were measured spectrophotometrically at 540 nm.

2.3. Scratch test

Scratch assay reflects the ability of adherent cells to migrate and "close" the artificial gap (scratch). Based on Liang et al. [36], undifferentiated and differentiated A172 cells were seeded at a density 25,000 cells/cm^2 in 24-well plates. After 24 h, confluent cell monolayers were scraped with a tip to create a "scratch". Subsequently, the medium was replaced with fresh medium supplemented with P2X7 purinergic receptor agonists: 100 μM ATP (in the presence of 100 μM BGO as ATP hydrolysis inhibitors) and 10 μM BzATP, or with 125/500 μM temozolomide (without and with ATP and BzATP for TMZ interplay with P2X7 receptor agonist analysis). The culture images were captured at the experiment beginning and after 4, 8, 12, and 24 h using the MOTIC AE30 microscope with x100 magnification and Motic Camera. Analysis of images was performed by Motic Images Plus 2.0 software (Motic Europe, Spain). Migration rate was calculated as a relative scratch closure, the scratch width at the time 0 was taken as 1.

2.4. Membrane and soluble enzymes activity assay

Undifferentiated and differentiated A172 cells were seeded in 6-well plates at a density 25,000 cells/cm^2. Enzymatic reactions were performed on the surface of the adherent cell layer (membrane ecto-enzymes), and in collected culture media (soluble and microvesicle membrane-anchored *exo*-enzymes). All enzymatic reactions were performed in triplicate. The reaction mixtures contained 35 mM Tris-HCl pH 7.0, 250 mM sucrose, 10 mM glucose, 3 mM Mg^{2+}, 2 mM Ca^{2+}, 0.1 mM dipyridamole, and 2 mM substrate (ATP, ADP or AMP). 2.5 mM levamisole (Sigma-Aldrich, Germany) was used as a phosphatase inhibitor, 10 μM Ap5A (diadenosine pentaphosphate pentasodium salt; Sigma-Aldrich, Germany) was used as an inhibitor of adenylate kinase and as a blocker of NPPase-mediated hydrolysis. After 90 min of incubation at 37 °C, the reaction was stopped by transferring the post-incubation mixture to a tube containing 1 M $HClO_4$ (POCh, Poland), and neutralized with 1 M KOH (Chempur, Poland). All samples were delipidated by shaking with n-heptane (POCh, Poland) and frozen for further analyses at −20 °C.

2.5. Protein concentration measurement

Determination of protein concentration in cell lysates after the reaction and in post-culture media was performed. Protein concentration was measured spectrophotometrically at 280 nm using an Epoch Take 3 reader and Epoch3 software, with the appropriate lysis buffer and control media as a blind sample.

2.6. High-performance liquid chromatography (HPLC)

The qualitative and quantitative composition of the reaction mixtures was analyzed by HPLC method using Waters chromatograph (In-Line Degasser AF, 515 HPLC Pump, Waters Pump Control Module, Waters 2487 Dual Absorbance Detector, Waters 717 Plus Autosampler) (Waters Corporation, USA), on Merck Chromolith Performance column (100 × 4.6 mm) with Merck Chromolith Performance pre-column (Merck, Germany). The separation was carried out under isocratic conditions with KH_2PO_4/K_2HPO_4 buffer pH 7.0 with 5 mM EDTA, 25 mM TBA, and 2.5% MeOH (J.T.Baker Chemical Company, USA) as the mobile phase.

20 μL of the delipidated and centrifuged samples (10 min, 10,000 *g*, Sartorius 3 K30) (Sartorius, Germany) was applied to the column. The separation was carried out at a flow rate of 1 mL/min. Compounds were identified on the basis of retention times of standard solutions at 260 nm. The compound concentration was calculated from the surface area using Millenium 32 software (Waters Corporation, USA).

2.7. Molecular docking studies

In Protein Data Bank (PDB) only rat (*Ratus norvegicus*) P2X7 receptors have complete structures determined by CryoEM technique [37]. Since amino acid sequences of a predominant isoform A of human P2X7R (UniProtKB ID: Q99572, GeneBank: CAA73360) and rat P2X7R are similar (>90%), we used the rat structure (PDB: 6U9V, closed state) as a template for the construction of hP2X7R model. The SWISS-MODEL server was used for this aim [38]. Hydrogen atoms corresponding to pH = 7 were added using Maestro code (Schroedinger Inc.). The quality of the resulting structure was verified with Procheck software [39]. The outcome was positive: only a few residues from loop regions located far from binding cavities important in this study had conformations slightly beyond a standard deviation. Thus, we are confident that focused docking of ATP, TMZ, BzATP and other ligands to this model is meaningful.

We performed molecular docking of ATP, TMZ, BzATP and MTIC to the hP2X7R model using SMINA package [40], a fork of Autodock Vina [41] that provides enhanced support for minimization and scoring. The docking region was restricted to 18x23x30 $Å^3$ box centered at ATP binding pocket delineated by Lys64, Lys66, Thr189, Lys193, Asn292, Arg294 and Lys311 residues. We performed 20 independent docking runs with flexible ligands, using default SMINA settings, generating 100 poses per run. For further analysis, poses with the best values (*i.e.*, the lowest values of SMINA scoring function, SSF) and located in the physiologically relevant region were chosen. We visualized results with the VMD code [42].

2.8. Ethidium bromide influx into A172 cells

Undifferentiated and differentiated A172 cells were seeded in 96-well plates and incubated in the presence of 10 μg/mL ethidium bromide for 10 min. Ethidium bromide influx was evaluated with a fluorescence plate reader (Epoch Take 3, excitation and emission wavelengths were 530 and 590 nm, respectively), upon addition of different P2X7 receptor ligands: 500 μM ATP, 50 μM BzATP, 125 μM TMZ (EC50 for differentiated A172 cells), or their combinations.

2.9. Statistical analyses

The experiments were performed in four independent replications. Statistical analyses were performed using the Past software version 4.02. Results are presented as means with error bars representing SD. The difference in gene expression value was determined using the Mann-Whitney test; the difference in cells viability was determined using the χ^2 test; the difference in migration assay was determined by two-way ANOVA followed by Tukey post-test for multiple comparisons. Differences were considered statistically significant at p-value ≤ 0.05. The statistical significance of the differences between samples is marked in the graphs with asterisks (* for $p \leq 0.05$, ** for $p \leq 0.01$, *** for $p \leq 0.001$).

3. Results

Fourteen-days treatment of A172 cells with 10 μM retinoic acid inhibited cell growth (Fig. 1C) and induced some alterations in cell culture arrangement – cells are orderly and do not form clumps (Fig. 1A, B). Marker gene expression analysis indicated that retinoic acid stimulated A172 differentiation predominantly to neuronal lineage cells, which was confirmed with up-regulation of nestin (NES) and neuron-specific beta-tubulin (TUJ1) marker genes (Fig. 1D).

Consequently, the expression of P2X7R – a nucleotide receptor abundantly expressed in neural cells has also been considerably up-regulated on the gene level and slightly increased on the protein level after differentiation (Fig. 1D and E). The P2X7R engagement in cell proliferation, cell growth, differentiation, and apoptosis of normal and cancer cells in the nervous system is widely reported [43,44]. Therefore, the observed changes should be reflected in alterations of glioma cells invasiveness and migration.

Bearing in mind the pivotal role of purinergic enzymes in regulating ecto-nucleotides and ecto-nucleosides concentrations, we decided to investigate how the retinoic acid-induced differentiation of A172 glioma cells has changed the expression and activity of ecto- end exoenzymes metabolizing nucleotides. Fig. 2A presents schematically the concerted action of various ecto-enzymes metabolizing nucleotides and controlling their levels.

In general, all the observed changes tend to decrease the genes expression and extracellular activity of nucleotide metabolizing enzymes, which will underlie the modified cell response to nucleotides and nucleosides. NTPDase1 is the only ecto-nucleotidase up-regulated in differentiated glioma cells (Fig. 2B), whereas NTPDase2, 3, and 8 are not expressed neither in undifferentiated nor in differentiated cells (data not shown). Thus, the decreased ecto-ATPase activity (Fig. 2C) can be ascribed rather to phosphatases than to NTPDase1. Together with the increased expression of P2X7R, it suggests the more pronounced cellular response to ATP stimulation. It can be both pro-proliferative and detrimental, depending on ATP concentration, cell type or extracellular microenvironment. Adenylate kinase expression and activity is also decreased, resulting in a lower level of phospho-transfer reactions. Decreased adenosine production from AMP by 5'NT indicates the lower sensitivity to its pro-proliferative influence.

Cell viability in different concentrations of extracellular adenosine, ADP and ATP has been determined – Fig. 3A-C. The obtained results confirmed the abovementioned assumption that differentiated A172 become more susceptible to microenvironmental purines. Adenosine influence on viability triggers the slight increase in cell number at 80 and 100 μM, and decrease in cell number at concentration 500 μM for undifferentiated A172 cells. For differentiated A172 cells, the effect of reduced viability is observed at 100–500 μM concentration (Fig. 3A). This changeability could be explained by the activation of different sensitivity P1 receptors. ADP influence on A172 cells reveals the initial rise in cell viability that can be ascribed to ADP hydrolysis to AMP and further to adenosine, and consequently to the pro-proliferative action of Ado low concentrations. Another possible explanation is the ADP-dependent activation of P2Y13 receptor, abundantly expressed in the nervous system cells, and promotion of cell growth as suggested in literature [45,46]. The only decrease in viable cell number was observed for differentiated cells (Fig. 3B). ATP-mediated decrease in cell viability was specifically more pronounced in differentiated cells at ATP concentrations around 80–100 μM (Fig. 3C). BGO as specific NTPDase inhibitor decreased the hydrolytic activity towards ATP and led to reduced cell viability. To confirm that increased sensitivity to ATP-induced cell death has been mediated mainly through P2X7 receptor signaling, we

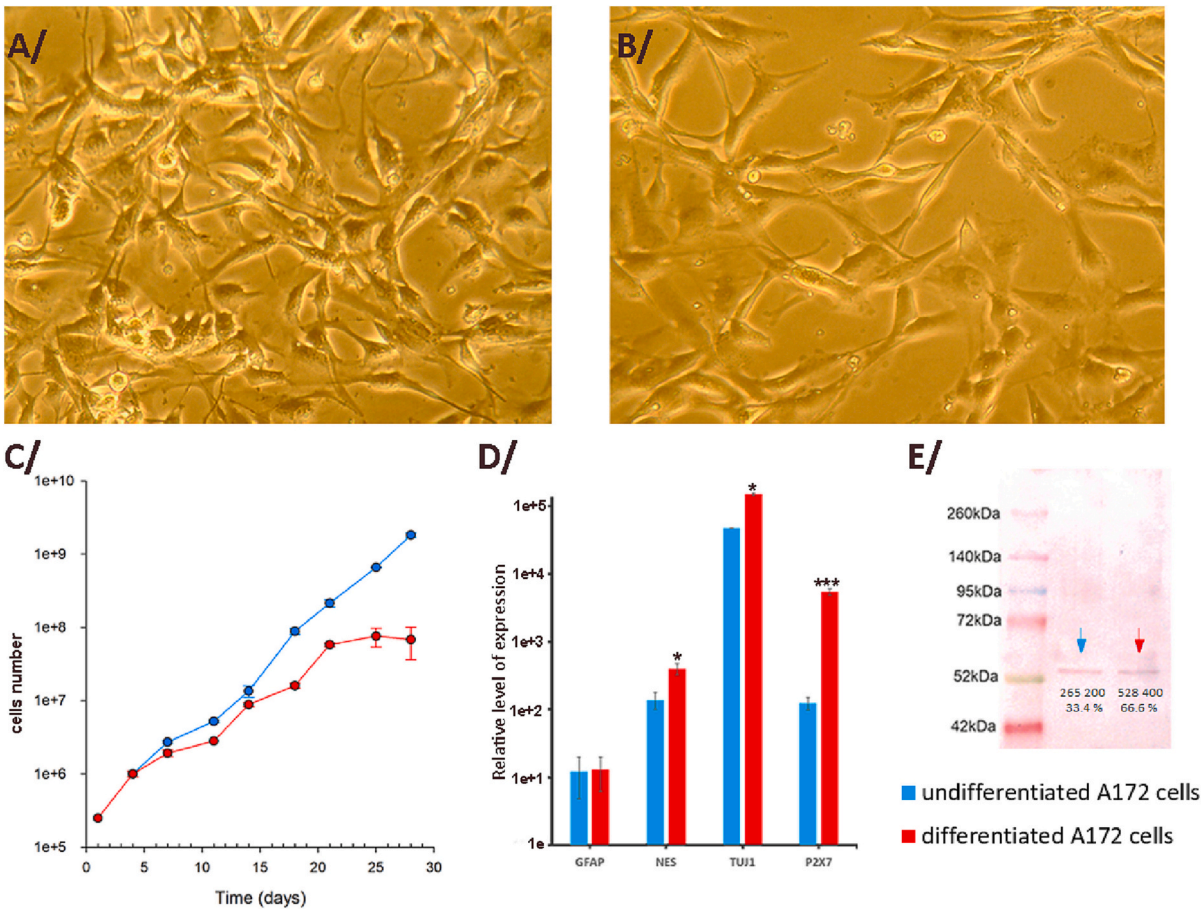

Fig. 1. Retinoic acid-induced differentiation of A172 cells: A/ representative image of undifferentiated A172 cells; B/ representative image of alterations triggered by 10 μM retinoic acid-induced differentiation procedure; C/ decreased proliferation observed during differentiation; D/ changes in P2X7 receptor and the marker genes expression; E/ changes in P2X7 receptor protein expression: the numbers indicate the absolute value of band intensity (arbitrary units) and the percentage of density. The statistical significance of the differences between undifferentiated and differentiated cells is marked in the graphs with asterisks (* for $p \leq 0.05$, *** for $p \leq 0.001$, number of samples $n = 4$).

determined the A172 viability in the presence of BzATP, a non-physiological and non-hydrolyzable ATP analogue that is considered an agonist of mainly P2X7R, but also of P2X1 and P2Y1 receptors – Fig. 3D.

This set of results confirmed that the glioma cells differentiation (followed by up-regulated expression of P2X7R, and together with decreased nucleotidase activity) underlies the changed strength of purinergic signals, mainly ATP. Moreover, we have assumed that these alterations are also potent for modifying the differentiated glioma cells response to commonly used chemotherapy. We decided to verify this hypothesis and disclose the nucleotides and nucleosides interplay with a chemotherapeutic agent – temozolomide (TMZ). TMZ itself decreases A172 cell proliferation with EC50 around 500 μM for undifferentiated cells and around 125 μM for differentiated ones (Fig. 4A). Thus, the described here differentiation procedure allows for reducing the drug effective dose by four times. Additionally, a combination of the half-maximal effective concentration of TMZ and purinergic compounds, P2X7 receptor ligands (in concentrations ranging from 80 to 500 μM for ATP and from 8 to 100 μM for BzATP) influenced the viability of A172 cells even stronger than TMZ alone, suggesting the enhancement of cytotoxic effect of the combined compounds, triggered mainly in differentiated glioma cells (Fig. 4B-C). We have analyzed the augmentation of TMZ efficacy by ATP – only 100 μM ATP, when added with TMZ (at a concentration equal to its EC50 value), has decreased cell viability by an additional 20–25% for undifferentiated cells, and by 75% for differentiated ones. Qualitatively similar results were also obtained for combined BzATP and TMZ action. Parallelly, the addition of 1 μM A740003 (specific antagonist of P2X7 receptors) reversed the cytotoxic effect in differentiated A172 cells – Fig. 4D-E. The improvement in cell viability may be due to the blockage of pore opening and the impeded influx of TMZ that confirms the pivotal role of P2X7 receptor.

Additional viability test were performed to confirm the decreased viability of A172 cells treated with two P2X7 receptor agonists: 100 μM ATP and 10 μM BzATP, alone or with 125/500 μM TMZ (Fig. 5A and B). Besides the limited viability of cells treated with ATP (or BzATP), especially when combined with TMZ, we have also proved their decreased migration rate – Fig. 5C. It is worth noting, that the scratch overgrowth is a result of various processes: cell proliferation, death, and only to some extent, migration. Despite the limitations, however, *in vitro* scratch assay can still be considered the method of choice to analyze cell migration, that is of great importance for the cancer cells potential to invade the adjacent tissues. Some representative photographs of fast *versus* slow scratch closure presented in Fig. 5D and E confirm this biological potential.

Looking closer to the obtained results, we can conclude that beneficial, as regarding anti-cancer activity, effect of combined ATP and TMZ action on differentiated A172 cells has probably been initiated *via* P2X7 receptor signaling. The higher number of P2X7 receptors on differentiated cells membrane and their activation with ATP (when concentrations ATP > TMZ) suggest the possibility of TMZ passing through the open receptor channel. Trying to explain this observation, we hypothesized that TMZ could interplay with elements of the purinergic

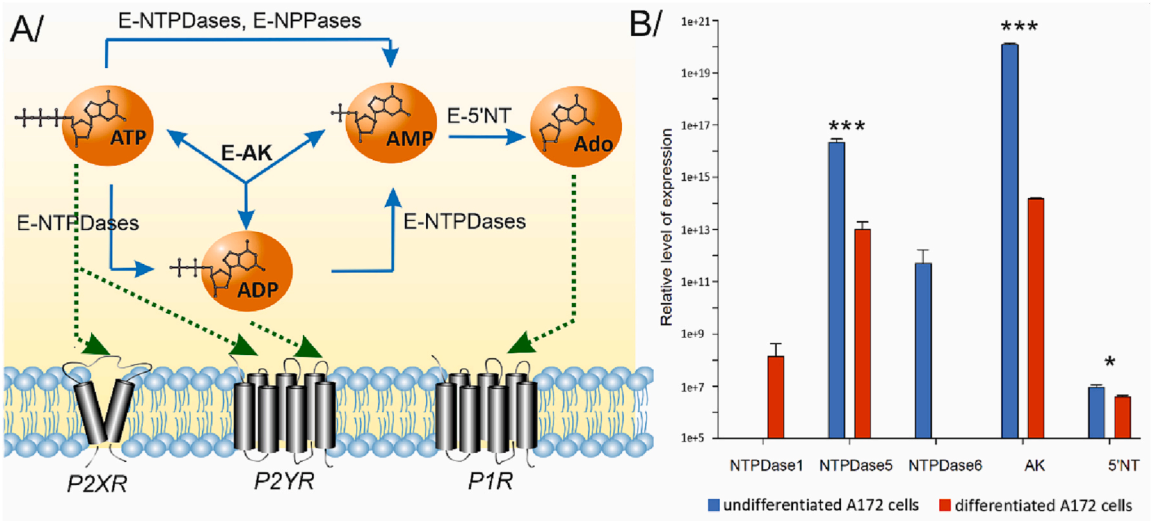

C/

Substrate	Enzyme	Activity [nmol · min^{-1} · mg protein^{-1}]			
		Undifferentiated cells		Differentiated cells	
		Ecto-enzymes	Exo-enzymes	Ecto-enzymes	Exo-enzymes
ATP	NTPDase/NPPase	0.305 ± 0.02	0.586 ± 0.03	0.126 ± 0.02	0.08 ± 0.02
ADP	NTPDase/NPPase	0.157 ± 0.08	0.063 ± 0.007	0.153 ± 0.02	0.001 ± 0.0003
	Adenylate kinase	2.733 ± 0.12	0.15 ± 0.004	1.482 ± 0.09	0.062 ± 0.005
AMP	5'-nucleotidase	1.202 ± 0.09	0.229 ± 0.02	0.687 ± 0.05	0.163 ± 0.03

Fig. 2. A/ Overview of the concerted action of various ecto-enzymes metabolizing nucleotides: AK – adenylate kinase, 5'NT – 5′-nucleotidase, NTPDases – ecto-nucleoside triphosphate diphosphohydrolases, NPPs – nucleotide pyrophosphatase/phosphodiesterases; B/ Changes in ecto- and *exo*-enzymes gene expression after A172 glioma cells differentiation; C/ Extracellular enzymatic activity towards ATP, ADP or AMP as a substrate. Ecto-enzymes are anchored in the cell membrane with their active center directed extracellularly, whereas exo-enzymes are released into the extracellular microenvironment as soluble molecules or anchored in the membrane of microvesicles. The activity values are presented as mean ± SD (for $n = 4$).

signaling pathway – primarily with the P2X7 receptor extracellular domains – due to its partial structural similarity to ATP. We performed molecular docking of ATP, TMZ, BzATP, and MTIC into the model of the human P2X7 receptor, which is presented in Fig. 6.

The human receptor trimeric structure contains three ligand-binding sites located in the easily accessible outer part of the receptor as indicated in Fig. 6. We used this region to test the hypothesis that TMZ competes for the same binding pocket as ATP, due to the structural similarities. Free energies (estimated by Smina scoring function, SSF) of the best poses for known ligands of P2X7R (ATP and BzATP) as well as for TMZ and its metabolite MTIC, are presented in Fig. 6E. All docking results are presented in SI in Tables S1-S4.

Relatively low free energy values for TMZ, in comparison with ATP or BzATP, indicate the possibility of molecule unspecific binding in the ATP binding pocket. A structural comparison of low energy poses of both ATP and TMZ is presented in Fig. 6C and D. Overlapping five best poses of ATP and TMZ within the ligand binding site are included in SI in Fig. S1 and S2, confirming that TMZ has potential to hamper ATP binding.

Summing the above docking results, they indicate that TMZ binding to P2X7 receptor is plausible and it interferes with ATP binding. Regarding cytophysiological effects of these TMZ interactions, blocking of P2X7R can be expected. We have confirmed it with the ethidium bromide influx into differentiated A172 cells treated with 500 μM ATP, 50 μM BzATP and 125 μM TMZ or their combinations (Fig. 6F). This set of results proved that binding of temozolomide molecules disables the P2X7 receptor activation and pore opening, and this effect can be overcome by increasing ATP concentration.

4. Discussion

During *in vitro* analysis of A172 cells purinome, we have observed that these cells were weakly sensitive to nucleotide signaling in the extracellular environment. Even high micromolar concentrations of ATP were not able to induce glioma cells death. Our observation stays in good agreement with literature data reporting that low-differentiated and fast proliferating cells (*e.g.*, cancer cells, stem cells or cancer stem cells) respond to ATP signal with higher proliferation rate, drug resistance, and survival [8,25,47,48]. Bearing in mind that cancer stem cells are the main factor responsible for cancer recurrence and, therefore, the critical target of therapeutic strategies [8,49], we concluded that correspondingly the differentiation of low-differentiated glioma cells would be a pivotal step in the therapeutic purines-based approach. Cytophysiological changes induced by retinoic acid-mediated differentiation of A172 altered the purinome, *inter alia* P2X7 receptor expression and ectonucleotidases expression and enzymatic activity. In contrary to

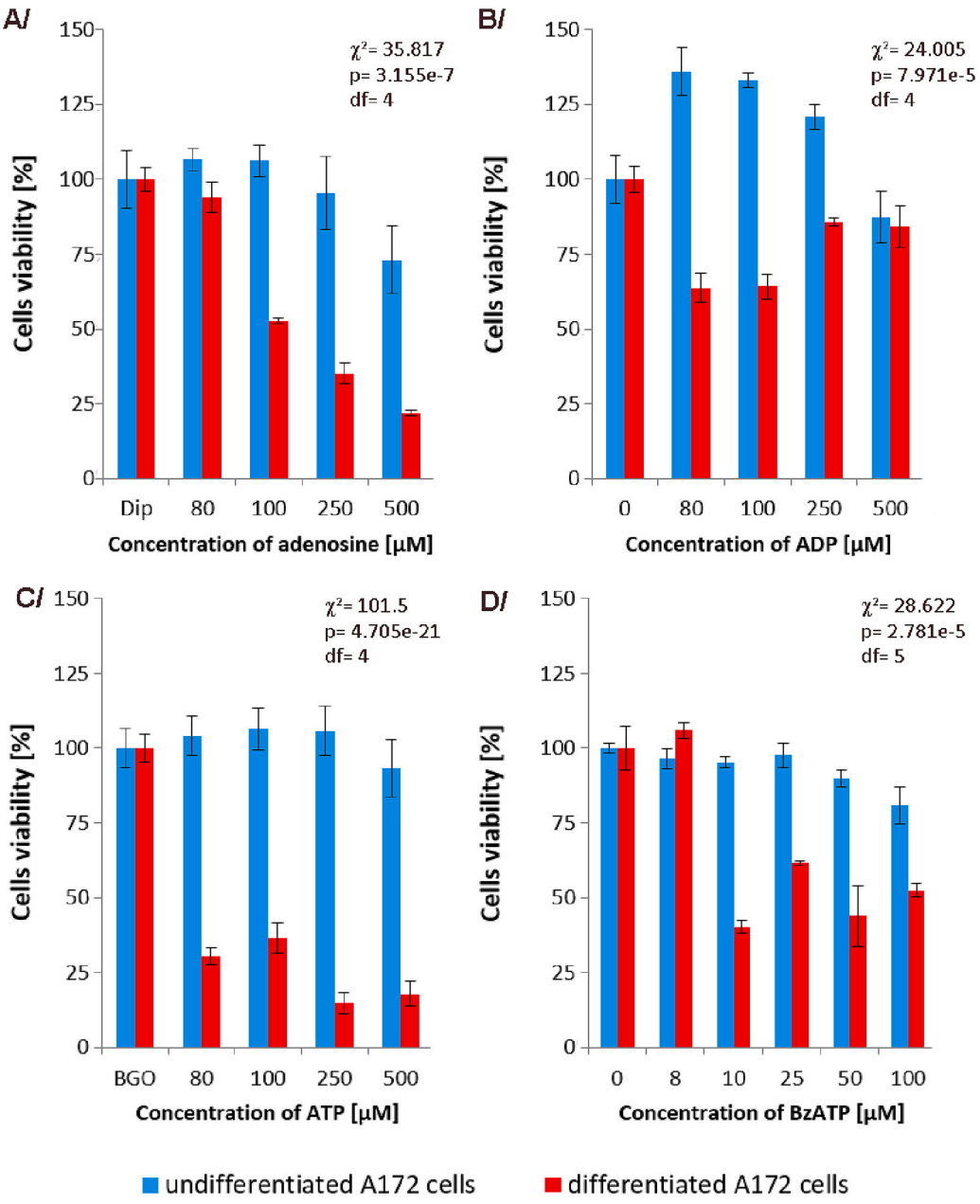

Fig. 3. Purinergic compounds influence on cell viability determined by MTT assay after 72 h-culture in the presence of: A/ adenosine (with dipirydamole as inhibitor of Ado re-uptake), B/ ADP, C/ ATP (with BGO as specific NTPDase inhibitor added to prevent ATP hydrolysis), D/ BzATP that is an agonist of P2 receptors. The bars present mean values ± SD (number of samples $n = 4$). The statistical analysis was performed using $\chi 2$ test and calculated parameters are given within panels.

the undifferentiated A172 glioma cells that seem to be more autonomous, the differentiated A172 become more homogenous, susceptible to environmental "danger" signals and reactive to them. Activation of P2X7R by its agonists – ATP and more potent derivative, BzATP, resulted in decreased viability of differentiated A172 cells. Up to date, it has been suggested rather that BzATP-treatment up-regulated EMT markers and increased invasiveness of glioma stem cells [50]. Our results are in contrast to the previous reports on undifferentiated glioma cells, and thus, they could be attributed to the differentiation-induced alterations [50,51].

The P2X7 receptor, activated by extracellular ATP, is a dual-function ion channel with multifaceted actions described by various research groups [52,53]. Its unique nature allows transmembrane passage of mono- and divalent cations on the one hand and the unrestricted influx of aqueous solutes of molecular mass up to 900 Da on the other. Small cation transfer is in principle associated with the activation of trophic functions, whereas free passage leads to multiple disturbances and cell death (necrosis, apoptosis, or pyroptosis). Some recent evidence suggests that the P2X7R might undergo a "controlled" activation, leading to opening the ion channel only and allowing for better control of the induced pathways [54]. Undoubtedly, it is the most interesting purinergic receptor, abundantly expressed in various cells, including but not limited to cancer and neuronal lineage cells [55,56].

P2X7R activation in glioma cells mediates multiple effects ranging from survival and immune system modulation to cell death [57,58]. The use of P2X7R agonists and antagonists, including BzATP, BBG, and OxATP, has shown varying and sometimes contrary effects in both animal and human glioma cells [58]. Nevertheless, several P2X7R-targeting compounds have been developed as drugs for a range of cancers; for review see [59]. A better understanding of P2X7 interactions with different ligands would create the opportunity to translate preclinical findings into the novel, more effective therapies. Remarkably,

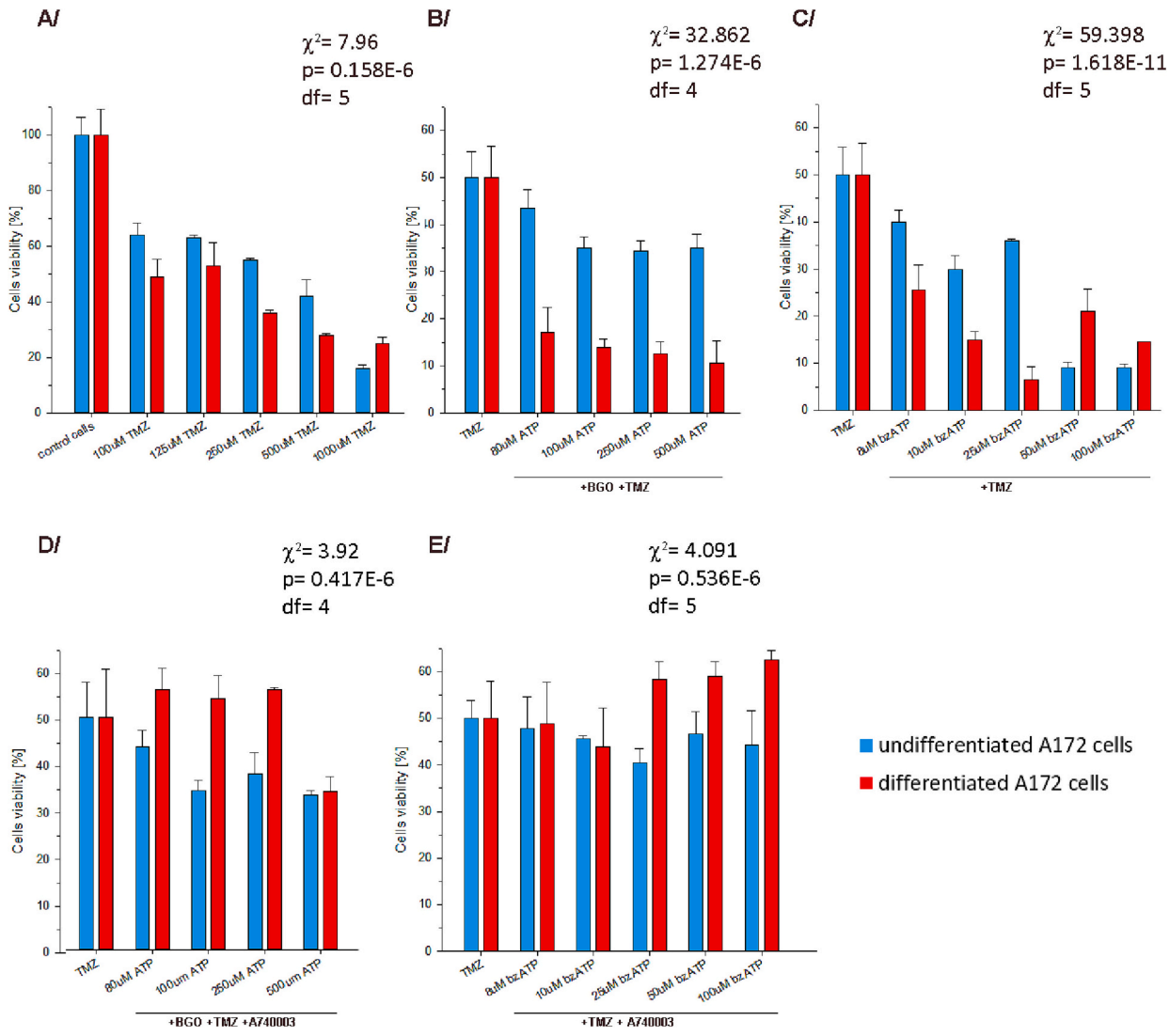

Fig. 4. A/ Concentration-dependent TMZ influence on undifferentiated and differentiated A172 cells determined by MTT assay after 72 h in culture; B/ combined action of ATP (added with BGO as nucleotidase activity inhibitor to prevent its hydrolysis) and TMZ; C/ combined action of BzATP and TMZ; D/ combined action of ATP and TMZ in the presence of P2X7 receptor antagonist (A740003); E/ combined action of bzATP and TMZ in the presence of P2X7 receptor antagonist (A740003). Experimental variants with TMZ were performed at its half-maximal effective concentration (different for both cell types, established here as 50% cell viability). The bars present mean values ± SD (number of samples $n = 4$). The statistical analysis was performed using $\chi 2$ test and calculated parameters are given within panels.

there has been a recent development of antibodies targeting a non-functional form of P2X7R (nfP2X7), which does not have the ability to form the pore state [60]. This is a result of the loss of two out of three ATP binding sites in nfP2X7, whereas the binding of ATP to all three ATP binding sites is required for pore formation.

In the presented experimental set, we aimed to shed more light on the role of purinergic system elements in glioma cancer progression and treatment. Based on our previous results and those reported in the literature, we assumed that micromolar ATP concentrations would open the P2X7 pore and facilitate the intracellular influx of cytotoxic drugs. We have verified this hypothesis using temozolomide – a chemotherapeutic agent with limited bioavailability. The observed enhancement of cytotoxic effect of TMZ and ATP in A172 glioma cells suggests that new interactions have to be considered beyond the undisputable transmembrane passage of TMZ and its interactions with DNA. Our results allow concluding that in the case of undifferentiated A172 cells, at TMZ exceeding ATP concentration, rather unspecific TMZ docking into P2X7 receptor blocks its activation through ATP and simultaneously inhibits pore formation. Regarding it, TMZ can only cross the cell membrane to interact with DNA, and the cell viability decreases by only 30% relative to control. Increasing ATP concentration up to 3 mM has not improved those outcomes. In the differentiated A172, due to enhanced P2X7R expression and lower TMZ effective concentration, cell viability in the presence of ATP decreases by 72%. This result is underlain by the consequent shortage of blocking TMZ molecules, and ATP-mediated activation of P2X7 receptor. The activated P2X7R opens a channel and facilitates TMZ influx into the cell, further increasing the bioavailability of TMZ. Noteworthy, not the ATP concentration alone but rather its ratio to TMZ is of decisive importance to this outcome. Therefore, the increase of ATP concentration rather than increase of TMZ dose should be considered for successful treatment of glioma.

The combined therapy consisting of nucleotide and chemotherapeutic has been previously tested on undifferentiated glioma cells isolated from three patients' tumors [57]. The human primary gliomas were sensitive to combined ATP and temozolomide therapy, however, the main disadvantage of that study was the small number of samples from hetereogenous primary tumors. Therefore, biased results reflecting the gliomas' sensitivity to drugs were obtained and reported in the literature for different human glioblastoma cell lines [11]. The described here procedure of initial differentiation allows overcoming these

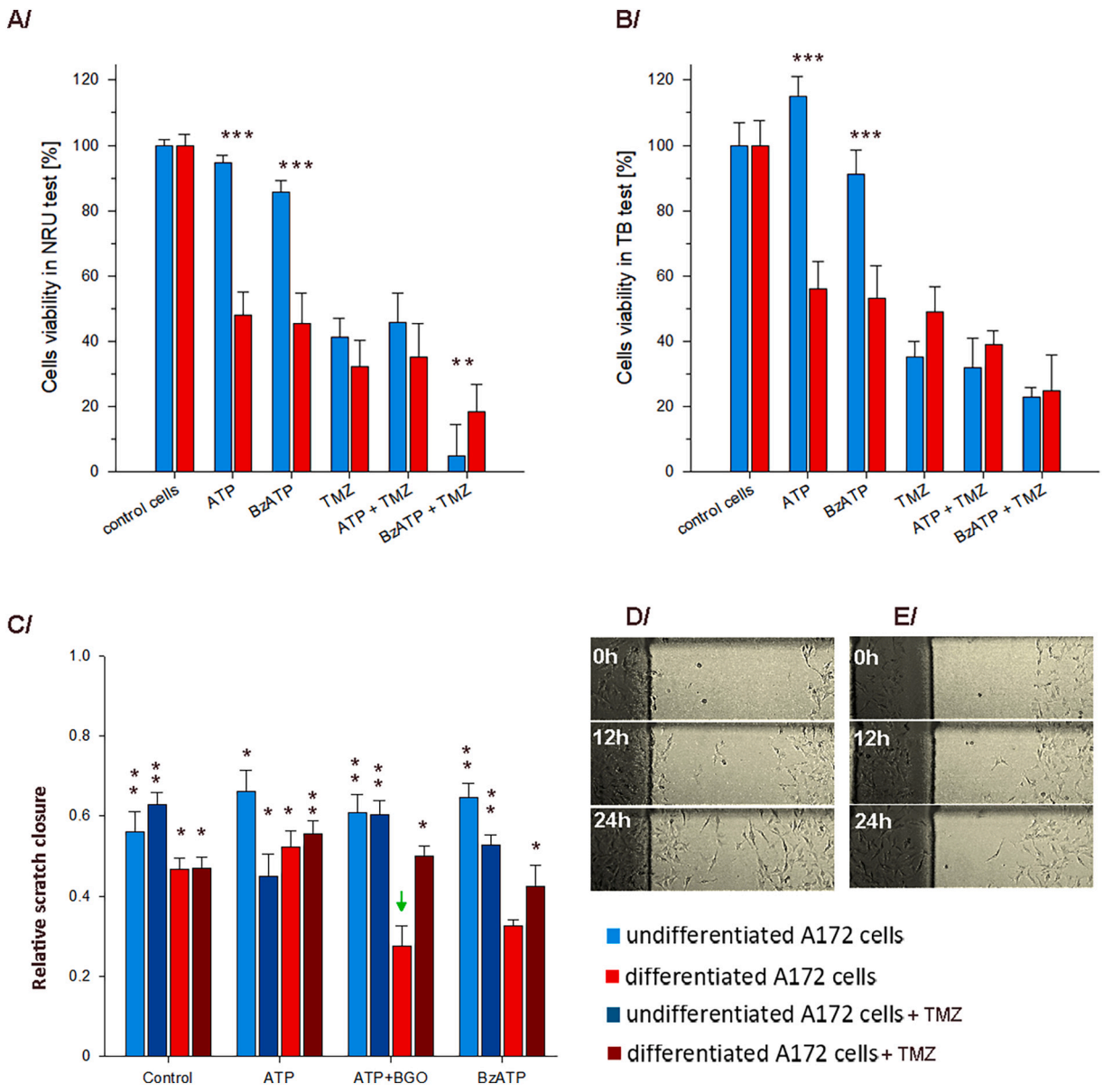

Fig. 5. A/ Influence of P2X7 receptor agonists: 100 μM ATP and 10 μM BzATP, alone or with 500/125 μM TMZ on undifferentiated and differentiated A172 cells assayed with NRU test after 72 h in culture; B/ Influence of P2X7 receptor agonists: 100 μM ATP and 10 μM BzATP, alone or with 500/125 μM TMZ on undifferentiated and differentiated A172 cells assayed with trypan blue staining after 72 h in culture; C/ Influence of 100 μM ATP and 10 μM BzATP, alone or with 500/125 μM TMZ on glioma cell scratch closure after 24 h (initial scratch width was taken as 1). The statistical significance of the differences between samples, compared to the best variant indicated with arrow, is marked in the graphs with asterisks (* for $p \leq 0.05$, ** for $p \leq 0.005$ *** for $p \leq 0.001$); D/ Representative images of fast migrating undifferentiated A172 cells; E/ Representative images of slow migrating differentiated A172 cells. (For interpretation of the references to colour in this figure legend, the reader is referred to the web version of this article.)

limitations, however, it should be further elucidated on various glioblastoma cells.

Additionally, a study on guanosine (GUO) and temozolomide combined therapy has been reported recently [61]. GUO or TMZ alone promoted a considerable decrease in A172 cell viability, and the drugs combination has not improved this effect. However, TMZ plus GUO prevented the migration of glioma cells after 24 h of treatment, indicating a decrease in metastatic growth ability in the presence of both compounds. To the best of our knowledge, no investigations revealed the possibility of TMZ interacting with purinergic receptors to induce the combined effect of drug and nucleotides/nucleosides, so far.

The 3D structure of the human P2X7 receptor is not known yet. Using the rat receptor structure determined by CryoEM technique as a template, we have constructed the hP2X7 receptor model. Structural data on hP2X7 receptor model confirm the presence of three equivalent ATP docking sites in the extracellular region of hP2X7R. Docking results reveal that ATP prefers binding to the same regions of hP2X7 receptor model as those observed in the homologous rat P2X7R experimental structure (see SI, Tables S1-S4). The values of SMINA scoring function (SSF), often used for relative comparisons of ligand binding affinities, indicate that the affinity of ATP to hP2X7 is moderate (−8.36 kcal/mol) and comparable with ligands of other receptors, for example, M1 muscarinic receptor, where values from −5.9 kcal/mol to −7.9 kcal/mol were calculated using SMINA [62].

The affinity of BzATP to hP2X7 receptor is substantially higher than that of ATP (−9.7 *vs.* -8.4 kcal/mol) that stays in agreement with experimental data [63,64]. TMZ has clear propensity to the same binding pocket, but the absolute value of its binding energy (−6.14 kcal/

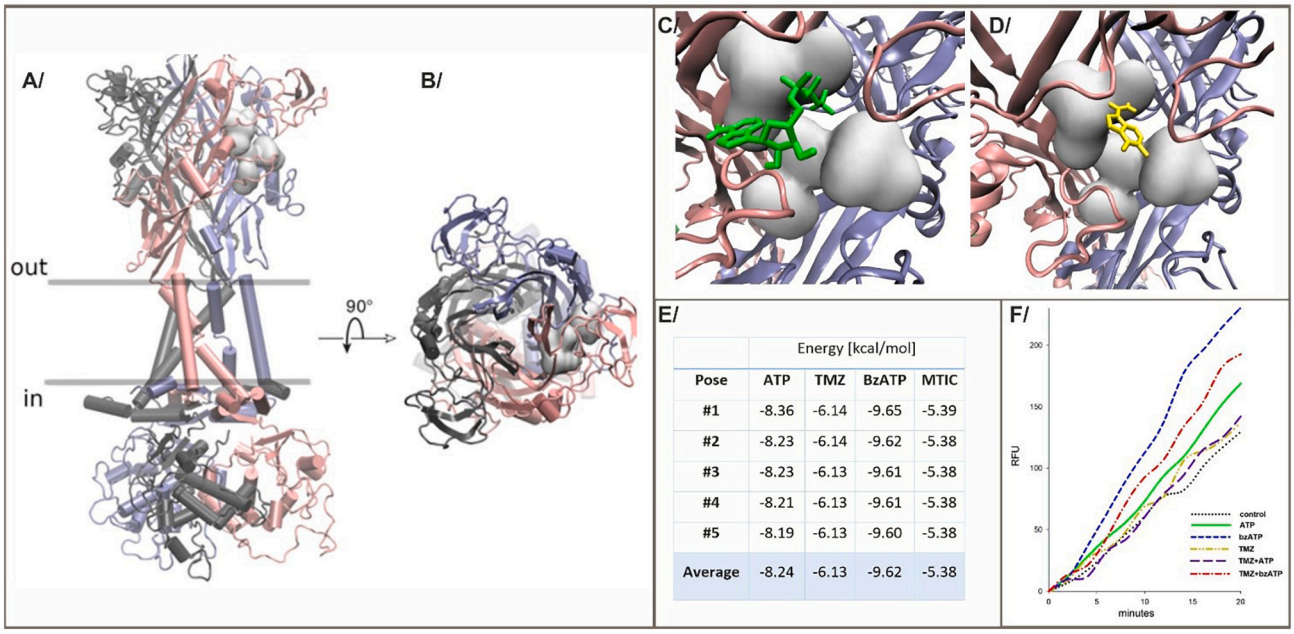

Fig. 6. General architecture and functionality of hP2X7 receptor: A/ side view, B/top view of receptor structure. One out of three ATP binding pockets is indicated as a grey cloud. Position of a cell membrane is schematically shown by grey bars. Structural comparison of the best docking poses of: C/ ATP, and D/ TMZ. Residues forming ATP binding site are shown as grey clouds; E/ Ligand binding energies (SSF, in kcal/mol) calculated by SMINA code for the best-docked poses in ATP binding site region of hP2X7 receptor; F/ Ethidium bromide influx into differentiated A172 cells subjected to 500 μM ATP, 50 μM BzATP and 125 μM TMZ treatment.

mol) is lower, so the affinity towards hP2X7R is lower than that of ATP. However, modelling indicated that ATP binding domain is the most preferred docking site of TMZ on the surface of a closed receptor. Additionally, MTIC molecule interacts even weaker (−5.4 kcal/mol) with the ATP binding site, but modelling shows that it can occupy the same ligand binding pocket as well. The binding of active molecules, TMZ and/or MTIC, disables the P2X7 receptor activation and pore opening, as well as decreases drug availability for glioma cells, what was experimentally proved with ethidium bromide uptake. Therefore, high TMZ concentrations in undifferentiated A172 cells, possessing a limited number of P2X7 receptors, resulted in a weak anti-cancer effect. Lowered TMZ concentration together with increased ATP level, and what is more important, the prior differentiation of A172 cells will enhance the effect of their decreased viability and migrative properties.

Summing up, in glioma cells microenvironment, ATP and TMZ can compete for the same binding sites in the extracellular part of hP2X7. The binding of TMZ molecules disables the P2X7 receptor activation and pore opening, and this effect can be overcome by RA-mediated differentiation, increased P2X7R expression and maintained ATP concentration in differentiated A172 glioblastoma cells.

5. Conclusions

Retinoic acid-induced differentiation of A172 glioma cells makes them more homogenous, reduces their proliferation and migration ability. Accordingly, differentiated cells are more susceptible to purine nucleotide signaling, TMZ alone, and to the concerted action of TMZ and ATP due to P2X7 receptor involvement. In differentiated A172 glioblastoma cells the appropriate ecto-ATP concentration will enhance the anti-tumor activity of TMZ. Remarkably, the increase and maintenance of ATP concentration rather than increase of TMZ dose should be considered for successful treatment of glioma. All that, in turn, could limit the side effects for the patient and shorten the therapy.

Structure availability: The structure of hP2X7 receptor model is available from authors upon request.

Credit author statement

Bartosz Szymczak: Investigation, Formal analysis, Visualization, Writing - original draft, Writing – review & editing. **Joanna Czarnecka:** Methodology, Investigation, Visualization, Writing - original draft, Writing - review & editing. **Sylwia Czach:** Investigation, Formal analysis, Visualization. **Wiesław Nowak:** Conceptualization, Formal analysis, Software, Writing - review & editing. **Katarzyna Roszek:** Conceptualization, Formal analysis, Resources, Writing - original draft, Wriitng - review & editing

Declaration of Competing Interest

The authors declare no conflicts of interest.

Data availability

Data will be made available on request.

Acknowledgments

JC acknowledges the financial support by the National Science Center grant 2019/03/X/NZ5/01409. WN acknowledges the partial financial support by the National Science Center grant 2016/23/B/ST4/01770. SC and WN are members of #MEMOBIT Team IDUB Nicolaus Copernicus University, Toruń, Poland.

Appendix A. Supplementary data

Supplementary data to this article can be found online at https://doi.org/10.1016/j.cellsig.2023.110641.

References

[1] H.J. Kim, J.W. Park, J.H. Lee, Genetic architectures and cell-of-origin in glioblastoma, Front. Oncol. 10 (2021), 615400, https://doi.org/10.3389/fonc.2020.615400.

[2] R.G.W. Verhaak, K.A. Hoadley, E. Purdom, et al., Integrated genomic analysis identifies clinically relevant subtypes of glioblastoma characterized by abnormalities in PDGFRA, IDH1, EGFR, and NF1, Cancer Cell 17 (2010) 98–110, https://doi.org/10.1016/j.ccr.2009.12.020.

[3] A. Vollmann-Zwerenz, V. Leidgens, G. Feliciello, et al., Tumor cell invasion in glioblastoma, Int. J. Mol. Sci. 21 (2020) 1–21, https://doi.org/10.3390/ijms21061932.

[4] M.C. de Gooijer, M. Guillén Navarro, R. Bernards, et al., An Experimenter's guide to glioblastoma invasion pathways, Trends Mol. Med. 24 (2018) 763–780, https://doi.org/10.1016/J.MOLMED.2018.07.003.

[5] F. Seker-Polat, N.P. Degirmenci, I. Solaroglu, T. Bagci-Onder, Tumor cell infiltration into the brain in glioblastoma: from mechanisms to clinical perspectives, Cancers (Basel) 14 (2022) 443, https://doi.org/10.3390/cancers14020443.

[6] W. Taal, J.E.C. Bromberg, Bent M.J. Van Den, CNS oncology chemotherapy in glioma, CNS Oncol. 4 (2015) 179–192, https://doi.org/10.2217/cns.15.2.

[7] M. Brada, S. Stenning, R. Gabe, et al., Temozolomide versus procarbazine, lomustine, and vincristine in recurrent high-grade glioma, J. Clin. Oncol. 28 (2010) 4601–4608, https://doi.org/10.1200/JCO.2009.27.1932.

[8] H. Zhang, A. Steed, M. Co, X. Chen, Cancer stem cells, epithelial-mesenchymal transition, ATP and their roles in drug resistance in cancer, Cancer Drug Resist. (Alhambra, Calif) 4 (2021) 684, https://doi.org/10.20517/cdr.2021.32.

[9] M.J. Ramalho, S. Andrade, M.Á.N. Coelho, et al., Biophysical interaction of temozolomide and its active metabolite with biomembrane models: the relevance of drug-membrane interaction for glioblastoma Multiforme therapy, Eur. J. Pharm. Biopharm. 136 (2019) 156–163, https://doi.org/10.1016/j.ejpb.2019.01.015.

[10] S.H. Bae, M.J. Park, M.M. Lee, et al., Toxicity profile of temozolomide in the treatment of 300 malignant glioma patients in Korea, J. Korean Med. Sci. 29 (2014) 980–984, https://doi.org/10.3346/jkms.2014.29.7.980.

[11] S.Y. Lee, Temozolomide resistance in glioblastoma multiforme, Genes Dis. 3 (2016) 198–210, https://doi.org/10.1016/j.gendis.2016.04.007.

[12] P. Cuevas, D. Díaz-González, M. Dujovny, Differentiation-inducing activity of neomycin in cultured rat glioma cells, Neurol. Res. 26 (2004) 401–403, https://doi.org/10.1179/016164104225016317.

[13] M. Dreyfus, M. El-Atifi, M. Court, et al., Reprogramming glioma cell cultures with retinoic acid: additional arguments for reappraising the potential of retinoic acid in the context of personalized glioma therapy, Glioma 1 (2018) 66, https://doi.org/10.4103/glioma.glioma_3_18.

[14] G. Burnstock, Pathophysiology and therapeutic potential of purinergic signaling, Pharmacol. Rev. 58 (2006), https://doi.org/10.1124/pr.58.1.5, 58 LP – 86.

[15] G. Burnstock, F. Di Virgilio, Purinergic signalling and cancer, Purinergic Signal 9 (2013) 491–540, https://doi.org/10.1007/s11302-013-9372-5.

[16] R. Lara, E. Adinolfi, C.A. Harwood, et al., P2X7 in Cancer: from molecular mechanisms to therapeutics, Front. Pharmacol. 11 (2020), https://doi.org/10.3389/fphar.2020.00793.

[17] F. Di Virgilio, P2X7 is a cytotoxic receptor….Maybe not: implications for cancer, Purinergic Signal 17 (2021) 55–61, https://doi.org/10.1007/s11302-020-09735-w.

[18] A.C. Sarti, V. Vultaggio-Poma, F. Di Virgilio, P2X7: a receptor with a split personality that raises new hopes for anti-cancer therapy, Purinergic Signal 17 (2021) 175–178, https://doi.org/10.1007/s11302-021-09783-w.

[19] C.F. Gelin, A. Bhattacharya, M.A. Letavic, P2X7 Receptor Antagonists for the Treatment of Systemic Inflammatory Disorders, 1st ed., Elsevier B.V, 2020.

[20] M. Shabbir, C. Thompson, M. Jarmulowiczc, et al., Effect of extracellular ATP on the growth of hormone-refractory prostate cancer in vivo, BJU Int. 102 (2008) 108–112, https://doi.org/10.1111/j.1464-410X.2008.07578.x.

[21] A. Lisa Giuliani, A. Clara Sarti, F. Di Virgilio, Ectonucleotidases in acute and chronic inflammation, Front. Pharmacol. 11 (2021), https://doi.org/10.3389/fphar.2020.619458.

[22] S. Ceruti, M.P. Abbracchio, Adenosine signaling in glioma cells, in: J. Barańska (Ed.), Glioma Signaling, Springer, Netherlands, Dordrecht, 2013, pp. 13–30.

[23] J. Spychala, Tumor-promoting functions of adenosine, Pharmacol. Ther. 87 (2000) 161–173, https://doi.org/10.1016/S0163-7258(00)00053-X.

[24] J.H. Azambuja, R.S. Schuh, L.R. Michels, et al., CD73 as a target to improve temozolomide chemotherapy effect in glioblastoma preclinical model, Cancer Chemother. Pharmacol. 85 (2020) 1177–1182, https://doi.org/10.1007/s00280-020-04077-1.

[25] E. Braganhol, M.R. Wink, G. Lenz, A.M.O. Battastini, Purinergic signaling in glioma progression, in: J. Barańska (Ed.), Glioma Signaling, Springer International Publishing, Cham, 2020, pp. 87–108.

[26] F.B. Morrone, M.C. Jacques-Silva, A.P. Horn, et al., Extracellular nucleotides and nucleosides induce proliferation and increase nucleoside transport in human glioma cell lines, J. Neuro-Oncol. 64 (2003) 211–218, https://doi.org/10.1023/A:1025699932270.

[27] Z. Ji, Y. Xie, Y. Guan, et al., Involvement of P2X7 receptor in proliferation and migration of human glioma cells, Biomed. Res. Int. 2018 (2018), https://doi.org/10.1155/2018/8591397.

[28] J. Liu, N. Li, R. Sheng, et al., Hypermethylation downregulates P2X7 receptor expression in astrocytoma, Oncol. Lett. 14 (2017) 7699–7704, https://doi.org/10.3892/ol.2017.7241.

[29] L.S. Bergamin, M. Capece, E. Salaro, et al., Role of the P2X7 Receptor in In Vitro and In Vivo Glioma Tumor Growth, 2019.

[30] M.P. Gehring, T.C.B. Pereira, R.F. Zanin, et al., P2X7 receptor activation leads to increased cell death in a radiosensitive human glioma cell line, Purinergic Signal 8 (2012) 729–739, https://doi.org/10.1007/s11302-012-9319-2.

[31] A. Yan, M.L. Joachims, L.F. Thompson, et al., CD73 promotes glioblastoma pathogenesis and enhances its chemoresistance via A2B adenosine receptor signaling, J. Neurosci. 39 (2019) 4387–4402, https://doi.org/10.1523/JNEUROSCI.1118-18.2019.

[32] Á. Torres, J.I. Erices, F. Sanchez, et al., Extracellular adenosine promotes cell migration/invasion of glioblastoma stem-like cells through A3 adenosine receptor activation under hypoxia, Cancer Lett. 446 (2019) 112–122, https://doi.org/10.1016/j.canlet.2019.01.004.

[33] H. Marcelino, T.M.A. Carvalho, J. Tomás, et al., Adenosine inhibits cell proliferation differently in human astrocytes and in glioblastoma cell lines, Neuroscience 467 (2021) 122–133, https://doi.org/10.1016/J.NEUROSCIENCE.2021.05.019.

[34] M.M. Shipley, C.A. Mangold, M.L. Szpara, Differentiation of the SH-SY5Y human neuroblastoma cell line, J. Vis. Exp. 2016 (2016) 1–11, https://doi.org/10.3791/53193.

[35] F.P. Gendron, O. Benrezzak, B.W. Krugh, et al., Purine signaling and potential new therapeutic approach: possible outcomes of NTPDase inhibition, Curr. Drug Targets 3 (2005) 229–245, https://doi.org/10.2174/1389450023347713.

[36] C.C. Liang, A.Y. Park, J.L. Guan, In vitro scratch assay: a convenient and inexpensive method for analysis of cell migration in vitro, Nat. Protoc. 2 (2007) 329–333, https://doi.org/10.1038/nprot.2007.30.

[37] A.E. McCarthy, C. Yoshioka, S.E. Mansoor, Full-length P2X7 structures reveal how Palmitoylation Prevents Channel desensitization, Cell 179 (2019), https://doi.org/10.1016/j.cell.2019.09.017, 659–670.e13.

[38] A. Waterhouse, M. Bertoni, S. Bienert, et al., SWISS-MODEL: homology modelling of protein structures and complexes, Nucleic Acids Res. 46 (2018) W296–W303, https://doi.org/10.1093/nar/gky427.

[39] R.A. Laskowski, M.W. MacArthur, D.S. Moss, J.M. Thornton, PROCHECK: a program to check the stereochemical quality of protein structures, J. Appl. Crystallogr. 26 (1993) 283–291, https://doi.org/10.1107/s0021889892009944.

[40] D.R. Koes, M.P. Baumgartner, C.J. Camacho, Lessons learned in empirical scoring with smina from the CSAR 2011 benchmarking exercise, J. Chem. Inf. Model. 53 (2013) 1893–1904, https://doi.org/10.1021/ci300604z.

[41] O. Trott, A.J. Olson, Software news and update AutoDock Vina: improving the speed and accuracy of docking with a new scoring function, efficient optimization, and multithreading, J. Comput. Chem. 31 (2010) 455–461, https://doi.org/10.1002/jcc.21334.

[42] W. Humphrey, A. Dalke, K. Schulten, VMD: Visual molecular dynamics, J. Mol. Graph. 14 (1996) 33–38, https://doi.org/10.1016/0263-7855(96)00018-5.

[43] E.M. Jimenez-Mateos, J. Smith, A. Nicke, T. Engel, Regulation of P2X7 receptor expression and function in the brain, Brain Res. Bull. 151 (2019) 153–163, https://doi.org/10.1016/J.BRAINRESBULL.2018.12.008.

[44] A. Pegoraro, E. De Marchi, E. Adinolfi, P2X7 variants in oncogenesis, Cells 10 (2021) 189, https://doi.org/10.3390/cells10010189.

[45] F.J. Jacques, T.M. Silva, F.E. da Silva, et al., Nucleotide P2Y13-stimulated phosphorylation of CREB is required for ADP-induced proliferation of late developing retinal glial progenitors in culture, Cell. Signal. 35 (2017) 95–106, https://doi.org/10.1016/J.CELLSIG.2017.03.019.

[46] C. Dsouza, S.V. Komarova, Characterization of potency of the P2Y13 receptor agonists: a Meta-analysis, Int. J. Mol. Sci. Artic. (2021), https://doi.org/10.3390/ijms22073468.

[47] F. Cavaliere, C. Donno, N. D'Ambrosi, Purinergic signaling: a common pathway for neural and mesenchymal stem cell maintenance and differentiation, Front. Cell. Neurosci. 9 (2015) 1–8, https://doi.org/10.3389/fncel.2015.00211.

[48] F. Di Virgilio, A.C. Sarti, S. Falzoni, et al., Extracellular ATP and P2 purinergic signalling in the tumour microenvironment, Nat. Rev. Cancer 18 (2018) 601–618, https://doi.org/10.1038/s41568-018-0037-0.

[49] A.K. Yadav, N.S. Desai, Cancer stem cells: acquisition, characteristics, therapeutic implications, targeting strategies and future prospects, Stem Cell Rev. Rep. 15 (2019) 331–355, https://doi.org/10.1007/s12015-019-09887-2.

[50] S. Ziberi, M. Zuccarini, M. Carluccio, et al., Transition markers and P2X7 receptors is associated to increased invasiveness caused by P2X7 receptor, Cells 9 (2020) 85, https://doi.org/10.3390/cells9010085.

[51] D. Matyśniak, V. Chumak, N. Nowak, et al., P2X7 receptor: the regulator of glioma tumor development and survival, Purinergic Signal 18 (2022) 135–154, https://doi.org/10.1007/s11302-021-09834-2.

[52] L.H. Jiang, E.A. Caseley, S.P. Muench, S. Roger, Structural basis for the functional properties of the P2X7 receptor for extracellular ATP, Purinergic Signal (2021), https://doi.org/10.1007/s11302-021-09790-x.

[53] R. Sluyter, The P2X7 receptor, Adv. Exp. Med. Biol. 1051 (2017) 17–53, https://doi.org/10.1007/5584_2017_59.

[54] L. Douguet, S. Janho Dit Hreich, J. Benzaquen, et al., A small-molecule P2RX7 activator promotes anti-tumor immune responses and sensitizes lung tumor to immunotherapy, Nat. Commun. 12 (2021) 1–17, https://doi.org/10.1038/s41467-021-20912-2.

[55] G. Martinez, P2X7 receptor in cardiovascular disease: the heart side, Clin. Exp. Pharmacol. Physiol. 46 (2019) 513–526, https://doi.org/10.1111/1440-1681.13079.

[56] A. Solini, I. Novak, Role of the P2X7 receptor in the pathogenesis of type 2 diabetes and its microvascular complications, Curr. Opin. Pharmacol. 47 (2019) 75–81, https://doi.org/10.1016/J.COPH.2019.02.009.

[57] I. D'Alimonte, E. Nargi, M. Zuccarini, et al., Potentiation of temozolomide antitumor effect by purine receptor ligands able to restrain the in vitro growth of human glioblastoma stem cells, Purinergic Signal 11 (2015) 331–346, https://doi.org/10.1007/s11302-015-9454-7.

[58] L.K. Kan, D. Williams, K. Drummond, et al., The role of microglia and P2X7 receptors in gliomas, J. Neuroimmunol. 332 (2019) 138–146, https://doi.org/10.1016/j.jneuroim.2019.04.010.
[59] G. Burnstock, G.E. Knight, Cellular distribution and functions of P2 receptor subtypes in different systems, Int. Rev. Cytol. 240 (2004) 31–304.
[60] J. Barden, A. Yuksel, J. Pedersen, et al., Non-functional P2X7: a novel and ubiquitous target in human Cancer, J. Clin. Cell Immunol. 05 (2014), https://doi.org/10.4172/2155-9899.1000237.
[61] K.A. Oliveira, T.A. Dal-Cim, F.G. Lopes, et al., Guanosine promotes cytotoxicity via adenosine receptors and induces apoptosis in temozolomide-treated A172 glioma cells, Purinergic Signal 13 (2017) 305–318, https://doi.org/10.1007/s11302-017-9562-7.
[62] E. Moreau, K. Mikulska-Ruminska, M. Goulu, et al., Orthosteric muscarinic receptor activation by the insect repellent IR3535 opens new prospects in insecticide-based vector control, Sci. Rep. 10 (2020) 1–15, https://doi.org/10.1038/s41598-020-63957-x.
[63] G. Lambrecht, Agonists and antagonists acting at P2X receptors: selectivity profiles and functional implications, Naunyn Schmiedeberg's Arch. Pharmacol. 362 (2000) 340–350, https://doi.org/10.1007/s002100000312.
[64] D.L. Donnelly-Roberts, M.T. Namovic, P. Han, M.F. Jarvis, Mammalian P2X7 receptor pharmacology: comparison of recombinant mouse, rat and human P2X7 receptors, Br. J. Pharmacol. 157 (2009) 1203–1214, https://doi.org/10.1111/j.1476-5381.2009.00233.x.

SUPPLEMENTARY INFORMATION TO:

Purinergic approach to effective glioma treatment with temozolomide reveals enhanced anti-cancer effects mediated by P2X7 receptor

Bartosz Szymczak[1], Joanna Czarnecka[1], Sylwia Czach[2], Wiesław Nowak[2], Katarzyna Roszek[1]

[1] Department of Biochemistry, Faculty of Biological and Veterinary Sciences, Nicolaus Copernicus University in Torun, Lwowska 1, 87-100 Torun, Poland

[2] Institute of Physics, Faculty of Physics, Astronomy and Informatics, Nicolaus Copernicus University in Torun, Grudziadzka 5, 87-100 Torun, Poland

CONTENT:

Figure S1. Overlap of five best (lowest binding energy) poses of ATP in the region of ATP-binding pocket in human P2X7 homology model.

Figure S2. Overlap of five best (lowest binding energy) poses of TMZ in the region of ATP-binding pocket in human P2X7 homology model.

Figure S3. Viability of human dermal fibroblasts (HDF) in the presence of various concentrations of ATP and TMZ after 72h in culture.

Table S1. Values of SMINA scoring function (in kcal/mol) for 20 best poses of ligands (ATP, TMZ, BzATP, MTIC) in human P2X7 homology model. In columns are shown results of 20 independent docking trials to the region of ATP-binding pocket.

Table S2. Values of SMINA scoring function (in kcal/mol) for 20 best poses of ligands (ATP, TMZ, MTIC) in human P2X7 homology model. In columns are shown results of 20 independent docking trials to the region of inhibitor-binding pocket.

Table S3. Values of SMINA scoring function (in kcal/mol) for 20 best poses of ligands (ATP, TMZ, BzATP, MTIC) in rat P2X7 structure (PDB 6U9V). In columns are shown results of 20 independent docking trials to the region of ATP-binding pocket.

Table S4. Values of SMINA scoring function (in kcal/mol) for 20 best poses of ligands (ATP, TMZ, MTIC) in rat P2X7 structure (PDB 6U9V). In columns are shown results of 20 independent docking trials to the region of inhibitor-binding pocket.

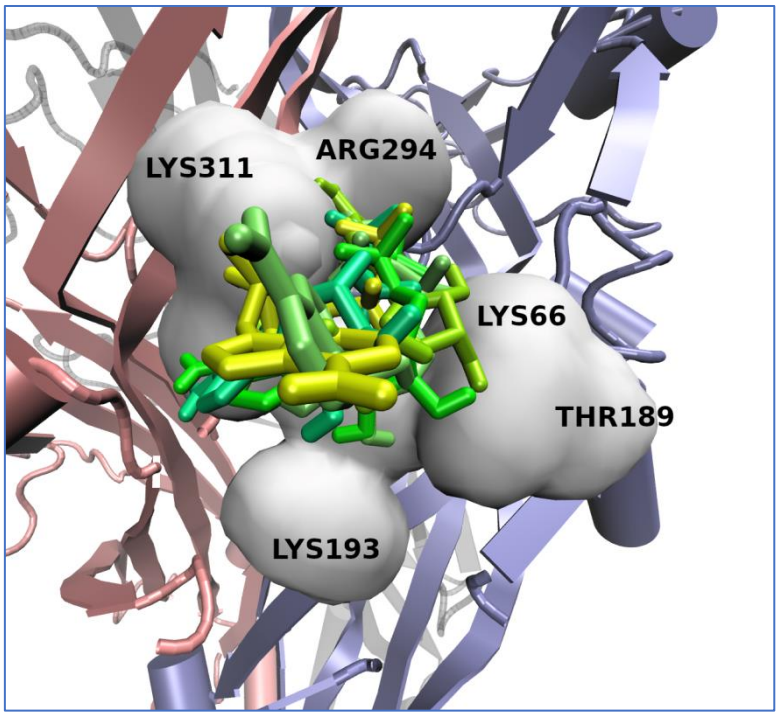

Figure S1. Overlap of five best (lowest binding energy) poses of ATP in the region of ATP-binding pocket in human P2X7 homology model. Deep green denotes the strongest binding.

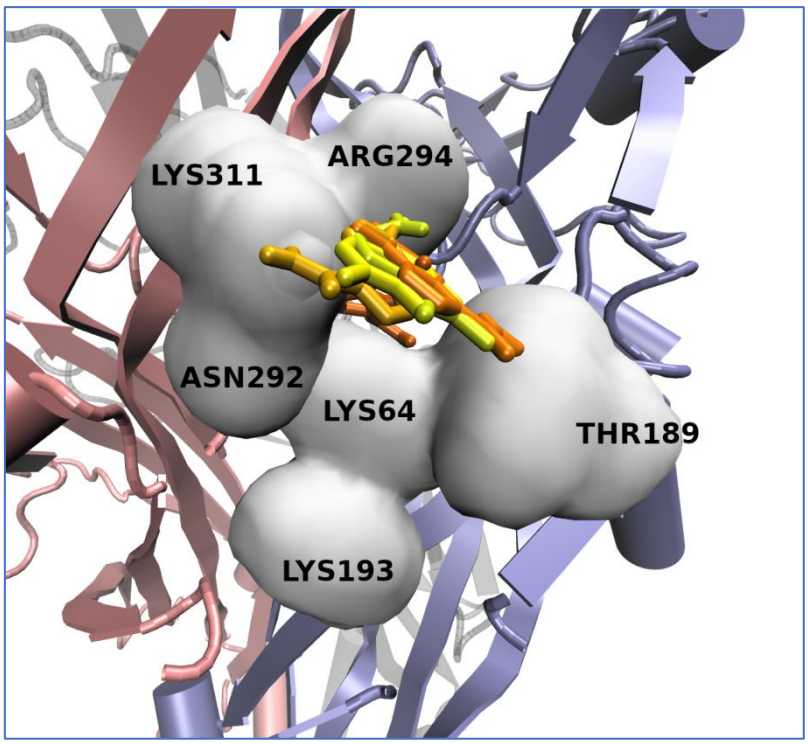

Figure S2. Overlap of five best (lowest binding energy) poses of TMZ in the region of ATP-binding pocket in human P2X7 homology model. Dark brown denotes the strongest binding pose.

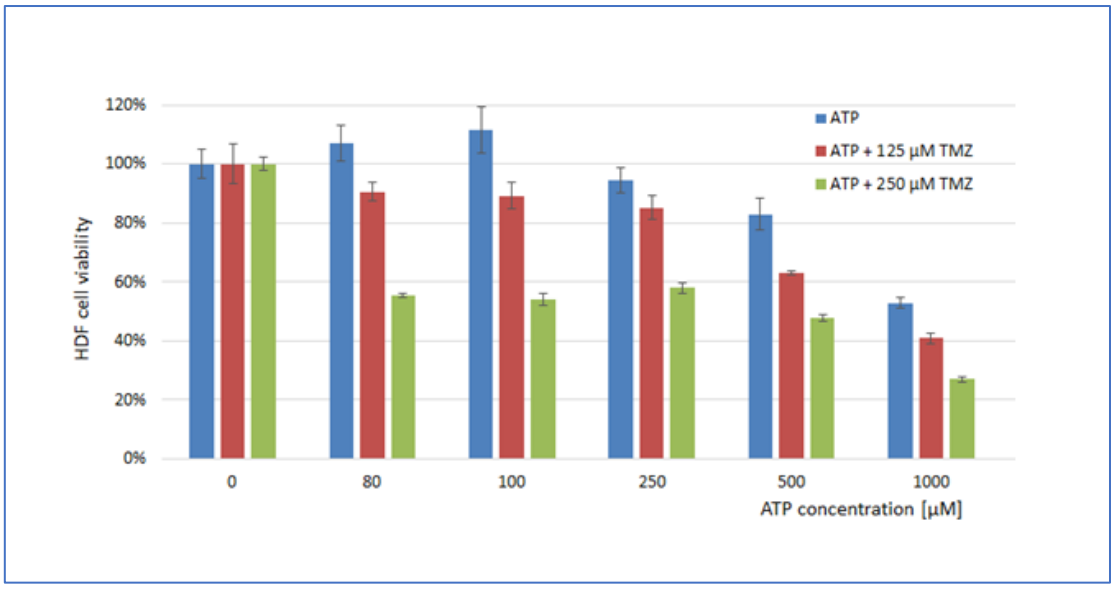

Figure S3. Viability of human dermal fibroblasts (HDF) in the presence of various concentrations of ATP and TMZ after 72h in culture. Experimental variants with TMZ were performed at 125 and 500 µM concentrations that are half-maximal effective concentration (EC50), different for undifferentiated and differentiated A172 cells.

Table S1. Values of SMINA scoring function (in kcal/mol) for 20 best poses of ligands (ATP, TMZ, BzATP, MTIC) in human P2X7 homology model. In columns are shown results of 20 independent docking trials to the region of ATP-binding pocket.

ATP	1	2	3	4	5	6	7	8	9	10
1	-7.946	-7.996	-8.081	-8.064	-8.087	-7.894	-8.139	-8.033	-8.144	-8.138
2	-7.723	-7.958	-7.836	-7.855	-8.044	-7.739	-8.048	-7.838	-7.978	-8.058
3	-7.686	-7.862	-7.790	-7.718	-8.036	-7.710	-7.871	-7.683	-7.880	-8.014
4	-7.638	-7.824	-7.625	-7.704	-7.901	-7.596	-7.722	-7.602	-7.829	-7.942
5	-7.609	-7.557	-7.621	-7.683	-7.837	-7.590	-7.600	-7.592	-7.737	-7.918
6	-7.545	-7.547	-7.555	-7.652	-7.835	-7.528	-7.561	-7.538	-7.726	-7.893
7	-7.536	-7.488	-7.520	-7.641	-7.831	-7.490	-7.543	-7.428	-7.720	-7.867
8	-7.469	-7.486	-7.513	-7.457	-7.789	-7.335	-7.529	-7.399	-7.489	-7.758
9	-7.358	-7.427	-7.330	-7.414	-7.775	-7.238	-7.525	-7.385	-7.358	-7.701
10	-7.345	-7.367	-7.312	-7.370	-7.773	-7.217	-7.457	-7.382	-7.307	-7.698
11	-7.244	-7.362	-7.302	-7.354	-7.752	-7.211	-7.427	-7.245	-7.287	-7.687
12	-7.190	-7.286	-7.258	-7.286	-7.743	-7.203	-7.408	-7.124	-7.278	-7.449
13	-7.165	-7.236	-7.216	-7.278	-7.717	-7.108	-7.383	-7.079	-7.220	-7.438
14	-7.129	-7.234	-7.193	-7.229	-7.691	-6.986	-7.327	-7.040	-7.201	-7.431
15	-7.127	-7.224	-7.178	-7.116	-7.658	-6.969	-7.322	-6.989	-7.195	-7.423
16	-7.127	-7.217	-7.163	-7.114	-7.630	-6.921	-7.312	-6.981	-7.189	-7.379
17	-7.063	-7.215	-7.134	-7.092	-7.620	-6.919	-7.306	-6.962	-7.186	-7.370
18	-7.048	-7.174	-7.118	-7.083	-7.548	-6.902	-7.305	-6.910	-7.167	-7.359
19	-7.020	-7.143	-7.118	-7.071	-7.517	-6.816	-7.222	-6.905	-7.147	-7.357
20	-7.006	-7.112	-7.114	-7.050	-7.424	-6.813	-7.156	-6.904	-7.122	-7.355
ATP	11	12	13	14	15	16	17	18	19	20
1	-8.088	-8.115	-7.962	-8.101	-8.033	-8.358	-8.087	-8.002	-8.232	-8.093
2	-8.036	-7.875	-7.921	-7.923	-7.805	-8.229	-7.908	-7.910	-8.214	-7.875
3	-7.765	-7.785	-7.868	-7.918	-7.755	-8.031	-7.888	-7.793	-8.189	-7.786
4	-7.739	-7.782	-7.724	-7.906	-7.499	-7.920	-7.687	-7.578	-8.121	-7.629
5	-7.721	-7.513	-7.555	-7.859	-7.457	-7.882	-7.660	-7.571	-8.020	-7.600
6	-7.709	-7.498	-7.542	-7.849	-7.387	-7.816	-7.620	-7.567	-7.997	-7.504
7	-7.676	-7.418	-7.504	-7.687	-7.374	-7.801	-7.460	-7.534	-7.971	-7.498
8	-7.552	-7.386	-7.448	-7.643	-7.260	-7.675	-7.449	-7.522	-7.935	-7.440
9	-7.430	-7.333	-7.367	-7.552	-7.246	-7.629	-7.445	-7.326	-7.793	-7.428
10	-7.242	-7.281	-7.320	-7.509	-7.235	-7.594	-7.426	-7.259	-7.765	-7.395
11	-7.203	-7.266	-7.291	-7.452	-7.199	-7.546	-7.325	-7.254	-7.728	-7.347
12	-7.192	-7.229	-7.255	-7.369	-7.170	-7.498	-7.247	-7.232	-7.703	-7.284
13	-7.173	-7.195	-7.211	-7.316	-7.136	-7.477	-7.235	-7.212	-7.614	-7.263
14	-7.122	-7.147	-7.133	-7.290	-7.099	-7.471	-7.207	-7.173	-7.567	-7.226
15	-7.118	-7.141	-7.097	-7.198	-7.095	-7.460	-7.177	-7.161	-7.557	-7.221
16	-7.053	-7.126	-7.085	-7.154	-7.080	-7.430	-7.131	-7.156	-7.531	-7.206
17	-7.050	-7.088	-7.056	-7.123	-7.044	-7.407	-7.117	-7.133	-7.469	-7.129
18	-7.036	-7.085	-7.054	-7.105	-7.021	-7.392	-7.104	-7.130	-7.430	-7.119
19	-7.035	-7.061	-7.024	-7.105	-7.003	-7.385	-7.037	-7.120	-7.418	-7.067
20	-7.007	-7.061	-6.959	-7.089	-6.991	-7.258	-7.022	-7.071	-7.416	-7.052

TMZ	1	2	3	4	5	6	7	8	9	10
1	-6.130	-6.059	-5.724	-6.052	-6.127	-6.130	-6.136	-6.135	-6.133	-6.131
2	-5.682	-5.913	-5.698	-5.700	-5.931	-5.682	-5.697	-5.683	-5.690	-5.691
3	-5.665	-5.896	-5.641	-5.667	-5.882	-5.663	-5.675	-5.675	-5.687	-5.674
4	-5.599	-5.870	-5.621	-5.622	-5.824	-5.457	-5.500	-5.611	-5.666	-5.508
5	-5.575	-5.604	-5.252	-5.583	-5.747	-5.294	-5.357	-5.596	-5.502	-5.353
6	-5.343	-5.533	-5.245	-5.229	-5.621	-5.235	-5.349	-5.519	-5.384	-5.241
7	-5.234	-5.501	-5.218	-5.188	-5.426	-5.161	-5.226	-5.247	-5.319	-5.234
8	-5.230	-5.496	-5.158	-5.162	-5.425	-5.027	-5.213	-5.243	-5.218	-5.227
9	-5.221	-5.470	-5.018	-5.134	-5.363	-5.008	-5.152	-5.214	-5.165	-5.191
10	-5.118	-5.352	-5.012	-5.073	-5.340	-4.964	-5.114	-5.149	-5.110	-5.148
11	-5.108	-5.330	-4.995	-5.006	-5.151	-4.909	-4.959	-5.029	-5.083	-5.130
12	-5.070	-5.305	-4.952	-4.923	-5.095	-4.909	-4.901	-5.005	-4.947	-5.062
13	-5.033	-5.202	-4.894	-4.909	-5.084	-4.882	-4.878	-4.966	-4.929	-5.039
14	-4.869	-5.185	-4.866	-4.891	-5.061	-4.855	-4.830	-4.957	-4.908	-5.030
15	-4.832	-5.172	-4.833	-4.826	-5.049	-4.851	-4.801	-4.908	-4.890	-4.981
16	-4.819	-5.073	-4.808	-4.809	-5.047	-4.831	-4.787	-4.889	-4.852	-4.937
17	-4.798	-5.032	-4.793	-4.796	-5.035	-4.803	-4.752	-4.879	-4.822	-4.919
18	-4.791	-5.022	-4.752	-4.789	-5.012	-4.772	-4.751	-4.875	-4.770	-4.860
19	-4.789	-4.996	-4.745	-4.781	-5.003	-4.733	-4.742	-4.853	-4.751	-4.855
20	-4.755	-4.978	-4.704	-4.773	-4.986	-4.704	-4.734	-4.816	-4.687	-4.831

TMZ	11	12	13	14	15	16	17	18	19	20
1	-5.687	-5.699	-6.127	-6.100	-6.110	-5.692	-6.137	-6.072	-6.121	-6.130
2	-5.676	-5.677	-5.706	-5.710	-5.702	-5.681	-5.705	-5.709	-5.698	-5.694
3	-5.626	-5.563	-5.689	-5.691	-5.663	-5.671	-5.638	-5.683	-5.692	-5.667
4	-5.606	-5.534	-5.666	-5.672	-5.654	-5.545	-5.604	-5.663	-5.655	-5.663
5	-5.586	-5.504	-5.565	-5.556	-5.613	-5.389	-5.581	-5.498	-5.570	-5.590
6	-5.215	-5.258	-5.358	-5.279	-5.357	-5.266	-5.394	-5.260	-5.501	-5.493
7	-5.167	-5.159	-5.217	-5.233	-5.231	-5.234	-5.328	-5.230	-5.388	-5.289
8	-5.046	-5.088	-5.175	-5.151	-5.111	-5.233	-5.242	-5.206	-5.371	-5.241
9	-4.976	-5.083	-5.166	-5.043	-5.029	-5.212	-5.228	-5.127	-5.247	-5.240
10	-4.954	-5.045	-5.037	-5.025	-4.993	-5.170	-5.205	-5.036	-5.222	-5.159
11	-4.914	-4.938	-4.949	-4.966	-4.990	-5.002	-5.145	-4.968	-5.161	-5.069
12	-4.873	-4.891	-4.942	-4.931	-4.941	-4.992	-5.034	-4.834	-5.034	-5.010
13	-4.859	-4.851	-4.912	-4.923	-4.929	-4.870	-4.987	-4.816	-4.997	-5.003
14	-4.829	-4.830	-4.891	-4.831	-4.921	-4.868	-4.935	-4.791	-4.868	-4.937
15	-4.812	-4.778	-4.867	-4.827	-4.903	-4.819	-4.830	-4.772	-4.818	-4.900
16	-4.810	-4.773	-4.859	-4.807	-4.819	-4.813	-4.809	-4.755	-4.806	-4.872
17	-4.807	-4.768	-4.840	-4.767	-4.792	-4.809	-4.804	-4.750	-4.797	-4.850
18	-4.805	-4.763	-4.822	-4.762	-4.747	-4.809	-4.780	-4.714	-4.771	-4.850
19	-4.804	-4.742	-4.808	-4.758	-4.722	-4.792	-4.741	-4.703	-4.767	-4.819
20	-4.796	-4.720	-4.803	-4.750	-4.687	-4.774	-4.730	-4.700	-4.763	-4.802

BzATP	1	2	3	4	5	6	7	8	9	10
1	-9.317	-9.617	-9.332	-9.334	-9.653	-9.285	-9.389	-9.362	-9.347	-9.404
2	-9.075	-9.612	-9.104	-9.196	-9.612	-8.912	-9.381	-9.298	-9.037	-9.262
3	-9.050	-9.231	-8.915	-8.955	-9.600	-8.904	-9.193	-9.131	-8.862	-9.151
4	-9.040	-9.179	-8.869	-8.804	-9.455	-8.833	-9.186	-9.037	-8.806	-9.015
5	-9.018	-9.128	-8.865	-8.798	-9.078	-8.810	-9.128	-8.924	-8.739	-8.841
6	-8.864	-9.088	-8.669	-8.736	-9.037	-8.799	-9.088	-8.765	-8.736	-8.795
7	-8.855	-9.007	-8.610	-8.614	-8.998	-8.791	-8.982	-8.606	-8.706	-8.738
8	-8.827	-8.965	-8.580	-8.566	-8.853	-8.702	-8.963	-8.504	-8.595	-8.698
9	-8.808	-8.920	-8.576	-8.422	-8.825	-8.658	-8.879	-8.498	-8.497	-8.677
10	-8.795	-8.912	-8.459	-8.401	-8.806	-8.632	-8.866	-8.484	-8.440	-8.641
11	-8.653	-8.860	-8.398	-8.396	-8.797	-8.614	-8.842	-8.477	-8.428	-8.578
12	-8.615	-8.857	-8.372	-8.367	-8.720	-8.573	-8.826	-8.428	-8.425	-8.532
13	-8.584	-8.824	-8.312	-8.282	-8.621	-8.557	-8.812	-8.409	-8.399	-8.407
14	-8.519	-8.698	-8.294	-8.239	-8.435	-8.498	-8.759	-8.392	-8.332	-8.400
15	-8.467	-8.692	-8.207	-8.220	-8.371	-8.404	-8.753	-8.360	-8.330	-8.397
16	-8.460	-8.667	-8.195	-8.173	-8.318	-8.237	-8.703	-8.214	-8.285	-8.365
17	-8.436	-8.621	-8.173	-8.159	-8.181	-8.225	-8.615	-8.126	-8.275	-8.137
18	-8.346	-8.553	-8.156	-8.139	-8.165	-8.220	-8.605	-8.066	-8.226	-8.117
19	-8.323	-8.522	-8.035	-8.061	-8.162	-8.189	-8.516	-7.991	-8.225	-7.939
20	-8.298	-8.494	-7.922	-8.060	-8.147	-8.101	-8.464	-7.970	-8.135	-7.888

BzATP	11	12	13	14	15	16	17	18	19	20
1	-9.348	-9.319	-9.214	-9.248	-8.316	-9.341	-8.653	-9.373	-8.948	-9.315
2	-9.103	-9.128	-9.148	-9.026	-8.137	-9.131	-8.613	-9.007	-8.839	-9.189
3	-9.021	-8.903	-8.974	-8.785	-8.042	-8.980	-8.566	-8.837	-8.635	-9.084
4	-8.948	-8.847	-8.798	-8.749	-8.014	-8.932	-8.560	-8.809	-8.600	-9.021
5	-8.915	-8.686	-8.759	-8.740	-7.957	-8.855	-8.503	-8.794	-8.488	-8.948
6	-8.864	-8.683	-8.742	-8.572	-7.954	-8.834	-8.474	-8.740	-8.482	-8.902
7	-8.860	-8.682	-8.640	-8.515	-7.812	-8.738	-8.474	-8.620	-8.470	-8.651
8	-8.770	-8.644	-8.631	-8.478	-7.732	-8.726	-8.399	-8.620	-8.463	-8.633
9	-8.738	-8.587	-8.595	-8.308	-7.652	-8.693	-8.347	-8.600	-8.459	-8.588
10	-8.706	-8.533	-8.564	-8.301	-7.569	-8.604	-8.338	-8.509	-8.341	-8.575
11	-8.611	-8.500	-8.497	-8.262	-7.514	-8.582	-8.262	-8.425	-8.306	-8.572
12	-8.593	-8.416	-8.472	-8.226	-7.485	-8.582	-8.253	-8.408	-8.253	-8.556
13	-8.540	-8.398	-8.418	-8.148	-7.348	-8.335	-8.101	-8.352	-8.166	-8.437
14	-8.503	-8.355	-8.339	-8.137	-7.288	-8.246	-8.032	-8.346	-8.050	-8.414
15	-8.276	-8.298	-8.334	-8.113	-7.251	-8.213	-8.025	-8.330	-7.978	-8.406
16	-8.266	-8.284	-8.321	-8.039	-7.136	-8.191	-7.953	-8.328	-7.878	-8.368
17	-8.168	-8.228	-8.266	-8.023	-7.112	-8.186	-7.704	-8.260	-7.852	-8.247
18	-8.149	-8.142	-8.215	-8.021	-6.926	-8.078	-7.631	-8.258	-7.822	-8.221
19	-8.121	-8.097	-8.197	-8.020	-6.857	-7.952	-7.536	-8.249	-7.760	-8.151
20	-7.991	-8.043	-8.122	-7.958	-6.782	-7.907	-7.505	-8.192	-7.589	-8.025

MTIC	1	2	3	4	5	6	7	8	9	10
1	-5.388	-5.382	-5.379	-5.224	-5.219	-5.380	-5.361	-5.378	-5.383	-5.248
2	-4.996	-5.252	-5.326	-5.044	-5.060	-5.201	-5.207	-5.041	-5.257	-5.063
3	-4.949	-5.080	-5.200	-4.906	-5.047	-5.057	-5.014	-4.912	-5.091	-4.985
4	-4.939	-5.071	-5.019	-4.899	-5.038	-5.022	-4.982	-4.840	-5.086	-4.941
5	-4.893	-4.932	-4.956	-4.854	-4.931	-4.884	-4.890	-4.802	-5.071	-4.917
6	-4.884	-4.895	-4.908	-4.809	-4.899	-4.835	-4.829	-4.713	-4.961	-4.836
7	-4.797	-4.851	-4.864	-4.636	-4.835	-4.825	-4.803	-4.620	-4.890	-4.831
8	-4.784	-4.642	-4.838	-4.598	-4.759	-4.810	-4.736	-4.606	-4.883	-4.826
9	-4.774	-4.632	-4.785	-4.517	-4.506	-4.797	-4.735	-4.595	-4.852	-4.738
10	-4.644	-4.622	-4.739	-4.422	-4.458	-4.795	-4.727	-4.466	-4.836	-4.629
11	-4.610	-4.601	-4.684	-4.397	-4.391	-4.720	-4.711	-4.325	-4.737	-4.609
12	-4.486	-4.555	-4.667	-4.306	-4.378	-4.556	-4.489	-4.234	-4.615	-4.596
13	-4.468	-4.516	-4.538	-4.277	-4.363	-4.549	-4.297	-4.225	-4.594	-4.518
14	-4.462	-4.276	-4.511	-4.257	-4.355	-4.523	-4.278	-4.220	-4.491	-4.510
15	-4.311	-4.268	-4.409	-4.256	-4.284	-4.480	-4.235	-4.206	-4.484	-4.441
16	-4.275	-4.225	-4.374	-4.250	-4.245	-4.441	-4.195	-4.192	-4.443	-4.424
17	-4.149	-4.205	-4.250	-4.203	-4.207	-4.348	-4.177	-4.094	-4.439	-4.311
18	-4.115	-4.180	-4.214	-4.146	-4.198	-4.297	-4.106	-4.065	-4.420	-4.282
19	-4.106	-4.170	-4.151	-4.111	-4.188	-4.216	-4.073	-4.044	-4.350	-4.273
20	-4.097	-4.157	-4.118	-4.109	-4.179	-4.206	-4.054	-4.033	-4.303	-4.212
MTIC	11	12	13	14	15	16	17	18	19	20
1	-5.278	-5.232	-5.375	-5.224	-5.384	-5.373	-5.353	-5.377	-5.375	-5.380
2	-5.207	-5.066	-5.356	-5.059	-4.939	-5.049	-5.338	-5.343	-5.047	-5.256
3	-5.037	-5.013	-4.907	-5.059	-4.917	-4.946	-5.211	-5.204	-4.811	-5.101
4	-5.035	-4.907	-4.876	-5.031	-4.883	-4.797	-5.060	-5.033	-4.800	-5.089
5	-4.946	-4.865	-4.825	-4.948	-4.654	-4.524	-4.884	-5.016	-4.706	-4.928
6	-4.887	-4.795	-4.799	-4.890	-4.589	-4.383	-4.846	-4.911	-4.633	-4.891
7	-4.831	-4.639	-4.777	-4.844	-4.552	-4.328	-4.617	-4.881	-4.562	-4.648
8	-4.762	-4.630	-4.734	-4.700	-4.523	-4.274	-4.566	-4.850	-4.429	-4.617
9	-4.726	-4.627	-4.693	-4.489	-4.507	-4.196	-4.525	-4.821	-4.304	-4.604
10	-4.667	-4.599	-4.584	-4.347	-4.453	-4.176	-4.516	-4.803	-4.240	-4.373
11	-4.571	-4.594	-4.570	-4.344	-4.412	-4.170	-4.460	-4.702	-4.117	-4.369
12	-4.509	-4.451	-4.491	-4.316	-4.358	-4.153	-4.390	-4.644	-4.054	-4.357
13	-4.484	-4.394	-4.452	-4.139	-4.337	-4.146	-4.389	-4.634	-4.010	-4.341
14	-4.475	-4.370	-4.443	-4.118	-4.318	-4.139	-4.311	-4.600	-3.999	-4.335
15	-4.448	-4.351	-4.323	-4.107	-4.288	-4.115	-4.307	-4.511	-3.985	-4.264
16	-4.394	-4.304	-4.322	-4.103	-4.276	-4.110	-4.277	-4.481	-3.963	-4.264
17	-4.362	-4.292	-4.271	-4.072	-4.265	-4.076	-4.273	-4.392	-3.951	-4.237
18	-4.275	-4.245	-4.235	-4.038	-4.233	-4.057	-4.221	-4.391	-3.947	-4.230
19	-4.267	-4.243	-4.204	-4.037	-4.176	-4.043	-4.160	-4.375	-3.930	-4.199
20	-4.226	-4.111	-4.194	-4.031	-4.169	-4.033	-4.083	-4.295	-3.907	-4.187

Table S2. Values of SMINA scoring function (in kcal/mol) for 20 best poses of ligands (ATP, TMZ, MTIC) in human P2X7 homology model. In columns are shown results of 20 independent docking trials to the region of inhibitor-binding pocket.

ATP	1	2	3	4	5	6	7	8	9	10
1	-7.854	-7.737	-7.944	-7.804	-7.393	-7.788	-7.876	-7.241	-7.278	-7.929
2	-7.756	-7.683	-7.873	-7.802	-7.370	-7.721	-7.787	-7.219	-7.253	-7.667
3	-7.711	-7.544	-7.787	-7.716	-7.278	-7.661	-7.780	-7.197	-7.228	-7.632
4	-7.657	-7.379	-7.703	-7.687	-7.269	-7.589	-7.715	-7.166	-7.144	-7.613
5	-7.644	-7.358	-7.701	-7.684	-7.261	-7.582	-7.715	-7.122	-7.121	-7.530
6	-7.602	-7.353	-7.676	-7.620	-7.203	-7.565	-7.690	-7.079	-7.106	-7.464
7	-7.542	-7.334	-7.671	-7.582	-7.156	-7.552	-7.571	-7.067	-7.067	-7.457
8	-7.540	-7.307	-7.656	-7.571	-7.150	-7.522	-7.537	-7.066	-7.059	-7.387
9	-7.511	-7.305	-7.647	-7.569	-7.129	-7.519	-7.536	-7.053	-7.030	-7.375
10	-7.454	-7.288	-7.646	-7.549	-7.073	-7.519	-7.535	-7.038	-7.019	-7.373
11	-7.453	-7.275	-7.629	-7.484	-7.071	-7.478	-7.514	-7.036	-7.012	-7.355
12	-7.421	-7.266	-7.607	-7.470	-7.012	-7.471	-7.446	-6.960	-7.010	-7.346
13	-7.399	-7.258	-7.585	-7.446	-7.009	-7.449	-7.439	-6.944	-6.936	-7.283
14	-7.358	-7.236	-7.566	-7.440	-6.997	-7.440	-7.424	-6.936	-6.925	-7.240
15	-7.296	-7.234	-7.532	-7.400	-6.977	-7.398	-7.411	-6.922	-6.905	-7.214
16	-7.284	-7.202	-7.490	-7.376	-6.954	-7.391	-7.407	-6.854	-6.903	-7.208
17	-7.283	-7.171	-7.489	-7.368	-6.939	-7.390	-7.375	-6.825	-6.875	-7.208
18	-7.282	-7.150	-7.457	-7.366	-6.916	-7.371	-7.352	-6.806	-6.875	-7.199
19	-7.279	-7.146	-7.433	-7.354	-6.907	-7.357	-7.345	-6.781	-6.857	-7.194
20	-7.245	-7.106	-7.419	-7.350	-6.899	-7.350	-7.323	-6.756	-6.834	-7.188
ATP	11	12	13	14	15	16	17	18	19	20
1	-7.688	-7.951	-7.421	-7.267	-7.447	-7.931	-7.436	-7.681	-7.455	-7.444
2	-7.504	-7.727	-7.397	-7.218	-7.359	-7.799	-7.405	-7.543	-7.397	-7.412
3	-7.495	-7.664	-7.381	-7.142	-7.357	-7.753	-7.363	-7.540	-7.382	-7.410
4	-7.439	-7.611	-7.289	-7.082	-7.356	-7.740	-7.348	-7.525	-7.369	-7.286
5	-7.361	-7.559	-7.248	-7.070	-7.249	-7.735	-7.189	-7.498	-7.333	-7.254
6	-7.323	-7.546	-7.215	-7.070	-7.244	-7.733	-7.167	-7.395	-7.227	-7.249
7	-7.243	-7.487	-7.215	-7.035	-7.213	-7.697	-7.165	-7.346	-7.218	-7.211
8	-7.229	-7.469	-7.212	-7.009	-7.194	-7.608	-7.136	-7.341	-7.217	-7.153
9	-7.228	-7.457	-7.157	-6.956	-7.194	-7.575	-7.122	-7.335	-7.207	-7.150
10	-7.211	-7.456	-7.105	-6.949	-7.188	-7.574	-7.113	-7.330	-7.200	-7.139
11	-7.203	-7.444	-7.096	-6.940	-7.181	-7.574	-7.112	-7.203	-7.187	-7.128
12	-7.202	-7.442	-7.086	-6.921	-7.170	-7.532	-7.098	-7.178	-7.167	-7.108
13	-7.195	-7.351	-7.035	-6.864	-7.166	-7.484	-7.094	-7.150	-7.165	-7.101
14	-7.179	-7.343	-7.011	-6.863	-7.101	-7.479	-7.091	-7.140	-7.130	-7.075
15	-7.175	-7.328	-7.000	-6.853	-7.072	-7.458	-7.056	-7.139	-7.071	-7.074
16	-7.171	-7.314	-7.000	-6.847	-7.064	-7.444	-7.033	-7.128	-7.053	-7.048
17	-7.168	-7.272	-6.990	-6.823	-7.036	-7.444	-7.022	-7.115	-7.048	-7.039
18	-7.140	-7.268	-6.981	-6.807	-7.036	-7.429	-7.015	-7.089	-7.041	-7.015
19	-7.134	-7.263	-6.977	-6.784	-6.962	-7.391	-7.005	-7.077	-7.036	-6.995
20	-7.115	-7.253	-6.970	-6.778	-6.956	-7.335	-6.999	-7.073	-6.993	-6.992

TMZ	1	2	3	4	5	6	7	8	9	10
1	-5.214	-5.239	-5.205	-5.227	-5.262	-5.239	-5.203	-5.259	-5.236	-5.211
2	-5.092	-5.094	-5.089	-5.088	-5.097	-5.041	-5.099	-5.104	-5.077	-5.102
3	-4.914	-4.989	-4.993	-4.874	-4.999	-4.915	-4.986	-4.945	-4.902	-4.845
4	-4.807	-4.919	-4.920	-4.760	-4.876	-4.858	-4.870	-4.909	-4.855	-4.805
5	-4.784	-4.873	-4.866	-4.738	-4.858	-4.804	-4.824	-4.875	-4.779	-4.762
6	-4.713	-4.780	-4.828	-4.711	-4.810	-4.704	-4.819	-4.807	-4.768	-4.727
7	-4.687	-4.710	-4.801	-4.659	-4.694	-4.607	-4.783	-4.799	-4.760	-4.625
8	-4.608	-4.686	-4.800	-4.641	-4.609	-4.582	-4.731	-4.742	-4.695	-4.601
9	-4.520	-4.670	-4.790	-4.639	-4.588	-4.581	-4.706	-4.730	-4.686	-4.537
10	-4.515	-4.657	-4.763	-4.577	-4.533	-4.518	-4.639	-4.728	-4.642	-4.521
11	-4.468	-4.580	-4.706	-4.526	-4.464	-4.508	-4.598	-4.539	-4.596	-4.516
12	-4.456	-4.456	-4.659	-4.525	-4.451	-4.404	-4.597	-4.522	-4.580	-4.509
13	-4.422	-4.431	-4.516	-4.479	-4.405	-4.384	-4.596	-4.434	-4.567	-4.483
14	-4.405	-4.417	-4.501	-4.478	-4.400	-4.343	-4.576	-4.429	-4.516	-4.439
15	-4.405	-4.406	-4.488	-4.474	-4.396	-4.343	-4.522	-4.404	-4.509	-4.424
16	-4.378	-4.399	-4.484	-4.393	-4.358	-4.335	-4.508	-4.402	-4.491	-4.422
17	-4.329	-4.323	-4.482	-4.381	-4.321	-4.317	-4.426	-4.387	-4.445	-4.417
18	-4.316	-4.301	-4.460	-4.280	-4.280	-4.316	-4.396	-4.380	-4.436	-4.411
19	-4.300	-4.293	-4.441	-4.276	-4.223	-4.307	-4.380	-4.361	-4.420	-4.401
20	-4.297	-4.290	-4.402	-4.258	-4.214	-4.297	-4.378	-4.352	-4.389	-4.389

TMZ	11	12	13	14	15	16	17	18	19	20
1	-5.237	-5.216	-5.260	-5.211	-5.244	-5.236	-5.230	-5.220	-5.255	-5.258
2	-5.095	-5.106	-5.102	-5.087	-5.098	-5.092	-5.100	-5.099	-5.092	-5.090
3	-4.928	-4.869	-4.902	-4.846	-4.906	-4.913	-4.872	-4.918	-4.910	-4.907
4	-4.829	-4.847	-4.829	-4.814	-4.894	-4.853	-4.830	-4.871	-4.897	-4.857
5	-4.828	-4.814	-4.801	-4.807	-4.875	-4.831	-4.829	-4.699	-4.868	-4.804
6	-4.722	-4.810	-4.780	-4.712	-4.819	-4.808	-4.810	-4.607	-4.826	-4.748
7	-4.635	-4.808	-4.766	-4.680	-4.706	-4.748	-4.766	-4.607	-4.802	-4.683
8	-4.599	-4.735	-4.749	-4.651	-4.631	-4.746	-4.726	-4.597	-4.771	-4.635
9	-4.599	-4.711	-4.746	-4.600	-4.627	-4.728	-4.635	-4.515	-4.727	-4.619
10	-4.581	-4.659	-4.696	-4.436	-4.601	-4.512	-4.611	-4.496	-4.701	-4.595
11	-4.530	-4.600	-4.632	-4.426	-4.595	-4.492	-4.534	-4.431	-4.623	-4.521
12	-4.516	-4.588	-4.569	-4.410	-4.583	-4.487	-4.516	-4.430	-4.622	-4.491
13	-4.497	-4.525	-4.528	-4.380	-4.507	-4.373	-4.408	-4.420	-4.498	-4.470
14	-4.397	-4.508	-4.515	-4.380	-4.418	-4.364	-4.347	-4.411	-4.446	-4.411
15	-4.370	-4.507	-4.500	-4.336	-4.384	-4.337	-4.335	-4.409	-4.444	-4.329
16	-4.341	-4.470	-4.498	-4.325	-4.383	-4.293	-4.314	-4.358	-4.439	-4.284
17	-4.332	-4.416	-4.419	-4.316	-4.378	-4.287	-4.295	-4.340	-4.413	-4.282
18	-4.288	-4.416	-4.353	-4.315	-4.375	-4.287	-4.277	-4.280	-4.400	-4.272
19	-4.269	-4.376	-4.332	-4.312	-4.367	-4.273	-4.275	-4.273	-4.331	-4.260
20	-4.261	-4.347	-4.321	-4.293	-4.314	-4.257	-4.231	-4.269	-4.296	-4.227

MTIC	1	2	3	4	5	6	7	8	9	10
1	-4.540	-4.534	-4.537	-4.980	-4.538	-4.917	-5.016	-4.528	-4.545	-4.547
2	-4.447	-4.429	-4.439	-4.766	-4.440	-4.708	-4.735	-4.416	-4.451	-4.379
3	-4.387	-4.424	-4.423	-4.645	-4.392	-4.633	-4.606	-4.375	-4.425	-4.355
4	-4.373	-4.378	-4.371	-4.614	-4.352	-4.591	-4.581	-4.345	-4.389	-4.347
5	-4.297	-4.375	-4.354	-4.606	-4.349	-4.566	-4.571	-4.283	-4.366	-4.309
6	-4.291	-4.374	-4.281	-4.605	-4.328	-4.549	-4.552	-4.226	-4.276	-4.156
7	-4.218	-4.363	-4.274	-4.495	-4.302	-4.513	-4.490	-4.195	-4.274	-4.096
8	-4.210	-4.263	-4.252	-4.490	-4.293	-4.508	-4.376	-4.181	-4.258	-4.039
9	-4.173	-4.206	-4.224	-4.440	-4.285	-4.489	-4.362	-4.180	-4.256	-4.035
10	-4.163	-4.146	-4.178	-4.438	-4.198	-4.387	-4.358	-4.114	-4.223	-4.029
11	-4.126	-4.120	-4.164	-4.436	-4.191	-4.377	-4.271	-4.087	-4.152	-4.015
12	-4.076	-4.076	-4.153	-4.413	-4.152	-4.344	-4.234	-4.019	-4.138	-3.983
13	-4.053	-4.072	-4.142	-4.360	-4.026	-4.316	-4.211	-3.960	-4.128	-3.957
14	-3.961	-4.064	-4.133	-4.345	-4.018	-4.301	-4.186	-3.945	-4.120	-3.953
15	-3.916	-4.041	-4.118	-4.272	-3.931	-4.254	-4.169	-3.921	-4.059	-3.899
16	-3.849	-4.017	-4.112	-4.253	-3.898	-4.239	-4.125	-3.902	-4.007	-3.888
17	-3.830	-4.002	-4.098	-4.188	-3.876	-4.107	-4.102	-3.858	-3.985	-3.866
18	-3.816	-3.979	-4.097	-4.177	-3.847	-4.059	-4.040	-3.821	-3.909	-3.811
19	-3.805	-3.928	-4.077	-4.164	-3.844	-4.019	-3.984	-3.805	-3.880	-3.792
20	-3.792	-3.885	-3.963	-4.157	-3.834	-4.019	-3.944	-3.762	-3.872	-3.783

MTIC	11	12	13	14	15	16	17	18	19	20
1	-4.538	-4.540	-4.538	-4.554	-4.546	-4.989	-4.545	-4.919	-4.555	-5.040
2	-4.397	-4.424	-4.450	-4.449	-4.446	-4.731	-4.464	-4.700	-4.384	-4.734
3	-4.379	-4.377	-4.379	-4.422	-4.363	-4.642	-4.403	-4.589	-4.378	-4.657
4	-4.375	-4.368	-4.344	-4.372	-4.319	-4.642	-4.394	-4.574	-4.373	-4.645
5	-4.294	-4.367	-4.314	-4.345	-4.309	-4.568	-4.374	-4.566	-4.364	-4.567
6	-4.244	-4.332	-4.293	-4.324	-4.300	-4.567	-4.373	-4.546	-4.339	-4.550
7	-4.227	-4.132	-4.288	-4.251	-4.222	-4.552	-4.369	-4.522	-4.272	-4.520
8	-4.225	-4.055	-4.268	-4.225	-4.195	-4.470	-4.296	-4.438	-4.242	-4.470
9	-4.220	-4.025	-4.268	-4.215	-4.183	-4.408	-4.235	-4.408	-4.237	-4.421
10	-4.215	-4.011	-4.223	-4.192	-4.182	-4.382	-4.220	-4.333	-4.225	-4.419
11	-4.214	-3.974	-4.190	-4.172	-4.153	-4.244	-4.206	-4.299	-4.164	-4.416
12	-4.181	-3.968	-4.168	-4.156	-4.143	-4.207	-4.092	-4.230	-4.148	-4.280
13	-4.176	-3.947	-4.146	-4.111	-4.139	-4.175	-4.082	-4.159	-3.977	-4.242
14	-4.170	-3.937	-4.138	-4.080	-4.103	-4.161	-4.053	-4.147	-3.922	-4.237
15	-4.159	-3.912	-4.108	-4.073	-4.098	-4.054	-3.986	-4.027	-3.909	-4.199
16	-4.105	-3.895	-4.103	-4.044	-4.094	-4.044	-3.974	-4.010	-3.901	-4.180
17	-4.077	-3.844	-4.043	-3.987	-4.065	-4.004	-3.970	-3.947	-3.872	-4.176
18	-4.029	-3.805	-4.028	-3.937	-4.030	-4.004	-3.935	-3.946	-3.829	-4.149
19	-4.022	-3.804	-4.016	-3.907	-3.982	-3.968	-3.913	-3.942	-3.796	-4.126
20	-4.018	-3.798	-4.015	-3.905	-3.963	-3.959	-3.902	-3.912	-3.794	-4.095

Table S3. Values of SMINA scoring function (in kcal/mol) for 20 best poses of ligands (ATP, TMZ, BzATP, MTIC) in rat P2X7 structure (PDB 6U9V). In columns are shown results of 20 independent docking trials to the region of ATP-binding pocket.

ATP	1	2	3	4	5	6	7	8	9	10
1	-7.954	-7.752	-7.709	-7.680	-7.659	-7.604	-7.733	-7.692	-7.832	-7.390
2	-7.823	-7.620	-7.666	-7.563	-7.556	-7.562	-7.528	-7.656	-7.609	-7.309
3	-7.738	-7.497	-7.602	-7.536	-7.484	-7.367	-7.507	-7.566	-7.555	-7.255
4	-7.720	-7.459	-7.497	-7.519	-7.482	-7.219	-7.460	-7.514	-7.450	-7.217
5	-7.719	-7.446	-7.422	-7.486	-7.423	-7.178	-7.455	-7.446	-7.422	-7.194
6	-7.690	-7.410	-7.412	-7.471	-7.378	-7.177	-7.334	-7.338	-7.392	-7.194
7	-7.572	-7.408	-7.367	-7.467	-7.378	-7.063	-7.310	-7.308	-7.093	-7.143
8	-7.558	-7.397	-7.311	-7.414	-7.364	-7.046	-7.284	-7.267	-7.047	-7.105
9	-7.526	-7.290	-7.302	-7.387	-7.355	-6.989	-7.261	-7.266	-7.020	-7.062
10	-7.515	-7.274	-7.290	-7.358	-7.348	-6.915	-7.192	-7.175	-7.010	-7.030
11	-7.306	-7.271	-7.192	-7.352	-7.301	-6.907	-7.128	-7.151	-6.937	-6.923
12	-7.303	-7.191	-7.134	-7.352	-7.144	-6.839	-7.076	-7.086	-6.843	-6.887
13	-7.271	-7.115	-7.078	-7.336	-7.122	-6.799	-7.052	-7.060	-6.835	-6.882
14	-7.205	-7.088	-7.047	-7.305	-6.986	-6.713	-7.009	-7.050	-6.787	-6.853
15	-7.167	-6.967	-7.028	-7.218	-6.964	-6.663	-6.996	-6.934	-6.786	-6.824
16	-7.165	-6.966	-7.028	-7.179	-6.935	-6.648	-6.913	-6.920	-6.773	-6.774
17	-7.161	-6.935	-7.016	-7.121	-6.911	-6.643	-6.876	-6.906	-6.751	-6.743
18	-7.042	-6.908	-6.913	-7.088	-6.822	-6.642	-6.851	-6.747	-6.735	-6.671
19	-7.016	-6.895	-6.813	-7.042	-6.818	-6.634	-6.833	-6.742	-6.721	-6.650
20	-6.998	-6.890	-6.702	-6.913	-6.790	-6.628	-6.730	-6.712	-6.705	-6.649
ATP	11	12	13	14	15	16	17	18	19	20
1	-7.448	-7.845	-7.767	-7.734	-7.845	-7.487	-7.493	-7.574	-7.396	-7.664
2	-7.345	-7.607	-7.723	-7.638	-7.787	-7.450	-7.323	-7.539	-7.379	-7.437
3	-7.315	-7.550	-7.627	-7.574	-7.709	-7.447	-7.312	-7.498	-7.346	-7.397
4	-7.312	-7.505	-7.613	-7.569	-7.698	-7.414	-7.277	-7.364	-7.324	-7.394
5	-7.276	-7.482	-7.590	-7.549	-7.613	-7.348	-7.250	-7.360	-7.220	-7.376
6	-7.220	-7.425	-7.558	-7.547	-7.567	-7.285	-7.227	-7.340	-7.185	-7.296
7	-7.184	-7.401	-7.531	-7.526	-7.551	-7.237	-7.146	-7.336	-7.123	-7.271
8	-7.084	-7.368	-7.523	-7.459	-7.528	-7.225	-7.082	-7.239	-7.115	-7.245
9	-7.065	-7.367	-7.441	-7.450	-7.515	-7.191	-7.035	-7.143	-7.095	-7.244
10	-7.019	-7.107	-7.420	-7.318	-7.484	-7.152	-6.990	-7.142	-7.072	-7.229
11	-6.975	-7.041	-7.368	-7.317	-7.438	-7.128	-6.902	-7.124	-6.972	-7.222
12	-6.962	-6.976	-7.327	-7.249	-7.437	-7.007	-6.897	-7.085	-6.872	-7.186
13	-6.923	-6.973	-7.318	-7.246	-7.404	-6.985	-6.897	-7.076	-6.845	-7.130
14	-6.871	-6.951	-7.157	-7.226	-7.315	-6.963	-6.832	-7.040	-6.831	-7.021
15	-6.836	-6.933	-7.114	-7.147	-7.314	-6.954	-6.753	-7.020	-6.772	-7.003
16	-6.815	-6.804	-7.099	-7.130	-7.138	-6.942	-6.741	-6.986	-6.640	-6.998
17	-6.801	-6.796	-7.087	-7.119	-7.118	-6.893	-6.672	-6.984	-6.537	-6.960
18	-6.773	-6.778	-7.086	-7.115	-7.102	-6.850	-6.625	-6.984	-6.498	-6.959
19	-6.769	-6.773	-7.056	-7.073	-7.091	-6.808	-6.578	-6.879	-6.464	-6.850
20	-6.694	-6.771	-7.028	-7.011	-7.017	-6.741	-6.506	-6.787	-6.450	-6.841

TMZ	1	2	3	4	5	6	7	8	9	10
1	-5.956	-6.531	-7.079	-7.082	-6.530	-6.664	-6.537	-7.058	-6.531	-6.344
2	-5.734	-6.407	-6.519	-6.512	-6.371	-6.353	-6.392	-6.511	-6.394	-5.910
3	-5.495	-6.087	-6.382	-6.392	-6.092	-5.874	-6.361	-6.363	-6.096	-5.817
4	-5.473	-5.928	-6.086	-6.078	-5.669	-5.593	-6.090	-5.829	-5.866	-5.548
5	-5.419	-5.815	-5.927	-6.040	-5.591	-5.575	-5.820	-5.594	-5.682	-5.243
6	-5.346	-5.679	-5.812	-5.830	-5.537	-5.450	-5.613	-5.328	-5.585	-4.948
7	-5.327	-5.587	-5.804	-5.641	-5.375	-5.436	-5.456	-4.973	-5.356	-4.930
8	-5.103	-5.375	-5.604	-5.586	-5.363	-5.417	-5.356	-4.948	-5.353	-4.916
9	-5.094	-5.339	-5.349	-5.329	-5.333	-5.204	-5.297	-4.910	-5.345	-4.885
10	-5.072	-5.232	-5.334	-5.207	-5.192	-5.196	-5.202	-4.908	-5.179	-4.867
11	-5.054	-5.203	-5.334	-5.162	-5.165	-5.191	-5.066	-4.895	-5.178	-4.807
12	-5.042	-5.172	-5.286	-5.130	-4.970	-5.189	-4.963	-4.874	-5.105	-4.772
13	-5.014	-5.146	-5.186	-5.064	-4.962	-5.162	-4.957	-4.863	-5.000	-4.767
14	-5.011	-4.971	-5.155	-4.949	-4.936	-5.128	-4.932	-4.859	-4.982	-4.765
15	-5.005	-4.945	-5.105	-4.913	-4.932	-5.108	-4.924	-4.808	-4.966	-4.745
16	-4.946	-4.943	-4.955	-4.884	-4.898	-5.077	-4.924	-4.773	-4.965	-4.726
17	-4.885	-4.942	-4.948	-4.882	-4.889	-5.032	-4.892	-4.766	-4.927	-4.636
18	-4.864	-4.923	-4.931	-4.868	-4.835	-5.012	-4.880	-4.713	-4.917	-4.587
19	-4.861	-4.901	-4.925	-4.865	-4.796	-5.005	-4.823	-4.661	-4.917	-4.585
20	-4.803	-4.895	-4.908	-4.824	-4.716	-4.993	-4.793	-4.628	-4.913	-4.528

TMZ	11	12	13	14	15	16	17	18	19	20
1	-6.051	-7.055	-7.052	-6.524	-7.053	-7.043	-7.076	-6.364	-6.617	-6.066
2	-5.961	-6.521	-6.392	-6.077	-6.517	-6.515	-6.342	-6.081	-5.833	-5.827
3	-5.669	-6.360	-6.348	-5.929	-6.381	-6.029	-6.072	-5.917	-5.611	-5.578
4	-5.597	-6.032	-6.028	-5.832	-6.360	-5.784	-5.598	-5.810	-5.542	-5.338
5	-5.413	-5.916	-5.809	-5.680	-6.085	-5.554	-5.455	-5.573	-5.530	-5.307
6	-5.312	-5.813	-5.806	-5.456	-5.927	-5.365	-5.297	-5.408	-5.415	-4.928
7	-5.100	-5.803	-5.592	-5.343	-5.827	-5.321	-5.269	-5.330	-5.392	-4.904
8	-5.100	-5.637	-5.347	-5.335	-5.816	-5.199	-5.144	-5.194	-5.258	-4.900
9	-5.093	-5.554	-5.330	-5.296	-5.631	-4.948	-4.960	-5.106	-5.179	-4.817
10	-5.093	-5.344	-5.317	-5.196	-5.602	-4.947	-4.956	-5.008	-5.176	-4.814
11	-5.070	-5.341	-5.199	-5.173	-5.303	-4.931	-4.953	-5.004	-5.147	-4.804
12	-5.048	-5.337	-5.175	-5.095	-5.299	-4.913	-4.942	-4.958	-5.147	-4.787
13	-4.931	-5.310	-5.138	-4.960	-5.167	-4.907	-4.922	-4.949	-5.138	-4.748
14	-4.891	-5.156	-4.982	-4.943	-5.156	-4.861	-4.919	-4.916	-5.093	-4.694
15	-4.879	-5.149	-4.948	-4.913	-5.133	-4.855	-4.900	-4.844	-5.083	-4.689
16	-4.863	-5.126	-4.935	-4.904	-5.055	-4.801	-4.873	-4.804	-5.067	-4.652
17	-4.828	-4.953	-4.883	-4.897	-4.951	-4.799	-4.871	-4.790	-5.031	-4.598
18	-4.812	-4.947	-4.850	-4.896	-4.912	-4.783	-4.761	-4.730	-4.990	-4.585
19	-4.781	-4.946	-4.832	-4.878	-4.879	-4.711	-4.709	-4.711	-4.953	-4.534
20	-4.755	-4.923	-4.798	-4.867	-4.852	-4.686	-4.706	-4.662	-4.932	-4.514

BzATP	1	2	3	4	5	6	7	8	9	10
1	-9.022	-9.280	-9.243	-8.945	-8.953	-8.937	-9.388	-8.883	-8.982	-9.239
2	-9.008	-9.249	-9.213	-8.759	-8.824	-8.881	-9.243	-8.845	-8.824	-9.163
3	-8.949	-9.158	-9.156	-8.717	-8.747	-8.830	-9.162	-8.765	-8.800	-9.116
4	-8.879	-9.120	-9.087	-8.623	-8.678	-8.824	-9.126	-8.757	-8.761	-9.107
5	-8.875	-9.057	-9.068	-8.620	-8.660	-8.775	-9.091	-8.692	-8.737	-9.049
6	-8.823	-9.048	-9.022	-8.618	-8.649	-8.769	-9.024	-8.655	-8.654	-9.008
7	-8.794	-9.027	-9.009	-8.616	-8.615	-8.728	-8.966	-8.631	-8.649	-8.991
8	-8.704	-9.001	-8.961	-8.512	-8.603	-8.666	-8.830	-8.577	-8.632	-8.979
9	-8.537	-8.993	-8.884	-8.447	-8.567	-8.607	-8.806	-8.539	-8.542	-8.930
10	-8.518	-8.965	-8.786	-8.391	-8.555	-8.604	-8.783	-8.531	-8.491	-8.842
11	-8.514	-8.905	-8.755	-8.322	-8.528	-8.566	-8.780	-8.436	-8.418	-8.663
12	-8.407	-8.861	-8.686	-8.179	-8.468	-8.542	-8.733	-8.400	-8.391	-8.632
13	-8.389	-8.856	-8.646	-8.167	-8.464	-8.535	-8.705	-8.267	-8.351	-8.570
14	-8.269	-8.807	-8.564	-8.149	-8.443	-8.512	-8.696	-8.136	-8.347	-8.540
15	-8.246	-8.754	-8.533	-8.139	-8.389	-8.480	-8.649	-8.095	-8.301	-8.519
16	-8.212	-8.698	-8.530	-8.046	-8.379	-8.385	-8.603	-8.081	-8.281	-8.509
17	-8.203	-8.612	-8.526	-8.044	-8.329	-8.323	-8.580	-8.067	-8.257	-8.492
18	-8.190	-8.575	-8.507	-8.033	-8.324	-8.261	-8.570	-8.008	-8.254	-8.486
19	-8.181	-8.522	-8.501	-7.954	-8.319	-8.216	-8.465	-7.998	-8.212	-8.413
20	-8.068	-8.506	-8.482	-7.886	-8.279	-8.209	-8.458	-7.940	-8.201	-8.379
BzATP	11	12	13	14	15	16	17	18	19	20
1	-9.313	-9.461	-8.977	-9.309	-9.259	-9.302	-9.316	-8.967	-8.896	-9.022
2	-9.244	-9.255	-8.937	-9.212	-9.169	-9.175	-9.114	-8.816	-8.894	-9.012
3	-9.193	-9.238	-8.883	-9.097	-9.155	-9.131	-9.107	-8.741	-8.732	-9.010
4	-9.167	-9.202	-8.872	-9.069	-9.019	-9.130	-9.062	-8.712	-8.718	-8.948
5	-9.153	-9.109	-8.817	-9.050	-9.007	-9.098	-9.040	-8.686	-8.706	-8.856
6	-9.115	-9.016	-8.792	-9.047	-8.993	-9.064	-9.028	-8.639	-8.624	-8.786
7	-9.087	-9.003	-8.770	-9.034	-8.946	-9.041	-9.018	-8.616	-8.585	-8.734
8	-9.085	-8.937	-8.531	-9.022	-8.880	-8.976	-8.999	-8.604	-8.566	-8.663
9	-9.005	-8.928	-8.494	-8.975	-8.871	-8.952	-8.874	-8.526	-8.500	-8.656
10	-8.986	-8.928	-8.449	-8.928	-8.808	-8.949	-8.867	-8.515	-8.441	-8.646
11	-8.898	-8.898	-8.435	-8.919	-8.768	-8.949	-8.687	-8.403	-8.399	-8.590
12	-8.898	-8.793	-8.433	-8.899	-8.752	-8.889	-8.543	-8.331	-8.386	-8.578
13	-8.846	-8.738	-8.407	-8.884	-8.612	-8.864	-8.520	-8.319	-8.380	-8.569
14	-8.748	-8.643	-8.348	-8.858	-8.567	-8.857	-8.515	-8.288	-8.332	-8.565
15	-8.747	-8.620	-8.290	-8.824	-8.514	-8.849	-8.508	-8.262	-8.252	-8.536
16	-8.703	-8.607	-8.287	-8.819	-8.511	-8.830	-8.417	-8.210	-8.136	-8.463
17	-8.683	-8.582	-8.222	-8.699	-8.490	-8.827	-8.399	-8.136	-8.081	-8.452
18	-8.673	-8.538	-8.206	-8.685	-8.486	-8.729	-8.397	-8.120	-8.048	-8.387
19	-8.598	-8.521	-8.175	-8.674	-8.467	-8.604	-8.371	-8.117	-8.031	-8.381
20	-8.482	-8.476	-8.170	-8.588	-8.465	-8.590	-8.361	-8.070	-8.029	-8.365

MTIC	1	2	3	4	5	6	7	8	9	10
1	-6.027	-5.985	-5.992	-5.880	-6.004	-5.883	-5.872	-5.989	-6.038	-5.862
2	-6.013	-5.964	-5.974	-5.757	-5.955	-5.711	-5.858	-5.970	-6.026	-5.721
3	-5.672	-5.835	-5.944	-5.709	-5.839	-5.551	-5.598	-5.840	-6.003	-5.590
4	-5.569	-5.799	-5.840	-5.458	-5.660	-5.467	-5.547	-5.800	-5.895	-5.551
5	-5.540	-5.648	-5.803	-5.424	-5.553	-5.423	-5.472	-5.635	-5.835	-5.471
6	-5.534	-5.632	-5.667	-5.033	-5.533	-5.291	-5.406	-5.549	-5.529	-5.402
7	-5.408	-5.549	-5.542	-4.775	-5.467	-5.185	-5.404	-5.545	-5.519	-5.303
8	-5.291	-5.475	-5.522	-4.731	-5.294	-5.158	-5.317	-5.282	-5.513	-5.294
9	-5.270	-5.467	-5.467	-4.688	-5.243	-5.051	-5.179	-5.242	-5.489	-5.162
10	-5.225	-5.413	-5.400	-4.580	-5.174	-4.952	-5.155	-5.087	-5.415	-5.073
11	-5.081	-5.372	-5.349	-4.562	-5.038	-4.814	-5.081	-5.043	-5.344	-5.051
12	-4.926	-5.252	-5.311	-4.532	-4.897	-4.808	-5.063	-5.040	-5.218	-4.958
13	-4.894	-5.240	-5.304	-4.356	-4.885	-4.768	-4.971	-4.893	-5.197	-4.955
14	-4.862	-5.220	-5.232	-4.255	-4.795	-4.755	-4.952	-4.864	-5.186	-4.816
15	-4.807	-5.155	-5.211	-4.245	-4.683	-4.689	-4.943	-4.850	-4.934	-4.813
16	-4.751	-5.154	-5.159	-4.227	-4.677	-4.664	-4.870	-4.781	-4.933	-4.775
17	-4.723	-5.154	-5.151	-4.220	-4.510	-4.607	-4.806	-4.750	-4.922	-4.745
18	-4.477	-5.148	-5.137	-4.204	-4.400	-4.525	-4.798	-4.738	-4.894	-4.689
19	-4.465	-5.140	-5.086	-4.182	-4.338	-4.503	-4.777	-4.690	-4.887	-4.664
20	-4.428	-5.100	-4.913	-4.132	-4.336	-4.392	-4.771	-4.661	-4.819	-4.659

MTIC	11	12	13	14	15	16	17	18	19	20
1	-5.888	-5.997	-6.042	-6.004	-5.877	-5.985	-5.966	-5.880	-6.010	-5.883
2	-5.862	-5.946	-6.006	-5.966	-5.544	-5.985	-5.857	-5.869	-5.999	-5.710
3	-5.755	-5.841	-5.850	-5.954	-5.288	-5.969	-5.830	-5.554	-5.878	-5.677
4	-5.717	-5.790	-5.834	-5.844	-5.283	-5.840	-5.684	-5.474	-5.845	-5.560
5	-5.553	-5.620	-5.833	-5.801	-5.261	-5.799	-5.564	-5.466	-5.681	-5.478
6	-5.469	-5.567	-5.696	-5.703	-5.154	-5.668	-5.517	-5.358	-5.673	-5.369
7	-5.233	-5.542	-5.677	-5.551	-5.124	-5.639	-5.462	-5.196	-5.577	-5.319
8	-5.179	-5.496	-5.602	-5.496	-5.086	-5.562	-5.398	-5.153	-5.520	-5.154
9	-5.154	-5.369	-5.529	-5.488	-5.078	-5.547	-5.351	-5.045	-5.447	-5.125
10	-5.044	-5.258	-5.515	-5.399	-5.064	-5.475	-5.273	-4.948	-5.404	-5.053
11	-4.994	-5.149	-5.411	-5.273	-5.055	-5.471	-5.255	-4.803	-5.354	-5.032
12	-4.994	-4.907	-5.298	-5.251	-4.953	-5.377	-5.173	-4.767	-5.283	-5.028
13	-4.961	-4.867	-5.274	-5.148	-4.811	-5.349	-5.160	-4.733	-5.279	-4.958
14	-4.959	-4.792	-5.172	-5.117	-4.772	-5.335	-5.064	-4.706	-5.266	-4.815
15	-4.954	-4.778	-5.078	-5.090	-4.685	-5.232	-5.042	-4.702	-5.179	-4.751
16	-4.945	-4.685	-5.074	-5.076	-4.684	-5.141	-5.037	-4.694	-5.114	-4.746
17	-4.813	-4.655	-5.073	-5.041	-4.620	-5.033	-4.935	-4.693	-5.074	-4.692
18	-4.783	-4.652	-4.938	-5.038	-4.606	-5.033	-4.886	-4.664	-5.073	-4.655
19	-4.767	-4.494	-4.915	-4.892	-4.573	-5.027	-4.845	-4.621	-5.056	-4.574
20	-4.724	-4.462	-4.900	-4.888	-4.561	-4.929	-4.831	-4.585	-4.924	-4.549

Table S4. Values of SMINA scoring function (in kcal/mol) for 20 best poses of ligands (ATP, TMZ, MTIC) in rat P2X7 structure (PDB 6U9V). In columns are shown results of 20 independent docking trials to the region of inhibitor-binding pocket.

ATP	1	2	3	4	5	6	7	8	9	10
1	-7.187	-7.193	-7.209	-7.206	-7.198	-7.213	-7.170	-6.993	-7.186	-7.175
2	-6.559	-6.862	-6.751	-6.745	-6.524	-6.913	-6.755	-6.621	-6.785	-6.892
3	-6.466	-6.638	-6.575	-6.595	-6.445	-6.483	-6.730	-6.555	-6.700	-6.765
4	-6.408	-6.549	-6.478	-6.379	-6.239	-6.412	-6.605	-6.473	-6.453	-6.725
5	-6.308	-6.529	-6.418	-6.368	-6.031	-6.389	-6.508	-6.032	-6.438	-6.560
6	-6.044	-5.958	-6.315	-6.129	-5.989	-6.312	-6.086	-5.788	-6.392	-6.490
7	-5.782	-5.947	-6.179	-6.065	-5.930	-6.027	-6.063	-5.668	-6.183	-6.469
8	-5.578	-5.934	-6.106	-6.033	-5.888	-6.020	-5.988	-5.631	-6.015	-6.298
9	-5.565	-5.823	-6.048	-5.729	-5.881	-5.956	-5.950	-5.591	-5.983	-6.097
10	-5.557	-5.578	-6.028	-5.587	-5.814	-5.927	-5.783	-5.513	-5.972	-5.920
11	-5.521	-5.536	-5.924	-5.527	-5.629	-5.840	-5.715	-5.439	-5.832	-5.712
12	-5.304	-5.394	-5.832	-5.477	-5.491	-5.761	-5.695	-5.347	-5.708	-5.622
13	-5.208	-5.295	-5.560	-5.446	-5.417	-5.597	-5.677	-5.295	-5.359	-5.450
14	-5.203	-4.968	-5.527	-5.393	-5.378	-5.533	-5.478	-5.178	-5.246	-5.408
15	-5.196	-4.930	-5.274	-5.347	-5.105	-5.526	-4.927	-5.065	-5.114	-5.313
16	-4.975	-4.895	-5.196	-5.345	-4.763	-5.456	-4.854	-5.055	-4.629	-5.310
17	-4.897	-4.837	-4.931	-5.339	-4.654	-5.252	-4.850	-5.035	-4.587	-5.131
18	-4.571	-4.769	-4.722	-5.219	-4.473	-5.082	-4.809	-4.975	-4.552	-5.131
19	-4.537	-4.663	-4.601	-5.125	-4.461	-4.973	-4.728	-4.869	-4.425	-5.129
20	-4.318	-4.556	-4.531	-5.088	-4.313	-4.957	-4.624	-4.619	-4.267	-4.602
ATP	11	12	13	14	15	16	17	18	19	20
1	-7.165	-7.259	-7.171	-7.192	-7.220	-7.105	-7.054	-7.120	-7.187	-7.082
2	-6.897	-6.857	-6.781	-7.064	-6.753	-6.930	-6.624	-6.807	-6.780	-6.974
3	-6.735	-6.855	-6.445	-6.734	-6.604	-6.920	-6.588	-6.696	-6.672	-6.583
4	-6.604	-6.800	-6.443	-6.696	-6.532	-6.776	-6.571	-6.456	-6.580	-6.544
5	-6.478	-6.507	-6.275	-6.333	-6.519	-6.570	-6.554	-6.430	-6.351	-6.170
6	-6.432	-6.288	-6.171	-6.320	-6.186	-6.448	-6.228	-6.409	-6.105	-6.092
7	-6.281	-6.280	-6.121	-6.313	-6.023	-6.383	-6.094	-6.134	-5.992	-6.033
8	-6.158	-6.181	-6.094	-6.289	-5.948	-6.338	-6.065	-6.065	-5.874	-5.966
9	-6.119	-6.109	-6.078	-6.229	-5.941	-6.319	-5.941	-5.925	-5.687	-5.883
10	-6.039	-5.955	-5.987	-6.071	-5.931	-6.306	-5.932	-5.903	-5.628	-5.207
11	-5.970	-5.903	-5.972	-5.686	-5.901	-6.091	-5.799	-5.754	-5.570	-5.194
12	-5.932	-5.659	-5.922	-5.483	-5.796	-5.833	-5.556	-5.626	-5.501	-5.172
13	-5.929	-5.583	-5.890	-5.393	-5.090	-5.775	-5.477	-5.592	-5.430	-5.107
14	-5.585	-5.472	-5.795	-5.362	-5.089	-5.442	-5.374	-5.400	-5.400	-5.064
15	-5.546	-5.410	-5.725	-5.150	-4.958	-5.437	-5.131	-5.384	-5.178	-4.808
16	-5.531	-5.135	-5.697	-4.936	-4.904	-5.354	-5.063	-5.180	-5.157	-4.515
17	-5.414	-5.118	-5.629	-4.680	-4.765	-4.815	-5.063	-5.089	-5.146	-4.450
18	-5.139	-5.000	-5.591	-4.467	-4.712	-4.669	-5.057	-4.835	-4.809	-4.447
19	-5.118	-4.712	-5.581	-4.437	-4.534	-4.668	-5.049	-4.530	-4.525	-4.399
20	-5.076	-4.421	-5.417	-4.355	-4.398	-4.516	-4.843	-4.425	-4.374	-4.175

TMZ	1	2	3	4	5	6	7	8	9	10
1	-6.557	-6.571	-6.567	-6.563	-6.562	-6.571	-6.558	-6.559	-6.563	-6.567
2	-6.228	-6.225	-6.205	-6.211	-6.207	-6.207	-6.214	-6.199	-6.097	-6.212
3	-6.121	-6.138	-6.141	-6.127	-6.132	-6.106	-6.103	-6.128	-5.740	-6.117
4	-5.968	-5.991	-5.842	-6.014	-5.987	-6.016	-5.991	-6.015	-5.736	-6.037
5	-5.853	-5.925	-5.807	-5.889	-5.901	-5.948	-5.979	-5.976	-5.718	-5.972
6	-5.737	-5.717	-5.753	-5.878	-5.743	-5.753	-5.751	-5.847	-5.682	-5.742
7	-5.717	-5.714	-5.723	-5.772	-5.739	-5.730	-5.716	-5.726	-5.674	-5.717
8	-5.683	-5.709	-5.694	-5.732	-5.715	-5.721	-5.661	-5.710	-5.634	-5.709
9	-5.658	-5.703	-5.667	-5.719	-5.687	-5.649	-5.654	-5.679	-5.620	-5.683
10	-5.630	-5.691	-5.657	-5.705	-5.625	-5.637	-5.630	-5.629	-5.615	-5.667
11	-5.629	-5.669	-5.633	-5.658	-5.618	-5.621	-5.588	-5.622	-5.605	-5.657
12	-5.582	-5.630	-5.629	-5.647	-5.568	-5.605	-5.559	-5.620	-5.574	-5.623
13	-5.567	-5.617	-5.623	-5.622	-5.562	-5.540	-5.548	-5.595	-5.548	-5.620
14	-5.544	-5.612	-5.611	-5.579	-5.544	-5.538	-5.523	-5.539	-5.510	-5.616
15	-5.520	-5.555	-5.604	-5.547	-5.506	-5.496	-5.517	-5.505	-5.498	-5.558
16	-5.507	-5.538	-5.559	-5.516	-5.506	-5.456	-5.509	-5.502	-5.459	-5.543
17	-5.484	-5.526	-5.552	-5.497	-5.506	-5.447	-5.487	-5.500	-5.450	-5.520
18	-5.441	-5.516	-5.521	-5.477	-5.422	-5.440	-5.428	-5.490	-5.404	-5.494
19	-5.427	-5.504	-5.500	-5.438	-5.402	-5.432	-5.409	-5.462	-5.383	-5.455
20	-5.374	-5.383	-5.445	-5.358	-5.388	-5.374	-5.392	-5.453	-5.383	-5.432

TMZ	11	12	13	14	15	16	17	18	19	20
1	-6.557	-6.567	-6.561	-6.562	-6.566	-6.570	-6.569	-6.568	-6.557	-6.625
2	-6.134	-6.218	-6.211	-6.213	-6.204	-6.200	-6.206	-6.217	-6.198	-6.179
3	-5.990	-5.980	-6.131	-5.985	-6.090	-6.127	-6.137	-6.136	-5.916	-5.778
4	-5.846	-5.956	-5.986	-5.941	-6.017	-6.040	-5.977	-5.799	-5.731	-5.759
5	-5.748	-5.744	-5.892	-5.751	-5.972	-5.895	-5.745	-5.722	-5.717	-5.666
6	-5.703	-5.719	-5.853	-5.741	-5.840	-5.737	-5.720	-5.719	-5.645	-5.653
7	-5.674	-5.668	-5.738	-5.715	-5.812	-5.702	-5.662	-5.642	-5.625	-5.653
8	-5.617	-5.650	-5.708	-5.706	-5.732	-5.675	-5.646	-5.633	-5.615	-5.580
9	-5.610	-5.627	-5.654	-5.684	-5.699	-5.627	-5.622	-5.624	-5.608	-5.557
10	-5.583	-5.623	-5.632	-5.627	-5.687	-5.613	-5.609	-5.621	-5.558	-5.547
11	-5.578	-5.598	-5.618	-5.619	-5.667	-5.613	-5.603	-5.621	-5.539	-5.533
12	-5.536	-5.580	-5.595	-5.596	-5.633	-5.612	-5.584	-5.609	-5.529	-5.443
13	-5.514	-5.535	-5.561	-5.586	-5.631	-5.538	-5.564	-5.538	-5.520	-5.394
14	-5.509	-5.519	-5.548	-5.544	-5.626	-5.535	-5.507	-5.503	-5.506	-5.386
15	-5.489	-5.494	-5.532	-5.536	-5.626	-5.525	-5.505	-5.497	-5.405	-5.340
16	-5.454	-5.484	-5.529	-5.534	-5.616	-5.510	-5.503	-5.442	-5.369	-5.337
17	-5.398	-5.461	-5.516	-5.515	-5.602	-5.507	-5.499	-5.392	-5.364	-5.317
18	-5.397	-5.457	-5.494	-5.512	-5.599	-5.498	-5.495	-5.366	-5.346	-5.206
19	-5.359	-5.418	-5.391	-5.506	-5.539	-5.485	-5.454	-5.341	-5.342	-5.195
20	-5.337	-5.390	-5.385	-5.422	-5.495	-5.430	-5.421	-5.335	-5.334	-5.152

MTIC	1	2	3	4	5	6	7	8	9	10
1	-5.700	-5.798	-5.698	-5.699	-5.807	-5.854	-5.695	-5.795	-5.693	-5.795
2	-5.661	-5.700	-5.662	-5.647	-5.732	-5.846	-5.643	-5.637	-5.659	-5.708
3	-5.601	-5.652	-5.575	-5.201	-5.643	-5.718	-5.599	-5.546	-5.588	-5.653
4	-5.485	-5.544	-5.480	-5.144	-5.546	-5.623	-5.490	-5.304	-5.429	-5.544
5	-5.447	-5.493	-5.448	-5.014	-5.161	-5.427	-5.421	-5.289	-5.267	-5.312
6	-5.267	-5.292	-5.165	-4.911	-5.011	-5.377	-5.247	-5.259	-5.217	-5.183
7	-5.197	-5.232	-5.119	-4.895	-4.951	-5.344	-5.230	-5.176	-5.178	-5.039
8	-5.139	-5.187	-4.996	-4.888	-4.851	-5.269	-5.204	-5.075	-5.071	-4.959
9	-5.126	-5.110	-4.937	-4.713	-4.831	-5.090	-5.195	-4.963	-5.020	-4.853
10	-5.098	-5.087	-4.929	-4.693	-4.804	-5.036	-5.126	-4.922	-4.883	-4.852
11	-5.089	-5.078	-4.909	-4.656	-4.789	-4.995	-5.020	-4.909	-4.843	-4.834
12	-5.022	-5.075	-4.892	-4.630	-4.745	-4.979	-4.960	-4.884	-4.831	-4.797
13	-4.897	-5.027	-4.792	-4.618	-4.657	-4.949	-4.895	-4.852	-4.826	-4.770
14	-4.866	-5.014	-4.778	-4.606	-4.644	-4.943	-4.883	-4.841	-4.730	-4.713
15	-4.844	-4.930	-4.776	-4.524	-4.621	-4.931	-4.838	-4.829	-4.722	-4.703
16	-4.802	-4.901	-4.759	-4.462	-4.569	-4.921	-4.788	-4.795	-4.658	-4.676
17	-4.798	-4.896	-4.666	-4.454	-4.560	-4.898	-4.773	-4.783	-4.549	-4.670
18	-4.768	-4.812	-4.617	-4.445	-4.552	-4.868	-4.759	-4.713	-4.470	-4.661
19	-4.748	-4.796	-4.586	-4.440	-4.529	-4.857	-4.748	-4.643	-4.462	-4.606
20	-4.744	-4.792	-4.583	-4.440	-4.526	-4.753	-4.736	-4.606	-4.459	-4.588

MTIC	11	12	13	14	15	16	17	18	19	20
1	-5.796	-5.697	-5.699	-5.803	-5.794	-5.838	-5.710	-5.792	-5.706	-5.837
2	-5.679	-5.656	-5.655	-5.754	-5.546	-5.751	-5.655	-5.758	-5.659	-5.829
3	-5.652	-5.590	-5.572	-5.655	-5.533	-5.644	-5.580	-5.647	-5.590	-5.704
4	-5.546	-5.479	-5.489	-5.545	-5.331	-5.564	-5.488	-5.545	-5.486	-5.414
5	-5.493	-5.310	-5.448	-5.488	-5.172	-5.411	-5.273	-5.296	-5.433	-5.376
6	-5.347	-5.121	-5.191	-5.075	-5.099	-5.355	-5.229	-5.296	-5.228	-5.314
7	-5.321	-5.116	-5.134	-4.959	-5.077	-5.285	-5.127	-5.252	-5.132	-5.262
8	-5.285	-5.060	-5.126	-4.857	-5.072	-5.135	-5.017	-5.183	-5.121	-5.185
9	-5.241	-5.010	-4.972	-4.806	-4.970	-5.059	-4.921	-5.182	-5.023	-5.164
10	-5.158	-4.905	-4.906	-4.787	-4.943	-4.980	-4.906	-5.076	-4.896	-5.154
11	-5.072	-4.902	-4.878	-4.776	-4.904	-4.966	-4.867	-4.949	-4.865	-5.044
12	-5.050	-4.841	-4.850	-4.771	-4.895	-4.928	-4.841	-4.928	-4.838	-4.949
13	-4.982	-4.800	-4.838	-4.760	-4.892	-4.903	-4.819	-4.916	-4.814	-4.873
14	-4.932	-4.766	-4.823	-4.679	-4.810	-4.900	-4.766	-4.853	-4.786	-4.854
15	-4.925	-4.748	-4.815	-4.651	-4.791	-4.798	-4.739	-4.846	-4.763	-4.838
16	-4.923	-4.730	-4.743	-4.587	-4.775	-4.774	-4.732	-4.816	-4.727	-4.804
17	-4.901	-4.726	-4.740	-4.570	-4.767	-4.712	-4.727	-4.792	-4.656	-4.763
18	-4.879	-4.718	-4.731	-4.544	-4.761	-4.699	-4.683	-4.782	-4.647	-4.762
19	-4.858	-4.691	-4.713	-4.542	-4.665	-4.697	-4.661	-4.747	-4.592	-4.752
20	-4.840	-4.675	-4.677	-4.541	-4.648	-4.679	-4.653	-4.732	-4.591	-4.692

Publikacja 3

Retinoic acid-induced alterations enhance eATP-mediated anti-cancer effects in glioma cells: implications for P2X7 receptor variants as key players.

Autorzy: **Szymczak, B.,** Pegoraro, A., De Marchi, E., Grignolo, M., Maciejewski, B., Czarnecka, J., & Roszek, K.

Rok publikacji: 2024

DOI:

Artykuł wysłany do czasopisma: Biochimica et Biophysica Acta (BBA) – Molecular Basis of Disease

Wydawnictwo: Elsevier

Punktacja według wykazu Ministerstwa Nauki i Szkolnictwa Wyższego (2024): 140 pkt

Journal Impact Factor (2023): 4,2 pkt

Liczba cytowań:

Retinoic acid-induced alterations enhance eATP-mediated anti-cancer effects in glioma cells: implications for P2X7 receptor variants as key players

Bartosz Szymczak[1], Anna Pegoraro[2], Elena De Marchi[2], Marianna Grignolo[2], Bartosz Maciejewski[3], Joanna Czarnecka[1], Elena Adinolfi[2], Katarzyna Roszek[1,] *

[1] Department of Biochemistry, Faculty of Biological and Veterinary Sciences, Nicolaus Copernicus University in Torun, Lwowska 1, 87-100 Toruń

[2]Department of Medical Sciences, Section of Experimental Medicine, University of Ferrara, Via Luigi Borsari 46, 44121 Ferrara, Italy

[3] Department of Immunology, Faculty of Biological and Veterinary Sciences, Nicolaus Copernicus University in Torun, Lwowska 1, 87-100 Toruń

* corresponding author: kroszek@umk.pl

ORCID numbers: 0000-0001-7597-4238 (BS), 0000-0002-7045-5161 (AP), 0000-0003-0064-4335 (EDM), 0000-0002-6268-3826 (JC), 0000-0001-8129-9929 (EA), 0000-0002-2854-6238 (KR)

ABSTRACT

Retinoic acid (RA) is a small, lipophilic molecule that inhibits cell proliferation and induces differentiation through activation of a family of nuclear receptors (RARs). The therapeutic potential of RA in the treatment of glioma was first evaluated two decades ago, but these attempts were considered not conclusive. Based on the complexity of tumor microenvironment and the role of purinergic signals within TME, we aimed to support RA-induced alterations in glioma cells with extracellular ATP.

Our experiments focused on defining the purinergic signaling dynamics of two different human glioma cell lines M059K and M059J subjected to RA-based differentiation protocol. The applied procedure caused considerable modulation in P2X7 receptor variants expression at the gene and protein level, and decrease in ecto-nucleotidase activity. Collectively, it led to the decrease in cell proliferation rate and migration, as well as boosted sensitivity to cytotoxic eATP influence. We confirmed that micromolar concentrations of ATP decreased cell viability by 40 and 20 % in RA-treated M059K and M059J cells, respectively. Moreover, the decrease in migration capability up to 60% in the presence of 100 µM ATP was observed. Both effects were mediated by P2X7R activation and reversed in the presence of A740003 antagonist, confirming the role of P2X7 receptor.

We postulate that retinoic acid-induced changes coupled with micromolar eATP could be effective as anti-cancer treatment affecting the purinergic signaling. The obtained results point out the role of P2X7R variants in influencing potential of glioma cells, as well as the possibility of using these isoforms as therapeutic targets.

KEY WORDS: glioma; retinoic acid-induced differentiation; eATP; P2X7 receptor; purinergic signaling

HIGHLIGHTS

- Retinoic acid (RA)-induced alterations decrease invasiveness of glioma cells
- RA-treated cells express changes in purinergic system components
- Increased expression of P2X7 receptor enhances cytotoxic effect of eATP

GRAPHICAL ABSTRACT

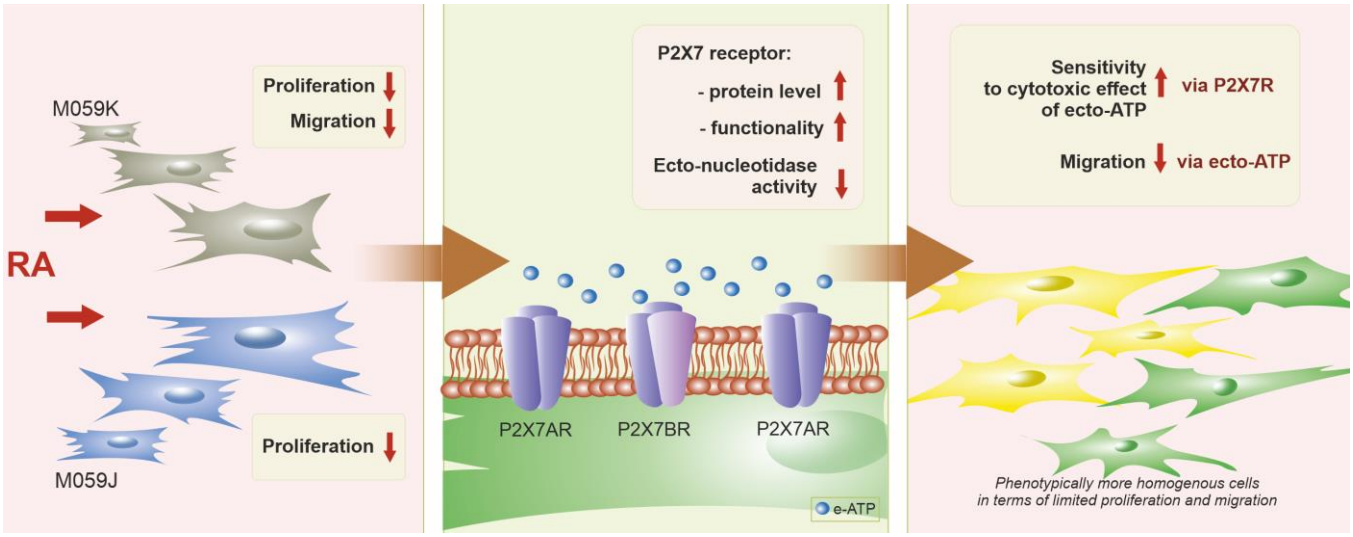

INTRODUCTION

Glioblastoma multiforme (GBM) is the most aggressive primary brain tumor, with a very poor prognosis and a median overall survival below 15 months [1]. The current standard treatment protocols involve surgical intervention followed by a combination of radiotherapy and chemotherapy with temozolomide (TMZ). However, prolonged monotherapy with TMZ tends to induce the phenomenon of selection pressure, fostering the formation of secondary chemoresistant tumors. Despite the implemented therapies, the relapse rate and the mortality linked to glioma remains high [2]. Differentiation of glioma cells using a differentiation agent such as retinoic acid (RA) seems to be a promising strategy to limit brain cancer progression [3–5].

RA is a small, lipophilic differentiation agent that acts as a ligand for a family of nuclear receptors (RARs) to regulate the expression of target genes. The main family of nuclear receptors comprises three genes, RARα, RARβ and RARγ, each coding for several isoforms. The selective stimulation of these isoforms with RA has been shown to mainly inhibit cellular proliferation but unexpectedly, also to promote such proliferation in some cases [6]. The ability of RA to induce post-mitotic, neural phenotypes in various stem cells, in vitro, served as early evidence that RA is involved in the switch between proliferation and differentiation. RA induces neuronal differentiation of mouse and human embryonic stem cells, neural stem cells, bone marrow hematopoietic stem cells, and cancer cells, such as teratocarcinoma and neuroblastoma cell lines [7], which is followed by the decrease in cell proliferation. The therapeutic potential of RA in the treatment of glioma was first evaluated two decades ago, but although some promising effects were initially reported, these attempts were considered not conclusive [6]. Therefore, we aimed to use this therapeutic approach in a novel way. In our earlier studies we confirmed that ATP in the extracellular environment supports the differentiation of mesenchymal stem cells into neuronal lineage [8]. Therefore, our aim was to support RA-induced alterations with extracellular ATP. It is commonly accepted that modern oncology requires a broader approach and combined therapies considering the tumor microenvironmental cues, which may influence the outcome. Purinergic signaling is one of the earliest evolutionary signaling systems comprising P2X and P2Y receptors, their purine ligands, and ectoenzymes metabolizing purine nucleotides, thus regulating purines levels in the microenvironment [9]. It is commonly accepted that critical pathophysiological processes such as tissue homeostasis, inflammation, and cancer are governed and modulated by purinergic signaling [10, 11].

Extracellular ATP (eATP) is a dominating purine component in the tumor microenvironment (TME) [11, 12]. It can be released following tumor and adjacent tissue necrosis or through active release, facilitated by proteins such as those of the ABC (ATP-binding cassette) transporter family, as well as inside vesicles released from the tumor, immune, and stromal cells [13]. eATP is the natural ligand of two distinct families of purinergic receptors: ionotropic P2Xs and metabotropic P2Ys. Among all of them, P2X7 is the most studied ATP receptor in cancer[11]. Numerous recent studies on ATP-gated ion channel P2X7 receptor, abundantly expressed on various cancer cells, indicate that it is characterized by its dual response to ATP stimulation, which may act as a „double-edged sword" [10, 14–16]. At low concentrations of ATP, the activated receptor creates a cation channel, whereas the prolonged exposure of P2X7R to high micromolar concentrations of ATP causes the activation of non-selective macropore, which is permeable to large organic cations such as N-methyl-D-glucamine ($NMDG^+$) or fluorescent dyes such as ethidium bromide, propidium iodide and Lucifer Yellow [17]. The macropore formation is reversible, but the only way to stop signaling is the hydrolysis of eATP, thus conferring an essential role to ATP degrading ectonucleotidases in this fine-tuned regulation. It is still

arguable whether the macropore-related effects are reliant only on pore permeabilization or also on accessory pathways of intracellular signaling. Nonetheless, it is generally accepted that the macropore opening is related to cytotoxicity, whereas the tonic activation of P2X7R with low ATP concentrations supports a trophic pro-proliferative effect [18–20]. Going deeper into cancer-promoting mechanisms, eATP acting through the P2X7R has been implicated in various processes such as induction of epithelial-mesenchymal transition, promotion of MMP and cathepsin secretion, and the increased motility and invasive capacity in human melanoma, breast, and prostate cancer cells *via* activation of Ca^{2+}-dependent potassium channels or the PI3K/AKT pathway [12, 13].

P2X7R stimulation leads to the activation of diverse intracellular signaling molecules, including protein kinases PKB/AKT, phospholipases, tyrosine phosphatases, epithelial membrane proteins, and the large molecular complex of NLRP3 inflammasome [19]. Over 50 different proteins have been identified to directly interact with the P2X7 receptor. However, for the vast majority of these proteins, the interaction domains and the physiological consequences of these connections are only poorly described [18]. The variability of the transduction pathways linked to P2X7R activation must be further interpreted based on the structural diversity of P2X7R domains which are surrounded by a specific molecular environment in each type of cell and each microenvironmental context [12, 13]. Undoubtedly, the P2X7 receptor plays an important role in regulating tumor cell growth, migration, and invasion. Some of the recently published data indicate that commonly accepted anti-cancer therapies, e.g. temozolomide treatment or irradiation, interfere with purinergic receptors [21–23].

The P2X7 receptor gene is located on human chromosome 12q24.31 and encodes the polypeptide of 595 amino acids. Two main human P2X7R variants, P2X7A and P2X7B, are expressed in most cell types, where their activation is associated with distinct biochemical and functional responses [16, 24]. The P2X7A receptor variant is subjected to post-translational modifications including *N*-linked glycosylation, palmitoylation, and ADP-ribosylation. The resulting protein product is typically 75 to 78 kDa in size compared to the predicted non-glycosylated size of 68 kDa. The P2X7B variant is 364 amino acid residues in length, lacks a part of the C-terminal domain of P2X7A, and is non-glycosylated. It can form functional ion channels but cannot create large pores - this property underlies its trophic role in cell proliferation [25, 26]. Ziberi and colleagues focused on examining P2X7 receptor splice variants in human glioblastoma stem cells (GSCs) [27]. The authors confirmed the expression of both P2X7 receptor isoforms in glioblastoma stem cells obtained from three different patients. Moreover, P2X7A and P2X7B levels were increased in GSCs resulting from treatment with the most potent agonist of P2X7 receptor, 2'(3')-O-(4-Benzoylbenzoyl)adenosine 5'-triphosphate (BzATP). Contrarily, pre-incubation of the cells with the P2X7R antagonist A438079 eliminates the effect of BzATP on P2X7A and P2X7B expression. In line with these findings, Zanoni and colleagues showed expression of both P2X7 isoforms in human glioblastoma cell lines and demonstrated how radiotherapy can differently affect P2X7A versus P2X7B expression [22] similarly to what was found in AML and neuroblastoma following chemotherapy administration [23, 26].

Our experiments aimed at defining the purinergic signaling dynamics of two different human glioma cell lines M059K and M059J subjected to retinoic acid-based differentiation. These cell lines were originally described as differing in sensitivity to ionizing radiation and chemotherapeutics, thus providing a useful model system for evaluating the cellular and molecular processes reflecting the tumor cell heterogeneity [28]. The applied RA-based differentiation procedure confirmed some differences and caused considerable modulation in purinergic signaling, including an increase in P2X7 receptor isoforms and a decrease in ecto-nucleotidase activity. Collectively, it led to a decrease in

proliferation rate, cell cycle synchronization, and an increase in the sensitivity to cytotoxic ecto-ATP influence. The obtained results point out the role of P2X7R variants and their expression level in regulating the biological potential of glioma cells, as well as the possibility of using these isoforms as therapeutic targets. Our detailed understanding of RA-induced processes and the following alterations in purinergic mechanisms will pave the way to harnessing such a complex approach in future anti-cancer treatment.

MATERIALS AND METHODS

Chemical reagents

All reagents used in the experimental part were of analytical grade and purchased as follow: Adenosine 5'-diphosphate monopotassium salt dihydrate (ADP), Adenosine 5'-monophosphate sodium salt (AMP), Adenosine 5'-triphosphate disodium salt solution (ATP), All-trans retinoic Acid (RA), 1-naphthol-3,6-disulfonic acid (BGO), 2'(3')-O-(4-Benzoylbenzoyl)adenosine 5'-triphosphate (BzATP), Diadenosine pentaphosphate pentasodium salt (Ap5A), N-(1-{[(cyanoimino)(5-quinolinylamino) methyl] amino}-2,2-dimethylpropyl)-2-(3,4-dimethoxyphenyl)acetamide (A740003), Dipyridamole, Levamisole, 3-(4,5-Dimethyl-2-thiazolyl)-2,5-diphenyl-2H-tetrazolium bromide (MTT), Ethidium bromide (EtBr) were from Sigma-Aldrich, Germany. Dipotassium and monopotassium phosphate for HPLC, Methanol for HPLC, Tetrabutylammonium (TBA) were from J.T.Baker Chemical Company, USA. ECL HRP Chemiluminescent Substrate ETA C ULTRA 2.0 was from Cyanagen Srl, Italy. All other basic reagents were purchased in POCh, Poland.

Cell culture and retinoic acid treatment

Cells of human glioma cell lines M059K and M059J, originating from the same male patient with glioblastoma, were purchased from American Type Culture Collection (ATCC) and grown according to manufacturer protocol in DMEM/F-12 medium supplemented with 10% fetal bovine serum (FBS), 100 IU/ml penicillin and 100 µg/mL streptomycin (all from Biowest, France) in a humidified incubator supplied with 5% CO_2 at 37 °C.

The RA-based neuronal differentiation protocol was based on the literature data [21]. Cells were seeded at a density of 10 000 cells/cm^2 in the culture medium described above. After adhesion, the culture medium was replaced with DMEM/F-12, 10% FBS, 100 IU/ml penicillin, and 100 µg/mL streptomycin supplemented with 10 µM retinoic acid (Sigma-Aldrich, Germany). The culture was carried out for 14 days, and the medium was changed every 72 hours.

The growth kinetics of RA-treated and non-treated M059K and M059J cells

Cell growth was assessed by determination of the total cell number and their proliferation rate. Initially, cells were seeded at a density of 2.5×10^5 per plate of 6 cm diameter, and cultured under standard conditions, with or without 10 µM retinoic acid (for RA-treated and non-treated cells, respectively). The cells were passaged every 3 days, and the cell number was counted using a Thoma chamber after 0.4% trypan blue staining.

The gene expression analysis in RA-treated and non-treated M059K and M059J cells

Gene expression was determined at the mRNA level. *RA-treated and non-treated* M059K and M059J cells in a subconfluent state were detached using 0.25% trypsin and subsequently suspended in a lysis buffer. mRNA isolation was performed using the RNeasy Mini Kit (Qiagen, Germany). The

concentration of the RNA sample was measured spectrophotometrically with an Epoch Take 3 reader (Agilent BioTek, USA). The obtained material underwent DNase treatment using the RNase-free DNase I kit (Thermo Fischer Scientific, USA). This step was carried out using the T100 Thermal Cycler (BioRad, USA). According to the producer's protocol.

The mRNA served as the substrate in the reverse transcription (RT) reaction, utilizing the RevertAid First Strand cDNA Synthesis Kit (Thermo Fischer Scientific, USA). This reaction was conducted over 60 minutes at 42°C and then terminated for 5 minutes at 70°C using a T100 Thermal Cycler (BioRad, USA). The resulting cDNA was utilized as a template for the quantitative analysis of gene expression levels in the Real-Time qPCR reaction.

The Real-Time PCR reaction was executed using the LightCycler 480 SYBR Green I Master kit (Roche, Switzerland), along with 50ng of cDNA and synthesized primers (provided by IBB PAN, Poland, see the table) at a final concentration of 0.4 µM. The reaction was carried out using the LightCycler 480 instrument (Roche, Switzerland), with the following sequential stages: initial denaturation at 95°C for 5 min (1 cycle); denaturation at 95°C for 10 s; annealing at 60°C for 20 s; extension at 72°C for 20 s (45 cycles). The results for the NES, NeuroD1, TUJ1, GFAP, N-cadherin, and E-cadherin genes were analyzed using the LightCycler 480 SW 1.5.1 software (Roche, Switzerland), regarding the expression level of the GAPDH gene.

For P2X7 isoforms expression, a comparative CT experiment (ΔΔCT) was run in AB PRISM 7300 Step One Real-Time PCR system (Applied Biosystems) using the following protocol: holding stage 50°C for 2 min, 95°C for 10 min followed by cycling stage 95°C for 15 s and 60°C for 1 min for a total of 40 cycles. Fold increase of the target cDNA in the test sample was determined relative to HEK cell line reference sample, which expresses minimal levels of P2X7A and P2X7B. The customized TaqMan primers and probes for P2X7A and B (Thermo Scientific, Applied Biosystem) were as previously described in Pegoraro et al. 2021 [29] and GAPDH (Thermo Scientific, Applied Biosystem) was used as a reference gene.

Marker	Forward (5'→3')	Reverse (5'→3')	Product (bp)	Annealing temp. (°C)
NES	GGAAGAGAACCTGGGAAAGG	GATTCAGCTCTGCCTCATCC	188	60/59.9
NeuroD1	GAACGCAGAGGAGGACTCAC	CTTGGGCTTTTGATCGTCAT	109	60/60.1
GFAP	GTGGTGAAGACCGTGGAGAT	CGGAGCAACTATCCTGCTTC	145	60/60
TUJ1	GAAGAGGGCGAGATGTACGA	TTTAGACACTGCTGGCTTCG	122	60/60
P2X7	GACGCTCTGTTCCTCTGACC	TCACAGGTCTTCTGGTTCCC	111	60/60

Western blotting analysis

RA-treated and non-treated M059K and M059J cells were cultured to reach a subconfluent state. Cells were then harvested with the use of 0.25% trypsin and subsequently re-suspended in lysis buffer (100 mM NaCl, 20 mM KCl, 10 mM $NaHCO_3$, 5 mM glucose, 4 mM $MgCl_2$, 2 mM $CaCl_2$, 1% Triton X-100, 25 mM Tris-Cl pH 7.4) to obtain protein lysate.

Protein lysate was loaded and separated in 4-12 % NuPAGE Bis-Tris precast gels (Thermo Scientific, USA) and then transferred onto a nitrocellulose membrane. Membranes were incubated overnight at 4°C with primary antibodies: anti-P2X7 diluted 1:300 (APR008, Alomone Labs, Israel) and anti-myosin II diluted 1:1000 (Sigma-Aldrich). Membranes were then incubated with HRP-conjugated secondary goat anti-rabbit at a 1:3000 dilution for an hour at room temperature. Protein bands were visualized using the ECL HRP Chemiluminescent Substrate ETA C ULTRA 2.0 (Cyanagen Srl, Italy) with a Licor C-Digit Model 3600, and intensity bands analysis was carried out with ImageJ software.

Cell viability assays

Cell viability screening was assessed using MTT test based on the activity of mitochondrial enzymes and their ability to reduce MTT salts to formazan. RA-treated and non-treated M059K and M059J cells were seeded at a density 15 000 cells/cm^2 in 48-well plates. After 24 hours, the culture media were replaced and supplemented with 10, 100 or 1000 µM ATP (Sigma-Aldrich, Germany) with or without NTPDase inhibitor 100 µM BGO (1-naphthol-3,6-disulfonic acid; BG0136, Sigma-Aldrich, Germany); with 1, 10 or 100 µM BzATP (2'(3')-O-(4-Benzoylbenzoyl)adenosine 5'-triphosphate; Sigma-Aldrich, Germany) or their combinations with 1 µM A740003 (Sigma-Aldrich, Germany). After 72 hours of incubation, the medium was replaced with 0.5 mg/ml MTT (Sigma-Aldrich, Germany) in the culture medium. After 30 minutes of incubation at 37°C, the MTT solution was removed, and the formed formazan crystals were dissolved in 300 µl of DMSO (Chempur, Poland). The absorbance of the solution was measured at 570 nm, using an Epoch Take 3 plate reader. The experiment was performed in 4 replications. Cell viability was calculated as a percentage of the untreated samples reflecting positive control (100%).

Scratch test

Scratch assay reflects the ability of adherent cells to migrate and "close" the artificial gap (scratch). Cells were seeded at a density of 25 000 cells/cm^2 in 24-well plates. After 24 h, confluent cell monolayers were scraped with a tip to create a "scratch". Subsequently, the medium was replaced with fresh medium supplemented with P2X7 purinergic receptor agonists: 100 µM ATP (in the presence of 100 µM BGO as ATP hydrolysis inhibitors) or 10 µM BzATP, without or with 1 µM A740003. The scratch images were captured during the experiment beginning and after 4, 8, 12, and 24 h using the MOTIC AE30 microscope with x100 magnification and Motic Camera. Analysis of images was performed by Motic Images Plus 2.0 software (Motic Europe, Spain). The migration rate was calculated as a relative scratch closure, and the scratch width at the time 0 was taken as 1.

Membrane and soluble enzymes activity assay

Enzymatic reactions were performed on the surface of adherent cells growing in 6-well plates (membrane ecto-enzymes), and in collected culture media (soluble and microvesicle membrane-anchored exo-enzymes). All enzymatic reactions were performed in triplicate. The reaction mixtures contained 35 mM Tris-HCl pH 7.0, 250 mM sucrose, 10 mM glucose, 3 mM Mg^{2+}, 2 mM Ca^{2+}, 0.1 mM dipyridamole, and 2 mM substrate (ATP, ADP or AMP). 2.5 mM levamisole (Sigma-Aldrich, Germany) was used as a phosphatase inhibitor, 10 µM Ap5A (diadenosine pentaphosphate pentasodium salt; Sigma-Aldrich, Germany) was used as an inhibitor of adenylate kinase and as a blocker of NPPase-mediated hydrolysis. After 90 min of incubation at 37°C, the reaction was stopped by transferring the post-incubation mixture to a tube containing 1 M $HClO_4$, (POCh, Poland) and neutralized with 1M KOH (Chempur, Poland). All samples were delipidated by shaking with n-heptane (POCh, Poland) and frozen at -20°C. Further analyses of qualitative and quantitative purines composition were performed with HPLC method.

Protein concentration measurement

Determination of protein concentration in cell lysates after the enzymatic activity assays and in post-culture media was performed. Protein concentration was measured spectrophotometrically at 280 nm

using an Epoch Take 3 reader and Epoch3 software, with the appropriate lysis buffer and control media as a blind sample.

High-performance liquid chromatography (HPLC)

The qualitative and quantitative composition of the reaction mixtures after enzymatic activity assays was analyzed by HPLC method using Waters chromatograph (In-Line Degasser AF, 515 HPLC Pump, Waters Pump Control Module, Waters 2487 Dual Absorbance Detector, Waters 717 Plus Autosampler) (Waters Corporation, USA), on Merck Chromolith Performance column (100 x 4.6mm) with Merck Chromolith Performance pre-column (Merck, Germany). The separation was carried out under isocratic conditions with KH_2PO_4/K_2HPO_4 buffer pH 7.0 with 5 mM EDTA, 25 mM TBA, and 2.5% MeOH (J.T. Baker Chemical Company, USA) as the mobile phase. 20 µl aliquots of the delipidated and centrifuged samples (10 min, 10000 g, Sartorius 3K30) (Sartorius, Germany) were applied to the column. The separation was carried out at a flow rate of 1 ml/min. Compounds were identified based on retention times of standard solutions at 260 nm. The compound concentration was calculated from the surface area using Millenium 32 software (Waters Corporation, USA).

Ethidium bromide influx

Cells were seeded in 96-well plates and incubated in the presence of 10 µg/mL ethidium bromide for 10 minutes. Ethidium bromide influx was evaluated with a fluorescence plate reader (Epoch Take 3, excitation and emission wavelengths were 530 and 590 nm, respectively), upon addition of 10 µM BzATP alone (as P2X7 receptor agonist), or with 1 µM A740003 as P2X7R antagonist.

Flow cytometry

Samples of 1 x 10^6 M059J and M059K cells, both RA-treated and non-treated , were harvested, washed twice with PBS, resuspended in 70% EtOH, and incubated at -20^{o}C overnight. Then cells were washed twice in PBS buffer and incubated with PI (20 µg/ml) and RNase A (50 µg/ml) for 60 minutes at 37^{o}C in the dark. Fluorescence intensity was measured using BriCyte E6 flow cytometer (Mindray, Shenzhen, China), with 488 nm excitation and 585 nm emission wavelengths. Data was analyzed using FCS Express 7 (De Novo Software, USA).

Enzyme-Linked Immunosorbent Assay (ELISA)

Commercially available ELISA kit, designed as a solid-phase sandwich (Thermo-Fisher Sci.) were used to measure the Akt and phospho-Akt (Ser 473) level in cell lysates according to the manufacturer's instructions. Results are expressed as the ratio of pAkt/Akt.

Statistical analyses

The difference in gene expression value, cell viability, and migration potential was determined using the Mann-Whitney test; the difference in migration assay and Akt-phosphorylation ratio were determined by two-way ANOVA followed by Tukey post-test for multiple comparisons. Differences were considered statistically significant at p-value ≤ 0.05. The statistical significance of the differences between samples is marked in the graphs with asterisks (* for $p \leq 0.05$, ** for $p \leq 0.01$, *** for $p \leq 0.001$). The experiments were performed in four independent replications. Statistical analyses were performed using the Past software version 4.02. Results are presented as means with error bars representing SD.

RESULTS

1. RA-based treatment decreases invasiveness of glioma cells

We have employed one of the widely accepted differentiation protocols, with 10 µM retinoic acid (RA) to differentiate M059 glioma cells. During RA treatment, the cells were cultured in a medium supplemented with 10% Fetal Bovine Serum (FBS) in the medium, as it mimics the natural niches of the human body. In the course of RA treatment, both glioma cell lines M059K and M059J decreased their proliferation rate (increasing population doubling time, PDT) and the plateau phase of the growth curve was established around the 21st day of the differentiation procedure – Figure 1A, 1E. Propidium iodide staining and cell cycle analysis indicated that in the case of RA-treated M059K cells, the limited proliferation reflects G1 phase arrest, a feature that is not observed in M059J cells after RA treatment– Figure 1D, 1H.

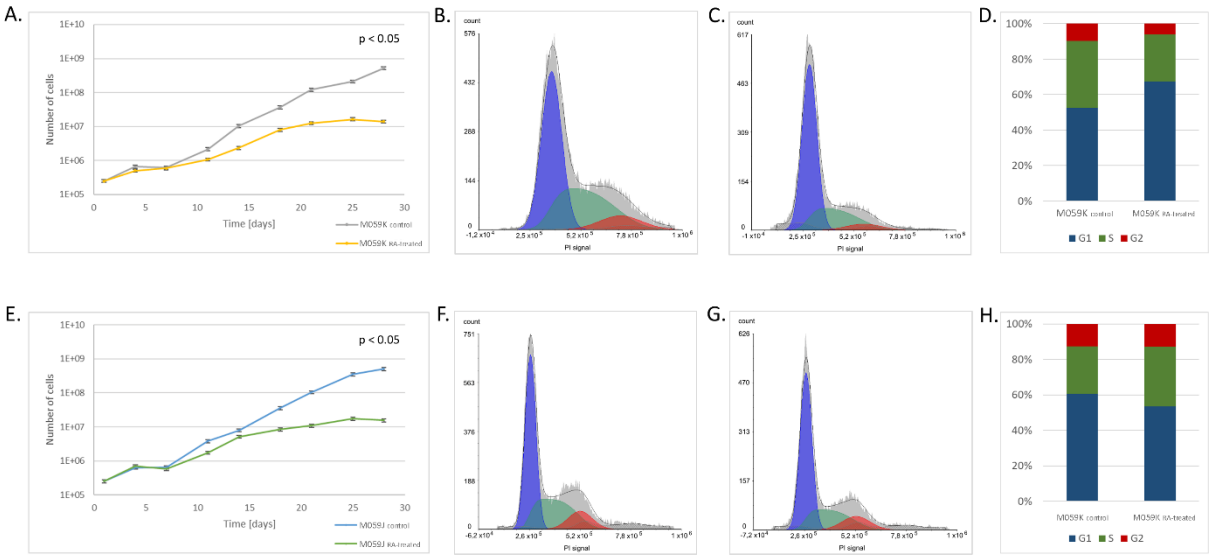

Figure 1. Changes in the proliferation rate (A, E) and cell cycle (B-D, F-H) of M059K (upper panel) and M059J (bottom panel) cells in the course of differentiation procedure with 10 µM retinoic acid (RA). The number of cells in 1A and 1E is presented as mean ± SD (for n=4). The statistical significance of the differences between control and RA-treated cells is marked in the graphs.

Initially, both types of glioma cells differ in their morphology, and migrative properties, as well as P2X7 receptor and cadherins expression. Control M059K exhibit high proliferation and migration potential due to lower E-cadherins and higher N-cadherins expression compared with M059J cells, and could represent the mesenchymal phenotype, whereas M059J are non-migratory, with higher E-cadherin expression and epithelial features. The RA-induced differentiation process changed considerably the neurogenic marker genes expression in M059J cells - increased *TUJ1*, *NES*, and

NeuroD1 expression and maintained the glial marker *GFAP* expression, whereas in M059K the alterations in tested genes expression levels were opposite and less pronounced (Figure 2A). Additionally, we have observed the rise in N-cadherins and relevant depletion of E-cadherins expression in both cell type, as well as changes in cell migration. The rate of wound closure of RA-treated M059K cells was decreased – Figure 2B, whereas the migrative properties of RA-treated M059J remained at the same level.

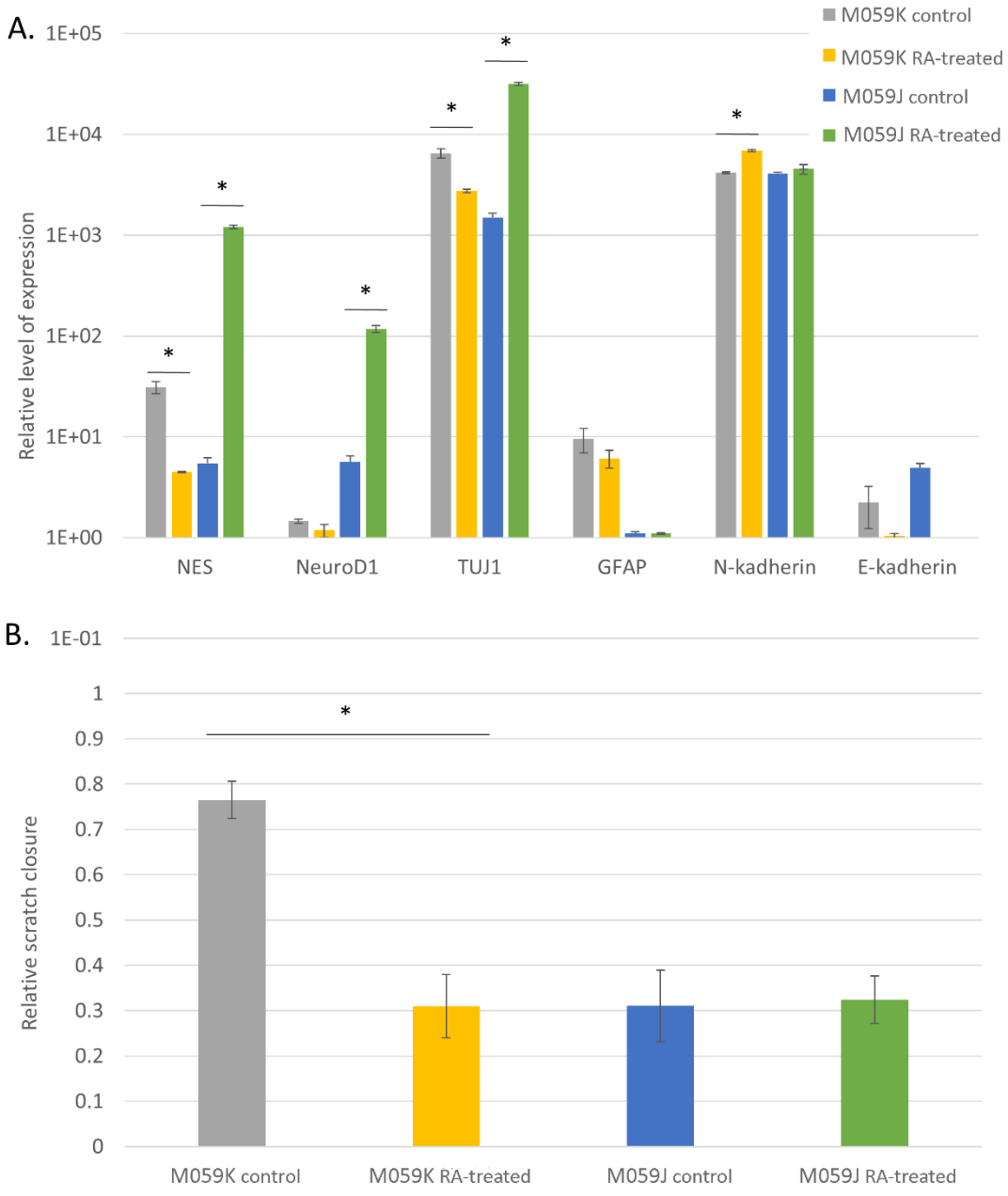

Figure 2. Changes in gene expression and migratory properties of M059K and M059J cells before and after RA treatment. A) expression of neurogenic markers: TUJ1, NES, NeuroD1, glial cells marker GFAP, and N- and E-cadherin genes; B) relative wound closure capability. The values are presented as mean ± SD (for n=4).The statistical significance of the differences between control and RA-treated cells is marked in the graphs with an asterisk (for $p \leq 0.05$).*

2. Changes in purinergic signaling after RA treatment

Definitely, after applied RA-treatment, we obtained phenotypically more similar cells in terms of limited proliferation and migration but differing in neurogenic markers expression. To define the purinergic signaling before and after the procedure, we have analyzed the alterations in P2X7 receptor expression on the gene and protein level (Figure 3). The determined increase in P2X7A and P2X7B receptor splice variants in both cell types were reflected in the presence and functions of receptors in the cells' membrane, which was confirmed experimentally with Western Blot analysis (Fig. 3B) and ethidium bromide uptake (Fig. 3C), respectively.

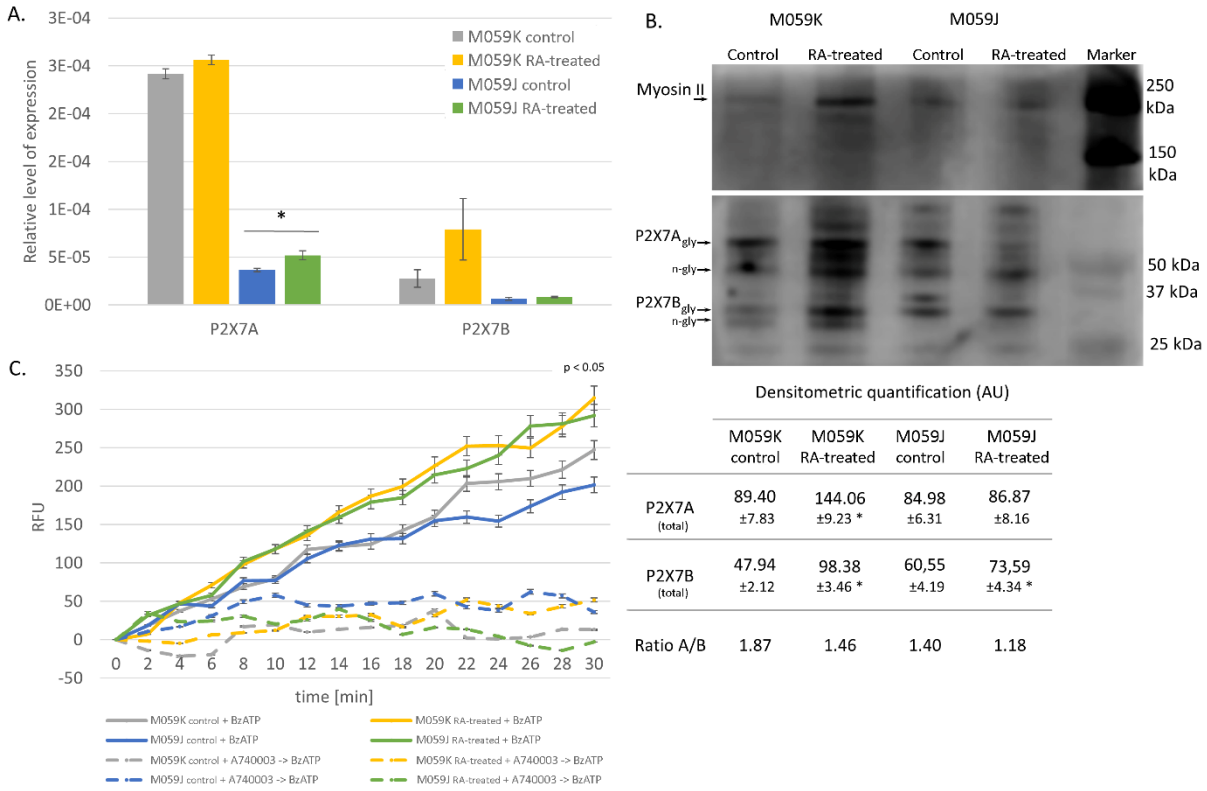

Densitometric quantification (AU)

	M059K control	M059K RA-treated	M059J control	M059J RA-treated
P2X7A (total)	89.40 ±7.83	144.06 ±9.23 *	84.98 ±6.31	86.87 ±8.16
P2X7B (total)	47.94 ±2.12	98.38 ±3.46 *	60,55 ±4.19	73,59 ±4.34 *
Ratio A/B	1.87	1.46	1.40	1.18

Figure 3. Changes in expression level of P2X7 receptor (isoforms A and B) genes (A), proteins (B), and their influence on P2X7R functionality (C) measured through ethidium bromide (EtBr) uptake. Different bands of P2X7A receptor in WB represent non-glycosylated (P2X7 n-gly) and glycosylated (P2X7 gly) proteins. Densitometric quantification presents the changes in receptor protein amount calculated from WB. For EtBr uptake the cells were stimulated with 10 µM BzATP alone (solid lines) to induce the P2X7 receptor opening or treated with 1 µM A740003 (dashed lines) acting as a specific P2X7 receptor antagonist and then stimulated with BzATP. The values in 3A, 3C, and in table are presented as mean ± SD (for n=4). The statistical significance of the differences between control and RA-treated cells is marked with an asterisk (for p ≤ 0.05).*

From the above presented results, it becomes evident, that M059K cells before RA treatment procedure have a considerably higher than M059J expression of both P2X7A and P2X7B genes that is also reflected in the level of receptor protein in WB analysis (Fig. 3A, B). The functionality of the P2X7 receptor in the cell membrane was confirmed through ethidium bromide uptake in cells stimulated with BzATP, and through uptake inhibition in the presence of P2X7 receptor antagonist, A740003 –

Figure 3C. It is consistent with the conclusions of Adinolfi and collaborators, that P2X7B variant coassembles with P2X7A into a heterotrimer potentiating all responses mediated by this latter receptor [30]. After RA treatment of M059 cells, we observed an increase in both P2X7 receptor isoforms expression at the gene and protein level. PCR data show that P2X7A rises only by 6% in M059K and by 42% in M059J cells afterRA treatment, whereas P2X7B rises by 300% and 30% in M059K and M059J cells after RA treatment, respectively. As a result, both M059 cells undergo an opposite shift in A and B isoforms: a decrease in the A to B ratio in M059K cells and a slight rise in the M059J cell line. In the case of protein expression, we observed a similar decrease in the A to B ratio in M059K and M059 cells. More importantly, in both cell types, the P2X7A to P2X7B receptor ratio was maintained in favor of the P2X7A splice variant.

Another pivotal alteration in purinergic signaling of RA-treated M059 cells was the decrease of ecto-and exo-enzymes activities that is followed by hampered cleavage of ATP, ADP, or AMP in the tumor microenvironment (Table 1). Collectively, the elevated expression of the P2X7 receptor makes the cells ATP-sensitive, and the higher ecto-nucleotides concentration in the case of RA-treated cells provides enough ligand for activation of the receptor.

Table 1. Comparison of ecto- and exo-enzymes activity towards various nucleotides in M059K and M059J cells before and after RA treatment. Membrane enzymes (ecto-enzymes) are anchored in the cell membrane and act extracellularly, whereas soluble enzymes (exo-enzymes) are released into the extracellular microenvironment. The activity values are presented as mean ± SD (for n=4). The statistical significance of the differences between control and RA-treated cells is marked with an asterisk (for p ≤ 0.05)*.

Cell line	Enzyme	Substrate	Activity [nmol of metabolized substrate × min^{-1} × mg $protein^{-1}$]			
			Control cells		RA-treated cells	
			soluble	membrane	soluble	membrane
M059K	NTPDase	ATP	0.67 ± 0.03	1.28 ± 0.02	0.15 ± 0.02 *	1.25 ± 0.13
	NTPDase	ADP	0.28 ± 0.01	0.79 ± 0.03	0 *	0 *
	Adenylate kinase	ADP	2.97 ± 0.13	3.25 ± 0.15	0 *	0.67 ± 0.03 *
	Ecto-5'-nucleotidase	AMP	0.74 ± 0.05	7.06 ± 0.25	0 *	0 *
M059J	NTPDase	ATP	1.65 ± 0.05	0.27 ± 0.03	0.44 ± 0.03 *	0.45 ± 0.08
	NTPDase	ADP	0.15 ± 0.01	0.73 ± 0.05	0.12 ± 0.007	0.17 ± 0.008 *
	Adenylate kinase	ADP	2.29 ± 0.08	5.77 ± 0.22	0 *	0
	Ecto-5'-nucleotidase	AMP	0.33 ± 0.06	4.04 ± 0.16	0.10 ± 0.005	0.86 ± 0.05 *

The results on P2X7 receptor expression and enzymes activity inspired us to further analyze the eATP influence on the regulation of RA-treated glioma cells' biological potential. To prove the presumed effects of efficient P2X7R activation due to increased eATP concentration, the cell viability

determination of M059K and M059J treated with different ligands of P2X7 receptor was performed, based on the cells' metabolic activity (MTT assay).

3. Increased P2X7 receptor enhances cytotoxic effect of eATP

Firstly, we determined the cytotoxicity of two different P2X7R antagonists – very specific A740003 and non-specific BBG (data not shown). A740003 is completely non-toxic in the tested range of concentrations, whereas BBG toxicity was observed exclusively for RA-treated cells and was concentration dependent. It is probably due to unspecific inhibition of other receptors or ecto-nucleotidases important for purinergic signaling. Therefore, 1μM A740003 was chosen for further experiments. A set of experiments with eATP and BzATP as P2X7 receptor agonists confirmed the different sensitivity of M059 glioma cells to purinergic compounds. Both cell types were treated for 72 h with ATP (in the presence of BGO as ectonucleotidases inhibitor) or BzATP (specific agonist of P2X7R) before and after RA treatment – see Figures 4 and 5. To confirm the involvement of P2X7R in the alterations of cells viability, we used 1 μM A740003 as a P2X7R antagonist.

Non-treated M059K cells are sensitive to cytotoxic influence of ATP in micromolar concentration, and this sensitivity rises after RA treatment (Figure 4A), presumably due to the increased P2X7R expression in RA-treated cells, and enhanced responses of heterotrimers as concluded from Figure 3. On the other hand, the cytotoxic effect is reversed in the presence of a specific P2X7R antagonist. In the case of M059J cells, the slightly cytotoxic influence of ATP was observed only at high ATP concentrations (Figure 4B). These results indicate that ATP-mediated decrease in cell viability can be linked with supported P2X7R activation, thus the more “ATP-resistant” phenotype is observed in case of M059J cells. These set of results is also related with the activity of ecto-enzymes metabolizing nucleotides (Table 1). M059J cells can partially hydrolyze ATP, and the outcomes of eATP signaling can be regulated/modified by exo-nucleotidases. In contrast, M059K cells have lower exo-nucleotidases activity than M059J, and thus their inability to hydrolyze ATP may also underlie the higher sensitivity to the cytotoxic effect of eATP. This relationship is even more pronounced after differentiation procedure, as all enzymatic activities decrease, and it was further confirmed with BzATP treatment of both cell types (Figure 5).

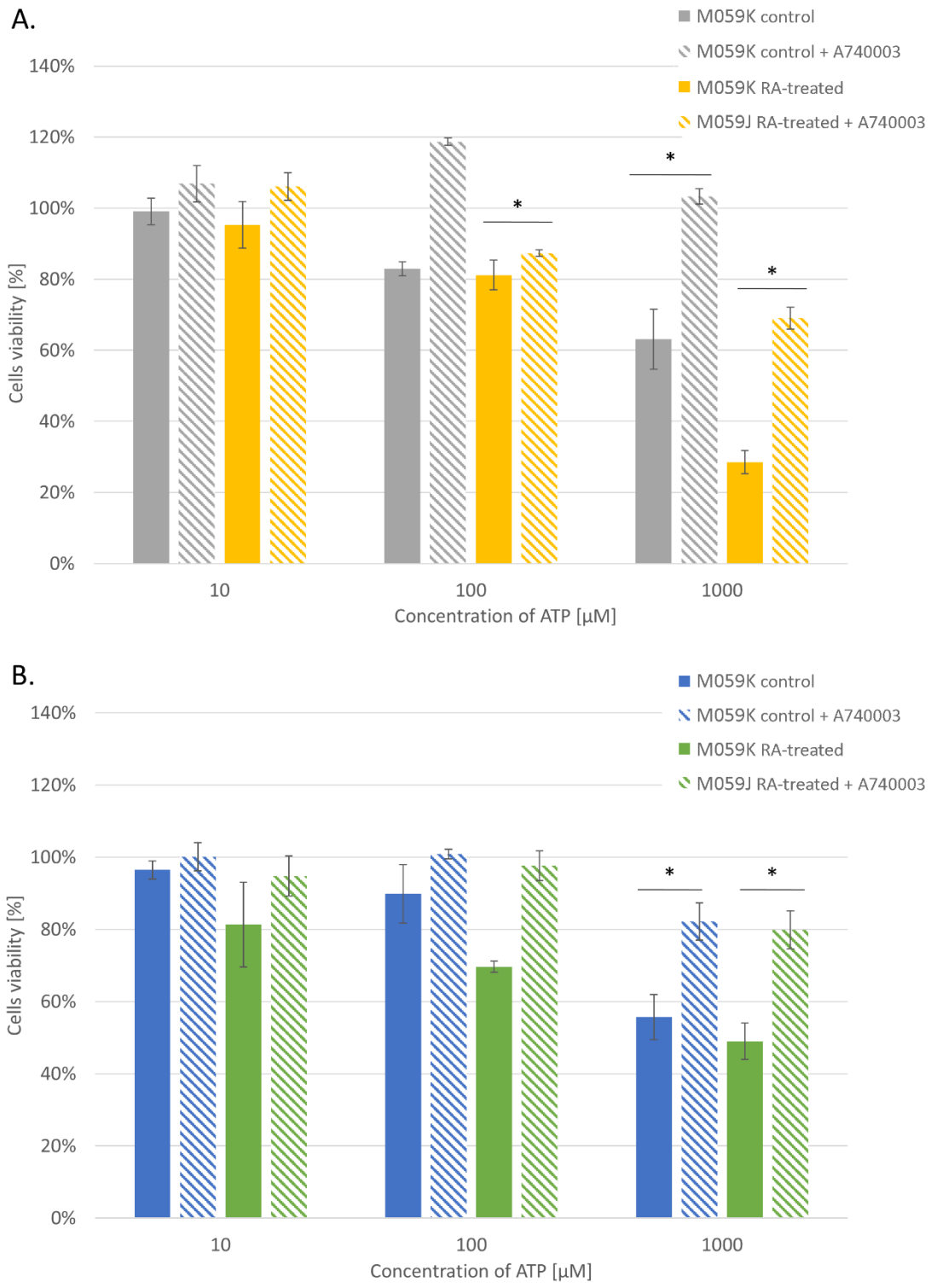

Figure 4. Changes in viability of M059K (A) and M059J (B) cells before and after RA treatment, treated for 72h with different concentrations of ATP in the presence of 100 µM BGO (ecto-nucleotidases inhibitor preventing the nucleotide cleavage) or ATP, BGO and 1 µM A740003 as *P2X7R antagonist. The values are presented as mean ± SD (for n=4). The statistical significance of the differences between control and RA-treated cells is marked in the graphs with an asterisk (* for p ≤ 0.05).*

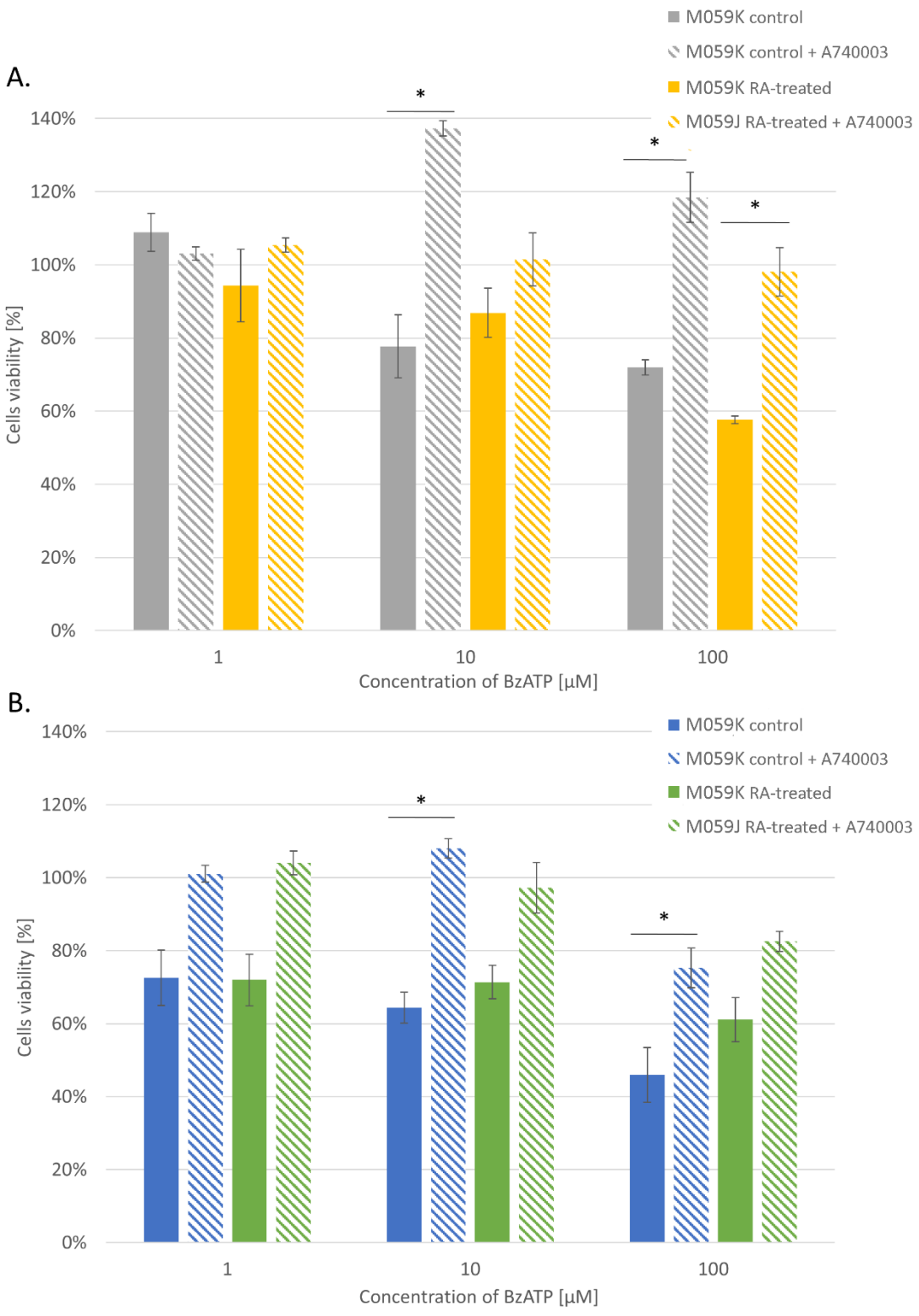

Figure 5. Changes in viability of M059K (A) and M059J (B) cells before and after RA treatment, treated for 72h with different concentrations of BzATP or BzATP with 1 µM A740003 as P2X7R antagonist. The values are presented as mean ± SD (for n=4). The statistical significance of the differences between control and RA-treated cells is marked in the graphs with an asterisk (for p ≤ 0.05).*

One of the parameters characteristic of cancer cells is their migration. Intrinsic migrative properties of M059K and M059J cells are different, and applied differentiation procedure decreases the migration rate of M059K cells as shown in Figure 2B. The addition of P2X7 receptor agonists - 100 µM ATP or 10 µM BzATP to non-treated and RA-treated M059K cells, significantly reduced their migration potential, and this process is reversed by adding the P2X7 receptor antagonist A740003 (Figure 6).

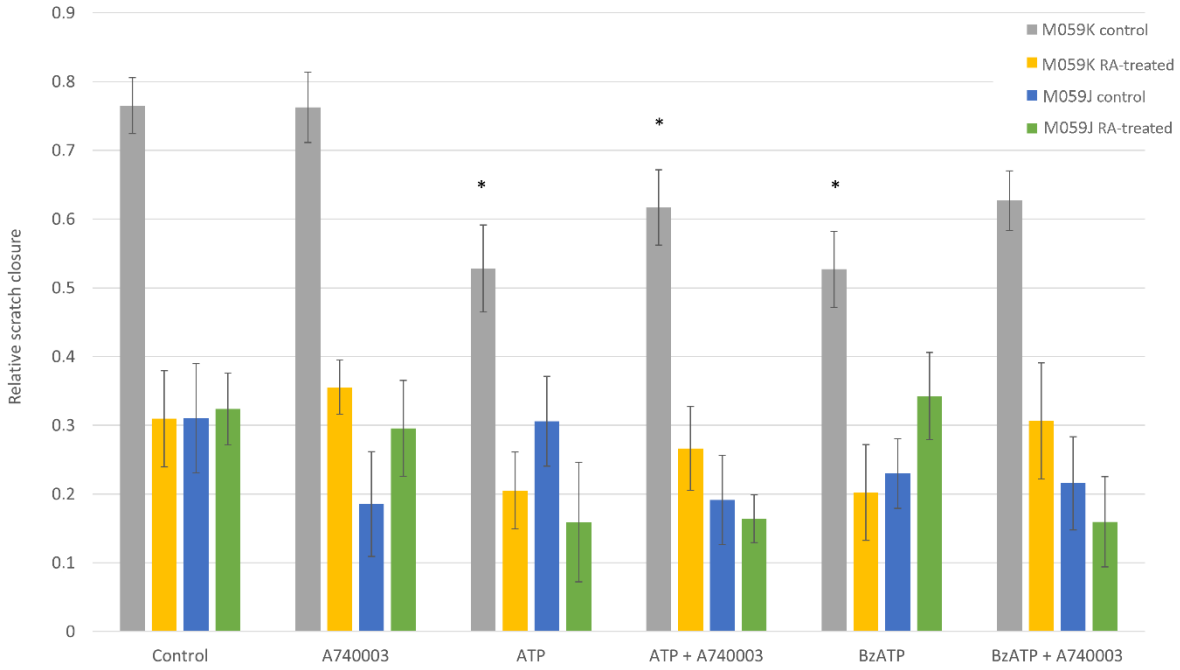

Figure 6. Changes in scratch closure capability (migration) of M059K and M059J cells before and afterRA treatment, under 24-hours treatment with different P2X7 receptor agonists (100 µM ATP or 10 µM BzATP) and antagonist (1 µM A740003). The values are presented as mean ± SD (for n=4). The statistical significance of the differences in comparison to appropriate control sample is marked in the graphs with an asterisk (for p ≤ 0.05).*

In the case of non-treated and RA-treated M059J cells, the addition of ATP also decreases the migration rate. However, the statistically significant decrease was achieved only in RA-treatedcells with BzATP treatment – Figure 6. Repeatedly, changes in migratory properties might be underpinned with general ATP-sensitivity that is due to enhanced P2X7A and P2X7B receptor expression, as well as to their coassembly.

4. Enhanced expression and activation of P2X7R affect intracellular Akt-mediated signaling

Finally, it has been determined how the process of RA-induced differentiation and stimulation of cells with P2X7 receptor ligands influences the intracellular signaling pathways related to cell proliferation. Non-treated M059K cells have the highest levels of phosphorylated protein kinase B (pAKT) reflecting their high proliferative potential – Figure 7.

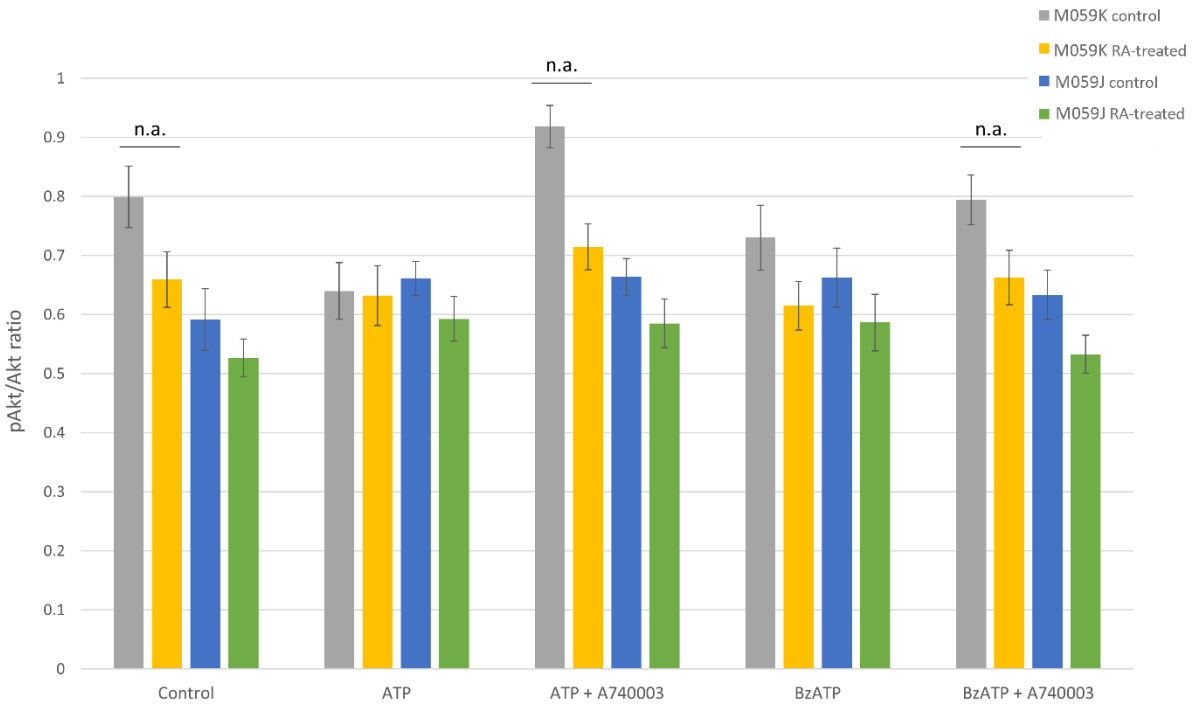

Figure 7. Relative pAKT expression level ratio in M059K and M059J cells before and after RA treatment, under 24-hours treatment with 100 µM ATP or 10 µM BzATP, with or without 1 µM A740003. The values are presented as mean ± SD (for n=4), the differences that are not statistically significant were marked as "n.a."

Treatment of these cells with ATP and BzATP reduced the amount of phosphorylated forms, while the addition of antagonist A740003 reversed this effect, suggesting the importance of P2X7R activation. In the case of RA-treated M059K cells, the stimulation with ATP and BzATP did not significantly change the ratio of phosphorylated to unphosphorylated forms, but still their influence was reversed with A740003. On the other hand, M059J cells treated with ATP and BzATP slightly increased the amount of phosphorylated proteins compared to the control, while the addition of A740003 scarcely decreased the amount of phosphorylated forms of the protein, but still above the control level. It can be concluded that a decrease in pro-proliferative pAKT level is connected with enhanced expression of both P2X7A and P2X7B variants and potentiated activation of P2X7 receptor by eATP. Such changes evoked by glioma cells RA-induced differentiation and subsequent P2X7R agonist treatment can strongly influence glioma cells' invasiveness.

DISCUSSION

Human glioma M059J and M059K cell lines were chosen as an example of cancer cells heterogeneity and, as expected, they reacted differently in the course of applied RA treatment. Retinoic acid-induced changes, even if the cells did not become fully differentiated, include increased neurogenic marker genes *TUJ1*, *NES*, and *NeuroD1* expression in M059J cells whereas it decreased their expression in M059K. Additionally, in both cell types we have observed the rise in N-cadherins and relevant depletion of E-cadherins expression, which could be ascribed to the EMT process. Definitely,

we obtained phenotypically altered cells, exhibiting limited proliferation and migration but differing in neurogenic markers expression.

Depletion of E-cadherins expression remains in contrast with the decreased rate of proliferation and wound closure capability in the case of RA-treated M059K cells, whereas the migrative properties of M059J remained at the same level. On the other hand, increased expression of N-cadherin in mouse glioma C6 cells also correlated with a dramatic decrease in invasiveness level *in vitro* [31]. It must be remembered that scratch overgrowth is a result of various processes including but not limited to migration. We can assume that the reduced migrative capability is also the aftermath of slowed proliferation. However, despite these limitations, *in vitro* scratch assay allows to analyze cell migration, that is of great importance for the cancer cells' potential to invade the adjacent tissues. Nevertheless, all the above alterations at the gene expression level underpin the cytophysiological properties of RA-treated glioma cells, predominantly influencing their proliferation and migration capability, but also altering the purinergic signaling dynamics.

Surprisingly, the expression of the P2X7R gene and functional protein has been changed oppositely to neurogenic markers, so we cannot conclude on positive relation between neurogenic differentiation and P2X7 receptor changes as it was described in case of A172 cells [21]. From the presented results it becomes clear that after applied RA-induced differentiation of M059 cells there is an increase in both P2X7 receptor isoforms expression at the gene and protein level. We can also conclude that the rise in P2X7 receptor expression is followed by increased ATP-mediated cytotoxicity, that can be explained with the P2X7A and P2X7B variants “cooperation” in opening the pore and making cells more sensitive to ATP. It stays in agreement with the study showing that P2X7 receptor variant A itself can form non-selective pores, and this activity is supported by the B variant in the receptor heterotrimer [16, 18, 20, 30, 32]. Adding to this picture the reduced ecto-nucleotidases activity and relatively high ATP concentration in the tumor microenvironment, RA-induced changes lead to mitigated biological potential of M059 glioma cells. More importantly, we can enhance the anti-cancer influence with ATP-assisted treatment directed toward the P2X7 receptor activation. We confirmed that micromolar concentrations of ATP decreased cell viability by 40 and 20 % in M059K and M059J cells, respectively. Additionally, a decrease in migration up to 60% in the presence of 100 µM ATP was observed. Both effects were mediated by P2X7R activation and reversed in the presence of the A740003 antagonist.

Recently, Ziberi et al. [27] suggested that the positive modulation of P2X7A and P2X7B expression levels following treatment with BzATP might support GSCs invasion, and consequently, P2X7 receptor may be considered as a potential pharmacological target to treat glioblastoma. However, in our study, we present a complex approach using retinoic acid-induced differentiation procedure combined with ATP treatment. In our case, the increased expression of P2X7A and P2X7B receptor variants due to RA treatmentwill lead to the increased sensitivity of glioma cells to ATP cytotoxic effect mediated by P2X receptor. Bearing in mind that eATP is one of the dominating purine components in the tumor microenvironment, additionally increased by radiation or other therapeutic approaches, the augmented ATP sensitivity seems very promising.

Increasing evidence published in recent years confirms that the P2X7B isoform might be of superior relevance in cancer cells. The expression of this isoform was initially associated with increased metabolic activities in HEK293 cells [30], then with a stem-like proliferation in osteosarcoma cells [25] or with the acquisition of a stem-like phenotype, the suppression of autophagy and induction of EMT in neuroblastoma cells [23]. These data are in line with those obtained by Tattersall and colleagues who examined osteosarcoma murine models. Their results demonstrated that P2X7B expression is

linked with reduced cell adhesion, promotion of invasiveness, and increased osteosarcoma progression in mouse lungs [33]. The dominant role of P2X7B variant in lung adenocarcinoma cells was also confirmed to correlate with tumor development [34]. However, from the presented here set of results, one can conclude that the rise in the P2X7B isoform is not always linked with elevated proliferation and invasive potential of cancer as long as both isoforms are expressed, and P2X7B may support pore opening and cytotoxic effects exerted *via* P2X7A activation. In glioma M059 cells subjected to RA-induced differentiation procedure, the changes in their phenotypes do not support proliferation and invasion if both P2X7A and P2X7B variants remain highly expressed. Not without significance is the phenomena of decreased activity of ecto-nucleotidases as a result of RA-induced differentiation. It considerably contributes to the modulation of tumor niche and allows to increase in the concentration of nucleotides, primarily cytotoxic ATP.

One of the signaling pathways implicated in ATP-mediated activation of the P2X7R in human melanoma, breast, and prostate cancer cells is the PI3K/AKT pathway [12]. A high level of phosphorylated AKT (pAKT) is generally ascribed to the rise in cells' proliferative potential and survival [35]. However, the literature data concerning P2X7 receptor and intracellular AKT-mediated signaling are ambiguous: in neuroblastoma cells, P2X7R inhibition was associated with neuritogenesis and increased AKT phosphorylation [36], and in contrast in pancreatic cancer cells, P2X7 receptor activation lead to nuclear AKT depletion and inhibited proliferation [37]. In the case of M059 cells, the decrease in pro-proliferative pAKT level is rather connected with activation of P2X7 receptor, that is also dependent on the amount of functional P2XRA variant.

The RA-induced differentiation and subsequent rise in the P2X7R variants seem to be beneficial regarding anti-cancer therapy. From all the above data it can be concluded that M059K cells in the course of differentiation undergo more modifications or exhibit stronger expressed changes that influence their invasive potential (proliferation and migration). We postulate that retinoic acid-induced differentiation together with micromolar ATP treatment could be an effective dual approach to maintain the balance of ecto-nucleotides in the tumor microenvironment, as well as to control P2X7 receptor activation. The plethora of various transduction pathways linked to P2X7R activation and its effects must be further interpreted based on the molecular context of the microenvironment and the cell type.

CONCLUSIONS

Described in this study the retinoic acid-induced differentiation decreases the proliferation potential of glioma cells and increases their sensitivity to cytotoxic eATP influence – these changes are underpinned with the decrease in ecto-nucleotidases activity, and the increase in P2X7R expression with splicing variant P2X7A as dominative. Decrease in viability, proliferation and migration of RA-treated glioma cells supported with eATP depends also on the presence of P2X7B variant supporting the pore opening. Collectively, the glioma cells become sensitive to micromolar eATP concentrations present in the tumor microenvironment. The intracellular pathway involved can be AKT-signaling as P2X7A receptor activation reduces the concentration of pAKT, and thus limits the pAKT-dependent pro-proliferative signaling.

STATEMENTS AND DECLARATIONS

FUNDING

This article is based upon work from PRESTO COST Action CA21130, supported by COST (European Cooperation in Science and Technology; www.cost.eu; www.p2xcost.eu). B.S. took part in a Short Term Mission funded by the Action to visit the laboratory of E.A. B.S. acknowledges the partial financial support by the Nicolaus Copernicus University grant 32/2021/Grants4NCUStudents. E.A. is supported by funding from TRANSCAN-3 JTC2021 funds (PUR-THER Project), and institutional funds from the University of Ferrara.

COMPETING INTERESTS

The authors have no relevant financial or non-financial interests to disclose.

AUTHORS CONTRIBUTION

Study conception and design were performed by K.R, E.A., J.C. and B.S. Material preparation, data collection and analysis were performed by B.S., A.P., E.M., M.G., B.M. The first draft of the manuscript was written by K.R. and all authors commented on previous versions of the manuscript. All authors read and approved the final manuscript.

DATA AVAILABILITY

The datasets generated during and/or analysed during the current study are available from authors upon reasonable request.

ETHICS APPROVAL

Not applicable.

CONSENT TO PARTICIPATE

Not applicable.

CONSENT TO PUBLISH

Not applicable.

REFERENCES

1. Stupp R, Brada M, van den Bent MJ, Tonn JC, Pentheroudakis G (2014) High-grade glioma: ESMO Clinical Practice Guidelines for diagnosis, treatment and follow-up. Ann Oncol Off J Eur Soc Med Oncol 25 Suppl 3:93–101. https://doi.org/10.1093/ANNONC/MDU050
2. Lee SY (2016) Temozolomide resistance in glioblastoma multiforme. Genes Dis 3:198–210. https://doi.org/10.1016/j.gendis.2016.04.007
3. Liang C, Yang L, Guo S (2015) All-trans retinoic acid inhibits migration, invasion and proliferation, and promotes apoptosis in glioma cells in vitro. Oncol Lett 9:2833–2838. https://doi.org/10.3892/ol.2015.3120
4. Shi L, Li H, Zhan Y (2017) All-trans retinoic acid enhances temozolomide-induced autophagy in human glioma cells U251 via targeting Keap1/Nrf2/ARE signaling pathway. In: Oncol. Lett. https://www.spandidos-publications.com/10.3892/ol.2017.6482. Accessed 9 Jun 2024
5. Shi Z, Lou M, Zhao Y, Zhang Q, Cui D, Wang K (2013) Effect of all-trans retinoic acid on the differentiation of u87 glioma stem/progenitor cells. Cell Mol Neurobiol 33:943–951.

https://doi.org/10.1007/S10571-013-9960-5/FIGURES/7
6. Dreyfus M, El-Atifi M, Court M, Bidart M, Coutton C, Leclech C, Ballester B, Garcion E, Bouamrani A, Berger F, Wion D (2018) Reprogramming glioma cell cultures with retinoic acid: Additional arguments for reappraising the potential of retinoic acid in the context of personalized glioma therapy. Glioma 1:66. https://doi.org/10.4103/glioma.glioma_3_18
7. Maden M (2007) Retinoic acid in the development, regeneration and maintenance of the nervous system. Nat Rev Neurosci 2007 810 8:755–765. https://doi.org/10.1038/nrn2212
8. Czarnecka J, Nemecz D, Bajek A, Hołysz M, Roszek K (2017) Neurogenic Differentiation of Mesenchymal Stem Cells Induces Alterations in Extracellular Nucleotides. Artic J Cell Biochem 118:478–486. https://doi.org/10.1002/jcb.25664
9. Burnstock G (2006) Pathophysiology and Therapeutic Potential of Purinergic Signaling. Pharmacol Rev 58:58 LP – 86. https://doi.org/10.1124/pr.58.1.5
10. Burnstock G, Di Virgilio F (2013) Purinergic signalling and cancer. Purinergic Signal 9:491–540. https://doi.org/10.1007/s11302-013-9372-5
11. Di Virgilio F, Adinolfi E (2017) Extracellular purines, purinergic receptors and tumor growth. Oncogene 36:293–303. https://doi.org/10.1038/ONC.2016.206
12. Cao Y, Chen E, Wang X, Song J, Zhang H, Chen X (2023) An emerging master inducer and regulator for epithelial-mesenchymal transition and tumor metastasis: extracellular and intracellular ATP and its molecular functions and therapeutic potential. Cancer Cell Int 23:. https://doi.org/10.1186/S12935-023-02859-0
13. Adinolfi E, De Marchi E, Grignolo M, Szymczak B, Pegoraro A (2023) The P2X7 Receptor in Oncogenesis and Metastatic Dissemination: New Insights on Vesicular Release and Adenosinergic Crosstalk. Int J Mol Sci 24:. https://doi.org/10.3390/IJMS241813906
14. Leung YM (2011) P2X7 receptor as a double-edged sword: Neurotrophic and neurotoxic effects. BioMedicine 1:16–20. https://doi.org/10.1016/J.BIOMED.2011.10.003
15. Sluyter R (2017) The P2X7 receptor. Adv Exp Med Biol 1051:17–53. https://doi.org/10.1007/5584_2017_59
16. Lara R, Adinolfi E, Harwood CA, Philpott M, Barden JA, Di Virgilio F, McNulty S (2020) P2X7 in Cancer: From Molecular Mechanisms to Therapeutics. Front Pharmacol 11:. https://doi.org/10.3389/fphar.2020.00793
17. Harkat M, Peverini L, Cerdan AH, Dunning K, Beudez J, Martz A, Calimet N, Specht A, Cecchini M, Chataigneau T, Grutter T (2017) On the permeation of large organic cations through the pore of ATP-gated P2X receptors. Proc Natl Acad Sci U S A 114:E3786–E3795. https://doi.org/10.1073/PNAS.1701379114
18. Kopp R, Krautloher A, Ramírez-Fernández A, Nicke A (2019) P2X7 Interactions and Signaling - Making Head or Tail of It. Front Mol Neurosci 12:. https://doi.org/10.3389/FNMOL.2019.00183
19. Martínez-cuesta MÁ, Blanch-ruiz MA, Ortega-luna R, Sánchez-lópez A, Álvarez Á (2020) Structural and Functional Basis for Understanding the Biological Significance of P2X7 Receptor. Int J Mol Sci 21:1–23. https://doi.org/10.3390/IJMS21228454
20. Bai X, Li Q, Peng X, Li X, Qiao C, Tang Y, Zhao R (2023) P2X7 receptor promotes migration and invasion of non-small cell lung cancer A549 cells through the PI3K/Akt pathways. Purinergic Signal 19:685–697. https://doi.org/10.1007/S11302-023-09928-Z
21. Szymczak B, Czarnecka J, Czach S, Nowak W, Roszek K (2023) Purinergic approach to effective glioma treatment with temozolomide reveals enhanced anti-cancer effects mediated by P2X7 receptor. Cell Signal 106:110641. https://doi.org/10.1016/J.CELLSIG.2023.110641
22. Zanoni M, Sarti AC, Zamagni A, Cortesi M, Pignatta S, Arienti C, Tebaldi M, Sarnelli A, Romeo A, Bartolini D, Tosatto L, Adinolfi E, Tesei A, Di Virgilio F (2022) Irradiation causes senescence, ATP release, and P2X7 receptor isoform switch in glioblastoma. Cell Death Dis 13:. https://doi.org/10.1038/S41419-022-04526-0
23. Arnaud-Sampaio VF, Bento CA, Glaser T, Adinolfi E, Ulrich H, Lameu C (2022) P2X7 receptor isoform B is a key drug resistance mediator for neuroblastoma. Front Oncol 12:.

https://doi.org/10.3389/FONC.2022.966404
24. Pegoraro A, De Marchi E, Adinolfi E (2021) P2X7 Variants in Oncogenesis. Cells 10:189. https://doi.org/10.3390/cells10010189
25. Giuliani AL, Colognesi D, Ricco T, Roncato C, Capece M, Amoroso F, Wang QG, De Marchi E, Gartland A, Di Virgilio F, Adinolfi E (2014) Trophic Activity of Human P2X7 Receptor Isoforms A and B in Osteosarcoma. PLoS One 9:e107224. https://doi.org/10.1371/JOURNAL.PONE.0107224
26. Pegoraro A, Orioli E, De Marchi E, Salvestrini V, Milani A, Di Virgilio F, Curti A, Adinolfi E (2020) Differential sensitivity of acute myeloid leukemia cells to daunorubicin depends on P2X7A versus P2X7B receptor expression. Cell Death Dis 2020 1110 11:1–12. https://doi.org/10.1038/s41419-020-03058-9
27. Ziberi S, Zuccarini M, Carluccio M, Giuliani P, Ciccarelli R (2020) Transition Markers and P2X7 Receptors Is Associated to Increased Invasiveness Caused by P2X7 Receptor. Cells 9:85. https://doi.org/10.3390/cells9010085
28. Allalunis-Turner MJ, Barron GM, Day RS, Dobler KD, Mirzayans R (1993) Isolation of Two Cell Lines from a Human Malignant Glioma Specimen Differing in Sensitivity to Radiation and Chemotherapeutic Drugs. Radiat Res 134:349–354. https://doi.org/10.2307/3578196
29. Pegoraro A, De Marchi E, Ferracin M, Orioli E, Zanoni M, Bassi C, Tesei A, Capece M, Dika E, Negrini M, Di Virgilio F, Adinolfi E (2021) P2X7 promotes metastatic spreading and triggers release of miRNA-containing exosomes and microvesicles from melanoma cells. Cell Death Dis 2021 1212 12:1–12. https://doi.org/10.1038/s41419-021-04378-0
30. Adinolfi E, Cirillo M, Woltersdorf R, Falzoni S, Chiozzi P, Pellegatti P, Callegari MG, Sandonà D, Markwardt F, Schmalzing G, Di Virgilio F (2010) Trophic activity of a naturally occurring truncated isoform of the P2X7 receptor. FASEB J 24:3393–3404. https://doi.org/10.1096/FJ.09-153601
31. Asano K, Duntsch CD, Zhou Q, Weimar JD, Bordelon D, Robertson JH, Pourmotabbed T (2004) Correlation of N-cadherin expression in high grade gliomas with tissue invasion. J Neurooncol 70:3–15. https://doi.org/10.1023/B:NEON.0000040811.14908.F2
32. De Marchi E, Orioli E, Dal Ben D, Adinolfi E (2016) P2X7 Receptor as a Therapeutic Target. Adv Protein Chem Struct Biol 104:39–79. https://doi.org/10.1016/BS.APCSB.2015.11.004
33. Tattersall L, Shah KM, Lath DL, Singh A, Down JM, De Marchi E, Williamson A, Di Virgilio F, Heymann D, Adinolfi E, Fraser WD, Green D, Lawson MA, Gartland A (2021) The P2RX7B splice variant modulates osteosarcoma cell behaviour and metastatic properties. J bone Oncol 31:. https://doi.org/10.1016/J.JBO.2021.100398
34. Benzaquen J, Dit Hreich SJ, Heeke S, Juhel T, Lalvee S, Bauwens S, Saccani S, Lenormand P, Hofman V, Butori M, Leroy S, Berthet JP, Marquette CH, Hofman P, Vouret-Craviari V (2020) P2RX7B is a new theranostic marker for lung adenocarcinoma patients. Theranostics 10:10849–10860. https://doi.org/10.7150/THNO.48229
35. Miras-Portugal MT, Ortega F, Gómez-Villafuertes R, Gualix J, Pérez-Sen R, Delicado EG (2021) P2X7 receptors in the central nervous system. Biochem Pharmacol 187:. https://doi.org/10.1016/J.BCP.2021.114472
36. Gómez-Villafuertes R, Del Puerto A, Díaz-Hernández M, Bustillo D, Díaz-Hernández JI, Huerta PG, Artalejo AR, Garrido JJ, Miras-Portugal MT (2009) Ca2+/calmodulin-dependent kinase II signalling cascade mediates P2X7 receptor-dependent inhibition of neuritogenesis in neuroblastoma cells. FEBS J 276:5307–5325. https://doi.org/10.1111/J.1742-4658.2009.07228.X
37. Mistafa O, Ghalali A, Kadekar S, Högberg J, Stenius U (2010) Purinergic receptor-mediated rapid depletion of nuclear phosphorylated Akt depends on pleckstrin homology domain leucine-rich repeat phosphatase, calcineurin, protein phosphatase 2A, and PTEN phosphatases. J Biol Chem 285:27900–27910. https://doi.org/10.1074/JBC.M110.117093

Oświadczenie o współautorstwie

Niniejszym oświadczam, że:

w pracy Adinolfi, E., De Marchi, E., Grignolo, M., **Szymczak, B.**, & Pegoraro, A. (2023). **The P2X7 receptor in oncogenesis and metastatic dissemination: New insights on vesicular release and adenosinergic crosstalk**. International Journal of Molecular Sciences, 24(18), 13906, mój udział polegał na przeprowadzeniu przeglądu literaturowego i uczestnictwu w pisaniu oryginalnego manuskryptu.

w pracy **Szymczak, B.**, Czarnecka, J., Czach, S., Nowak, W., & Roszek, K. (2023). **Purinergic approach to effective glioma treatment with temozolomide reveals enhanced anti-cancer effects mediated by P2X7 receptor**. Cellular Signalling, 106, 110641, mój udział polegał na opracowaniu konceptu badań, przygotowaniu przeglądu literaturowego, sporządzeniu protokołów eksperymentalnych, przeprowadzeniu większości doświadczeń, analizy statystycznej wyników, wizualizacji wyników, współudziale w pisaniu manuskryptu publikacji oraz edycji i odpowiedziach na recenzje.

w pracy **Szymczak, B.**, Pegoraro, A., De Marchi, E., Grignolo, M., Maciejewski, B., Czarnecka, J., & Roszek, K. (2024). **Retinoic acid-induced alterations enhance eATP-mediated anti-cancer effects in glioma cells: implications for P2X7 receptor variants as key players**. (BBA - Molecular Basis of Disease – praca po drugiej odpowiedzi na recenzje) mój udział polegał na opracowaniu konceptu badań, przygotowaniu przeglądu literaturowego, sporządzeniu protokołów eksperymentalnych, przeprowadzeniu większości doświadczeń, analizy statystycznej wyników, wizualizacji wyników, współudziale w pisaniu manuskryptu publikacji oraz edycji i odpowiedziach na recenzje.